University of Alberta

Mid-infrared spectroscopy estimates nutrient digestibility in pigs to improve in vitro digestion models

by

Lifang Wang

A thesis submitted to the Faculty of Graduate Studies and Research
in partial fulfillment of the requirements for the degree of

Doctor of Philosophy

in

Animal Science

Department of Agricultural, Food and Nutritional Science

Spring 2014
Edmonton, Alberta

DEDICATION

Dedicated to my father Guigen Wang, my mother Lanying Chen,

my daughter Fulin Wang, and my wife Chonglan Zhou

ABSTRACT

Co-products are increasingly used as alternative feedstuffs for pigs, but their nutritional quality varies largely. Rapid evaluation of energy digestibility of co-products is important for the feed industry and pork production. In vitro digestion (IVD) models have been used to evaluate nutritional quality of feedstuffs, but not rigorously tested on co-products. In study 1, we examined the performance of an IVD model to predict the apparent total tract digestibility (ATTD) of energy of 30 co-product samples of canola meal, corn dried distillers grain with solubles (DDGS), soybean meal, and wheat millrun, and compared with the predictions based on chemical analyses. The IVD model explained 69% of the variation in ATTD of energy among the co-products, but the prediction error was large. Furthermore, the IVD model underestimated the ATTD of energy of corn DDGS and wheat millrun, and poorly described the variation of the ATTD of energy within co-products of canola meal, corn DDGS, and soybean meal. Currently, chemical analyses had greater accuracy than the IVD model to predict the ATTD of energy of co-products, but its prediction based on multiple chemical analyses is not favorable. To determine issues of IVD model for its further improvement, identification of discrepancies between IVD and in vivo digestion of nutrients is essential. In study 2, a novel approach of using functional group digestibility (FGD) was proposed to estimate crude protein (CP) digestibility. The apparent ileal digestibility (AID) of CP of wheat was accurately estimated (R^2 = 0.99) using the FGD determined with the absorbance in the amide I region (1,689-1,631 cm^{-1}) of Fourier transform infrared (FT-IR) spectra scanned with an

attenuated total reflection (ATR) attachment and ratio of an inorganic indigestible marker in diet and digesta. In study 3, a spectroscopic method was proposed to evaluate fat digestibility. The AID of total fatty acids (R^2 = 0.75) and ATTD of ether extract (R^2 = 0.90) of flaxseed and field pea were estimated with the FGD at ca. 2,923 cm^{-1} and 1,766-1,695 cm^{-1} of ATR FT-IR spectra, respectively. Our findings can assist the further improvement of IVD model to evaluate energy digestibility of co-products.

ACKNOWLEDGEMENTS

I would like to express my gratitude to my supervisor, Dr. Ruurd T. Zijlstra, for giving me the opportunity to pursue my PhD study, and his enormous support and encouragement during my study in all aspects. His scope of knowledge, attitude on scientific research, and his hard-work influenced me and were greatly appreciated. I would like to give sincere thanks to Dr. Mary-Lou Swift for bringing me into the world of spectroscopy and helping me throughout my research. I appreciate Dr. Eduardo Beltranena, Dr. Doug Korver, and Dr. Masahito Oba for your instructions and help during my PhD study. I thank Dr. Peiqiang Yu, Dr. Scott Jeffrey, and Dr. Paul Stothard for your precious time spent on my thesis defense and for your helpful comments. I would like to give thanks to Dr. James A. de Haseth, Dr. Franklin E. Barton, II, Dr. Isao Noda, Dr. Peter R. Griffiths, and Dr. Bob Hannah for mentoring me on infrared spectroscopy. I appreciate Dr. Allan Schaefer, Professor Jinyu Wang, and Professor Rongbin Jing for supplying references to make my PhD study possible. I am very grateful to Queen Elizabeth II Graduate Scholarship (Doctoral) for funding during my PhD study. The funding from the Alberta Crop Industry Development Fund (Lacombe, AB) and Nutreco Canada Inc. (Guelph, ON) for the research projects are also highly appreciated. I would like to acknowledge the help and academic feedback from Dharma Shrestha, Krishna Kandel, Ruwani Senerviratne, Miladel Casano, Kim Williams, Dr. Jorge Yañez, Dr. Jose Landero, Dr. Guishan Huang, Dr. John Htoo, Dr. Tofuko Woyengo, Dr. Adrienne Woodward, Dr. Zahid Nasir, Dr.

Rajesh Jha, Dr. Prajwal Regmi, Janelle Fouhse, Xun Zhou, Hong Anh Le Minh, and Kimberley Berendt.

I would like to express my sincerest gratitude to my parents for their persistent encouragement of my studies and for taking care of themselves. I would like to thank all my family members and relatives for their kindness and patience, especially for forgiving me not visiting them during my entire PhD study. I would like to give thanks to Mrs. Kathleen Lewanczuk and Dr. Richard Lewanczuk, for their kind help to my family during my PhD study in Edmonton. I would like to express my best wishes from my heart to my deceased uncle, my deceased grandmother, and my wife's deceased grandmother, and my sincerest apologies for not coming back to see them for the last time while I was pursuing my PhD study abroad.

I would like to thank my wife Chonglan and my daughter Fulin for supporting my studies, and also for being so understanding and forgiving for hardly bringing them outdoor for activities during my PhD study.

TABLE OF CONTENTS

LIST OF TABLES

LIST OF FIGURES

LIST OF ABBREVIATIONS

2DCOS	Two-dimensional correlation spectroscopy
a.u.	Arbitrary unit
AA	Amino acids
ADF	Acid detergent fiber
AID	Apparent ileal digestibility
ANF	Anti-nutritional factor
ATR	Attenuated total reflection
ATTD	Apparent total tract digestibility
CF	Crude fiber
CLA	Conjugated linoleic acid
CP	Crude protein
DDGS	Distillers dried grains with solubles
DE	Digestible energy
DM	Dry matter
DRIFTS	Diffuse reflectance Fourier transform infrared spectroscopy
EE	Ether extract
FA	Fatty acids
FFA	Free fatty acids
FGD	Functional group digestibility
FT-IR	Fourier transform infrared
GC	Gas chromatography
GLC	Gas-liquid chromatography

IR	Infrared
IRE	Internal reflection element
IVD	In vitro digestion
ivED	In vitro energy digestibility
ivR	In vitro residues
MCFA	Medium-chain fatty acid
ME	Metabolizable energy
MIR	Mid infrared
MNBT	Mobile nylon bag technique
MRT	Mean retention time
MSC	Multiplicative scatter correction
MW	Molecule weight
NDF	Neutral detergent fiber
NIR	Near infrared
NIRS	Near infrared reflectance spectroscopy
NMR	Nuclear magnetic resonance
NSP	Non-starch polysaccharides
OM	Organic matter
PC	Principal component
PCA	Principal component analysis
PLS	Partial least squares
PUFA	Polyunsaturated fatty acid
RDS	Rapidly digestible starch

RS	Resistant starch
SCFA	Short-chain fatty acids
SDS	Slowly digestible starch
SECV	Standard error of cross validation
SEP	Standard error of prediction
SID	Standardized ileal digestibility
TID	True ileal digestibility
VBA	Visual Basic for Applications
VFA	Volatile fatty acid

Chapter 1 Introduction

Established in vitro digestion (**IVD**) models accurately predicted energy digestibility of cereal grains and among feedstuffs in pigs (Chapter 2). Likewise, chemical analyses accurately predicted digestible energy (**DE**) value of wheat grain and apparent total tract digestibility (**ATTD**) of energy for 114 mixed diets (Noblet and Perez, 1993; Zijlstra et al., 1999). However, IVD models and predictions based on chemical analyses have not been rigorously tested for co-products. Co-products of cereal grains, legumes, and oilseeds are increasingly used as alternative feedstuffs, but they are rich in fiber, protein, or fat. It remains unclear if IVD or proximate analyses can predict energy digestibility of co-products.

Identification of discrepancies between IVD and in vivo digestion of nutrients is essential to improve IVD techniques. However, the small quantity of undigested residue of IVD hampers chemical analyses to determine nutrient concentration and digestibility. Spectroscopy can predict nutrient concentration or digestible nutrient content, but calibrations require reference data, and those are not available in this particular situation (Chapter 3). Thus, the ideal methods need to be applicable for small sample quantities and do not rely on reference data from chemical analyses to build calibrations. The Fourier transform infrared (**FT-IR**) spectrometer with an attenuated total reflection (**ATR**) accessory permits analysis on small quantity of samples (Chapter 3). It remains unknown if nutrient digestibility can be estimated using ATR FT-IR spectroscopy without calibration.

1.1 Hypotheses

The hypotheses of the thesis were:

a) IVD and chemical analyses can predict the ATTD of energy of co-products of cereal grains and oilseeds in pigs;
b) Absorbance of ATR FT-IR spectra in the amide I region, methylene stretching region, and carbonyl in free fatty acids (**FFA**) and ester region reflects concentration of crude protein (**CP**), fatty acids (**FA**), ether extract (**EE**), respectively;
c) Digestibility of CP, FA, and EE can be estimated using ATR FT-IR spectra and the ratio of an indigestible marker in diet and undigested residue without calibration.

1.2 Objectives

The objectives were to examine if IVD and chemical analyses can predict energy digestibility of co-products in pigs, and to develop non-calibration spectroscopic methods to estimate digestibility of CP, FA, and EE for identification of discrepancies between IVD and in vivo digestion of nutrients. Specific objectives were:

1. To examine if IVD and chemical analyses can predict the ATTD of energy of co-products from canola, corn, wheat grain, and soybean in pigs (Chapter 4);
2. To examine relationships between absorbance of ATR FT-IR spectra and concentration of CP of digesta samples of wheat grain (Chapter 5), concentration of FA of ingredients, diets, and digesta samples of co-extruded

flaxseed and field pea, and concentration of EE of ingredients, diets, and fecal samples of co-extruded flaxseed and field pea (Chapter 6);

3. To develop a non-calibration spectroscopic method to estimate apparent ileal digestibility (**AID**) of CP of diet containing wheat grain in pigs (Chapter 5);
4. To develop a non-calibration spectroscopic method to estimate AID of FA and ATTD of EE of diets containing co-extruded flaxseed and field pea in pigs (Chapter 6).

1.3 References

Noblet, J., and J. M. Perez. 1993. Prediction of digestibility of nutrients and energy values of pig diets from chemical analysis. J. Anim. Sci. 71:3389–3398.

Zijlstra, R. T., C. F. M. de Lange, and J. F. Patience. 1999. Nutritional value of wheat for growing pigs: chemical composition and digestible energy content. Can. J. Anim. Sci. 79:187–194.

Chapter 2 In vitro digestion model to simulate nutrient digestion of feedstuffs in monogastric animals: A review

2.1 Abstract

In vitro digestion (IVD) models mimic in vivo digestion and are promising as an alternative to using animals to evaluate feed quality. A detailed understanding of IVD technique to evaluate nutrient digestion of feedstuffs for monogastric animals is required. Therefore, key steps of IVD models were compared with in vivo digestion of nutrients at each section of digestive tract. The lack of fat digestion in the second step and enzymatic digestion of fiber in the third step of IVD models do not match with in vivo digestion. Apart from digestion, fermentation by microbiota in the digestive tract of animals poses a challenge for using IVD models to simulate protein and fat digestion. The IVD models predicted energy digestibility within cereal grains and among feedstuffs, but not for co-products of cereal grains and oilseeds rich in fiber, protein, and/or fat. Characterization of discrepancies between in vitro and in vivo digestion of energy-yielding nutrients are essential to improve IVD technique for accurate evaluation of energy digestibility.

2.2 Introduction

Feed accounts for more than 65% of the total cost of monogastric livestock production (Steiner and Aufy, 2011; Williams et al., 2011); thus, accurate feed quality information is important. However, nutritional value varies

largely even within feedstuffs (Yin et al., 1993; Zijlstra and Beltranena, 2008) due to genetics, agronomics, harvest, storage (Canibe and Eggum, 1997; van Barneveld, 1999), and processing conditions (Hernot et al., 2008). For example, the digestible energy (**DE**) value varied by up to 3.7 MJ/kg DM for wheat grain and 4.3 MJ/kg DM for barley grain in pigs (van Barneveld, 1999; Zijlstra et al., 2011). Such magnitude of variation in DE is economically important to livestock producers. Feed producers need timely feed quality information to formulate production diets close to target nutrient requirements and to properly determine cost of feedstuffs. Thus, rapid and accurate feed quality assessment of digestible nutrient content of feedstuffs is important (Noblet and Henry, 1993). Poor estimation of digestible nutrient content in feedstuffs may reduce predictability of animal performance (Boisen, 2000), increase feed cost, reduce profit margin (de Lange and Birkett, 2005), and may cause environmental issues (Dourmad et al., 1999; Boisen, 2007a).

Among feed quality evaluation methods, physical measurements such as density or 1,000-kernel weight were used traditionally to describe feed quality, but do not predict DE or metabolizable energy (**ME**) values of cereal grains, and are inferior to predictions based on chemical measurements (Fairbairn et al., 1999; Zijlstra et al., 1999). Although equations exist to predict DE or ME values based on proximate analysis (Noblet and Perez, 1993; Goff and Noblet, 2001), time required for acquiring data and analytical error especially for fiber limits accuracy of prediction. Modern technologies, such as near-infrared reflectance spectroscopy (**NIRS**), can predict DE of cereal grains in pigs (van Barneveld et al.,

1999; Zijlstra et al., 2011); however, NIRS must be supported by reference data to develop calibrations. Using in vivo data as reference is expensive and time consuming. The IVD models are promising for feed quality assessment (Boisen and Fernandez, 1997; Moughan, 1999), and may replace predictions based on proximate analyses (Spanghero and Volpelli, 1999; Mould, 2002). The mobile nylon bag technique (**MNBT**) has also been used to evaluate nutrient digestibility (Sauer et al., 1983; Thacker and Qiao, 2001). This technique offers advantages over conventional digestibility methods, such as fast turnover, fewer pigs required, and exclusion of basal diet and indigestible marker (Qiao and Thacker, 2004). However, this technique is affected by wash time and mesh size of nylon bags (Yin et al., 2002) and prediction accuracy was similar to IVD models (Beames et al., 1996). Historical development of IVD models to estimate digestibility of foods and feed grains for pigs has been reviewed (Boisen and Eggum, 1991; Savoie, 1994; Moughan, 1999). Thus, the present review focuses on the identification of weaknesses of IVD models to evaluate nutrient digestibility with emphasis on pigs.

2.3 Overview of in vitro digestion systems

More than 50 years have passed since the first use of pepsin to predict the biological value of egg protein (Sheffner et al., 1956). Many IVD models have been developed, but need to be characterized for their efficacy to describe feeding value for animals and their practical application. A 2-step IVD model is commonly used to simulate nutrient digestion in stomach (Step 1) and the small

intestine (Step 2), plus Step 3 to simulate digestion in the large intestine accounting for total tract digestion. Three categories of IVD system exist (Table 2.1):

1. Use of digestive fluid or microflora collected from living animals for all digestion simulation steps of an IVD model, such as the use of duodenal or fecal extractions for entire digestion simulation (Lowgren et al., 1989);
2. Use of digestive fluid or microflora in part of simulation steps, such as the IVD models using pepsin in Step 1 and intestinal fluid of pigs in Step 2 to predict ileal dry matter (**DM**) and crude protein (**CP**) digestibility (Furuya, 1979); or using fecal inocula in Step 3 for in vitro fermentation trials (Gajda et al., 2005);
3. Use of commercially-available purified enzymes for all simulation steps, as represented by a 3-step IVD procedure (Boisen and Fernandez, 1997) to predict the apparent total tract digestibility (**ATTD**) of energy.

To evaluate the extent of digestion or absorption, four types exist (Table 2.2):

I. Measure digesta directly for liberated H^+ as peptide bonds split, e.g., pH change or concentration change, for instance, pH-drop (Hsu et al., 1977) or pH-stat method (Pedersen and Eggum, 1983) to predict protein digestibility, by regressing in vivo data against uptake of alkali titrant;

II. Separate the undigested from the digested fractions by filtration or centrifugation and measure undigested mass or nutrients;

III. Mimic absorption by dialysis with a cut-off molecular weight (**MW**) and then measure concentration of absorbed nutrients to assess protein or AA digestibility (Gauthier et al., 1982; Savoie and Gauthier, 1986);

IV. Measuring products from digestion, such as gas production during fermentation (Coles et al., 2005). This type of measurement is not discussed in this review.

According to the control of the digestion process, IVD models can be divided into static models that represent most, and dynamic models that represent a few (Moughan, 1999; Smeets-Peeters et al., 1999; Chiang et al., 2008).

Use of Categories 1 (Table 2.3) and 2 (Table 2.4) IVD models has decreased, while use of Category 3 (Table 2.5) models has increased in the last decade. This change reflects that IVD models exist to enable rapid evaluation of nutritional quality of feedstuffs with minimal use of animals. Purified microbial enzyme complexes (e.g., Viscozyme, a mixed multi-enzyme complex containing a wide range of microbial carboanhydrases including arabinase, cellulase, β-glucanase, hemicellulase, xylanase, and pectinase) can be used to mimic digestion of fiber in the hind gut (Boisen and Fernandez, 1997). Similarly, cellulase can also be used to mimic fiber digestion and support accurate prediction of ATTD of energy for barley grain in pigs (van der Meer and Perez, 1992; Huang et al., 2003a). Thus, hind gut digestion can be simulated without living microflora. Benefits of using purified enzymes include avoiding use of animal and greater repeatability among batches of IVD measurements (Noblet and Jaguelin-Peyraud, 2007; Regmi et al., 2008, 2009). Regarding using digestive fluid, concerns exist

about efficiency of digestive enzymes, because diets fed to donor animals may influence enzyme composition and activity (Furuya et al., 1979; Corring, 1980). Fluctuating enzyme activity hampers standardization of IVD models among batches and laboratories.

Dynamic in vitro systems, with sophisticated control of pH, secretion of enzymes and simulated movement of gut were proposed (Minekus et al., 1995, 1999; Smeets-Peeters et al., 1999). However, dynamic in vitro systems are used less for feed quality evaluation and more for functional food and pharmaceutical research (Marteau et al., 1997; Venema et al., 2000, 2003). Ileal organic matter (**OM**) digestibility (65.1%) was severely underestimated by a dynamic in vitro system (24.0%) for fibrous feedstuffs as compared with a static 3-step IVD model (74.0%; Meunier et al., 2008). The reason for the underestimation is not clear. It is unknown whether inclusion of simulation of large intestine digestion into dynamic in vitro systems can improve their accuracy (Minekus et al., 1999). With simple static or sophisticated dynamic in vitro models, simulation of all digestion and absorption processes within the gut is too complex and nearly impossible. However, with defined goals, IVD models can estimate the nutritive value of feedstuffs. Encouraging examples do exist. The IVD models described 81-98% variation of CP digestibility and 82-97% variation of energy digestibility of feedstuffs for monogastric animals (Table 2.6).

Some IVD models have been used for practical routine evaluation. Notably, the feed evaluation system for pigs based on an IVD model became official in Denmark in 2004 (Boisen and Tybirk, 2005). Among IVD models, the

3-step IVD model developed by Boisen and Fernandez (1997) received wide attention (Moughan, 1999). However, IVD models require improvements, because conflicting or less satisfactory data exist. For example, predictions had high accuracy (R^2 = 0.93) for the apparent ileal digestibility (AID) of CP of wheat grain in pigs with a 2-step IVD model, but were low (R^2 = 0.03-0.60) for *Phaseolus* bean, pea, rapeseed meal, and soybean meal (Cone and Vanderpoel, 1993).

Prediction accuracy for CP and AA digestibility of feedstuffs and feed mixtures for pigs was so high (Boisen and Fernandez, 1995) that future studies with surgically-modified pigs to analyze AID of AA in protein sources were questioned (Boisen, 2007b). However, poor to moderate accuracy to predict protein digestibility for soybean meal (R^2 = 0.59), rapeseed meal (R^2 = 0.33; Swiech et al., 2001) and feather meal for poultry (R^2 < 0.16) was also reported (Papadopoulos, 1987). Moreover, validation of the IVD model with 48 feed mixtures had moderate prediction accuracy (R^2 = 0.57) for protein digestibility (Boisen and Fernandez, 1995).

A linear relation between IVD of OM and in vivo ATTD of energy was achieved with a 3-step IVD model, but five samples of meat and bone meal and raw potato starch were overestimated or underestimated, respectively (Boisen and Fernandez, 1997). Using the same IVD model for corn co-products, including corn distillers dried grain with solubles (**DDGS**), the accuracy of using in vitro digestibility of OM to predict in vivo DE value was moderate (R^2 = 0.63). The relation was reduced (R^2 = 0.29) when corn oil was removed from regression

analysis, because corn oil was washed away by filtration with acetone (Anderson, 2009). In a validation of the IVD model on 113 compound feeds and 66 ingredients, full-fat rapeseed was excluded for the regression as an outlier (Noblet and Jaguelin-Peyraud, 2007). The IVD model poorly (R^2 = 0.12) predicted the ATTD of neutral detergent fiber (**NDF**) of DDGS from corn, sorghum, or blended corn and sorghum in growing pigs (Urriola, 2010).

All these poor results indicate that IVD models are far from robust. We need to review whether IVD models properly simulate nutrient digestion in monogastric animals.

2.4 In vitro simulation of gastric digestion

Simulation of oral digestion is omitted from IVD models, because minimal amounts of starch and fat are digested in the mouth due to limited activity of salivary amylase (Hudman et al., 1957) and lingual lipase (Dicklin et al., 2006). Optimal pH for salivary α-amylase is 6.7 and pH is above 5.0 in the cardiac gland region of stomach; thus, gastric starch digestion may continue temporarily and then stop in the gastric fundus with a pH below 3.6 (Yen, 2001). In static IVD models, pH is normally around 2.0 in Step 1; thus, starch digestion is not simulated. Among macronutrients, protein digestion is initiated in the stomach by gastric proteases and HCl. The step simulating gastric digestion is often Step 1 in 3-step IVD models.

2.4.1 Enzyme, pH and digestion time

Gastric proteases produced in the porcine gastric mucosa are pepsins A, B and C and chymosin (Yen, 2001). Pepsins have two pH optima, one at pH 2 and one near 3.3 (Bottger and Holler, 1974). Most IVD models using pepsin have a pH around 2.

Incubation time to simulate gastric digestion varies greatly among 2- or 3-step IVD models and lacks standardization. Among studies, digestion time ranged from 0.5 to 6 h: 0.5 h (Savoie et al., 2005), 1 h (van der Meer and Perez, 1992), 1.5 h (Cone and Vanderpoel, 1993), 2 h (Boisen and Fernandez, 1997) and 6 h (Boisen and Fernandez, 1995; Huang et al., 2003a). Because digestion is a function of enzyme activity and time, increased digestion time will increase protein or AA digestibility. Information about length of simulation of gastric digestion is not conclusive for in vivo digestion. Mean retention time (**MRT**) was 1 h in the stomach (Wilfart et al., 2007) and increasing dietary insoluble fiber did not affect gastric MRT. But, the MRT ranged from 3 h for a maize starch-based diet to 12.8 h for a soy hull diet (van Leeuwen and Jansman, 2007). Enzyme activity and concentration drastically influence digestion of substrates and are difficult to compare, because enzyme sources differ among studies. With excess enzyme concentration, enzyme specificity is likely more important.

2.4.2 Protein digestion

Pigs are normally cannulated at the ileum; thus, gastric digestibility of CP is rarely reported. Protein digestibility estimates at 2 to 4 h of incubation time in a static IVD model were similar to in vivo digestibility when concentration of

pepsin (1,000 units/mL 0.1 M HCl) was close to stomach concentration of pigs (Chiang et al., 2008). Digestibility of CP in the dynamic IVD model increased with time similar to in vivo studies in pigs (Chiang et al., 2008).

2.4.3 Fat digestion

Similar to protein, digestion of fat is initiated in the stomach with lipase secreted from gastric mucosa in the fundic region (Armand et al., 1992). Although lipase activity in gastric tissue is 3% of that of pancreas, it has broad optimal pH ranging from 2.2 to 6.4. About 25 to 50% of dietary lipid in newborn pigs is hydrolyzed in the stomach into diacylglycerols, monoacylglycerols and free fatty acids (**FFA**; Gu and Li, 2003). About 10 to 30% of fat is hydrolyzed in the stomach by lingual lipase with substrate specificity. Medium-chain triglycerides were hydrolyzed at rates 5 to 8-fold greater than long-chain triglycerides (Liao et al., 1984). An IVD model using lipase with simulated gastric conditions released enzymatically up to 20% of medium-chain fatty acids (**MCFA**) into the medium (Dierick et al., 2002). For IVD models with only pepsin included in Step 1 and lacking gastric movement, fat digestion in Step 1 of IVD model remains unknown.

2.5 In vitro simulation of digestion in small intestine

2.5.1 Enzyme, pH and digestion time

The small intestine is the major site of digestion for starch, fat, protein, but not for non-starch polysaccharides (**NSP**). Simulation of this digestion is often Step 2 of the IVD model. In contrast to the low pH in the stomach, the pH is neutral in the small intestine and also in the Step 2 of most IVD models. Enzymes

secreted into small intestine are complex, including pancreatic amylase, trypsin, chymotrypsin and lipase for luminal digestion (Yen, 2001). Apart from these enzymes, brush border enzymes further cleave peptides and dextrin, etc. (Yen, 2001). These enzymes are not included in most 3-step IVD models. Thus, the IVD end-products are not the same as those of in vivo digestion.

Time to simulate the small intestine digestion in Step 2 of IVD models varies considerably, ranging from 1 h (van der Meer and Perez, 1992), 4 h (Boisen and Fernandez, 1997), 12 h (Graham et al., 1989) to 18 h (Huang et al., 2003a). For in vivo digestion, MRT averaged 4 h in the small intestine and decreased with increasing dietary insoluble fiber content (Wilfart et al., 2007). However, the MRT in the small intestine ranged from 5 h for a corn starch-based control diet to 21 h for a diet with high water-holding capacity (van Leeuwen and Jansman, 2007). Optimum IVD time to simulate digestion in the small intestine requires further investigation.

Enzyme activity seems less of a concern, as pancreatic enzymes can digest about 10 times the quantity of feed typically ingested by pigs under normal physiological conditions (Corring, 1980). Moreover, a great surplus of enzyme activity is added in most IVD models (Boisen and Eggum, 1991).

The physical environment of IVD models differs from in vivo digestion. For IVD models, the constant watery digestion condition does not reflect viscosity of the intestinal tract, as increasing viscosity of gastrointestinal tract contents alters physiologic responses in many species (Dikernan et al., 2007).

2.5.2 Protein digestion

Comparing digestibility of CP among various digestion times in IVD models is difficult, as digestibility of CP varies with digestion time. For example, digestion of CP of rapeseed protein increased linearly for 18 h (Gauthier et al., 1982). With trypsin incubation, CP digestibility was greater at 24 h than at 4 h, and increased continually from 4 h to 24 h. The IVD of CP also increased with trypsin concentration increasing from 0.1 to 2 mg/mL (Huang et al., 2000). These examples indicate that selection of digestion time requires further study.

In vitro protein digestion with 4 h in Step 2 is less complete when comparing digestion end products with in vivo digestion (Qiao et al., 2004). For in vivo digestion, soluble but unabsorbed peptides were smaller than 1 kDa, indicating that size of soluble peptides prevents their absorption. For IVD, 88% of soluble peptides were smaller than 1 kDa and 12% between 1 and 5 kDa. Thus, soluble peptides in IVD could be considered digested, because large soluble peptides whose size prevented absorption were not observed for in vivo digestion (Qiao et al., 2004). Based on a dialysis system, precision was lacking for highly water-soluble AA, especially lysine, and digestibility for less water-soluble AA was underestimated, e.g., histidine, isoleucine, leucine and phenylalanine. However, the peptides with larger MW might not be a problem for IVD models using filtration systems with a large pore size.

Substrate specificity also exists for protein digestion. For example, rapeseed protein that is poor in aromatic AA is a poor substrate for pepsin (Gauthier et al., 1982). Generally, animal proteins were digested at a greater rate

than plant proteins (Savoie et al., 2005). For protein sources with peptide fractions with a MW exceeding 10 kDa (basic-neutral, BN > 10), protein was hydrolyzed rapidly during the first 2 h of pancreatin digestion, except for gluten (Savoie et al., 2005). Specificity also exists for AA. Peptides rich in proline and glutamic acid are more resistant to digestion; threonine and proline proportions were relatively high in BN > 10 and in peptide fractions with MW between 10-1 kDa (BN 10-1), while fractions with tyrosine, phenylalanine, lysine, and arginine dominated in the low MW (<1 kDa) fraction (Savoie et al., 2005).

2.5.2.1 Endogenous N

For protein digestion in the small intestine, ileal digestibility is often used. Many studies have correlated AID of CP or AA to IVD of protein or AA. Some may attribute the discrepancy of CP or AA digestibility between in vivo digestion and IVD entirely to the endogenous N loss, but neither is appropriate. The IVD model does not have the same endogenous losses that occur in vivo. In young pigs, the epithelium of small intestine is replaced every 3 to 4 days and that of large intestine every 4 to 8 days (Yen, 2001). However, the IVD model is not void of endogenous protein. Enzymes added are equivalent to endogenous, and surplus enzyme is added in most IVD models (Boisen and Eggum, 1991). For in vivo digestion, 70 to 80% of endogenous N is digested and reabsorbed (Souffrant et al., 1993). For IVD, especially for filtration units with a large pore size, enzyme would be ‘absorbed’; thus, in vitro digestibility should be deemed as true ileal digestibility (**TID**) of protein.

Evaluated using a casein-based diet, basal endogenous loss reached 63 mg total N/g digesta DM at the distal ileum and 73% was proteinaceous (Miner-Williams et al., 2009). Mucin contributed 10% of N lost and was the most abundant endogenous loss. Bacterial N (45%) combined with ammonia and urea N represented 61% of total N lost (Miner-Williams et al., 2009). Gut microflora of pigs synthesize essential AA and microbial AA that can be absorbed (Torrallardona et al., 2003). The largest proportion of endogenous protein is due to microbial activity in the stomach and small intestine of the pig (Miner-Williams et al., 2009). The composition of endogenous protein was relatively constant (Pedersen et al., 2002). Using the ^{15}N-isotope dilution technique, the ingredient-specific endogenous loss induced was characterized (de Lange, 1989). Dietary pectin can induce greater endogenous protein losses at the distal ileum (24 g/kg DM intake) comparing with endogenous protein losses (20, 23, 20 g/kg DM intake, respectively) for diets based on N-free, cellulose, and canola oil. Pectin thus increases microbial activity and thereby microbial contributions in the endogenous loss. Canola meal induced greater endogenous loss (31 g/kg DM intake) than soybean meal, wheat, and barley (26, 27, 28 g, respectively; de Lange, 1989). The mechanical effect of fiber may stimulate mucosa production and increase sloughed-off mucosal cells (Bergner et al., 1975; Farness and Schneeman, 1982). Regarding this loss, digestibility of threonine of IVD may not match in vivo digestion (Pujol and Torrallardona, 2006). Endogenous losses have been reviewed (Boisen and Moughan, 1996; Nyachoti et al., 1997; Stein et al., 2007). Thus, for fibrous and highly fermentable feedstuffs, endogenous losses may be

underestimated with the correction of basal endogenous and the TID of protein or AA might be overestimated. Microbial activity has thus not been considered in IVD models using purified enzymes; and this activity should be considered. In summary, IVD should be compared with the TID or, as a minimum, with the standard ileal digestibility (SID) of CP or AA (Moughan, 1999).

2.5.3 Starch digestion

For in vivo digestion, pancreatic α-amylase is the sole active luminal carbohydrase. Digestion end products include maltose, maltotriose, α-limit dextrin and some glucose (Yen, 2001). The end products of the IVD model using pancreatin would be similar to digesta of in vivo digestion. However, for in vivo digestion, maltose, maltotriose, and α-limit dextrin from luminal starch digestion are further degraded into monosaccharides by brush border enzymes, including sucrase, isomaltase and maltases II and III (Yen, 2001). For IVD, mucosal digestion is lacking, thus, digestion end products might be a mix of monosaccharide, disaccharides and low-MW polymers of carbohydrates. However, the lack of simulation of mucosal digestion in IVD models is likely not a major issue, except in dialysis systems with restricting cut-off MW.

From the literature, IVD digestion of starch in cereal grains does not seem a problem. Starch is a high-molecular carbohydrate composed of linear (amylose) and branched (amylopectin) chains of glucose residues. Raw plant starch, e.g. from cereals, is subject to complete but slow digestion. The 4 h IVD of starch was well correlated ($r = 0.96$) to in vivo ileal digestion of starch in poultry. Also, digestion rate was well correlated to in vivo digestion ($r = 0.87$) among starch of

potato, legume, cereal grains, and rapidly-digestible tapioca (Weurding et al., 2001), indicating that IVD of starch could describe in vivo starch digestion. The in vivo portal glucose appearance data can be predicted effectively (R^2 = 0.95) from IVD data after correction for gastric emptying for in vivo digestion of four heterogeneous starch sources (Kempen et al., 2010). However, other results exist. Rate of disappearance of starch between in vivo digestion and IVD models agreed minimally (Bauer et al., 2003). The classification of starch into rapidly digestible starch (**RDS**) and slowly digestible starch (**SDS**) components was not accomplished for a range of starch sources, in particular for corn starch (Bauer et al., 2003). In addition, starch may occur in a form incapable of enzymatic hydrolysis, referred to as resistant starch (**RS;** Leszczynski, 2004). The amount of RS that cannot be digested in the small intestine can be predicted from IVD measurements, but RS is fermentable (Silvester et al., 1995). The fractions of RDS, SDS and RS may have less biological relevance in pigs and thus have little value to predict in vivo responses among starch sources (Kempen et al., 2010). Enzyme access issues occasionally occur for starch digestion, because digestion for one nutrient may affect digestion for others. For example, pepsin and bile may enhance IVD of slowly-digestible starch, as starch encapsulated in the endosperm protein matrix was released, making starch accessible to amylolytic enzymes (Aura et al., 1999).

2.5.4 Fat digestion

For most 3-step IVD models, simulation of fat digestion is probably the weakest component. Few investigations included a fat digestion simulation step,

or fat was inadequately washed out with acetone at the end of Step 3 of IVD model. Fat digestion may have little effect on protein digestion. In 23 food samples, fat extraction prior to IVD did not increase protein digestibility (Hsu et al., 1977). Thus, removal of fat might not be needed for IVD models to evaluate protein digestibility. The enzymatic digestion of fat is not critical in IVD models to predict in vivo digestible CP content. Moreover, enzymatic IVD of fat is laborious (Babinszky et al., 1990). However, fat may still affect digestion of other nutrients. The addition 0.3 g fat to 1 g of a cereal/legume sample during gelatinization decreased in vitro digestibility of carbohydrates (Madhuri et al., 1996). The affected digestion of one nutrient may hinder digestion of other nutrients. The matrix of fat with other nutrients required further research.

For simulation of fat digestion, efficacy of fat digestion by including pancreatic lipase and bile salts was not determined. Using IVD model, long-chain triglycerides emulsified with phospholipid were not available for hydrolysis by pancreatic lipase even with bile salts and colipase present (Borgstrom, 1980). The inhibition could be overcome by pancreatic phospholipase A2. In contrast, non-oxidized fat was rapidly hydrolyzed in an IVD model using pancreatic lipase, but fat digestion was severely inhibited by oxidized oil (Verleyen et al., 2006).

For in vivo digestion, the main digestion site of fat is the small intestine (Embleton and Pouton, 1997). Complete hydrolysis of fat may take 12 h (Borgstrom, 1952). Optimal pH for digestion of fat is 8.1-9.0 (Hamosh and Scow, 1971; Gargouri et al., 1990). In contrast to lingual lipase cleaving FA at the sn-3 ester linkage in preference to the sn-1 position (Staggers et al., 1981), sn-2

monoglycerides and FA are the final products of pancreatic lipase hydrolysis (Paltauf et al., 1974). The hydrolysis is fully functional only in the presence of oil-water emulsions. Pure bile salts are extremely poor emulsifiers of fat. Its combination with lipolytic products present in intestine may participate in triglyceride emulsification (Linthorst et al., 1977). Bile salts inhibit lingual and pancreatic lipase to various degrees (Liao et al., 1984). With bile salts and phospholipids absent, lipase can bind to the triglyceride-water interface by hydrophobic interactions. Pancreatic lipase, colipase, phospholipase A_2, calcium and bile salts act synergistically in the small intestine (Carey et al., 1983). Size of emulsion particles was less than 0.6 μm (Linthorst et al., 1977). Products of partial digestion of lipids are negatively charged polymolecular aggregates called micelles with a 5 nm diameter, much smaller than un-hydrolyzed precursor particles. This size will allow the micelles access to intramicrovillus spaces (50~100 nm) of intestinal membranes (Groff and Gropper, 1999). In the IVD models with large pore size (25 to 90 μm) filtration system, the emulsified droplet can pass through filtration device theoretically without digestion.

Purified enzymes may replace gastric or pancreatic fluid to simulate fat digestion. The in vitro specific activity of human gastric and pancreatic lipase in the gastric or pancreatic juice and their purified form with co-lipase were in the same range with in vivo values, only lower for solid meals comparing with in vivo digestion, but still enough for fat digestion (Carriere et al., 2000).

An emulsifier is needed to digest fat in a sophisticated IVD model to simulate fat digestion in mouth, stomach and small intestine with various

emulsifiers. The initial emulsifier used to stabilize oil-in-water emulsions had a limited effect on microstructure changes that occurred during digestion of lipid droplets, though appreciable differences occurred among behaviour of emulsions within the IVD model. Simulating the complex physicochemical and physiological processes in the gastrointestinal tract remains difficult (Hur et al., 2009).

The IVD of fat was emphasized, because fat may limit digestion of other nutrients. Fat reduced IVD of DM with olive cake, added fat reduced OM digestibility of oat hay, and extraction of fat with acetone increased OM digestibility (Zaidi et al., 2008). If fat digestion limits digestion of other nutrients, removal of fat at the end of Step 3 of IVD models will not alleviate reduced nutrient digestion in Steps 2 or 3. The effect might be pronounced for high fat co-products, such as corn DDGS. Prediction accuracy of IVD model for corn co-products is poor (Urriola, 2010). As fat was mostly digested before the distal ileum (Shi and Noblet, 1994), using acetone to remove fat is an alternative to replace enzymatic digestion of fat in IVD model.

2.5.5 Fiber fermentation

Fiber digestion is not simulated in Step 2 of most IVD models. Although certain NSP ferment in small intestine, the large intestine is the major site for NSP fermentation.

2.6 In vitro simulation of digestion in the large intestine

2.6.1 Hydrolysis vs. fermentation

Without Step 3 simulating digestion in the large intestine, evaluation of energy digestion is not complete, because hindgut fermentation contributes 7 to 40% to energy maintenance requirement of pigs, depending on body weight of pigs and dietary fiber content (Breves et al., 1993; Shi and Noblet, 1994). Digestion in the large intestine is simulated using living microflora or purified microbial enzymes. Generally, purified microbial enzyme is used to investigate digestibility of energy or OM, whereas living microflora are used to determine fermentability using gas or short-chain fatty acid (SCFA) production, or disappearance of NSP or OM. Using purified enzymes to digest fiber is a simple approach to replace living microflora. The advantages of using purified enzymes include standardized enzyme activity, without using living animals and higher repeatability with great potential to evaluate energy digestibility. However, we need to scrutinize the potential drawbacks of using purified enzymes.

For in vivo digestion, microflora in the large intestine contains highly active cellulolytic and hemicellulolytic bacterial species, including *Fibrobacter succinogenes (intestinalis), Ruminococcus albus, Ruminococcus flavefaciens, Butyrivibrio spp., Prevotella ruminicola*, and a cellulolytic bacterium, *Clostridium herbivorans* (Varel and Yen, 1997). For IVD models, two commonly used purified enzymes are Viscozyme (Boisen and Fernandez, 1997) and cellulase (Huang et al., 2003b). Viscozyme is a multi-enzyme complex containing carbohydrases, including cellulase, hemicellulase, arabinase, xylanase, P-

glucanase and pectinase, produced from a selected strain of *Aspergillus* (Boisen and Eggum, 1991). Cellulase is obtained from specific bacterial species such as *Aspergillus* sp. or *Trichoderma viridae* etc. (Regmi et al., 2008). Bacterial species involved to produce purified enzyme is limited. For in vivo digestion, oligosaccharides are rapidly fermented by intestinal bacteria such as *Bifidobacteria* (Smiricky-Tjardes et al., 2003; Hernot et al., 2009). The *B. adolescentis* utilized a range of oligosaccharides with a wide range of glycosidases. Enzymes purified from *B. adolescentis* can degrade arabinoxylan (Laere, 2000). Whether purified enzyme from a narrow band of bacterial species will degrade various substrates, including types of NSP, undigested starch and protein is not clear. In an IVD model using purified cellulase to simulate digestion of 89 diets in the large intestine, the natural logarithm of crude fiber as an additional variable together with in vitro OM digestibility in the regression model increased the prediction accuracy (R^2 = 0.90) of OM digestibility, indicating that the IVD model did not simulate fiber digestion in pigs (van der Meer and Perez, 1992). A 3-step IVD model severely underestimated OM digestibility of raw potato starch in pigs (Boisen and Fernandez, 1997). Raw potato starch contains more RS, therefore, its underestimation is indicative of short digestion time of Step 2 or inability of purified Viscozyme in Step 3 to hydrolyze raw potato starch. For in vivo digestion, starch and mixed-linked β-glucans can be degraded rapidly and pectic substances are also easily metabolized by human fecal flora (Lebet et al., 1998). However, degradation of NSP varies for different types of fiber. Uronic acid and arabinose were the most extensively fermented sugars, whereas xylose

and glucose were the least fermented by human fecal microflora (Guillon et al., 1995). In contrast to arabinose, uronic acids and galactose are fermented mostly in the proximal large intestine and xylose and glucose are fermented more distally in the colon of pigs to a lower extent at a slower rate (Canibe et al., 1997). Barley fiber concentrate was poorly fermented using human fecal inocula and its in vitro fermentability did not predict NSP degradability in humans (Daniel et al., 1997), Fiber of corn co-products from ethanol production is mostly insoluble, with cellulose being predominant followed by xylose, and is poorly fermented by dog microbiota (Guevara et al., 2008). The residue left after hydrolytic digestion of corn was also poorly fermented using canine fecal inoculum (Gajda et al., 2005). Type and extent of links between polymers and lignin rather than amount of lignin are important to determine degradability of carbohydrates in pigs (Glits et al., 2000).

In vitro fermentation has been validated with in vivo digestion. For example, net disappearance of NSP during in vitro fermentation is highly correlated ($r = 0.96$) with in vivo digestion of NSP by pigs (Anguita et al., 2006). Disappearance of OM ($r = 0.77$), NSP ($r = 0.89$), arabinose ($r = 0.65$), xylose ($r = 0.81$) and glucose ($r = 0.96$) in the large intestine matched in vitro data of NSP digestion in pigs (Christensen et al., 1999). However, hydrolysis using purified fiber-degrading enzyme to simulate digestion in the large intestine was not validated with in vivo digestion.

As digestion of one nutrient may influence digestion of other nutrients, multi-enzyme methods may be most reliable (Boisen and Eggum, 1991). Thus,

more attention should be paid to specificity of microbial enzyme used. However, use of purified enzymes was rarely compared with in vivo digestion.

For IVD model using purified enzymes, hydrolysis but not fermentation occurs (Cores et al., 2005). Two methods yielded different digestion end-products. For fermentation using microflora, the end products are SCFA and gases (Jørgensen et al., 1997). For purified enzymes, the end digestion products are simple sugars or low MW polymers. Thus, using microflora for fermentation is closer to in vivo digestion. Nevertheless, using purified enzymes is promising (Boisen and Fernandez, 1997; Huang et al., 2003a; Noblet and Jaguelin-Peyraud, 2007; Regmi et al., 2008; Regmi et al., 2009) but should be validated with in vivo digestion.

2.6.2 Repeatability

Using living microflora is not free from problems. Dietary fiber level may affect cecal cellulolytic fungal counts, and specific activity of the cellulase enzyme complex and cellulolytic fungi in the pig caecum (Rodriguez et al., 2000). The rate of degradation of fiber using an IVD model can be affected by donor animal (Dung and Udén, 2002). The antibiotic Nebacitin can reduce microbial activity and may reduce energy digestibility of a barley diet in rats (Eggum et al., 1984). The degradation of carbohydrates in poultry can be affected by antibiotics (Marounek et al., 1999). These factors may compromise repeatability among measurements. For instance, amounts of SCFA produced from feces varied considerably among pigs fed the same diet, and feces from the same pig adapted to different diets (Christensen et al., 1999). Colonic inoculum sources influenced

profiles of SCFA. Extent of substrate fermentation varied among inoculum donors, indicating that colonic microbial activities differ among individuals (Bourquin et al., 1992). The fermentation method is qualified for ranking digestibility, but differences occurred with respect to absolute values (Barry et al., 1995). Adaptation of donors to experimental diets was not an influential factor, and inter-laboratory differences were reduced by adding less substrate during incubations or using less-diluted inocula (Barry et al., 1995).

In vitro fermentation can use fecal, cecal, or rectal inocula to simulate digestion in the large intestine. Rectal contents could replace cecum-colon contents as inocula sources to measure NDF degradation without impact on estimations of NDF degradation kinetics (Dung and Uden, 2002). Equine feces could be suitable as microbial inoculum for in vitro gas production studies (Lowman et al., 1999). Pig fecal inoculum might be used to simulate digestion of fiber in broiler diets (Marrero et al., 1998). However, using cecal microflora as inoculum provided a more accurate index of fermentation during transit through the large intestine (Monsma and Marlett, 1996).

2.6.3 Digestion time

Digestion time of Step 3 to simulate digestion in the large intestine varies. For IVD models using purified enzymes, Step 3 usually lasts 18 h (Boisen and Fernandez, 1997) or 24 h (Huang et al., 2003a), but 2 h also exists (van der Meer and Perez, 1992). For fermentation with living microflora, in vitro fermentation time also varies. A 24-h in vitro incubation was sufficient to mimic NSP degradation in humans (Wisker et al., 1998) while 36-h incubation had the best

relation between the IVD and in vivo digestion for NDF (Dung et al., 2002). Longer incubation time using pig fecal inocula exists, such as 48 h (Graham et al., 1989; Anguita et al., 2006) and 72 h (Christensen et al., 1999) and both had good results, although the best time to reflect in vivo digestion is not clear. The 48-72 h incubation simulated digestion in the large intestine of pigs (Lowgren et al., 1989); and 36-48 h incubation was recommended to estimate fermentation kinetics of non-lignified samples (Dung and Udén, 2002).

For in vivo digestion, MRT averaged 38 h in the large intestine of pigs (Wilfart et al., 2007). Increase in either soluble or insoluble dietary fiber content decreased MRT of both solid and liquid phases in the large intestine (43 to 29 h). Similarly, total tract MRT for banana sheaths solid diet in pigs were 22 h and ranged from 33-39 h for five other tropical fiber source diets (Dung et al., 2002). However, the MRT in the large intestine was 45 h for a high water holding capacity diet and 73 h for a maize starch-based control diet in pigs (van Leeuwen and Jansman, 2007). The 3-step IVD model for pigs used 18 h in Step 3 to simulate fiber digestion in the large intestine, seems not enough for certain fibrous feedstuffs. However, the proper digestion time needs further investigation.

2.6.4 Fat modification

Fat is almost completely digested by the distal ileum of pigs (Shi and Noblet, 1994). However, digesta stearic acid increased by the distal ileum with a greater increase in the large intestine. These trends did not occur in germ-free pigs (Carlson and Bayley, 1968). This phenomenon might be caused by bio-hydrogenation of unsaturated FA in the large intestine (Duran-Montgé et al.,

2007). The antibiotic Nebacitin considerably reduced hydrogenation of unsaturated FA, especially linoleic acid (Eggum et al., 1982). Intestinal bacteria can metabolize undigested unsaturated FA, such as linoleic acid, into stearic acid or conjugated linoleic acid (**CLA;** Devillard et al., 2009) in a process similar to rumen hydrogenation. Thus AID might be greater than ATTD of FA (de Souza et al., 1995), notably of palmitic and stearic acids (Hamilton, 1968; Hamilton and McDonald, 1969; Fakler, 1992; Mountzouris et al., 1999). However, bio-hydrogenation is not that simple, because hydrogenation only changes double bonds to single bonds by adding hydrogen to unsaturated FA, which means shifting digestibility between saturated and unsaturated FA. For IVD models using purified enzymes, hydrogenation did not occur during IVD. Because less microbial activity exists in the small intestine than in the large intestine and absorption of long-chained lipids in the colon does not occur (Carey et al., 1983), IVD of fat should be compared with AID of fat and FA.

The property of fecal fat differs from fat in diets. In humans, fat content was high in feces and soap form could account for more than 60% of total fat (Tidwell and Holt, 1936). Most Ca soaps are absorbed, particularly Ca oleate (91%), palmitate (65%), and stearate (45%; Boyd et al., 1932). Absorption of Ca was inversely correlated with chain length and saturation of FA (Gacs and Barltrop, 1977).

For in vitro fermentation with living microflora, hydrogenation was simulated somewhat, but the formation of oil soaps was not. Polyunsaturated fatty acids (**PUFA**) were extensively bio-hydrogenated in an in vitro fermentation

model. Bio-hydrogenation of PUFA is more complete for C18:0 in full-fat soybean than linseed, reflecting PUFA composition (Lee et al., 2003). Factors affecting fat digestion cannot be examined by measuring apparent or corrected FA digestibility (Carlson and Bayley, 1972); thus, whether IVD models using purified enzyme instead of living microflora properly simulate fat saturation in the hind gut is unknown. Currently, an effective correction does not exist, especially to evaluate fat or energy digestibility, as fecal energy excretion increased in parallel with total fecal fat excretion in the form of Ca soap (Bendsen et al., 2008).

2.7 Separation of digesta and measurement of in vitro digestibility

Next to simulation of digestion, measurement of digestibility is a critical part of an IVD model that may require digesta separation. Digestibility can be predicted without separation of digested from undigested digesta. For instance, pH change can be measured during protein digestion due to formation of carboxyl groups after liberation of AA released following protein hydrolysis. The pH change of initial digestion with proteolytic enzymes after 10 min was a good indicator ($r = 0.90$) of CP digestibility (Hsu et al., 1977; Pedersen and Eggum, 1981). Interestingly, correlations between IVD and in vivo CP digestibility for pH at 10 min ($r = 0.75$) was stronger than for pH at 20 min ($r = 0.52$; Moughan et al., 1989). Alternatively, pH can be kept constant by neutralizing digesta with alkali. Prediction accuracy of CP digestibility using pH-stat was greater than pH-drop method (Pedersen and Eggum, 1983). However, released AA is not the only cause for pH changes. Free fatty acids can change pH, and indicate fat digestion using

the pH-stat method (Carriere et al., 2000), which may confound prediction of protein digestibility.

Another method without separation of undigested or digested fractions from digesta is measuring gas production. This method is limited to in vitro fermentation using living microflora. Although the gas production model was primarily developed to evaluate ruminant feedstuffs, it is also applied to hindgut fermentation of monogastric animals (Krishnamoorthy et al., 2005). Automated gas production apparatuses using electronic pressure transducers with electric valves to release overpressure during incubation is helpful to study fermentation kinetics (Cone et al., 1996). The in vitro gas production model can study microbial fermentation in pig cecum, but composition of ileal content as affected by feed composition and self-fermentation of cecal contents must be considered (Fondevila et al., 2002). Methane production to indicate extent of fermentation might be misleading (Zhu et al., 1988), because methane production in pigs does not reliably predict fermentation rate in the digestive tract (Shi and Noblet, 1994).

Minimal separation is often needed to measure digested or undigested fractions. Using centrifugation, supernatant or residues can be analyzed. For example, SCFA concentration is used to indicate fermentation extent. Total SCFA production was highly correlated with OM digestibility (Bourquin et al., 1996), energy absorption (McBurney and Sauer, 1993) and disappearance of NSP, thus allows rapid prediction of energy values of dietary fiber (Barry et al., 1995). Fourier transform infrared (**FT-IR**) transmission spectroscopy can measure nutrients in supernatant and predict starch digestion extent (Uden, 2009).

Measurements of pH, gas production and SCFA are indirect, and require regression analyses to predict digestibility or without regression analyses to rank feedstuffs. Concentrations of nutrients can be measured in residues, e.g., protein, starch, fat, and fiber. But, crude fiber (**CF**), NDF and acid detergent fiber (**ADF**) did not accurately describe fiber digestion. Fiber degradation in the hindgut could be underestimated by 100% compared with using NSP values (Vervaeke et al., 1991).

A common method to separate the undigested from the digested fractions is filtration, either with filter paper (Regmi et al., 2008) or with glass fiber crucibles (Boisen and Fernandez, 1997). Media for filtration includes water (Regmi et al., 2008), or sequential use of water, ethanol and acetone (Boisen and Fernandez, 1997). Filtration using acetone may remove fat from undigested residues depending on duration. The proper filtration method for IVD model requires further investigation.

A key point for filtration in IVD model is selection of correct pore size. The selection of pore size was discussed for the MNBT, but is also applicable to IVD models. The upper pore size limit is mainly set by sample particle size and risk of losing undegraded feed particles. A pore size of 20 µm permits bacterial exchange (Lindberg et al., 1984). In a MNBT study with pigs, increasing bag pore size from 10 to 36 µm did not influence DM disappearance of barley or whole-crop pea (Graham et al., 1985). Using bags with 5-µm pores reduced OM digestibility by 3% and increased protein digestibility by 17% compared with in vivo values (Petry & Handlos, 1978). In contrast, protein degradability

determined with bags of 50 μm pore size was similar to traditional cannulation (Sauer et al., 1983). However, larger pores may lose undigested feed particles, as evidenced by washing bags with pore size of 48 μm, which greatly overestimated nutrient digestibility obtained with MNBT (Qiao and Thacker, 2001).

For 3-step IVD models, the pore size was 20~25 μm for filter paper (Regmi et al., 2008) and 40~90 μm for glass fiber crucible (Boisen and Fernandez, 1997). In terms of digestion end products, the pore size, especially for 40~90 μm, seems too big, with higher risks of losing undigested fine feed particles and may overestimate digestibility (Boisen and Fernandez, 1997).

The ultimate separation method is dialysis that rigorously tests digestion and absorption. However, this method is not simple or rapid. With a cut-off MW of 12,000 Da, digestibility of CP and AA for four feedstuffs used for growing pigs was accurately predicted (R^2 = 0.92-0.98; Huang et al., 2000). Similar to pore size, MW cut-off size varies. A MW cut-off of 3000 Da to determine ileal endogenous N and AA was recommended (Hodgkinson and Moughan, 2003). The MW of digestion products ranged from 500 to 10 000 Da, with a cut-off of 6 to 8 residues for proteins (around 1000 Da; Savoie, 1994). For in vivo digestion, soluble but unabsorbed peptides were smaller than 1000 Da; but for IVD, only 88% was smaller than 1000 Da (Qiao et al., 2004). Different selection of MW cut-off may under- or over-estimate digestibility. Dialysis methods were not commonly used for digestibility analyses, possibly for its greater cost, more sophisticated instrumentation and more time for separation (24 h; Savoie and Gauthier, 1986).

2.8 Evaluation of energy digestibility

2.8.1 Two- or three-step in vitro model

Energy is not a nutrient, but yields from nutrients, e.g., fat, starch, protein and fiber. Energy represents the greatest single factor of feed cost (de Lange and Birkett, 2005). Thus, evaluation of energy digestibility is important. Some may evaluate IVD of DM (Lowgren et al., 1992) or OM (Boisen and Fernandez, 1997) to predict energy digestibility. The in vitro DM digestibility of barley was strongly correlated to in vitro energy digestibility in pigs (Regmi et al., 2008). Simulation of energy digestion involves digestion in the entire digestive tract. The 3-step IVD model is superior to the 1- or 2-step model, as validated using an IVD of energy for hull-less barley (Beames et al., 1996). The one step digestion system with two enzymes only correlated moderately to energy digestibility for corn in swine and poorly for poultry (Kim, 2001). The OM digestibility of 39 mixed pig feeds was predicted within 2% accuracy using a multi-step IVD model, but not the HCl-pepsin/cellulase method (Kirchgessner et al., 1992). Overall, a 3-step IVD model worked well to predict energy digestibility for cereal grains, as tested in wheat, barley and hull-less barley (Beames et al., 1996; Huang et al., 2003a; Regmi et al., 2008; Regmi et al., 2009). However, a 3-step IVD model worked well for mash feed, but not for pelleted feed (Noblet and Jaguelin-Peyraud, 2007).

2.8.2 Test on diets or ingredients

Single ingredients and mixed diets have been used for IVD trials. As starch in cereal grains is easily digested, tests on compound diets might be less rigorous than on ingredients and may hide underlining drawbacks of IVD models.

The IVD models worked well among ingredients, but few have been tested within ingredients. The purpose of energy digestibility evaluation is not to identify feeds, but to detect small differences in energy digestibility within ingredients (Moughan, 1999), thus, IVD models should be tested rigorously within ingredients.

2.8.3 Special concerns for co-products of grains and oilseeds

Co-products of grains and oilseeds are characterized by high protein, high fiber, and/or high fat, and are increasingly used as animal feed. Existing IVD models are not accurate to evaluate energy digestibility of co-products. Prediction accuracy for co-products was poor or co-products were excluded as outliers. For example, rapeseed meal and lupin meal were excluded from statistical analysis as outliers (Graham and Lowgren, 1991; Noblet and Jaguelin-Peyraud, 2007). Likewise, prediction accuracy for energy digestibility was poor for corn DDGS (R^2 = 0.29; Anderson, 2009).

The IVD model could not predict energy digestibility of DDGS, whereas it accurately evaluated their parent grains. Ethanol production removes most starch while the remaining is mostly fiber, protein, fat and RS. This combination may pose a serious challenge for IVD models. Although bioethanol processing may change the structure of nutrients (Yu et al., 2010, 2011), pigs have the capacity to utilize these feedstuffs (Stein and Shurson, 2009; Urriola, 2010; Kandel, 2011). Fiber digestion seems a major complication of IVD models for co-products. An IVD model explained only 12% variation of in vivo ATTD of NDF of corn DDGS, sorghum DDGS and a blend of corn and sorghum DDGS in growing pigs (Urriola, 2010). As digestion of one nutrient may affect digestion of other

nutrients, the lack of fat digestion simulation in IVD models might affect fiber digestion. The issue of enzyme lacking access may exist. Fat as a coating substance may reduce total gas production and speed of fermentation for cereal grains (Mohammadian-Tabrizi et al., 2011). In vitro degradable N, total gas and methane production declined with increasing fat content (Lovedeep et al., 1999). The enzyme access issue did not occur with oil supplementation, which did not affect basal parameters (pH, total SCFA production, digestibility of DM and fiber) of rumen fermentation (Jalc et al., 2006). Conversely, for nutrients entrapped in the fiber matrix, fiber prevents enzymes access to digest other nutrients. Obviously, existing IVD models are not suitable for the evaluation of energy digestibility for co-products.

2.9 Other considerations for the simulation of digestion

2.9.1 Age and physiological states of animal

Existing IVD models are static. Enzyme and incubation time remain unchanged once procedures are developed and validated. Adult pigs have greater capacity to digest fiber (Etienne et al., 1997; Noblet, 2000), especially in feedstuffs with a higher degree of lignification (Noblet and Bach Knudsen, 1997). A static IVD model will not work for both growing and adult pigs as demonstrated with 113 compound feeds and 66 ingredients (Noblet and Jaguelin-Peyraud, 2007). A change of Step 3 digestion time might be needed, because the greater ability of heavy pigs or adult sows than lighter growing pigs to digest fiber may be not due to an increased intrinsic ability of microbial flora to degrade fiber

(Goff et al., 2003). Even for pigs with similar age, MRT also differs among fiber types or amount of fiber included.

2.9.2 Animal response to diets, group feedstuffs

Pigs can respond well to feeds, regarding enzyme secretion, activity and digestion time etc. There is adaptive mechanism when pigs encounter diet change. For instance, pancreatic amylase of pig is very sensitive to any change in starch intake. Specific amylase activity in rat pancreatic tissue can increase 6-fold (Corring, 1980). The specific lipase activity in pig pancreatic juice is 7 times higher when the daily amount of dietary triglyceride intake increases from 30 to 220 g (Corring, 1980). Are these responses of the pig to diet change futile? Should IVD models also respond to different feedstuffs? Is the excess use of enzyme in the static IVD models able to explain the nutritive values of all kinds of feedstuffs? It might be a safe approach to develop IVD models for specific feedstuff or group of feedstuffs with similar properties. For example, a better in vitro prediction of protein digestibility was obtained when the specific protein category regression equation was used, because the digestion of animal proteins was different from the digestion of plant proteins (Marshall et al., 1979).

2.9.3 Is in vitro digestion more susceptible to anti-nutritional factors?

Pigs respond to nutrient content in diet, but also to anti-nutritional factors (**ANF**). Many feedstuffs for monogastric animals, such as barley, rye, wheat, triticale, maize, rice, sorghum, oats, contain ANF (Boisen, 1983) that may interfere with digestion and utilization of dietary nutrients (Hedemann et al., 1999; de Lange et al., 2000). The IVD model can detect effects of trypsin inhibitor and

heat treatment on protein digestibility of various protein sources (Hsu et al., 1977). It is unclear if IVD models are more susceptible to anti-nutritional factors than animals. A 1% increase in tannic acid content added to barley diet decreased in vitro digestibility of protein by 3-4 %, whereas 1% increase in tannic acid content added to soybean protein diet decreased in vivo digestibility of protein by 6% (Pedersen and Eggum, 1981). Although not a side-by-side comparison, the IVD model and in vivo digestion suffered from ANF. Unlike the response in animal, such as increased pancreas weight and trypsin activity (Pedersen and Boisen, 1982), IVD model would remain static to ANF in terms of the amount and activity of enzymes.

2.9.4 Particle size

To compare with in vivo digestibility, the particle size used for IVD model should be scrutinized. For in vivo digestion, particle size is reduced through mastication (pigs) or gizzard action (poultry); while it remains static for IVD model. Beads may be used in an IVD model, but it remains unknown if this could achieve equivalent particle size reduction to that of animals. As we know, smaller particle size will result in higher digestibility values for both in vivo digestion and IVD. Reducing particle size from 900 to 600 μm increased the ATTD of N and energy by 3%, and increased the AID of N by 9% and energy by 11% (Oryschak and Zijlstra, 2002). Increase of particle size from 1 mm to 3 mm resulted in a decrease of OM digestibility by 2.3 for barley and 3.8 for peas in %-units (Boisen and Fernandez, 1997). The rate for starch digestion decreases with grain particle size, and starch digestion in IVD models might be controlled by diffusion of

enzyme through grain fragment (Al-Rabadi et al., 2009). In IVD models, energy digestibility and average geometric particle size were negatively and linearly correlated for maize, wheat bran, dehulled soybean meal, cotton seed meal and rapeseed meal (Wang et al., 2003). Thus, to achieve similar digestibility, the particle size of feed for IVD should be same as or smaller than that for in vivo digestion.

2.9.5 Inhibition by digestion end products

Inhibition by digestion end products are not considered in most IVD models. The inhibition might be minor, for the enzyme used in IVD models is often in excess. Inhibition of enzyme can be reversible or irreversible. For reversible inhibition, it can be competitive or non-competitive. A competitive inhibitor has a shape and structure similar to substrate, so it competes with substrate for binding to the active site of enzyme (Smith, 2010). The inhibition of digestion end products seems mostly competitive, if there are any. However, it is a normal digestion process that substrate, e.g. intermediate digestion product, binds to enzyme. The inhibition effect of IVD end product is still controversial. The increased frequency of buffer replacement was reported as improving dialysis speed, and was claimed as alleviation of possible inhibition of enzyme action by digestion products (Gauthier et al., 1982). However, it is questionable as to whether digestion or absorption is increased. The inhibition effect of digestion end products appears to be a non-issue in a closed-system with excess enzyme concentration. In vitro protein digestibility of meat and bone meal was 87.5%, much higher than the in vivo protein digestibility of 55.5% (Boisen and Fernandez,

1995); thus, this sample was excluded from regression as an outlier. However, using living microflora, there is a possibility of inhibition of microbial growth by the accumulation of fermentation end products (Abe and Kumeno, 1973).

2.10 Methodologies to improve in vitro digestion models

Due to the nature of IVD models, amounts of undigested residue are often limited; thus, posing a challenge for using proximate analyses to determine nutrient digestibility. For instance, to evaluate IVD of energy, we need to examine if macronutrients were digested similarly to in vivo digestion, rather than simply oxidize undigested residues for calorimetry, leaving macronutrient digestibility unknown. Spectroscopy is a non-destructive method to obtain qualitative and quantitative chemical information, and may assist to identify limits of IVD models in simulating in vivo digestion (Chapter 2). Mathematical modelling might assist design of IVD models to define optimum digestion parameters, by describing kinetics of digestion and absorption in growing pigs (Strathe et al., 2008).

2.11 Conclusions

In vitro simulation of in vivo digestion is a challenge, especially for microbial modification of fat, microbial contribution of endogenous protein losses and simulation of fat digestion. As a result, existing IVD models do not evaluate co-products of cereal grains and oilseeds correctly. Specificity of enzyme is more important than amount of enzyme. Specifically, digestibility increases with

increasing enzyme concentration, but will plateau and then not respond to excess enzyme (Huang et al., 2000). Synergistic effects should be studied, because one undigested nutrient may prevent digestion of other nutrients. The instrumentation, such as proper pore size of filtration units, should be studied to avoid overestimation of digestibility. Finally, in vivo digestibility should be the reference for IVD models. New technologies, such as spectroscopy may assist to identify issues in IVD models for their further improvements. Refined IVD models can then evaluate feed quality, but also provide reference data for more rapid techniques, such as NIRS, which might be more desirable for commercial application to support decision making.

2.12 References

Abe, M., Kumeno, F., 1973. In vitro simulation of rumen fermentation: apparatus and effects of dilution rate and continuous dialysis on fermentation and protozoal population. J. Anim. Sci. 36, 941–948.

Al-Rabadi, G.J.S., Gilbert, R.G., Gidley, M.J., 2009. Effect of particle size on kinetics of starch digestion in milled barley and sorghum grains by porcine alpha-amylase. J. Cereal. Sci. 50, 198–204.

Anderson, P., 2009. Energy determination of corn co-products in finishing pigs and the use of an in vitro organic matter digestibility assay to predict in vivo energy. MSc Diss., Iowa State Univ., Ames, IA, USA.

Anderson, P.V., Kerr, B.J., Weber, T.E., Ziemer, C.J., Shurson, G.C., 2012. Determination and prediction of digestible and metabolizable energy from

chemical analysis of corn coproducts fed to finishing pigs. J. Anim. Sci. 90, 1242–1254.

Anguita, M., Canibe, N., Perez, J.F., Jensen, B.B., 2006. Influence of the amount of dietary fiber on the available energy from hindgut fermentation in growing pigs: use of cannulated pigs and in vitro fermentation. J. Anim. Sci. 84, 2766–2778.

Armand, M., Borel, P., Rolland, P.H., Senft, M., Andr é, M., Lafont, H., Lairon, D., 1992. Adaptation of gastric lipase in mini-pigs fed a high-fat diet. Nutr. Res. 12, 489–499.

Aura, A.M., Harkonen, H., Fabritius, M., Poutanen, K., 1999. Development of an in vitro enzymatic digestion method for removal of starch and protein and assessment of its performance using rye and wheat breads. J. Cereal. Sci. 29, 139–152.

Babinszky, L., van der Meer, J.M., Boer, H., den Hartog, L.A., 1990. An in-vitro method for prediction of the digestible crude protein content in pig feeds. J. Sci. Food Agric. 50, 173–178.

Barry, J.L., Hoebler, C., Macfarlane, G.T., Macfarlane, S., Mathers, J.C., Reed, K.A., Mortensen, P.B., Nordgaard, I., Rowland, I.R., Rumney, C.J., 1995. Estimation of the fermentability of dietary fiber in-vitro - a European interlaboratory study. Br. J. Nutr. 74, 303–322.

Bauer, L.L., Murphy, M.R., Wolf, B.W., Fahey, G.C., Jr., 2003. Estimates of starch digestion in the rat small intestine differ from those obtained using in vitro time-sensitive starch fractionation assays. J. Nutr. 133, 2256–2261.

Beames, R.M., Helm, J.H., Eggum, B.O., Boisen, S., Knudsen, K.E.B., Swift, M.L., 1996. A comparison of methods for measuring the nutritive value for pigs of a range of hulled and hulless barley cultivars. Anim. Feed Sci. Technol. 62, 189–201.

Bendsen, N.T., Hother, A.L., Jensen, S.K., Lorenzen, J.K., Astrup, A., 2008. Effect of dairy calcium on fecal fat excretion: a randomized crossover trial. Int. J. Obesity 32, 1816–1824.

Bergner, H., Simon, O., Zimmer, M., 1975. Effect of natural crude fibre content in rat diets on amino acid absorption. Arch. Anim. Nutr. 25, 95–104.

Boisen, S., 1983. Protease inhibitors in cereals. Occurrence, properties, physiological role, and nutritional influence. Acta Agric. Scand. 33, 369–381.

Boisen, S., 2000. A simple nutrient-based production model for the growing pig. CABI Publishing, Cambridge, MA, USA.

Boisen, S., 2007a. A new concept for practical feed evaluation systems. Faculty of Agricultural Sciences, Univ. of Aarhus, Tjele, Denmark.

Boisen, S. 2007b. In vitro analyses for predicting standardised ileal digestibility of protein and amino acids in actual batches of feedstuffs and diets for pigs. Livest. Sci. 109:182–185.

Boisen, S., Eggum, B.O., 1991. Critical evaluation of in vitro methods for estimating digestibility in simple-stomach animals. Nutr. Res. Rev. 4, 141–162.

Boisen, S., Fernandez, J.A., 1995. Prediction of the apparent ileal digestibility of

protein and amino-acids in feedstuffs and feed mixtures for pigs by in-vitro analyses. Anim. Feed Sci. Technol. 51, 29–43.

Boisen, S., Fernandez, J.A., 1997. Prediction of the total tract digestibility of energy in feedstuffs and pig diets by in vitro analyses. Anim. Feed Sci. Technol. 68, 277–286.

Boisen, S., Moughan, P.J., 1996. Dietary influences on endogenous ileal protein and amino acid loss in the pig - A review. Acta Agr. Scand. A-An. 46, 154–164.

Boisen, S., Tybirk, P., 2005. Implementation of a new feed evaluation system for pigs. Manipulating pig production X. In: Proc. 10th Biennial Conf. Austral. Pig Sci. Assoc. (APSA), Christchurch, New Zealand. p. 116.

Borgstrom, B., 1952. On the action of pancreatic lipase on triglycerides in vivo and in vitro. Acta Physiol. Scand. 26, 328–347.

Borgstrom, B., 1980. Importance of phospholipids, pancreatic phospholipase A2, and fatty acid for the digestion of dietary fat. In vitro experiments with the porcine enzymes. Gastroenterol. 78, 954–962.

Bottger, G., Holler, H., 1974. Agar electrophoretic demonstration of proteolytic activity in extracts of the pig gastric mucosa. Zentralblatt fur Veterinarmedizin 21A, 243–252.

Bourquin, L.D., Titgemeyer, E.C., Fahey, G.C., 1993. Vegetable fiber fermentation by human fecal bacteria: cell wall polysaccharide disappearance and short-chain fatty acid production during in vitro fermentation and water-holding capacity of unfermented residues. J. Nutr.

123, 860–869.

Bourquin, L.D., Titgemeyer, E.C., Fahey, G.C., 1996. Fermentation of various dietary fiber sources by human fecal bacteria. Nutr. Res. 16, 1119–1131.

Bourquin, L.D., Titgemeyer, E.C., Garleb, K.A., Fahey, G.C., 1992. Short-chain fatty-acid production and fiber degradation by human colonic bacteria - effects of substrate and cell-wall fractionation procedures. J. Nutr. 122, 1508–1520.

Boyd, O.F., Crum, C.L., Lyman, J.F., 1932. The absorption of calcium soaps and the relation of dietary fat to calcium utilization in the white rat. J. Biol. Chem. 95, 29–41.

Breves, G., Schulze, E., Sallmann, H.P., Gadeken, D., 1993. The application of C-13-labeled short chain fatty-acids to measure acetate and propionate production-rates in the large-intestines - studies in a pig model. Z. Gastroent. 31, 179–182.

Canibe, N., Eggum, B.O., 1997. Digestibility of dried and toasted peas in pigs. 2. Ileal and total tract digestibilities of amino acids, protein and other nutrients. Anim. Feed Sci. Technol. 64, 311–325.

Canibe, N., Knudsen, K.E.B., Eggum, B.O., 1997. Apparent digestibility of non-starch polysaccharides and short chain fatty acids production in the large intestine of pigs fed dried or toasted peas. Acta Agr. Scand. A-An. 47, 106–116.

Carey, M.C., Small, D.M., Bliss, C.M., 1983. Lipid digestion and absorption. Annu. Rev. Physiol. 45, 651–677.

Carlson, W.E., Bayley, H.S., 1968. Utilization of fat by young pigs: fatty acid composition of ingesta in different regions of the digestive tract and apparent and corrected digestibilities of corn oil, lard and tallow. Can. J. Anim. Sci. 48, 315–322.

Carlson, W.E., Bayley, H.S., 1972. Digestion of fat by young pigs: a study of the amounts of fatty acid in the digestive tract using a fat-soluble indicator of absorption. Br. J. Nutr. 28, 339–346.

Carriere, F., Renou, C., Lopez, V., Caro, J.D., Ferrato, F., Lengsfeld, H., Caro, A.D., Laugier, R., Verger, R., 2000. The specific activities of human digestive lipases measured from the in vivo and in vitro lipolysis of test meals. Gastroenterol. 119, 949–960.

Chiang, C., Chuang, S., Yu, B., 2008. A dynamic system simulating pigs' stomach to evaluate the protein digestibility of pig diet. J. Chin. Soc. Anim. Sci. 37, 131–143.

Cho, J.H., Kim, I.H., 2011. Evaluation of the apparent ileal digestibility (AID) of protein and amino acids in nursery diets by in vitro and in vivo methods. Asian-Australas. J. Anim. Sci. 24, 1007–1010.

Christensen, D.N., Knudsen, K.E.B., Wolstrup, J., Jensen, B.B., 1999. Integration of ileum cannulated pigs and in vitro fermentation to quantify the effect of diet composition on the amount of short-chain fatty acids available from fermentation in the large intestine. J. Sci. Food Agric. 79, 755–762.

Coles, L.T., Moughan, P.J., Darragh, A.J., 2005. In vitro digestion and fermentation methods, including gas production techniques, as applied to

nutritive evaluation of foods in the hindgut of humans and other simple-stomached animals. Anim. Feed Sci. Technol. 123–124, 421–444.

Cone, J.W., Vanderpoel, A., 1993. Prediction of apparent ileal protein digestibility in pigs with a 2-step in-vitro method. J. Sci. Food Agric. 62, 393–400.

Cone, J.W., van Gelder, A.H., Visscher, G.J.W., Oudshoorn, L., 1996. Influence of rumen fluid and substrate concentration on fermentation kinetics measured with a fully automated time related gas production apparatus. Anim. Feed Sci. Technol. 61, 113–128.

Corring, T., 1980. The adaptation of digestive enzymes to the diet: its physiological significance. Reprod. Nutr. Dev. 20, 1217–1235.

Daniel, M., Wisker, E., Rave, G., Feldheim, W., 1997. Fermentation in human subjects of nonstarch polysaccharides in mixed diets, but not in a barley fiber concentrate, could be predicted by in vitro fermentation using human fecal inocula. J. Nutr. 127, 1981–1988.

de Lange, C.F.M., 1989. Endogenous protein in digestibility studies in pigs. PhD Diss. Univ. of Alberta, Edmonton, AB, Canada.

de Lange, C.F.M., Birkett, S.H., 2005. Characterization of useful energy content in swine and poultry feed ingredients. Can. J. Anim. Sci. 85, 269–280.

de Lange, C.F.M., Nyachoti, C.M., Verstegen, M.W.A., 2000. The significance of antinutritional factors in feedstuffs for monogastric animals, In: Moughan, P.J., Verstegen, M.W.A., Visser-Reyneveld, M.I. (Eds.), Feed evaluation: principles and practice. p. 169–188.

de Souza, T.R., Peiniau, J., Mounier, A., Aumaitre, A., 1995. Effect of addition of tallow and lecithin in the diet of weanling piglets on the apparent total tract and ileal digestibility of fat and fatty acids. Anim. Feed Sci. Technol. 52, 77–91.

Decuypere, J.A., Knockaert, P., Henderickx, H.K., 1981. In vitro and in vivo protein digestion in pigs fed diets containing soybean protein isolates with different physical properties. J. Anim. Sci. 53, 1297–1308.

Devillard, E., McIntosh, F.M., Paillard, D., Thomas, N.A., Shingfield, K.J., Wallace, R.J., 2009. Differences between human subjects in the composition of the faecal bacterial community and faecal metabolism of linoleic acid. Microbiol. (Reading) 155, 513–520.

Dicklin, M.E., Robinson, J.L., Lin, X., Odle, J., 2006. Ontogeny and chain-length specificity of gastrointestinal lipases affect medium-chain triacylglycerol utilization by newborn pigs. J. Anim. Sci. 84, 818–825.

Dierick, N.A., Decuypere, J.A., Molly, K., Van Beek, E., Vanderbeke, E., 2002. The combined use of triacylglycerols containing medium-chain fatty acids (MCFAs) and exogenous lipolytic enzymes as an alternative for nutritional antibiotics in piglet nutrition: I. In vitro screening of the release of MCFAs from selected fat sources by selected exogenous lipolytic enzymes under simulated pig gastric conditions and their effects on the gut flora of piglets. Livest. Prod. Sci. 75, 129–142.

Dikernan, C.L., Barry, K.A., Murphy, M.R., Fahey, G.C., 2007. Diet and measurement techniques affect small intestinal digesta viscosity among

dogs. Nutr. Res. 27, 56–65.

Dourmad, J.Y., Seve, B., Latimier, P., Boisen, S., Fernandez, J., van der Peet-Schwering, C., Jongbloed, A.W., 1999. Nitrogen consumption, utilization and losses in pig production in France, The Netherlands and Denmark. Livest. Prod. Sci. 58, 261–264.

Dung, N.N.X., 2001. Evaluation of green plants and by-products from the Mekong Delta with emphasis on fibre utilisation by pigs, PhD Diss. Sveriges Lantbruksuniversitet, Sweden.

Dung, N.N.X., Manh, L.H., Udén, P., 2002. Tropical fibre sources for pigs-digestibility, digesta retention and estimation of fibre digestibility in vitro. Anim. Feed Sci. Technol. 102, 109–124.

Dung, N.N.X., Udén, P., 2002. Estimation of neutral detergent fibre degradation in pigs by an in vitro method. Anim. Feed Sci. Technol. 95, 205–214.

Duran-Montgé, P., Lizardo, R., Torrallardona, D., Esteve-Garcia, E., 2007. Fat and fatty acid digestibility of different fat sources in growing pigs. Livest. Sci. 109, 66–69.

Eggum, B.O., Andersen, J.O., Rotenberg, S., 1982. The effect of dietary fibre level and microbial activity in the digestive tract on fat metabolism in rats and pigs. Acta Agric. Scand. 32, 145–150.

Eggum, B.O., Beames, R.M., Wolstrup, J., Knudsen, K.E.B., 1984. The effect of protein quality and fibre level in the diet and microbial activity in the digestive tract on protein utilization and energy digestibility in rats. Br. J. Nutr. 52, 305–314.

Embleton, J.K., Pouton, C.W., 1997. Structure and function of gastro-intestinal lipases. Adv. Drug Del. Rev. 25, 15–32.

Etienne, M., Noblet, J., Dourmad, J.Y., Castaing, J., 1997. Digestive utilization of feeds in lactating sows. Comparison with growing pigs, In: Digest. Physiol. Pigs. Proc. 7th Int. Symp. St. Malo, France. p. 583–586.

Fairbairn, S.L., Patience, J.F., Classen, H.L., Zijlstra, R.T., 1999. The energy content of barley fed to growing pigs: characterizing the nature of its variability and developing prediction equations for its estimation. J. Anim. Sci. 77, 1502–1512.

Fakler, T.M., 1992. Effect of supplemental fat in prestarter diets on performance and apparent absorption of fatty acids in the early-weaned pig. PhD Diss. Oklahoma State Univ., OK, USA.

Farness, P.L., Schneeman, B.O., 1982. Effects of dietary cellulose, pectin and oat bran on the small intestine in the rat. J. Nutr. 112, 1315–1319.

Fondevila, M., Morales, J., Perez, J.F., Barrios-Urdaneta, A., Baucells, M.D., 2002. Microbial caecal fermentation in Iberic or Landrace pigs given acorn/sorghum or maize diets estimated in vitro using the gas production technique. Anim. Feed Sci. Technol. 102, 93–107.

Furuya, S., Sakamoto, K., Takahashi, S., 1979. New in vitro method for the estimation of digestibility using the intestinal fluid of the pig. Br. J. Nutr. 41, 511–520.

Gacs, G., Barltrop, D., 1977. Significance of Ca-soap formation for calcium absorption in the rat. Gut 18, 64–68.

Gajda, M., Flickinger, E.A., Grieshop, C.M., Bauer, L.L., Merchen, N.R., Fahey, G.C., Jr., 2005. Corn hybrid affects in vitro and in vivo measures of nutrient digestibility in dogs. J. Anim. Sci. 83, 160–171.

Gargouri, Y., Moreau, H., Verger, R., 1990. Gastric lipases: Biochemical and physiological studies (BBA 53261). BBA.-Lipid. Lipid Met. 1042, 421–421.

Gauthier, S.F., Vachon, C., Jones, J.D., Savoie, L., 1982. Assessment of protein digestibility by in vitro enzymatic-hydrolysis with simultaneous dialysis. J. Nutr. 112, 1718–1725.

Glits, L.V., Jensen, B.B., Knudsen, K.E.B., 2000. In vitro fermentation of rye carbohydrates including arabinoxylans of different structure. J. Sci. Food Agric. 80, 1211–1218.

Graham, H., Aman, P., Newman, R.K., Newman, C.W., 1985. Use of a nylon-bag technique for pig feed digestibility studies. Br. J. Nutr. 54, 719–726.

Graham, H., Lowgren, W., 1991. Prediction of the energy value of non-ruminant feeds using in vitro digestion with intestinal fluid and other chemical methods, In: Fuller, M.F., (Ed.), In vitro digestion for pigs and poultry. CAB International, Wallingford, UK. p. 128–134.

Graham, H., Lowgren, W., Aman, P., 1989. An in vitro method for studying digestion in the pig. 2. Comparison with in vivo ileal and faecal digestibilities. Br. J. Nutr. 61, 689–698.

Groff, J.L., Gropper, S.S., 2000. Advanced nutrition and human metabolism. Wadsworth Publishing Company, Inc., Belmont, CA, USA.

Gu, X., Li, D., 2003. Fat nutrition and metabolism in piglets: a review. Anim. Feed Sci. Technol. 109, 151–170.

Guevara, M.A., Bauer, L.L., Abbas, C.A., Beery, K.E., Holzgraefe, D.P., Cecava, M.J., Fahey, G.C., Jr., 2008. Chemical composition, in vitro fermentation characteristics, and in vivo digestibility responses by dogs to select corn fibers. J. Agric. Food Chem. 56, 1619–1626.

Guillon, F., Barry, J.L., Thibault, J.F., 1992. Effect of autoclaving sugar-beet fiber on its physicochemical properties and its in vitro degradation by human fecal bacteria. J. Sci. Food Agric. 60, 69–79.

Guillon, F., Renard, C., Hospers, J., Thibault, J.F., Barry, J.L., 1995. Characterization of residual fibers from fermentation of pea and apple fibers by human fecal bacteria. J. Sci. Food Agric. 68, 521–529.

Guo, L., Piao, X., Li, D., Li, S., 2004. The apparent digestibility of corn by-products for growing-finishing pigs in vivo and in vitro. Asian-Australas. J. Anim. Sci. 17, 379–385.

Hamilton, R.M.G., 1968. Effect of dietary fat source on fat utilization by the young pig. M.Sc. dissertation, McGill Univ., Montreal, QC, Canada.

Hamilton, R.M.G., McDonald, B.B., 1969. Effect of dietary fat source on the apparent digestibility of fat and the composition of fecal lipids of the young pig. J. Nutr. 97, 33–41.

Hamosh, M., Scow, R.O., 1971. Lipoprotein lipase activity in guinea pig and rat milk. BBA.-Lipid. Lipid Met. 231, 283–289.

Hedemann, M.S., Welham, T., Boisen, S., Canibe, N., Bilham, L., Domoney, C.,

1999. Studies on the biological responses of rats to seed trypsin inhibitors using near-isogenic lines of Pisum sativum L (pea). J. Sci. Food Agric. 79, 1647–1653.

Hernot, D.C., Boileau, T.W., Bauer, L.L., Middelbos, I.S., Murphy, M.R., Swanson, K.S., Fahey, G.C., Jr., 2009. In vitro fermentation profiles, gas production rates, and microbiota modulation as affected by certain fructans, galactooligosaccharides, and polydextrose. J. Agric. Food Chem. 57, 1354–1361.

Hernot, D.C., Boileau, T.W., Bauer, L.L., Swanson, K.S., Fahey, G.C., Jr., 2008. In vitro digestion characteristics of unprocessed and processed whole grains and their components. J. Agric. Food Chem. 56, 10721–10726.

Hodgkinson, S.M., Moughan, P.J., 2003. The enzyme hydrolysed protein method for the determination of endogenous ileal nitrogen and amino acid flows - a modification. Anim. Feed Sci. Technol. 108, 207–214.

Hoebler, C., Guillon, F., Fardet, A., Cherbut, C., Barry, J.L., 1998. Gastrointestinal or simulated in vitro digestion changes dietary fibre properties and their fermentation. J. Sci. Food Agric. 77, 327–333.

Hsu, A., 1983. Prediction of energy value and nitrogen digestibility of feeds from chemical and enzymatic methods for swine. PhD Diss. Kansas State Univ., Manhattan, KS, USA.

Hsu, H.W., Vavak, D.L., Satterlee, L.D., Miller, G.A., 1977. A multienzyme technique for estimating protein digestibility. J. Food Sci. 42, 1269–1273.

Huang, G., Sauer, W.C., He, J., Hwangbo, J., Wang, X., 2003a. The nutritive

value of hulled and hulless barley for growing pigs. 1. Determination of energy and protein digestibility with the in vivo and in vitro method. J. Anim. Feed Sci. 12, 759–769.

Huang, G., Sauer, W.C., He, J., Ramirez, M., 2003b. The nutritive value of hulled and hulless barley for growing pigs. 2. Determination of in vivo and in vitro energy and in vivo ileal amino acid digestibility. J. Anim. Feed Sci. 12, 771–784.

Huang, R.L., Tan, Z.L., Xing, T.X., Pan, Y.F., Li, T.J., 2000. An in vitro method for the estimation of ileal crude protein and amino acids digestibility using the dialysis tubing for pig feedstuffs. Anim. Feed Sci. Technol. 88, 79–89.

Hudman, D.B., Friend, D.W., Hartman, P.A., Ashton, G.C., Catron, D.V., 1957. Digestive enzymes of the baby pig. Pancreatic and salivary amylase. J. Agric. Food Chem. 5, 691–693.

Hur, S.J., Decker, E.A., McClements, D.J., 2009. Influence of initial emulsifier type on microstructural changes occurring in emulsified lipids during in vitro digestion. Food Chem. 114, 253–262.

Jalc, D., Potkanski, A., Szumacher-Strabel, M., Kowalczyk, J., Cieslak, A., 2006. The effect of a forage diet and different fat sources on rumen fermentation in vitro. J. Anim. Feed Sci. 15, 129–132.

Jørgensen, H., Larsen, T., Zhao, X., Eggum, B.O., 1997. The energy value of short-chain fatty acids infused into the caecum of pigs. Br. J. Nutr. 77, 745–756.

Kandel, K.P., 2011. Nutritional characterization of wheat distillers dried grains

with solubles in grower-finisher pigs. M.Sc. Thesis. Univ. of Alberta, Edmonton, AB, Canada.

Kim, I.B., 2001. Development of in vitro technique for bioavailable corn energy value. Asian-Australas. J. Anim. Sci. 14, 1645–1646.

Kirchgessner, M., Gerstl, R., Windisch, W., Roth, F.X., 1992. In vitro method for estimating energy feed value of high protein mixed feeds for pigs. Agribiol. Res. 45, 333–343.

Krishnamoorthy, U., Rymer, C., Robinson, P.H., 2005. The in vitro gas production technique: limitations and opportunities. Anim. Feed Sci. Technol. 123–124, 1–7.

Le Goff, G.., Noblet, J., 2001. Comparative total tract digestibility of dietary energy and nutrients in growing pigs and adult sows. J. Anim. Sci. 79, 2418–2427.

Le Goff, G., Noblet, J., Cherbut, C., 2003. Intrinsic ability of the faecal microbial flora to ferment dietary fibre at different growth stages of pigs. Livest. Prod. Sci. 81, 75–87.

Lebet, V., Arrigoni, E., Amado, R., 1998. Measurement of fermentation products and substrate disappearance during incubation of dietary fibre sources with human faecal flora. Food. Sci. Technol. 31, 473–479.

Lee, S.H., Choi, N.J., Maeng, W.J., 2003. Effects of full-fat soybeans and linseed as dietary fat sources on in vitro ruminal disappearances of dry matter and C18-unsaturated fatty acids and fatty acids profile. J. Anim. Sci. Technol. 45, 443–454.

Leszczynski, W., 2004. Resistant starch - classification, structure, production. Pol. J. Food. Nutr. Sci. 13, 37–50.

Liao, T.H., Hamosh, P., Hamosh, M., 1984. Fat digestion by lingual lipase: mechanism of lipolysis in the stomach and upper small intestine. Pediatr. Res. 18, 402–409.

Lindberg, J.E., Kaspersson, A., Ciszuk, P., 1984. Studies on pH, number of protozoa and microbial ATP concentrations in rumen-incubated nylon bags with different pore sizes. J. Agr. Sci., UK 102, 501–504.

Linthorst, J.M., Bennett Clark, S., Holt, P.R., 1977. Triglyceride emulsification by amphipaths present in the intestinal lumen during digestion of fat. J. Colloid Interface Sci. 60, 1–10.

Losada, B., Garcia-Rebollar, P., Cachaldora, P., Alvarez, C., Mendez, J., de Blas, J.C., 2009. A comparison of the prediction of apparent metabolisable energy content of starchy grains and cereal by-products for poultry from its chemical components, in vitro analysis or near-infrared reflectance spectroscopy. Span. J. Agric. Res. 7, 813–823.

Lovedeep, Y., Tewatia, B.S., Virk, A.S., 1999. Effect of fat content in various oil cakes on rumen fermentation. Indian J. Anim. Nutr. 16, 123–127.

Lowgren, W., Graham, H., Aman, P., 1989. An in vitro method for studying digestion in the pig. 1. Simulating digestion in the different compartments of the intestine. Br. J. Nutr. 61, 673–687.

Lowgren, W., Graham, H., Aman, P., Raj, S., Kotarbinska, M., 1992. Predicting the energy value of pig feeds using in vitro or analytical methods. Anim.

Feed Sci. Technol. 39, 183–191.

Lowman, R.S., Theodorou, M.K., Hyslop, J.J., Dhanoa, M.S., Cuddeford, D., 1999. Evaluation of an in vitro batch culture technique for estimating the in vivo digestibility and digestible energy content of equine feeds using equine faeces as the source of microbial inoculum. Anim. Feed Sci. Technol. 80, 11–27.

Madhuri, K., Pratima, S., Rao, B.Y., 1996. Effect of processing on in vitro carbohydrate digestibility of cereals and legumes. J. Food Sci. Technol. (Mysore) 33, 493–497.

Marounek, M., O. Suchorska, and O. Savka. 1999. Effect of substrate and feed antibiotics on in vitro production of volatile fatty acids and methane in caecal contents of chickens. Anim. Feed Sci. Technol. 80:223–230.

Marrero, A.I., Dihigo, L.E., Savon, L., Machin, L., Orta, M., 1998. The utilization of the faecal content of pigs to determine in vitro digestion of fibre diets for broilers. Cuban J. Agr. Sci. 32, 165–169.

Marshall, H.F., Jr., Wallace, G.W., Satterlee, L.D., 1979. Prediction of protein digestibility by an in vitro procedure using human, porcine, and rat pancreatin preparations. Nutr. Rep. Int. 19, 901–913.

Marteau, P., Minekus, M., Havenaar, R., Huis in't Veld, J.H.J., 1997. Survival of lactic acid bacteria in a dynamic model of the stomach and small intestine: validation and the effects of bile. J. Dairy Sci. 80, 1031–1037.

McBurney, M.I., Sauer, W.C., 1993. Fiber and large-bowel energy-absorption - validation of the integrated ileostomy-fermentation model using pigs. J.

Nutr. 123, 721–727.

McBurney, M.I., Thompson, L.U., 1989. Dietary fiber and energy balance: Integration of the human ileostomy and in vitro fermentation models. Anim. Feed Sci. Technol. 23, 261–275.

Meunier, J.P., Manzanilla, E.G., Anguita, M., Denis, S., Perez, J.F., Gasa, J., Cardot, J.M., Garcia, F., Moll, X., Alric, M., 2008. Evaluation of a dynamic in vitro model to simulate the porcine ileal digestion of diets differing in carbohydrate composition. J. Anim. Sci. 86, 1156–1163.

Minekus, M., Marteau, P., Havenaar, R., Huisintveld, J.H.J., 1995. A multicompartmental dynamic computer-controlled model simulating the stomach and small-intestine. ATLA-Altern. Lab. Anim. 23, 197–209.

Minekus, M., Smeets-Peeters, M., Bernalier, A., Marol-Bonnin, S., Havenaar, R., Marteau, P., Alric, M., Fonty, G., Huis in't Veld, J.H.J., 1999. A computer-controlled system to simulate conditions of the large intestine with peristaltic mixing, water absorption and absorption of fermentation products. Appl. Microbiol. Biotechnol. 53, 108–114.

Miner-Williams, W., Moughan, P.J., Fuller, M.F., 2009. Endogenous components of digesta protein from the terminal ileum of pigs fed a casein-based diet. J. Agric. Food Chem. 57, 2072–2078.

Mohammadian-Tabrizi, H.R., Sadeghipanah, H., Chamani, M., Ebrahim-Nejad, Y., Fazaeli, H., 2011. In vitro gas production of wheat grain flour coated with different fat types and levels. Afr. J. Biotechnol. 10, 7710–7716.

Monsma, D.J., Marlett, J.A., 1996. Fermentation of carbohydrate in rat ileal

excreta is enhanced with cecal inocula compared with fecal inocula. J. Nutr. 126, 554–563.

Moughan, P.J., 1999. In vitro techniques for the assessment of the nutritive value of feed grains for pigs: a review. Aust. J. Agric. Res. 50, 871–879.

Moughan, P.J., Schrama, J., Skilton, G.A., Smith, W.C., 1989. In-vitro determination of nitrogen digestibility and lysine availability in meat and bone meals and comparison with in-vivo ileal digestibility estimates. J. Sci. Food Agric. 47, 281–292.

Mould, F.L., 2002. Predicting feed quality - chemical analysis and in vitro evaluation. In: International Workshop "Approaches to improve the utilization of food-feed crops", Addis Ababa, Ethiopia. p. 31–44.

Mountzouris, K.C., Fegeros, K., Papadopoulos, G., 1999. Utilization of fats based on the composition of sow milk fat in the diet of weanling pigs. Anim. Feed Sci. Technol. 77, 115–124.

Noblet, J., 2000. Digestive and metabolic utilization of feed energy in swine: application to energy evaluation systems. J. Appl. Anim. Res. 17, 113–132.

Noblet, J., Bach Knudsen, K.E., 1997. Comparative digestibility of wheat, maize and sugar beet pulp non-starch polysaccharides in adult sows and growing pigs, In: Digestive physiology in pigs. Proc. 7th Int. Symp. St. Malo, France. p. 571–574.

Noblet, J., Henry, Y., 1993. Energy evaluation systems for pig diets - a review. Livest. Prod. Sci. 36, 121–141.

Noblet, J., Jaguelin-Peyraud, Y., 2007. Prediction of digestibility of organic matter and energy in the growing pig from an in vitro method. Anim. Feed Sci. Technol. 134, 211–222.

Noblet, J., Perez, J.M., 1993. Prediction of digestibility of nutrients and energy values of pig diets from chemical-analysis. J. Anim. Sci. 71, 3389–3398.

Nyachoti, C.M., de Lange, C.F.M., McBride, B.W., Schulze, H., 1997. Significance of endogenous gut nitrogen losses in the nutrition of growing pigs: a review. Can. J. Anim. Sci. 77, 149–163.

Oryschak, M.A., Zijlstra, R.T., 2002. Effect of dietary particle size and nutrient supply on energy digestibility and nitrogen excretion in ileal cannulated grower pigs. Can. J. Anim. Sci. 82, 603–606.

Paltauf, F., Esfandi, F., Holasek, A., 1974. Stereospecificity of lipases. Enzymic hydrolysis of enantiomeric alkyl diacylglycerols by lipoprotein lipase, lingual lipase and pancreatic lipase. Febs Lett. 40, 119–123.

Papadopoulos, M.C., 1987. In vitro and in vivo estimation of protein quality of laboratory treated feather meal. Biol. Waste. 21, 143–148.

Pedersen, B., Boisen, S., 1982. The nutritional effect of a pepsin stable trypsin inhibitor from barley grains. Z. Tierphysiol. Tierer. 48, 65–75.

Pedersen, B., Eggum, B.O., 1983. Prediction of protein digestibility by an in vitro enzymatic pH-stat procedure. Z. Tierphysiol. Tierer. 49, 265–277.

Pedersen, C., Boisen, S., Fernandez, J.A., 2002. Studies on the effect of dietary crude protein supply on the composition of ileal endogenous crude protein loss in growing pigs. Acta Agric. Scand. A 52, 141–149.

Pedersen, N., Eggum, B.O., 1981. Prediction of protein digestibility by in vitro procedures based on two multi-enzyme systems. Z. Tierphysiol. Tierer. 45, 190–200.

Pettersson, A., Lindberg, J.E., Thomke, S., Eggum, B.O., 1996. Nutrient digestibility and protein quality of oats differing in chemical composition evaluated in rats and by an in vitro technique. Anim. Feed Sci. Technol. 62, 203–213.

Pujol, S., Torrallardona, D., 2006. Evaluation of in vitro methods to estimate the in vivo nutrient digestibility of barley in pigs, In: Proc. 10th Int. Symp. Digest. Physiol. Pigs, Vejle, Denmark. p. 186–188.

Qiao, S., Thacker, P.A., 2001. A comparison of washed and unwashed bags to determine the apparent fecal digestibility of dry matter, energy and crude protein in feeds for swine using the mobile nylon bag technique. Can. J. Anim. Sci. 81, 371–378.

Qiao, S., Thacker, P.A., 2004. Use of the mobile nylon bag technique to determine the digestible energy content of traditional and non-traditional feeds for swine. Arch. Anim. Nutr. 58, 287–294.

Qiao, Y., Lin, X., Odle, J., Whittaker, A., van Kempen, T.A.T.G., 2004. Refining in vitro digestibility assays: Fractionation of digestible and indigestible peptides. J. Anim. Sci. 82, 1669–1677.

Regmi, P.R., Ferguson, N.S., Zijlstra, R.T., 2009. In vitro digestibility techniques to predict apparent total tract energy digestibility of wheat in grower pigs. J. Anim. Sci. 87:3620–3629.

Regmi, P.R., Sauer, W.C., Zijlstra, R.T., 2008. Prediction of in vivo apparent total tract energy digestibility of barley in grower pigs using an in vitro digestibility technique. J. Anim. Sci. 86, 2619–2626.

Rodriguez, Z., Lopez, A., Riveri, Z., 2000. Effect of fibre level on the number and activity of the cellulolytic microflora in the caecum of pigs. Cuban J. Agr. Sci. 34, 47–55.

Salvador, V., Cherbut, C., Barry, J.L., Bertrand, D., Bonnet, C., Delortlaval, J., 1993. Sugar composition of dietary fiber and short-chain fatty-acid production during in-vitro fermentation by human bacteria. Br. J. Nutr. 70, 189–197.

Satterlee, L.D., Marshall, H.F., Tennyson, J.M., 1979. Measuring protein quality. J. Am. Oil Chem. Soc. 56, 103–109.

Sauer, W.C., Jørgensen, H., Berzins, R., 1983. A modified nylon bag technique for determining apparent digestibilities of protein in feedstuffs for pigs. Can. J. Anim. Sci. 63, 233–237.

Savoie, L., 1994. Digestion and absorption of food - usefulness and limitations of in-vitro models. Can. J. Physiol. Pharmacol. 72, 407–414.

Savoie, L., Gauthier, S.F., 1986. Dialysis cell for the in vitro measurement of protein digestibility. J. Food Sci. 51, 494–498.

Savoie, L., Gauthier, S.F., Marin, J., Pouliot, Y., 2005. In vitro determination of the release kinetics of peptides and free amino acids during the digestion of food proteins. J. AOAC Int. 88, 935–948.

Schmidt, L.D., Blank, G., Boros, D., Slominski, B.A., 2007. The nutritive value of

egg by-products and their potential bactericidal activity: in vitro and in vivo studies. J. Sci. Food Agric. 87, 378–387.

Sheffner, A.L., Eckfeldt, G.A., Spector, H., 1956. The pepsin-digest-residue (PDR) amino acid index of net protein utilization. J. Nutr. 60, 105–120.

Shi, X.S., Noblet, J., 1994. Effect of body weight and feed composition on the contribution of hindgut to digestion of energy and nutrients in pigs. Livest. Prod. Sci. 38, 225–235.

Silvester, K.R., Englyst, H.N., Cummings, J.H., 1995. Ileal recovery of starch from whole diets containing resistant starch measured in-vitro and fermentation of ileal effluent. Am. J. Clin. Nutr. 62, 403–411.

Smeets-Peeters, M.J.E., Minekus, M., Havenaar, R., Schaafsma, G., Verstegen, M.W.A., 1999. Description of a dynamic in vitro model of the dog gastrointestinal tract and an evaluation of various transit times for protein and calcium. ATLA-Altern. Lab. Anim. 27, 935–949.

Smiricky-Tjardes, M.R., Grieshop, C.M., Flickinger, E.A., Bauer, L.L., Fahey, G.C., 2003. Dietary galactooligosaccharides affect ileal and total-tract nutrient digestibility, ileal and fecal bacterial concentrations, and ileal fermentative characteristics of growing pigs. J. Anim. Sci. 81, 2535–2545.

Smith, J.G., 2010. General, organic, and biological chemistry. McGraw-Hill Companies, Inc., New York, NY, USA.

Souffrant, W.B., Rerat, A., Laplace, J.P., Darcy-Vrillon, B., Kohler, R., Corring, T., Gebhardt, G., 1993. Exogenous and endogenous contributions to nitrogen fluxes in the digestive tract of pigs fed a casein diet. 3. Recycling

of endogenous nitrogen. Reprod. Nutr. Dev. 33, 373–382.

Spanghero, M., Volpelli, L.A., 1999. A comparison of the predictions of digestible energy content of compound feeds for pigs by chemical or in vitro analysis. Anim. Feed Sci. Technol. 81, 151–159.

Staggers, J., Fernando-Warnakulasuriya, G.J.P., Wells, M.A., 1981. Studies on fat digestion, absorption, and transport in the suckling rat. 2. Triacylglycerols: molecular species, stereospecific analysis, and specificity of hydrolysis by lingual lipase. J. Lipid Res. 22, 675–679.

Stein, H.H., Seve, B., Fuller, M.F., Moughan, P.J., de Lange, C.F.M., 2007. Invited review: amino acid bioavailability and digestibility in pig feed ingredients: terminology and application. J. Anim. Sci. 85, 172–180.

Stein, H.H., Shurson, G.C., 2009. Board-Invited Review: The use and application of distillers dried grains with solubles in swine diets. J. Anim. Sci. 87, 1292–1303.

Steiner, T., Aufy, A., 2011. Phytogenics and managing feed cost in poultry production. Poultry: Middle East & North Africa 33, 78–126.

Strathe, A.B., Danfar, A., Chwalibog, A., 2008. A dynamic model of digestion and absorption in pigs. Anim. Feed Sci. Technol. 143, 328–371.

Sun, T., Lærke, H.N., Jørgensen, H., Knudsen, K.E.B., 2006. The effect of extrusion cooking of different starch sources on the in vitro and in vivo digestibility in growing pigs. Anim. Feed Sci. Technol. 131, 67–86.

Sunvold, G.D., Fahey, G.C., Jr., Merchen, N.R., Reinhart, G.A., 1995a. In vitro fermentation of selected fibrous substrates by dog and cat fecal inoculum:

influence of diet composition on substrate organic matter disappearance and short-chain fatty acid production. J. Anim. Sci. 73, 1110–1122.

Sunvold, G.D., Hussein, H.S., Fahey, G.C., Merchen, N.R., Reinhart, G.A., 1995b. In vitro fermentation of cellulose, beet pulp, citrus pulp, and citrus pectin using fecal inoculum from cats, dogs, horses, humans, and pigs and ruminal fluid from cattle. J. Anim. Sci. 73, 3639–3648.

Swiech, E., Buraczewska, L., 2006. The energy value of pig diets estimated in vitro and in vivo. In: Proc. 3rd Conf. Physiol. Biochem. Anim. Nutr., Warsaw, Poland. p. 85–88.

Swiech, E., Buraczewska, L., 2001. In vivo and in vitro protein and amino acid digestibility of soybean and rapeseed products in pig diets, In: Lindberg, J.E., Ogle, B., editors, Digest. Physiol. Pigs. Proc. 8th Symp., Swedish Univ. Agr. Sci., Uppsala, Sweden. p. 354–356.

Thacker, P. A., and S. Qiao. 2001. Further modifications to the mobile nylon bag technique to determine nutrient digestibility for swine. Asian-Australas. J. Anim. Sci. 14:1149-1156.

Tidwell, H.C., Holt, L.E., Jr., 1936. The estimation of the total lipids and the lipid partition in feces. J. Biol. Chem. 112, 605–613.

Titgemeyer, E.C., Bourquin, L.D., Fahey, G.C., Jr., Garleb, K.A., 1991. Fermentability of various fiber sources by human fecal bacteria in vitro. Am. J. Clin. Nutr. 53, 1418–1424.

Torrallardona, D., Harris, C.I., Fuller, M.F., 2003. Pigs' gastrointestinal microflora provide them with essential amino acids. J. Nutr. 133, 1127–1131.

Uden, P., 2009. Estimating residual starch from in vitro fermentations by Fourier transform mid-IR transmission spectroscopy. Anim. Feed Sci. Technol. 152, 133–140.

Urriola, P.E., 2010. Digestibility of dietary fiber by growing pigs. PhD Diss. Univ. of Illinois at Urbana-Champaign, IL, USA.

Valdes, E.V., Leeson, S., 1992. Measurement of metabolizable energy in poultry feeds by an in vitro system. Poult. Sci. 71, 1493–1503.

van Barneveld, R.J., 1999. Chemical and physical characteristics of grains related to variability in energy and amino acid availability in pigs: a review. Aust. J. Agric. Res. 50, 667–687.

van Barneveld, R.J., Nuttall, J.D., Flinn, P.C., Osborne, B.G., 1999. Near infrared reflectance measurement of the digestible energy content of cereals for growing pigs. J. Near Infrared Spectrosc. 7, 1–7.

van der Meer, J.M., Perez, J.M., 1992. In vitro evaluation of European diets for pigs - prediction of the organic-matter digestibility by an enzymatic method or by chemical-analysis. J. Sci. Food Agric. 59, 359–363.

van Kempen, T.A.T.G., Regmi, P.R., Matte, J.J., Zijlstra, R.T., 2010. In vitro starch digestion kinetics, corrected for estimated gastric emptying, predict portal glucose appearance in pigs. J. Nutr. 140, 1227–1233.

van Laere, K., 2000. Degradation of structurally different non-digestible oligosaccharides by intestinal bacteria: glycosylhydrolases of Bifidobacterium adolescentis. Wageningen Agr. Univ., Wageningen, The Netherlands.

van Leeuwen, P., Jansman, A.J.M., 2007. Effects of dietary water holding capacity and level of fermentable organic matter on digesta passage in various parts of the digestive tract in growing pigs. Livest. Sci. 109, 77–80.

Varel, V.H., Yen, J.T., 1997. Microbial perspective on fiber utilization by swine. J. Anim. Sci. 75, 2715–2722.

Venema, K., Nuenen, M.v., Smeets-Peeters, M., Minekus, M., Havenaar, R., 2000. TNO's in vitro large intestinal model: an excellent screening tool for functional food and pharmaceutical research. Ernahrung 24, 558–564.

Venema, K.M.M.H.R., 2003. Advanced in vitro models of the gastrointestinal tract - novel tools to study functionality of dietary fibres, Dietary fibre: bio-active carbohydrates for food and feed. In: Proc. Dietary Fibre 2003 Conference, The Netherlands. p. 112.

Verleyen, T., van Dyck, S., Adams, C.A., 2006. In vitro model relating lipid digestibility and quality. In: Proc. 12th European Poultry Conference, Verona, Italy. p. 123.

Vervaeke, I.J., Graham, H., Dierick, N.A., Demeyer, D.I., Decuypere, J.A., 1991. Chemical analysis of cell wall and energy digestibility in growing pigs. Anim. Feed Sci. Technol. 32, 55–61.

Villamide, M.J., Carabano, R., Maertens, L., Pascual, J., Gidenne, T., Falcao-e-Cunha, L., Xiccato, G., 2009. Prediction of the nutritional value of European compound feeds for rabbits by chemical components and in vitro analysis. Anim. Feed Sci. Technol. 150, 283–294.

Wang, W., Lu, P., Wang, J., Xiong, Y., Liu, H., 2003. Effect of particle sizes on in vitro protein digestibility and energy consumption of seven feed ingredients. Chin. J. Anim. Sci. 39, 18–20.

Weurding, R.E., Veldman, A., Veen, W.A.G., van der Aar, P.J., Verstegen, M.W.A., 2001. In vitro starch digestion correlates well with rate and extent of starch digestion in broiler chickens. J. Nutr. 131, 2336–2342.

Wiesemuller, W., Poppe, S., 1990. Protein digestion in pigs measured in vitro. Arch. Anim. Nutr. 40, 689–693.

Wilfart, A., Jaguelin-Peyraud, Y., Simmins, H., Noblet, J., Milgen, J.v., Montagne, L., 2006. A step-wise in vitro method to estimate kinetics of hydrolysis of feeds. In: 10th Int. Symp. Digest. Physiol. Pigs, Vejle, Denmark. p. 179–181.

Wilfart, A., Jaguelin-Peyraud, Y., Simmins, H., Noblet, J., van Milgen, J., Montagne, L., 2008. Kinetics of enzymatic digestion of feeds as estimated by a stepwise in vitro method. Anim. Feed Sci. Technol. 141, 171–183.

Wilfart, A., Montagne, L., Simmins, H., Noblet, J., Milgen, J.v., 2007. Digesta transit in different segments of the gastrointestinal tract of pigs as affected by insoluble fibre supplied by wheat bran. Br. J. Nutr. 98, 54–62.

Williams, N.H., Klenk, S., Christianson, B., 2011. Production costs in the Americas. In: Proc. 2011 Banff Pork Seminar, Banff, Alberta. p. 277–282.

Wisker, E., Daniel, M., Rave, G., Feldheim, W., 1998. Fermentation of non-starch polysaccharides in mixed diets and single fibre sources: comparative studies in human subjects and in vitro. Br. J. Nutr. 80, 253–261.

Yen, J.T., 2001. Anatomy of the digestive system and nutritional physiology, In: Lewis, A.J., Southern, L.L., (Eds.), Swine Nutrition, 2nd ed., CRC Press, Boca Raton, FL, USA. p. 31–64.

Yin, Y.L., Huang, R.L., Zhang, H.Y., Chen, C.M., Li, T.J., Pan, Y.F., 1993. Nutritive value of feedstuffs and diets for pigs: I. Chemical composition, apparent ileal and faecal digestibilities. Anim. Feed Sci. Technol. 44, 1–27.

Yin, Y.L., Huang, R.L., Zhong, H.Y., Li, T.J., Souffrant, W.B., de Lange, C.F.M., 2002. Evaluation of mobile nylon bag technique for determining apparent ileal digestibilities of protein and amino acids in growing pigs. J. Anim. Sci. 80, 409–420.

Yu, P., 2011. Study the sensitivity of molecular functional groups to bioethanol processing in lipid biopolymer of co-products using DRIFT molecular spectroscopy. Spectrochim. ACTA A 82, 1–7.

Yu, P., Niu, Z., Damiran, D., 2010. Protein molecular structures and protein fraction profiles of new coproducts from bioethanol production: a novel approach. J. Agric. Food Chem. 58, 3460–3464.

Zaidi, F., Hassissene, N., Boubekeur, N., Bouaiche, A., Bouabdellah, A., Grongnet, J.F., Bellal, M.M., Youyou, A., 2008. In vitro study of limiting factors of nutritive value of olive cake: effects of fats and secondary metabolites. Livest. Res Rural Dev. 20, 46.

Zhu, J.Q., Fowler, V.R., Fuller, M.F., 1988. The production of methane and volatile fatty acids resulting from the fermentation of sugar beet pulp in

the gut of growing pigs, In: Digest. Physiol. Pigs. Proc. 4th Int. Seminar, Jabonna, Poland. p. 180–187.

Zijlstra, R.T., Beltranena, E., 2008. Variability of quality in biofuel co-products, Recent advances in animal nutrition 2008. In: Proc. 42nd Univ. of Nottingham Feed Conf., Nottingham. p. 313–326.

Zijlstra, R.T., de Lange, C.F.M., Patience, J.F., 1999. Nutritional value of wheat for growing pigs: chemical composition and digestible energy content. Can. J. Anim. Sci. 79, 187–194.

Zijlstra, R.T., Swift, M.L., Wang, L.F., Scott, T.A., Edney, M.J., 2011. Near infrared reflectance spectroscopy accurately predicts the digestible energy content of barley for pigs. Can. J. Anim. Sci. 91, 301–304.

Table 2.1 Categories of enzyme origin for simulation of digestion with examples for each step

Step[a]	All from living animal	Partly from living animal	Purified enzyme
1	Jejunum fluid	Pepsin	Pepsin
2	Intestinal fluid	Pancreatin	Pancreatin
3	Fecal inocula	Fecal inocula	Viscozyme[b], cellulase

[a] Step 1 represents in vitro digestion simulating digestion in stomach of pigs; Step 2 represents in vitro digestion simulating digestion in small intestine of pigs; and Step 3 represents in vitro digestion simulating digestion in large intestine of pigs (Boisen and Fernandez, 1997).

[b] Viscozyme is a mixed multi-enzyme complex containing a wide range of microbial carboanhydrases including arabinase, cellulase, β-glucanase, hemicellulase, xylanase, and pectinase.

Table 2.2 Type of measurement of digestion or absorption

	Type			
Item	I	II	III	IV
Measure approach	Digested[a]	Undigested[b]	Absorbed[c]	Produced[d]
Example	Digesta, centrifuged digesta	Residue after filtration or centrifuge	Digestion product with dialysis	Gas production during fermentation
Measurements	pH, concentration of nutrients	Weight, concentration of nutrients	Concentration of nutrients	Gas production

[a] Hsu et al., 1977.

[b] Boisen and Fernandez, 1997.

[c] Savoie and Gauthier, 1986.

[d] Coles et al., 2005.

Table 2.3 In vitro digestibility studies using digestive fluid or microflora collected from animals for all digestion simulation steps[a]

Author and year	In vitro model brief	Substrates	Nutrients	Model	Type[b]
Lowgren et al., 1989	Duodenal, ileal, fecal inocula	sugar-beet pulp, wheat bran	CP	Pig	II
Graham et al., 1989	Duodenal, ileal, fecal inocula	wheat bran, sugar-beet pulp, pea	CP, starch, energy, DM	Pig	II
McBurney and Thompson, 1989	Fermentation: fecal inocula	food	Energy	Human	II
Titgemeyer et al., 1991	Fecal inocula	various fiber sources		Human	I
Graham and Lowgren, 1991	Intestinal fluid	non-ruminant feeds	Energy	Pig, poultry	II
Guillon et al., 1992	Fecal inocula	sugar-beet fiber		Human	I
Lowgren et al., 1992	Ileal or fecal inocula	cereals, lupin, rapeseed meal	ME, DE	Pig	II
Salvador et al., 1993	Fermentation: fecal inocula	wheat bran, sugar beet, maize, pea hulls	SCFA	Human	I
Bourquin et al., 1993	Fermentation: fecal inocula	8 vegetables	DM	Human	I, II
Silvester et al., 1995	Fermentation: fecal inocula	starchy foods	RS	Human	I
Sunvold et al., 1995a	Fermentation: fecal inocula	fibrous substrates	OM, SCFA	Dog, cat	I, II

Author and year	In vitro model brief	Substrates	Nutrients	Model	Type[b]
Sunvold et al., 1995b	Fermentation	cellulose, beet pulp, citrus pulp	OM, SCFA	Pig, etc.	I, II
Barry et al., 1995	Fermentation: fecal inocula	5 fiber sources	SCFA, NSP	Human	I, II
Bourquin et al., 1996	Fermentation: fecal inocula	11 fiber-rich substrates	OM, SCFA	Human	I, II
Monsma and Marlett, 1996	Caecal or fecal inocula	dietary fiber	Carbohydrates	Mouse	II

[a] CP, crude protein; DE, digestible energy; DM, dry matter; SCFA, short-chain fatty acid; ME, metabolizable energy; NSP, non-starch polysaccharides; OM, organic matter; RS, resistant starch.

[b] Types for measurement of digestion or absorption were defined in Table 2.2.

Table 2.4 In vitro digestibility studies using digestive fluid or microflora in part of simulation steps[a]

Author and year	In vitro model brief	Substrates	Nutrients	Model	Type[b]
Furuya et al., 1979	Pepsin + jejunum intestinal fluid	grain, soybean meal	CP	Pig	II
Hoebler et al., 1998	Fermentation	wheat bran, barley bran, beet fiber	Polysaccharides	Pig	II
Dung, 2001	Caecum-colon and rectal inocula	green plants, by-products	OM, NDF	Pig	II
Dung et al., 2002	Caecum-colon and rectal inocula	tropical fiber sources	Fiber	Pig	II
Dung and Udén, 2002	α-amylase; pepsin; caecum-colon or inoculum from rectum	rice bran, tofu residue, water spinach	NDF	Pig	II
Guo et al., 2004	Filter bag and dialysis	10 corn by-products	Energy, CP, DM	Pig	III
Guevara et al., 2008	Fecal inocula	corn co-products	Fiber	Dog	I
Urriola, 2010	Fecal inocula	DDGS	OM	Pig	II

[a] CP, crude protein; DDGS, dried distillers grains with solubles; DM, dry matter; OM, organic matter.

[b] Types for measurement of digestion or absorption were defined in Table 2.2.

Table 2.5 In vitro digestibility studies using commercially-available purified enzymes for all simulation steps[a]

Author and year	In vitro model brief[b]	Substrates	Nutrients	Model	Type[c]
Sheffner et al., 1956	Pepsin; pancreatin; erepsin	casein, whole egg	Protein, AA	Human, mouse	I
Hsu et al., 1977	pH drop (10 min)	23 protein sources	Protein	Mouse	I
Marshall et al., 1979	Pancreatin	33 foods	Protein	Pig, human, mouse	I
Satterlee et al., 1979	pH drop (20 min)	foods	Protein, AA	Human, mouse	I
Decuypere et al., 1981	Pepsin; trypsin	soy protein isolate	CP	Pig	II
Pedersen and Eggum, 1983	pH state, 10 min	30 protein samples	Protein	Mouse	I
Hsu, 1983	Pepsin, amylase, pancreatin	9 ingredients, 12 diets	N, DM, energy	Pig	II
Moughan et al., 1989	pH-drop	20 meat and bone	N, Lysine	Mouse	I
Wiesemuller and Poppe, 1990	Pepsin-HCl or pepsin + trypsin	soybean meal	CP, AA	Pig	I
Babinszky et al., 1990	A:Fat-extracted feed samples B: pancreatic lipase, bile salts	7 feedstuffs, 16 diets	CP	Pig	II
Valdes and Leeson, 1992	Pepsin; pancreatin; bile salts, etc.	71 diets	AME	Poultry	II
Kirchgessner et al., 1992	HCl-pepsin/cellulase	39 mixed pig feeds	OM	Pig	II
van der Meer and Perez, 1992	Pepsin; pancreatin, cellulase	89 samples of diets	OM	Pig	II

Author and year	In vitro model brief[b]	Substrates	Nutrients	Model	Type[c]
Cone and Vanderpoel, 1993	Pepsin/HCl, pancreatin, amylase	5 common feedstuffs	CP	Pig	II
Boisen and Fernandez, 1995	Pepsin 6h, pancreatin 18h	15 common feedstuffs	CP, AA	Pig	II
Madhuri et al., 1996	Salivary, pancreatic amylases	cereals, legumes	Carbohydrates		I
Pettersson et al., 1996	Pepsin; pancreatin; Viscozyme	oats	DM, CP	Mouse	II
Beames et al., 1996	Pepsin; pancreatin; Viscozyme	barley	Energy, protein	Pig, mouse	II
Boisen and Fernandez, 1997	Pepsin; pancreatin; Viscozyme	31 feeds	Energy	Pig	II
Aura et al., 1999	Amylase; pepsin; pancreatin; bile	cereal samples	Starch, CP		I
Spanghero and Volpelli, 1999	Pepsin; pancreatin; Viscozyme	compound pig feeds	DE	Pig	II
Huang et al., 2000	Dialysis	4 feedstuffs	CP AA	Pig	III
Weurding et al., 2001	In vitro starch digestion, kinetics	12 starch sources	Starch	Poultry	I
Kim, 2001	One step, 2 enzymes	corn hybrids	Energy	Pig, poultry	II
Bauer et al., 2003		starch sources	Starch	Mouse	I
Huang et al., 2003b	Pepsin, pancreatin; cellulase	barley	Energy	Pig	II
Huang et al., 2003a	Pepsin, pancreatin; cellulase	barley	Energy, CP	Pig	II

Author and year	In vitro model brief[b]	Substrates	Nutrients	Model	Type[c]
Qiao et al., 2004	Pepsin; pancreatin	animal proteins	Protein, peptide	Pig	I
Savoie et al., 2005	Dialysis cell with continuous removal of digestion products	casein, cod protein, soy protein, gluten	Peptide		III
Verleyen et al., 2006	Pancreatic lipase	oxidized lard	Lipids		I
Sun et al., 2006	Amyloglucosidase; invertase	barley, pea, etc.	Starch	Pig	I
Pujol and Torrallardona, 2006	Pepsin and pancreatin	barley	AA, CP; OM	Pig	II
Boisen, 2007b	Pepsin and pancreatin	feedstuffs, diets	CP, AA	Pig	II
Swiech and Buraczewska, 2006	Pepsin; pancreatin; Viscozyme	29 formulated diets	DE, ME	Pig	II
Wilfart et al., 2006	Pepsin; pancreatin; Viscozyme	wheat, barley, wheat bran, soybean meal	OM, N, starch	Pig	II
Noblet and Jaguelin-Peyraud, 2007	Pepsin; pancreatin; Viscozyme	113 compound feeds, 66 ingredients	OM, energy	Pig	II
Schmidt et al., 2007	Dialysis system	egg by-products	CP	Mouse	III
Chiang et al., 2008	Dynamic gastric digestion	grower diet	CP	Pig	II
Regmi et al., 2008	Pepsin; pancreatin, cellulase	barley	Energy	Pig	II
Wilfart et al., 2008	Pepsin; pancreatin; Viscozyme	4 common feedstuffs	OM, N, starch	Pig	II

Author and year	In vitro model brief[b]	Substrates	Nutrients	Model	Type[c]
Meunier et al., 2008	Dynamic vs. static in vitro	fibrous diets	OM, CP, starch	Pig	III
Regmi et al., 2009	Pepsin; pancreatin; Viscozyme	wheat	Energy	Pig	II
Villamide et al., 2009	Pepsin; pancreatin; Viscozyme	164 rabbit diets	Energy	Rabbit	II
Losada et al., 2009	Pepsin; pancreatin; Viscozyme	grains, by-products	ME	Poultry	II
Anderson, 2009	Pepsin; pancreatin; Viscozyme	corn co-products	OM	Pig	II
Cho and Kim, 2011	Pepsin and pancreatin	nursery diets	CP, AA	Pig	II
Anderson et al., 2012	Pepsin; pancreatin; Viscozyme	corn co-products	OM	Pig	II

[a] AA, amino acids; AME, apparent metabolizable energy; CP, crude protein; DE, digestible energy; DM, dry matter; ME, metabolizable energy; NDF, neutral detergent fiber; OM, organic matter.

[b] Viscozyme is a mixed multi-enzyme complex containing a wide range of microbial carboanhydrases including arabinase, cellulase, β-glucanase, hemicellulase, xylanase, and pectinase.

c Types for measurement of digestion or absorption were defined in Table 2.2.

Table 2.6 Example performance of in vitro digestibility assays to predict digestibility of CP, starch, OM, and energy[a]

Author and year	Nutrients	Feedstuffs	Animal model	R^2
Hsu et al., 1977	CP	23 protein sources	rat	0.81
Furuya et al., 1979	CP	grains and soybean meal	pig	0.96
Pedersen and Eggum, 1983	CP	30 protein samples	rats	0.92
Babinszky et al., 1990	CP	7 feedstuffs and 16 diets	pig	0.98
Huang et al., 2000	CP and AA	4 feedstuffs	pig	0.92-0.98
Weurding et al., 2001	Starch	12 diets	chicken	0.92
Lowgren, 1992	DE and ME	cereals, lupin, rapeseed oilmeal	pig	0.94
van der Meer and Perez, 1992	OM	89 samples	pig	0.85
Boisen and Fernandez, 1997	energy	90 samples of 31 feeds	pig	0.88
Huang et al., 2003a	energy	hulled and hull-less barley	pig	0.93
Noblet and Jaguelin-Peyraud, 2007	OM and energy	113 compound feeds	pig	0.83
Regmi et al., 2008	energy	barley	pig	0.97
Regmi et al., 2009	energy	wheat	pig	0.82

[a] AA, amino acids; CP, crude protein; DE, digestible energy; ME, metabolizable energy; OM, organic matter.

Chapter 3 Application of vibrational spectroscopy to characterize nutrient digestion discrepancies between monogastric animals and in vitro digestion models: Critical review and research perspectives

3.1 Abstract

To select infrared instrumentation to identify discrepancies in nutrient digestion between in vitro and in vivo digestion models, the application of near-infrared (NIR) and mid-infrared (MIR) spectroscopy was reviewed. The capability, advantages, and limitations of NIR and MIR to identify nutrients and their structural changes during digestion and to predict nutrient content or digestibility are discussed. The small amount of residue following in vitro digestion means that a Fourier transform infrared (FT-IR) spectrometer with attenuated total reflection (ATR) is a feasible option to qualitatively identify discrepancies in digestion using MIR spectroscopy. Then, a non-calibration method is desired to quantitatively characterize discrepancies between in vitro and in vivo digestion.

3.2 Introduction

3.2.1 A need to characterize in vitro digestion

Simulation of digestion with in vitro digestion (**IVD**) models is a promising approach to evaluate nutrient and energy digestibility of feedstuffs (Boisen and Fernandez, 1997; Moughan, 1999; Noblet and Jaguelin-Peyraud, 2007; Regmi et al., 2008; Regmi et al., 2009). A validated IVD model might be

attractive to supply reference data to develop near-infrared (**NIR**) reflectance spectroscopy (**NIRS**) calibrations (Regmi et al., 2008; Losada et al., 2010). However, established IVD models did not accurately predict digestible energy (**DE**) for corn co-products in pigs (Anderson, 2009). To determine energy digestibility in these IVD studies, undigested residues of the IVD model were burnt using bomb calorimetry (Regmi et al., 2009). Thus, information about digestion of energy yielding macronutrients was not obtained. To improve the IVD technique, identification of discrepancies between IVD and in vivo digestion of nutrients is essential. However, the small quantity of undigested residue following IVD (50 to 200 mg) is not sufficient for conventional chemical analysis; thus, characterization of problems with IVD models is limited.

3.2.2 Vibrational spectroscopy, a promising method

To identify discrepancies between IVD and in vivo digestion of nutrients, candidate methods must be able to detect nutrients qualitatively and quantitatively in small amounts of sample. Vibrational spectroscopy, measuring molecular vibrations (Griffiths, 2002b), may assist to unveil these discrepancies. Spectra that are induced by molecule vibrations contain a wealth of chemical information. Equipment such as Fourier transform infrared (**FT-IR**) equipped with attenuated total reflection (**ATR**) permits acquisition of information on small amounts of residues from IVD models (Hannah, 2002; Milosevic, 2004). Other vibration techniques, such as nuclear magnetic resonance (**NMR**) spectrometry, X-ray diffraction, and mass spectrometry may take precedence over infrared (**IR**) spectrometry to determine molecular structure. However, IR spectrometry

requires less expensive instrumentation (Griffiths, 2002b) and is not limited by molecular weight of an analyte. For instance, NMR spectroscopy can only be applied to proteins with molecular weights less than 20,000 Da (Jackson and Mantsch, 1995).

Vibrational spectroscopy has wide application in pharmaceutical, and natural sciences (Chalmers and Griffiths, 2002). In agriculture, NIRS has been used for several decades to predict quality of agricultural products, such as grain moisture (Williams, 1975), wheat protein (Williams and Cordeiro, 1979), wheat amino acids (**AA**) (Williams et al., 1984), wheat hardness (Norris et al., 1989), and acid detergent fiber (**ADF**) in forages (Barton, 1991). The NIRS methods to determine moisture (forage), ADF (forage) and protein (forage, wheat) did become official methods (AOAC, 2006). The use of NIRS can also predict digestible nutrient values of feed, such as dry matter (**DM**) digestibility of forages (Norris et al., 1976), crude protein (**CP**) digestibility of silage (Swift, 2003), digestible AA of feedstuffs in poultry (van Kempen and Bodin, 1998) and DE value of barley in pigs (McCann et al., 2006; Zijlstra et al., 2011). Applications of NIRS in animal nutrition have been reviewed previously (Givens and Deaville, 1999).

For most applications, spectroscopy was a secondary method to predict chemical content or nutritive values of feed, rather than to evaluate nutrient digestion using digesta or feces. Still, fecal spectra were used to investigate nutrient digestion in herbivores (Dixon and Coates, 2009), cattle (Coleman and Murray, 1993; Purnomoadi et al., 1998; Boval et al., 2004; Garnsworthy and Unal,

2004), rabbit (Meineri et al., 2009), and sheep (Decandia et al., 2009). Mid-infrared (**MIR**) spectroscopy, such as ATR FT-IR spectroscopy and diffuse reflectance FT-IR spectroscopy (**DRIFTS**), was widely used to characterize nutritive quality of feed (Mahesar et al., 2011; Yu, 2011). To evaluate IVD, FT-IR has been used rarely, such as prediction of residual starch from in vitro fermentation (Udén, 2009), volatile fatty acid (**VFA**) concentrations (Udén and Sjaunja, 2009), and starch crystallinity changes during enzymatic IVD (Shrestha et al., 2010). To our knowledge, the application of IR spectroscopy to characterize undigested residues from IVD simulating nutrient digestion in pigs has not been reported.

As each type of spectroscopy has its particular characteristics, a critical review with a research perspective is needed to scrutinize if available IR spectroscopy fulfills the need to characterize nutrient digestion discrepancies between IVD and in vivo digestion.

3.3 General considerations on the selection of infrared spectroscopy

Each type of spectroscopy has strengths and weaknesses. The infrared spectrum is divided into 3 wavelength regions (Osborne et al., 1993), NIR (750–2,500 nm or 13,333–4,000 cm^{-1}), MIR (2,500–25,000 nm or 4,000–400 cm^{-1}), and far-infrared (**FIR;** 25–1,000 μm or 400–10 cm^{-1}). The NIR, MIR, and FIR differ in wavelength, and also in transitions between quantized vibrational energy states (Griffiths, 2002b). When molecules are excited by IR radiation energy, the vibrational frequencies change to higher states (ν_0 to ν_n). Fundamental energy

differences (ν_0 to ν_1) are measured in the MIR spectrum (Griffiths, 2002b). The MIR spectra are easy to interpret, because peaks above 1,500 cm^{-1} of MIR spectra can be assigned confidently to specific functional groups, e.g. O-H, C-H, N-H, C=O etc. (Miller, 2004b). Samples for MIR measurement using DRIFTS often need dilution to avoid specular reflection (Yu, 2011), which may distort band intensity in the fingerprint region (Olinger and Griffiths, 1993; Pandey and Theagarajan, 1997). The dilution process is inconvenient. The ATR technique requires minimal sample preparation and permits gathering quantitative information on small quantities of sample; thus, it is more convenient than DRIFTS (Kos et al., 2004). However, ATR has a shallow penetration depth, usually only a couple of micrometers (Ekgasit and Ishida, 2002), which is smaller than the particle size (4.8-60.0 μm) of starch granules (Sevenou et al., 2002; Warren et al., 2011; Uarrota et al., 2013). The small quantity of sample and shallow penetration depth may raise a concern regarding sample homogenization. Nevertheless, ATR can be used for quantitative analysis (Coates, 2002).

In the NIR region, the spectrum is mainly composed of overtone and combination bands of fundamental frequencies measured in the MIR region. Overtones are higher vibrational frequencies of molecule ($\geq\nu_2$) and have weaker intensity compared with fundamental bands. Samples can be measured without dilution; thus, require minimal sample preparation. Another advantage of NIRS over MIR is that NIR light penetrates deeper into a sample than MIR radiation. For NIRS measurements, penetration depth, also known as path length, depends on particle size and packing density, but starts at 0.1 mm for most powders and

increases to several millimeters as the visible region (700 nm) is approached (DeThomas and Brimmer, 2002). However, in contrast to the small quantity of sample used for ATR FT-IR, NIR requires more sample for analysis, which limits investigation of undigested residues of IVD, because it may require pooling from many replicates just for one scan (Wilman et al., 2000). The NIR spectra are not as easy to interpret as MIR spectra, because broad bands are derived from several functional groups, but they are amenable to multivariate statistical analysis (Griffiths, 2002b). The NIRS predictions rely on multivariate calibration and also accurate reference analysis (Blakeney and Flinn, 2005).

For quantitative analysis, Beer's law is the fundamental law of quantitative absorption spectroscopy, and denotes that absorbance is proportional to concentration of an analyte (Griffiths, 2002b). Notably, linear absorbance of IR spectra is rarely measured directly (Griffiths, 2002b). Some factors may cause deviation of Beer's law, such as variation of absorptivity caused by high concentration and intermolecular interactions, detector nonlinearity with FT-IR spectrometers, etc. (Griffiths, 2002a). These factors may guide the selection of FT-IR instrument and proper spectra acquisition. For instance, response linearity of FT-IR spectrometer equipped with deuterated triglycine sulfate pyroelectric detectors is better than that with mercury cadmium telluride detectors, especially if the sample has several strongly absorbing bands for which a linear variation of absorbance with concentration is desired (Griffiths, 2002a). Peak absorbance is also meaningful for Beer's law, and should not be greater than 4 absorbance units (**AU**), and ideally less than 1 AU, to ensure Beer's law is obeyed (Griffiths,

2002a). Beer's law assumes that the absorbing medium is homogeneous and does not scatter radiation. When samples scatter incident radiation, the effective path length can vary drastically and may cause deviations from Beer's law. To consider this potential deviation, samples being prepared as KBr disks or mineral oil mulls should be ground finely, ideally to a particle size of less than 1 μm (Griffiths, 2002a).

To grind small amounts of IVD residue to such a fine particle size is a challenge. Using ATR FT-IR, very fine particles in mixtures with coarse particles may result in a non-linear relation between absorbance (peak height) and concentration of a component (Planinšek et al., 2006). Other factors, such as a small air gap between the internal reflection element (**IRE**) of ATR, may cause a large decrease in spectral intensity, according to the nature of the mean square electric field; thus, perfect optical contact between the IRE of ATR and sample is required (Ekgasit and Ishida, 2002). Beer's law also indicates that absorbance is proportional to path length; thus, the use of band ratios for applications involving an indeterminate path length (variations in sample thickness) is common practice (Coates, 2002).

To investigate nutrient digestion quantitatively, high quality of spectra is essential. Normally, the detector of NIR spectrometers is more sensitive than that of MIR spectrometers. The signal to noise ratio of NIR spectra could be as high as 10,000:1, whereas MIR was questioned in the past for quantitative analysis because of a low signal to noise ratio (Givens and Deaville, 1999). With improved technology (Milosevic, 2004), the ATR FT-IR instrument could nowadays have a

signal to noise ratio as high as 50,000:1 (ABB, 2011). As most quantitative measurements can be accomplished with a signal-to-noise ratio in the range 1,000:1 to 5,000:1 (Coates, 2002), the ATR FT-IR ought to be capable of quantitative analysis. This capability was evidenced by slightly better calibrations using MIR than NIRS for predicting carbon content in soils (McCarty and Reeves, 2006; Bellon-Maurel and McBratney, 2011), and for AA content in 141 meat and bone meal samples (Qiao and van Kempen, 2004). However, single reflection ATR is signal-limited when compared with transmission spectroscopy (van de Voort et al., 2007), and multiple reflection ATR FT-IR could extend the detection limit (Mossoba et al., 2012). Both NIR and MIR spectroscopy have potential for quantitative analysis (Reeves, 2010). However, a high detection limit of NIRS means NIRS is not suitable for trace analysis (Luypaert et al., 2007). Because NIRS is sensitive to water content (Munck et al., 2004), analysis of dried undigested residue for IVD and in vivo digestion is practical. An NIRS calibration on dried silage samples was more accurate than a calibration based on undried silage samples (Castro et al., 2002). Methods to prepare dry samples, e.g., oven- or freeze-drying, can affect NIR spectra; thus, consistent sample preparation is important (Alomar et al., 1999).

3.4 Qualitative characterization of digestion discrepancies

To characterize discrepancies in nutrient digestion between IVD and in vivo digestion, use of spectroscopy for qualitative analysis of digesta (intermediate digestion product) or final undigested residue needs examination. One elemental

question is whether spectroscopy can detect nutrient disappearance or appearance, and chemical structure changes of diets during digestion. Another question would be how we can better characterize digestion discrepancies by applying spectroscopic methods.

3.4.1 Nutrient disappearance and appearance

Chemical composition of samples could be determined by detecting the position and intensity of a specific peak or area with spectroscopy. According to vibrational theory, spectra bands in the MIR region are well defined and linked to functional groups (Shurvell, 2002) and can be used to judge the absence or presence of specific functional groups of nutrients. Peaks of NIR spectra of biological samples overlap and are less distinctive than MIR spectra peaks; thus, to conclude the absence of certain functional groups simply by visual examination of NIR spectra might be difficult. Semi-empirical methods are often used to assign NIR bands (Weyer and Lo, 2002). Characteristic bands of macronutrients in MIR and NIR are outlined in Table 3.1. However, we need to scrutinize the application of spectroscopy to characterize the presence or absence of nutrients in feed and undigested residues.

3.4.1.1 Protein

Proteins are large polymers of AA with 4 levels of structure: primary, secondary, tertiary, and quaternary (Smith, 2010). In MIR, protein can be identified by a contour of 2 diagnostic peaks (Figure 3.1) of amide I and II (Miller, 2003). The amide I peak centered at ca. 1,650 cm^{-1} is induced primarily by carbonyl (C=O) stretching plus minor contributions from C-N stretching of

peptide links in the secondary amide of protein and polypeptides (Barth, 2007). The analyses of α-helix and β-sheet peaks in amide I region were used to characterize protein molecular structure of yellow and brown *Brassica* canola seed (Yu, 2008). The amide II peak centered at ca. 1,550 cm^{-1} is induced by a mixture of the C–N stretch and the N–H in-plane bending (Miller, 2003). The amide I and II peaks were used as evidence of little protein being present in pericarp and more protein being present in endosperm of corn (Yu et al., 2004b). Other protein peaks, e.g., amide A (3,300 cm^{-1}), amide B (3,100 cm^{-1}), and amide III-VII also indicated the presence of protein (Carbonaro and Nucara, 2010). The amide III region (1,301-1,229 cm^{-1}) was used to analyze protein secondary structure, because this region is free from the interference of the strong absorption by water between 1,640 and 1,650 cm^{-1} in amide I region. However, it suffers from interference from the side chain of peptide in the amide III region and weak absorbance in this region (Fu et al., 1994; Cai and Singh, 2004). Also, the ester in fat has a peak in this region due to the anti-symmetric stretching of C-O-C (Shurvell, 2002). Thus, the amide III region is less useful for visual examination of protein presence or disappearance. Side chains of protein might also be inspected with MIR spectra, such as proteins with tyrosine residue having a strong peak at 1,515 cm^{-1} (Bendit, 1967). The use of MIR to characterize protein has been reviewed (Jackson and Mantsch, 1995; Schweitzer-Stenner, 2006; Barth, 2007).

The first overtone of the fundamental N-H stretch vibrational mode is in the NIR region. However, the first overtone of C=O in amide still occurs in the

MIR region, and the second overtone of C=O appears in the NIR region. Because intensities decrease usually by a factor of 10 to 100 for each step from fundamental to overtone, intensity of C=O in the NIR region is negligible (Siesler, 2001). Thus, N-H overtones dominate the presence of protein in the NIR region. Important wavelengths for protein include the carbonyl stretch of the primary amide at 2,060 nm, and 2,168 to 2,180 nm as combination band consisting of N-H bending second overtone, C-H stretching, C=O stretch, N-H in-plane bending, and C-N stretching (Workman and Weyer, 2012). The bands at 2,050 to 2,060 nm indicating N-H stretching vibrations are also useful (Shenk et al., 2001). The 2,070 nm wavelength was characteristic of N-H stretching in R-CO-NH_2 in ammoniated barley straw (Barton et al., 1986). The NIR spectral regions of amide A/II at 2,055-2,065 nm and amide I/III at 2,175-2,180 nm were used to visually compare changes of protein content during wheat maturation (Gergely and Salgo, 2007); bands at 1,506, 2,167 nm (amide B/II), 2,184 nm (glutamine) and 2,209 nm (amide A/III) were also linked to protein in barley, gluten powder, and wheat grain (Fox et al., 2002; Bruun et al., 2007; Butkute and Ceseviciene, 2009).

3.4.1.2 Fat and fatty acids (FA)

Fats in animal- or plant-based feedstuffs are mainly triacylglycerols. Triacylglycerols, or triglycerides, are triesters of glycerol with 3 molecules of FA (Smith, 2010). Free fatty acids (**FFA**) exist in feed, such as in distillers dried grains with solubles (**DDGS**) from ethanol processing of corn (Moreau et al., 2011). In digesta and feces, FFA also exist (Holtug et al., 1992).

Functional groups of fat include methyl, methylene, ester, and the

backbone of the carbon chain with double or single bonds. In the MIR region, peaks of functional groups of fat are prominent. The aliphatic carbon chain composed of methylene has typical and prominent C-H anti-symmetric and symmetric stretching peaks at 2,926 ± 10 cm^{-1} and 2,853 ± 10 cm^{-1} (Figure 3.1) and the all-in-phase methylene rocking mode of $(-CH_2-)_n$ near 720 ± 3 cm^{-1} (Mayo, 2004). For triglyceride, the ester carbonyl (C=O) peak (Figure 3.1) appears at 1,742 to 1,749 cm^{-1} (Yang and Irudayaraj, 2000; Budevska, 2002; Larkin, 2011). The ester peak at 1,736 cm^{-1} was used as evidence of lipid presence in pericarp of corn (Yu et al., 2004b). For FFA, the peak of C=O in carboxylic acids appears at 1,710-1,712 cm^{-1} (Lanser et al., 1991; Yu et al., 2011b). For unsaturated fat or FA, a sp^2 carbon (-C=C-H) peak exists at 3,010 cm^{-1} depending on the extent of unsaturation and polyunsaturated fatty acid (**PUFA**) species (Yoshida and Yoshida, 2003; Miller, 2004a). Combining information of these peak positions can give decisive information to determine the existence of fat or FFA.

In the NIR region, the first overtones of C-H stretching occur between 1,650 and 1,850 nm (Westad et al., 2008). The asymmetric and symmetric modes of the combination of C-H stretching and CH_2 bending motions present 2 strong bands near 2,307 and 2,347 nm as Fermi resonance which occurs when an overtone or combination band absorbs at approximately the same frequency of a fundamental mode involving the same atoms (Ricard-Lespade et al., 1990). These bands are prominent in spectra of pig fat (Pérez-Marín et al., 2007), feces (Coleman and Murray, 1993), edible oils (Hourant et al., 2000), and other high fat products (Kays and Barton, 2002). The band with a maximum around 1,210 nm

and a shoulder at 1,164 nm may indicate degree of unsaturation (Hourant et al., 2000; Westad et al., 2008). However, peaks/bands in NIR spectra were broader and weaker than those in MIR spectra. The NIRS was less efficient than MIR spectroscopy to discriminate and classify oils and fats (Yang et al., 2005).

3.4.1.3 Starch

Starch is a polymer of repeating glucose units joined in α-glycosidic linkages (Smith, 2010). In MIR, starch has strong and broad absorption bands at 3,900 to 3,000 cm^{-1} due to O-H stretching, and at 1,200 to 900 cm^{-1} due to ring vibrations overlapped by stretching vibrations of C-OH side groups and C-O-C glycosidic bond vibration (García et al., 2009; Uarrota et al., 2013; Zhang et al., 2013). Starch has some featured peaks, such as a peak at ca. 1,022 cm^{-1} and another peak at ca. 995 cm^{-1} (García et al., 2009). The peak at 1,022 cm^{-1} is also observed in α-D-glucose (Vasko et al., 1972), and collectively induced by C-O (55%), C-OH (24%), and C-C (17%; Vasko et al., 1972). The peak at 995 cm^{-1} is sensitive to changes in degree of crystallinity, domain size, molecular arrangement, and moisture content during retrogradation (van Soest et al., 1995; Smits et al., 1998). The peak at ca. 1,078 cm^{-1} is related to starch, starch digestion intermediates, or end products (Schindler et al., 1997). The peak at ca. 1,076 cm^{-1} was also observed in α-D-glucose, and was collectively induced by C-O (57%), C-C (25%), and C-OH (23%; Vasko et al., 1972). The peak at ca. 1,047 cm^{-1} is characteristic of crystalline starch and observed in native rice starch (Smits et al., 1998; Nakorn et al., 2009). Starch also has a glycosidic linkage peak at ca. 1,149 cm^{-1} (Kuhnen et al., 2010). In the anomer region associated with configuration of

anomeric carbon (Dauchez et al., 1994), starch has peaks of α-anomers at 930 and 857 cm^{-1} due to C-H bending (Zhbankov, 1992; Irudayaraj and Yang, 2002) that differ from cellulose with β-anomers at 897 cm^{-1} (Zhbankov, 1992; Kačuráková et al., 2000). The peaks at 1,025, 929, and 860 cm^{-1} were used as evidence of non-structural carbohydrate such as starch in the endosperm of corn grain (Yu et al., 2004b). Field pea starch also has peaks at 985 and 1,074 cm^{-1} that are characteristic of the anhydroglucose ring O-C stretch (Zhang and Han, 2006). The molecular structure of starch is mainly linear α-1,4 D-glucan for amylose; and α-1,4 with branched α-1,6 D-glucan for amylopectin (Zobel, 1988). Dextran, an intermediate luminal digestion product (Yen, 2001), is mainly α-(1→6)-linked glucan (Mischnick and Momcilovic, 2010). The α-(1→4) linkage (930 ± 4 cm^{-1}, type 1; and 758 ± 2 cm^{-1}, type 3) can be distinguished from the α-(1→6) linkage (917 ± 2 cm^{-1}, 768 ± 1 cm^{-1}; Mathlouthi and Koenig, 1987).

The first overtone of featured bands of starch in MIR at 1,200-800 cm^{-1} is still in the MIR region, and only the first overtone of O-H is in the NIR region. Thus, NIR spectra are less diagnostic for presence or disappearance of starch. Indeed, NIR spectra do contain information associated with starch. With calibrations, NIRS can predict starch content in feed grains (Kim and Williams, 1990), wheat (Garnsworthy et al., 2000), barley grain (Byung Joo et al., 1995), whole kernels of maize (Wei et al., 2004; Jiang et al., 2007), alfalfa (Albrecht et al., 1987), and cotton leaves (Hattey et al., 1994). The NIRS can predict different starch types, such as resistant starch (**RS**) in sweet potato (Tang et al., 2011) and amylose content in rice starch (Jinsong et al., 2007). The NIR can evaluate starch

hydrolysis by monitoring the dextrose equivalent (Blanco et al., 2000; Storz and Steffens, 2004). Some bands related to starch were documented, such as main absorbance of starch in wheat at 2,060, 2,096, and 2,282 nm (Kim and Williams, 1990); in cotton leaves at 1,548, 1,588, 2,328, and 2,338 nm (Hattey et al., 1994). The peaks around 700, 1,962, 2,290, and 2,330 nm have also been linked to starch (Butkute and Ceseviciene, 2009). Three important wavelengths at 970 nm, 1,155 nm, and 1,395 nm were associated with amylopectin retrogradation (Xie et al., 2004). The spectrum between waxy and non-waxy grains also displayed different profiles, especially in the region from 1,932 to 2,292 nm: waxy rice displayed a 'W' shape of profile, while the non-waxy rice displayed relatively linear lines (Jinsong et al., 2007). Overall, it is less conclusive to define specific wavelengths for the identification of starch.

3.4.1.4 Fiber

Non-starch polysaccharides (**NSP**) are the non-α-glucan polysaccharides in plant tissue (Englyst et al., 1982), including cellulose, hemicellulose, and pectin. Unlike starch, NSP are resistant to pancreatic amylase (Englyst and Cummings, 1985). Globally, the amount of co-products in swine diets in expected to continue to increase; thus, pigs are fed diets with a greater NSP content than traditional cereal-based diets (Zijlstra et al., 2010). Thus, evaluation of NSP digestion is crucial for both IVD and in vivo digestion.

For MIR, NSP have a broad band of O-H stretch (Mathlouthi and Koenig, 1987), with differing band shapes for NSP (Zhbankov, 1992; Zhbankov et al., 2002). With visual examination, the broad O-H stretch area has less diagnostic

value. However, NSP have distinct absorption band maxima in the MIR region at 1,200-800 cm^{-1} (Kačuráková et al., 2000). This region is dominated by ring vibrations overlapped with stretching vibrations of side groups (C-OH) and the glycosidic (C-O-C) bond vibration (Kačuráková et al., 2000). The region at 950-750 cm^{-1} is useful to distinguish bands characteristic for α and β anomers (Mathlouthi and Koenig, 1987; Kačuráková and Wilson, 2001).

Cellulose, an unbranched polymer composed of repeating 1→4-β-linked glucose units (Smith, 2010) has a characteristic band at about 898 cm^{-1} (Figure 3.1) for the β-anomer (Kačuráková et al., 2000; Yuen et al., 2009; Rana et al., 2010). Hemicellulose also has a band at 898 cm^{-1} (Pandey and Theagarajan, 1997). The anomer peak position differs with cellulose type as a consequence of rotations around C5C6 and C6O6 bonds and intra- and intermolecular hydrogen bonds. For celluloses I, II, and III, the anomer peaks are at 894 cm^{-1}, 898 cm^{-1}, and 894 cm^{-1} respectively (Zhbankov et al., 2002). Cellulose also has other featured bands. The peak at 1,106-1,107 cm^{-1} is associated with C-O, C-C, and ring vibrations, and was observed in spectra of wood (Pizzo et al., 2013), β-(1→3)-D-xylan (Kačuráková et al., 1999), and carboxy-methylated NSP (Yuen et al., 2009). The peak at 1,113 cm^{-1} was assigned to the O-H association band in cellulose and hemicellulose; and at 667 cm^{-1} was assigned to C-OH out of plane bending in cellulose (Pandey and Theagarajan, 1997). Moreover, peak intensity at 897 (R^2 = 0.95) and 667 cm^{-1} (R^2 = 0.94) correlated with percentage of cellulose analyzed chemically (Abidi et al., 2013). The band at 1,033 cm^{-1} is characteristic of native crystalline cellulose (Nakashima et al., 2008). The absence of peak at

1,033 cm^{-1} could indicate absence of cellulose or at low concentrations (Philippe et al., 2006).

The glycosidic region at ca. 1,160 cm^{-1}, induced by the glycosidic linkage C-O-C, is useful to distinguish fiber from starch and different NSP, such as 1,161 cm^{-1} for β-(1→4)-glucan, 1,155 cm^{-1} for galactose, 1,153 cm^{-1} for xyloglucan, 1,151 cm^{-1} for β-(1→4)-xylan (Kačuráková et al., 2000). The peak at 1,158 cm^{-1} was assigned to C-O-C asymmetric stretch vibration in cellulose and hemicellulose (Pandey and Theagarajan, 1997), whereas the peak for starch was at 1,149 cm^{-1} (Kuhnen et al., 2010). The vibrational modes of C-O-C in triglycerides have a peak at 1,159-1,161 cm^{-1} (Yoshida and Yoshida, 2003).

Hemicelluloses include xyloglucans, xylans, glucomannans, and galactoglucomannans (Kačuráková et al., 2000). Arabinoxylan is a xylan-type hemicellulose and rich in wheat bran. Cereal arabinoxylan has main chains composed of (1→4)-linked β-D-xylopyranosyl residues and has typical bands at 1,045 and 898 cm^{-1} (Hromádková et al., 2013). Two bands at 984 and 958 cm^{-1} were highly related to degree of substitution of the xylose backbone by arabinose side units in wheat endosperm (Robert et al., 2005; Philippe et al., 2006). The ratio of peak intensity at 1,164 and 990 cm^{-1} can indicate arabinofuranosyl (Kačuráková et al., 1994), which is valuable to study arabinoxylan type polysaccharides and xylan component behaviour of plant materials. For α-linked arabinan, the band maximum was at 1,039 cm^{-1} (Kačuráková et al., 2000).

The β-glucans are linear 1→4 β-linked glucose polymers and mixed linkage β-glucans contain 1→3 linkages interspersed with 1→4 linkages. They

are rich in cereal grains such as oat and barley (George et al., 2000; Izydorczyk and Dexter, 2008; Vasanthan and Temelli, 2008). In the anomer region, pure barley β-glucan shows a peak at 895 cm^{-1} (Seefeldt et al., 2009). The absorption bands at 1,155 and 1,078 cm^{-1} were observed in spectra of aleurone cell walls of wheat grain (Jamme et al., 2008). The band centered at 991 cm^{-1} characterized the presence of β-(1→3)(1→4) glucans in cell wall of wheat grain (Philippe et al., 2006). The peak area at 1,420 cm^{-1} could be used to detect β-glucan in canola seed (Yu et al., 2005).

Pectins are complex polysaccharides with a linear backbone built up of (1→4)-linked α-D-galacturonan with regions of alternating (1→4)-α-D-galacturonic acid and (1→2)-α-L-rhamnopyranosyl residues (Kačuráková et al., 2000). Pectin has strong bands at 1,100 and 1,017 cm^{-1} (Kačuráková et al., 2000).

Lignins are polymeric aromatic constituents in plant cell walls and are not NSP (Derkacheva and Sukhov, 2008). Aromatic skeletal vibrations of lignin have a characteristic peak at 1,505-1,510 cm^{-1}, and other bands at 1,465, 1,270, 1,140, and 1,030 cm^{-1} (Derkacheva and Sukhov, 2008; Gelbrich et al., 2008; Rana et al., 2010; Zhou et al., 2011).

For NIR, the first overtone of O-H stretch is in the NIR region, but the first overtone of vibrations in the anomer region of fiber is in the MIR region. The combination of O-H bending and C-O stretch overtones have a strong peak centered at 2,100 nm (Workman and Weyer, 2012), which is characteristic of alcohols. This peak appears in compounds possessing alcoholic OH groups, such as sugars, starch, and cellulose. Information from 2,000-2,200 nm is repeated at

1,400-1,500 nm in the second overtone region, but it may be easily confused with water having a similar absorbing band (Coleman and Murray, 1993). For cellulose, bands of functional groups include C-H at 2336 nm, CH_2 at 2270 nm, and O-H groups at 2,044-2,164 nm (Munck et al., 2004; Modzelewska et al., 2011). The NIRS may verify high (1→3, 1→4)-β-glucan and low starch content in barley (Munck et al., 2004). Wavelengths at 2,325 nm is associated with indigestible fiber (Barton et al., 1986).

For lignin, the most prominent band is the first overtone of the C-H stretching vibration of aromatics near 1,672 nm. Another characteristic lignin band is located near 1,446 nm; this band is assigned to the phenolic hydroxyl group of lignin (Krongtaew et al., 2010). When amount of lignin in sample is small, lignin is difficult to detect in the NIR spectra. Absorption for lignin was less pronounced in the combination region at 2,260-2,280 nm. However, this absorption is shared with cellulose (Coleman and Murray, 1993).

3.4.2 Identification of nutrients structural changes

3.4.2.1 Protein structure change

Denaturation (unfolding) of protein in a gastric acid environment involves disruption of hydrogen bonding interactions between polar AA (Herman, 2006; Smith, 2010). Denatured protein is broken down by protease into small peptides and free AA (Yen, 2001). Digestion of protein thus changes protein structure. The MIR spectroscopy is an established tool to characterize protein structure (Jackson and Mantsch, 1995), such as monitoring structural changes during protein folding and unfolding (Fabian et al., 1993; Chung et al., 2004; Buchner et al., 2011).

Denaturation and aggregation of protein coincided with fewer α-helices at 1,644-1,653 cm^{-1} and turns at 1,672 cm^{-1}, and a simultaneous increase of intermolecular anti-parallel β-sheets at 1,620-1,632 and 1,681-1,690 cm^{-1} (Fabian and Naumann, 2004; Sokolowski and Naumann, 2005). The MIR could detect the formation of non-native β-sheets and provide a clearer picture of structural changes than circular dichroism method (Fabian et al., 2005). Two-dimensional MIR spectroscopy revealed that unfolding of α-helices temporally proceeds before temporal changes in regions of its native β-sheet structure (Fabian et al., 2010). In feed science, protein structure changes induced by gene-transformation, heating, and bio-ethanol processing were investigated (Yu, 2010). Protein structure changes in co-products were linked to metabolizable protein available to dairy cattle (Yu and Nuez-Ortin, 2010). Multi-component peak modeling is often used to quantify protein secondary structures. The Gaussian method is more accurate for fitting multi-peak curves of protein secondary structures of various plant seed tissues than the Lorentzian method (Yu, 2005). The method for curve-fitting is valuable to characterize protein secondary structure changes between IVD and in vivo digestion. Notably, sample moisture may affect determination of secondary structure of the protein, because of its interfering absorbance in amide I area (Wong et al., 2009; Buchner et al., 2011).

The NIRS can monitor protein secondary changes (Bruun et al., 2007). The increases of peak intensity at 2,209 nm and decreases of peak intensity at 2,167-2,182 nm in second-derivative spectra were attributed to heat denaturation and an indication of α-helix to β-sheet transformation. The NIR spectra were

interpreted by comparison to existing knowledge of gluten protein obtained in ATR FT-IR and NMR studies.

3.4.2.2 Fat structure change

Digestion of dietary fats with gastric and pancreatic lipase breaks down triglycerides into diglycerides, monoglycerides, and FFA; the unsaturated FFA may then be hydrogenated by gut microflora before forming Ca soaps (Yen, 2001).

Triglycerides are tri-esters of glycerol with 3 molecules of FA (Smith, 2010), with a characteristic ester C=O peak at ca. 1,743 cm^{-1} in MIR spectra due to stretching vibration of the carbonyl group (Moya Moreno et al., 1999). Oxidation of fat broadens the band at 1,743 cm^{-1} to lower wavenumber; and the absorbance maximum of decomposed products of fat is between 1,700 and 1,726 cm^{-1}. Thus, the total carbonylic compounds formed after fat decomposition can be quantified by measuring the broadening area between 1,700 and 1,726 cm^{-1} compared with between 1,840 and 1,743 cm^{-1} that is proportional to esters exclusively (Moya Moreno et al., 1999). For diacylglycerolipids, the absorption bands of sn-1 and sn-2 ester C=O stretching with maximum at 1,733 cm^{-1} are usually resolved into 2 comparably intense components that exhibit maxima near 1,743 and 1,728 cm^{-1} (Lewis et al., 1994). The absorption band of ester C=O in monoglyceride is at 1,710-1,729 cm^{-1} (Das et al., 2013). When fat breaks down to FFA, absorption of the ester C=O stretch peak at 1,743 cm^{-1} decreases, whereas absorbance of the peak of C=O in carboxylic acids at 1,710 cm^{-1} increases (Jakobs et al., 2000). The peak of FFA at 1,712 cm^{-1} has been used in a direct method to

determine FFA in edible oils (Yu et al., 2011b).

Fat changes in the hind gut can be summarized as saturation, formation of trans fat and oil soap (Hamilton and McDonald, 1969; Devillard et al., 2009). Fat saturation was monitored by the cis-alkene (H-C=C-H) absorption bands around 3,010 cm^{-1} for the C-H stretching vibrational mode (Yoshida and Yoshida, 2003), because saturated fats do not have double bonds; hence, this peak is absent. The cis double bonds in unsaturated fat introduce kinks in the long hydrocarbon chain, and make close packing of molecules difficult. For saturated fat without double bonds, the three side chains of saturated lipid lie parallel; thus, the triacylglycerol molecules may pack efficiently in a crystalline lattice (Smith, 2010). The band position of the symmetric CH_2 stretching vibration corresponds with the conformational state at ca. 2,850 cm^{-1} for the fully ordered state and at ca. 2,854 cm^{-1} for the fully disordered state (Wolkers, 2009).

For trans-fat formation during digestion, the C-H out-of-plane deformation band at 966 cm^{-1} is characteristic of isolated double bonds with trans configuration (Mossoba et al., 2007; van de Voort et al., 2008). Using this peak in ATR FT-IR spectra to determine total trans content in oil is an official method (AOCS, 1993; Mossoba et al., 1996). The ATR FT-IR spectroscopy can also determine trans FA in ground cereal products without oil extraction (Kim et al., 2007).

The MIR spectroscopy might detect oil soap formation during digestion. Soaps are metal salts of FA (Smith, 2010). The C=O stretch in carboxylate has a band at ca. 1,570 cm^{-1} (Yu et al., 2011b). Opposite to triglycerides, the FA salt,

e.g. Ca palmitic acid salt, does not have a peak in ester C=O region at 1,743 cm^{-1} (Larkin, 2011). With Ca-soap formation in feces (Gacs and Barltrop, 1977), Ca carboxylate may contain carboxylate groups coordinated with Ca ions in unidentate and bidentate modes with a doublet at 1,540 and 1,575 cm^{-1} in MIR spectra (Lu and Miller, 2002). However, validation with feces is required.

3.4.2.3 Starch crystallinity change

Starch crystallinity and structure type of granule (A, B, C) differ with starch source and digestibility with α-amylase (Zobel, 1988; Regmi et al., 2011). The MIR spectroscopy can elucidate starch crystallinity. The MIR spectrum of starch is sensitive to changes in short-range structure in the C-C and C-O stretching region at 1,300-800 cm^{-1} (van Soest et al., 1995). The band at 1,047 cm^{-1} is sensitive to crystalline starch and the band at 1,022 cm^{-1} is characteristic of amorphous starch (van Soest et al., 1995; Nakorn et al., 2009). Intensity of the band at ca. 1,022 cm^{-1} increases with decreasing crystallinity (García et al., 2009). The absorbance ratio at 1,045 and 1,022 cm^{-1} can follow crystallinity of starch components during storage, because the amount of amorphous starch decreases with a concomitant increase in crystallinity. When the ratio of peak intensity at 1,045 and 1,022 cm^{-1} increased, crystallinity was greater in tortillas (Hernandez-Uribe et al., 2010). The ratio of 1,018 and 999 cm^{-1} indicated amylose and amylopectin in maize flours (Kuhnen et al., 2010); and the ratio of bands at 1,022 and 1,000 cm^{-1} can index the proportion of ordered to amorphous starch structure (Warren et al., 2011). With this relation, factors affecting α-amylase-catalysed hydrolysis kinetics of starch were investigated. Using ATR FT-IR, IVD of

extruded high amylose maize starch was investigated (Shrestha et al., 2010). However, ATR FT-IR is insensitive to long range crystalline ordering of starch granules. Instead, ATR FT-IR provides a measure indicating the amount of short range carbohydrate structuring (Warren et al., 2011). The ATR is a surface specific technique, because the IR beam only penetrates about 2 μm deep in the region 1,200-800 cm^{-1} used in studies of starch structure (Sevenou et al., 2002). The ATR FT-IR cannot differentiate between A- and B-type crystallinity of external regions of starch granules (Sevenou et al., 2002). Limits of ATR FT-IR spectroscopy was also reported for quantifying molecular order in starches (Htoon et al., 2009). For gelatinized starch, peak shifts exist in FT-IR spectra compared with the native starch (Rashid et al., 2012).

3.4.2.4 Fiber crystalline structures change

Crystallinity of fiber connects to fiber digestion, because crystalline regions are less accessible to cellulase enzymes than amorphous regions (Cyr et al., 1990). The X-ray diffraction and differential scanning calorimetry can determine degree of crystallinity. A spectrum of a molecule depends on its physical state and will change depending on its crystalline state, conformation, configuration and method of sample preparation (Griffiths, 2002b), The MIR can monitor cellulose crystallinity (Ciolacu et al., 2011). The symmetric CH_2 bending vibration band at 1,430 cm^{-1} is the "crystallinity band"; its decrease in intensity reflects reduced crystallinity. The β-(1→4)-glycosidic linkage band at 898 cm^{-1} is an "amorphous" absorption band; an increase in its intensity occurs in amorphous samples (Ciolacu et al., 2011). Crystallinity of cellulose may change with

chemical treatment (Oh et al., 2005); thus, it also changes during digestion (Cyr et al., 1990). Due to crystallinity change, bands of MIR spectra of cellulose may shift and absorbance may change after chemical treatment (Oh et al., 2005). The cellulose peaks at 1,431, 1,373, 1,319, 1,282, 1,236, 1,202, 1,165, 1,032, and 897 cm^{-1} may shift to 1,419, 1,376, 1,317, 1,278, 1,228, 1,200, 1,162, 1,019, and 894 cm^{-1}; and absorbance at 1,263, 993, 897, and 668 cm^{-1} may increase (Oh et al., 2005). These changes indicate that spectra of digested samples should be analyzed carefully. The ratios of CH_2 bending band at 1,431 (1,419) cm^{-1}, CH_2 wagging band at 1,376 (1,373) cm^{-1} to C-O-C bands in β-glycosidic linkage at 897 (894) cm^{-1}, C-OH bending at 1,263 cm^{-1}, C-OH out of plane at 668 cm^{-1} indicated cellulose crystallinity (Oh et al., 2005).

For NIR, areas with bands centered at 1,428 nm, 1,488 nm, 1,548 nm, and 1,592 nm were assigned to amorphous, semicrystalline, and two crystalline regions in cellulose, respectively (Mitsui et al., 2007). Changes in lignin, hemicelluloses, and amorphous, semi-crystalline, and crystalline regions of cellulose moieties of pretreated straw were characterized by NIR (Krongtaew et al., 2010).

3.4.3 Other forms of spectroscopy

3.4.3.1 Raman

Raman spectroscopy, measuring the energy of scattered photons, may complement IR (Griffiths, 2002b). First, some bands, such as S–S, C-C and C=C stretching, that are weak in IR spectra are strong in Raman spectra (Edwards, 2002), which may support qualitative characterization of digestion discrepancies.

Second, some Raman bands have characteristic frequencies. For instance, mono-substituted aromatic compounds, together with 1,3-disubstituted and 1,3,5-trisubstituted aromatics, have an intense band at 1,000 cm^{-1} (Griffiths, 2002b). Third, Raman spectroscopy is less affected by water than IR and does not require sample preparation or contact with sample. Raman spectra can be obtained for samples in a vial (Schulz and Baranska, 2007). Thus, Raman spectroscopy may be applied to fresh digesta, feces, or digesta of IVD without interfering with digestion. Peaks in Raman spectra exhibit less overlap (Yang and Ying, 2011), which may facilitate quantitative analysis without calibration. Raman spectroscopy can support qualitative analysis, such as classifying cereal foods based on nutritional components (Sohn et al., 2005), discriminant analysis of edible oils and fats (Yang et al., 2005), and assessing cellulose for crystallinity and allomorph structure (Szymanska-Chargot et al., 2011). Raman spectroscopy can support quantitative analysis, such as predicting content of protein and amylose in rice (Sohn et al., 2004), unsaturation of fat in vegetable oils (Barthus and Poppi, 2001), total dietary fiber in cereal foods (Archibald et al., 1998), but cannot predict AA content in meat and bone meal (Qiao and van Kempen, 2004). Raman spectroscopy is applied widely in biological tissues, agricultural products, and food analysis (Movasaghi et al., 2007; Yang and Ying, 2011). Raman spectroscopy might be useful to investigate digestion process for both in vivo and IVD models.

3.4.3.2 Micro-spectroscopy

The extent of digestion is not only affected by the amount of nutrients, but

also by the distribution of nutrients and other constituents, such as lignin, fat, etc. that might restrict enzyme access to substrate. Micro-spectroscopy may supply information on spatial distribution of nutrients in feedstuffs, which is helpful to investigate the digestion of feedstuffs. Synchrotron micro-spectroscopy can explore the chemical makeup of intact plant tissue with a high signal to noise ratio at spatial resolutions as fine as 3~10 μm (Yu et al., 2004a). This technique can provide information related to quantity, composition, structure, and distribution of chemical constituents and functional groups in tissue.

Chemical distribution of plant tissues such as lignin, cellulose, protein, lipid, and total carbohydrate could be mapped (Yu et al., 2003). With synchrotron micro-spectroscopy, the distribution of nutritional components in corn grain was revealed. Specifically, pericarp contains more lignin (1,510 cm^{-1}), cellulose (1,246 cm^{-1}), and lipid (1,738 cm^{-1}) and less protein (1,650 cm^{-1}, 1,550 cm^{-1}) than endosperm that was rich in protein and starch (1,025 cm^{-1}; Yu et al., 2004b). With micro-spectroscopy, changes in endosperm cell wall composition were detected during wheat grain development for individual constituents and the fine structure of arabinoxylans (Philippe et al., 2006). With micro-spectroscopy, spatial distribution of starch, protein, and lipid in corn and oat flour-based extrudates were revealed, and inversely related distributions of starch and protein were characterized (Cremer and Kaletunç, 2003). Using micro-spectroscopy, the biochemical nature of aleurone cell walls of wheat grain was characterized (Jamme et al., 2008).

3.4.4 Useful spectral techniques and chemometrics

Qualitative analysis may answer questions related to digestion, such as nutrients or structures that are responsible for the low digestibility.

3.4.4.1 Difference spectroscopy

Difference spectroscopy allows decomposition of spectra into their basic components (Grdadolnik and Maréchal, 2003). The NIR difference spectra revealed effects of ammoniation of barley straw (Barton et al., 1986). Using difference spectra, 2 spectral regions (1,430-1,620 and 1,960-2,230 nm) were associated with increased cell wall degradability of wheat silage (Wilman et al., 2000). Difference spectra and principal component analysis (**PCA**) revealed effects of oven- and freeze-drying on chemical composition of pasture silage (Alomar et al., 1999). Difference spectra revealed that lignin (1,670 and 2,250 nm) was associated with low rumen degradability of forages (Deaville and Givens, 1998). Feed-feces differences of NIR spectra defined nutrient digestion of hay by cattle (Coleman and Murray, 1993).

Subtraction of spectra should be done carefully prior to performing the intensity-based calculations to prevent data distortions. Moreover, over- or under-subtraction of spectra will cause indefinable and unquantifiable errors in analysis (Coates, 2002). If bands of interest in the original spectra strongly overlap and are extracted from difference spectra, use of second and fourth derivatives is mandatory (Grdadolnik, 2003).

3.4.4.2 Simple correlation analysis

With correlation analysis of absorbance in each wavelength with organic

matter digestibility, the band at 1,662 nm (supposedly close to 1,668 nm, one of the absorption peaks of extracted lignin) was responsible (r = -0.97) for digestibility change of ammonia treated cereal straw (Guzmán et al., 1996).

3.4.4.3 Principal component analysis

The PCA is used in analysis of spectral data. The PCA converts original variables of spectral data into latent variables. These latent variables, principal components (**PC**), are linear combinations of original variables, absorptions at different wavelengths of spectra. The first PC represents the largest variation. The second PC is orthogonal to the first PC and accounts for the maximum possible residual variance in the data set (Mark, 2008), and so on. The concept of PCA is to reduce dimensionality of data sets consisting of multiple interrelated variables, while retaining maximum variation (Jolliffe, 2002). Using PCA on second derivative NIR spectra, high lysine mutants were characterized in barley (Munck et al., 2004). With PCA, alterations of chemical structure of straw after pre-treatment could be differentiated (Krongtaew et al., 2010). The PCA can reveal carbohydrate structural changes due to bioethanol processing (Yu et al., 2011a).

3.4.4.4 Two-dimensional analysis

Two-dimensional correlation spectroscopy (**2DCOS**) is a powerful technique applicable to vibrational spectroscopy (Noda, 2002). Statistical 2DCOS is based on correlation coefficient mapping. The plot of intensity in 2 orthogonal axes with 2 independent spectra variables (wavelength or wavenumber) can give intuitive relation between variables (Barton et al., 1992). It can simplify the complexity of spectra consisting of many overlapped peaks, also has the benefit of

spectral resolution enhancement and unambiguous assignments of bands. The 2DCOS may be applied to aid the interpretation of NIR spectra of agricultural materials by comparing them with their MIR spectra (Aït Kaddour et al., 2008) or other spectra (Liu et al., 2004). It can also be used to investigate spectral variations based on external perturbations, such as temperature, concentration, chemical reactions (Isao, 2008). Using 2DCOS, interactions between and within the cellulose polymer chains could be revealed (Hinterstoisser and Salmén, 2000).

3.5 Evaluation of nutrient digestibility with spectroscopy

One method to determine digestibility is to predict nutrient content in diets and undigested residue (digesta, feces, or IVD residue) with spectroscopy, then calculate digestibility or digestible nutrients of diets. The other method is to predict digestibility directly from spectra of diets or undigested residues.

3.5.1 Predict nutrient concentrations in feeds and undigested residues

3.5.1.1 Protein

In 1975, NIRS calibration was used to predict grain protein content (Williams, 1975). The NIRS method to predict protein content in wheat and forage has become official (AOAC, 2006). This AOAC method applies to wheat containing 9–16% protein. The NIRS can predict protein content accurately in whole maize kernels (Jiang et al., 2007), rice (Sohn et al., 2004), grains (Williams and Sobering, 1993), wheat (Garnsworthy et al., 2000), and other animal feedstuffs (Gonzalez-Martin et al., 2006), and may predict essential AA (Fontaine et al., 2004). The NIRS can predict N content in feces accurately (Picarelli et al., 1995). However, accurate predictions were based on calibrations separate for each

sample set. Without reference data, building robust calibrations for undigested IVD residues remains a challenge.

The MIR is often used to elucidate protein structures and less used to predict protein content. However, MIR spectroscopy can also predict protein content, e.g., for rice (Shao et al., 2011), and AA content in meat and bone meal (Qiao and van Kempen, 2004).

3.5.1.2 Fat and FA

The NIRS can predict oil content in maize (Jiang et al., 2007), total FA in freeze-dried poultry ileal digesta and excreta (Philipps et al., 2005), fat content in wet feces (Picarelli et al., 1995), and FA composition in meat (Pla et al., 2007; Guy et al., 2011; Zomeno et al., 2012), milk (Coppa et al., 2010), oilseed (Koprna et al., 2006), fish oil (Cozzolino et al., 2005), and edible oils (Azizian and Kramer, 2005). However, prediction for certain FA was not satisfactory. The NIRS does not require derivatization of fats to FA methyl esters, thus has an advantage compared with gas chromatography (**GC**) method (Azizian and Kramer, 2005).

The MIR accurately quantifies fat and FA content. Single reflection ATR FT-IR spectroscopy can predict (R^2 = 0.999) the main FA groups (saturated, trans, mono- and poly-unsaturated) in edible oils (Sherazi et al., 2009). Quantification of fat and FFA with FT-IR is successful in many samples, such as high-fat products (van de Voort et al., 1993), trans fats (Mossoba et al., 2007), rumen samples (Udén and Sjaunja, 2009), fish oils (Aryee et al., 2009; Vongsvivut et al., 2012), and edible oils (Al-Alawi et al., 2006). First derivative transformation of the 1,475-650 cm^{-1} spectral region best predicted unsaturated fat (Mahesar et al.,

2011). The ATR FT-IR also predicted fecal fat using partial least squares (**PLS**) regression (Franck et al., 1996).

3.5.1.3 Starch

The extent of starch hydrolysis, which is characterized by the dextrose equivalent value, could be accurately predicted by NIRS (Storz and Steffens, 2004). The NIRS predicted starch digestion pattern with α-amylase of rice flour (Osawa and Inoue, 2008) and starch content in poultry excreta (Bastianelli et al., 2010).

The MIR can evaluate residual starch after in vitro fermentation for variable lengths of time. A successful calibration of MIR absorbance spectra against enzymatically determined starch remaining after rumen IVD incubations was demonstrated (Udén, 2009). Starch analysis by MIR is precise and simplifies the analyses and reduces cost. However, this finding was hard to apply to investigate starch digestion discrepancies between IVD and in vivo digestion, because acquisition of digesta from different segments of the digestive tract of pigs is not convenient. Moreover, absorption of digestion end product of starch occurs, and water content is not identical in undigested residue between IVD and vivo digestion. A quantitative relation between specific peaks of MIR spectra and starch digestion exists. Peak intensity at 1,078 and 1,020 cm^{-1} identified ($r = 0.99$) enzyme activity of amyloglucosidase on starch (Schindler et al., 1997).

3.5.1.4 Fiber

Determination of ADF content in forages by NIRS has become an official method (AOAC, 2006). Moreover, NIRS can predict total dietary fiber in cereal

grain products and barley cultivars (Kays et al., 1996; Archibald et al., 1998; Kays et al., 2005). Likewise, NIRS can predict crude fiber (**CF**), ADF, acid detergent lignin (**ADL**) content of whole crops of oats, barley, triticale, wheat, ryegrass, and sorghum (Bruno-Soares et al., 1998). Finally, NIRS can predict cellulose in forage and feces (Decruyenaere et al., 2009), and in situ degradation characteristics of neutral detergent fiber (**NDF**) in temperate grasses and red clover (Nordheim et al., 2007).

Using ATR FT-IR spectroscopy with PLS regression, lignin content in triticale and wheat straws could be accurately predicted (Tamaki and Mazza, 2011). The ATR FT-IR spectroscopy can predict sugar conversions and yields from enzymatic hydrolysis of pretreated plant biomass (Sills and Gossett, 2012). The ratio of lignin (1,510 cm^{-1}) and carbohydrate (1,050 cm^{-1}) of MIR spectra was highly correlated to 48 h in sacco dry matter degradability of cell wall in cereal straw (Russell et al., 1989). Nevertheless, using MIR had the advantage of confident assignment of spectra bands to functional groups.

3.5.2 Prediction of digestibility or digestible nutrients

3.5.2.1 Calibration method

Many efforts were made to predict digestibility or digestible nutrients of diets with NIRS (Swift, 2003; Zijlstra et al., 2011). The DE content of a range of cereal grains (wheat, barley, sorghum, triticale, maize) in pigs was predicted with a standard error of cross validation (**SECV**) of 96 kcal kg^{-1} (van Barneveld et al., 1999). The quality of reference data for calibration is important. The DE content of barley for pigs was predicted accurately with a SECV of 67 kcal kg^{-1} (McCann

et al., 2006) and an even lower SECV of 57 kcal kg^{-1} (Zijlstra et al., 2011). The low SECV indicates that NIRS may predict the nutritive value of barley accurately for growing pigs. However, prediction accuracy was poor for DE (R^2 = 0.17) and N digestibility (R^2 = 0.22) in pigs, and slightly better for true and apparent metabolizable energy in broiler chicks (R^2 = 0.52, 0.45, respectively) (Garnsworthy et al., 2000).

Different calibrations to predict digestible nutrients or nutrient digestibility are needed for different species of animals at different physiological stages and age, because animal maturity influences nutrient digestibility. For the IVD model, any adjustment of digestion environment settings, e.g., digestion time or enzyme, may change digestibility of the diet. Thus, predictions using diet spectra are not suitable to evaluate nutrient digestibility during the development of an IVD model.

Fecal NIR spectra can predict nutrient digestibility of forage in ruminants (Givens and Deaville, 1999; Landau et al., 2006; Fanchone et al., 2007; Dixon and Coates, 2009). Fecal NIR spectra can better predict (R^2 = 0.92) in vivo total tract organic matter digestibility in sheep than forage NIR spectra (R^2 = 0.86) (Decruyenaere et al., 2009). However, supplying reference data with small amounts of IVD residues is a challenge for calibration; thus, a non-calibration method would be desirable.

3.5.2.2 Non-calibration method

As opposed to multivariate calibration, classical methods for quantitative analysis could be an alternative solution (Coates, 2002). The ideal situation is to

locate an isolated absorption band of the specific analyte, and to extract relevant intensity information by peak height or area, which varies linearly with concentration. For many spectra, especially for NIR, this ideal situation does not exist, because absorption bands are broad and diffuse (Coates, 2002). Instead, strong and distinct MIR spectra are more suitable to develop a non-calibration spectroscopic method.

To our knowledge, non-calibration methods to predict nutrient digestibility for monogastric animals have not been published. The K-matrix multiple linear regression method using composite samples accurately predicted starch, lipid, and protein with less than 5% standard error of prediction (Gordon et al., 1993), which may give some ideas to predict digestibility. However, this method relied heavily on pure component spectra, which is difficult to prepare from complex digestion end products. An issue that requires resolution is that pigs normally eat mixed diets, whereas single ingredients are often used for IVD models. Adding spectra from component spectra may then assist to investigate discrepancies between IVD and in vivo digestion (Coates, 2002). The spectral additivity in the fingerprint region of MIR spectra has been validated with sugar mixtures in culture media (Hashimoto et al., 2005).

3.6 Conclusions

Both NIR and MIR can predict nutrient content. However, the use of NIRS is not ideal to identify or elucidate chemical structure changes of nutrients during digestion. The MIR has the advantage of identifying specific nutrients, and is expected to have adequate quantitative accuracy. For IVD models, the adoption of

NIRS may require pooling of IVD residues to obtain enough sample mass for spectra acquisition. With the ability of sampling on small quantity and without dilution of samples, the ATR FT-IR is a promising solution. As reference data from IVD residues are the bottleneck to build calibrations, the non-calibration method is ideal to handle small quantities of IVD residues. Thus future research should develop a non-calibration method to enable quantitative evaluation of nutrient digestibility. Discrepancies between IVD and in vivo digestion of nutrients can then be identified, and its resolution can supply a scientific base to improve IVD techniques.

3.7 References

Aït Kaddour, A., M. Mondet, and B. Cuq. 2008. Application of two-dimensional cross-correlation spectroscopy to analyse infrared (MIR and NIR) spectra recorded during bread dough mixing. J. Cereal. Sci. 48:678–685.

ABB. 2011. MB3000 FT-IR laboratory analyzer brochure. http://www.abb.ca/product/seitp330/2f0aefb9d5d936d18525728300630dc9.aspx. (Accessed 9 September 2011).

Abidi, N., L. Cabrales, and C. H. Haigler. 2013. Changes in the cell wall and cellulose content of developing cotton fibers investigated by FTIR spectroscopy. Carbohydr. Polym. http://dx.doi.org/10.1016/j.carbpol.2013.01.074.

Al-Alawi, A., F. R. van de Voort, J. Sedman, and A. Ghetler. 2006. Automated FTIR analysis of free fatty acids or moisture in edible oils. J. Lab. Autom.

11:23–29.

Albrecht, K. A., G. C. Marten, J. L. Halgerson, and W. F. Wedin. 1987. Analysis of cell-wall carbohydrates and starch in alfalfa by near-infrared reflectance spectroscopy. Crop Sci. 27:586–588.

Alomar, D., R. Fuchslocher, and S. Stockebrand. 1999. Effects of oven- or freeze-drying on chemical composition and NIR spectra of pasture silage. Anim. Feed Sci. Technol. 80:309–319.

Anderson, P. 2009. Energy determination of corn co-products in finishing pigs and the use of an in vitro organic matter digestibility assay to predict in vivo energy. MSc Diss. Iowa State University, Ames, IA.

AOAC. 2006. Official methods of analysis. 18th ed. Assoc. Off. Anal. Chem., Arlington, VA.

AOCS. 1993. Isolated trans isomers infrared spectrometric method (Cd 14-61). In: D. Firestone, editor, Official methods and recommended practices of the American oil chemists' society. AOCS Press, Champaign, IL.

Archibald, D. D., S. E. Kays, D. S. Himmelsbach, and F. E. Barton II. 1998. Raman and NIR spectroscopic methods for determination of total dietary fiber in cereal foods: A comparative study. Appl. Spectrosc. 52:22–31.

Aryee, A. N. A., F. R. van de Voort, and B. K. Simpson. 2009. FTIR determination of free fatty acids in fish oils intended for biodiesel production. Process Biochem. 44:401–405.

Azizian, H., and J. Kramer. 2005. A rapid method for the quantification of fatty acids in fats and oils with emphasis on trans fatty acids using Fourier

transform near infrared spectroscopy (FT-NIR). Lipids 40:855–867.

Barth, A. 2007. Infrared spectroscopy of proteins. Biochim. Biophys. Acta, Bioenerg. 1767:1073–1101.

Barthus, R. C., and R. J. Poppi. 2001. Determination of the total unsaturation in vegetable oils by Fourier transform Raman spectroscopy and multivariate calibration. Vib. Spectrosc. 26:99–105.

Barton, F. E., D. S. Himmelsbach, J. H. Duckworth, and M. J. Smith. 1992. Two-dimensional vibration spectroscopy: Correlation of mid- and near-infrared regions. Appl. Spectrosc. 46:420–429.

Barton, F. E. 1991. New methods for the structural and compositional analysis of cell walls for quality determinations. Anim. Feed Sci. Technol. 32:1–11.

Barton, F. E., J. H. Wolsink, and H. M. Vedder. 1986. Near infrared reflectance spectroscopy of untreated and ammoniated barley straw. Anim. Feed Sci. Technol. 15:189–196.

Bastianelli, D., L. Bonnal, H. Juin, S. Mignon-Grasteau, F. Davrieux, and B. Carre. 2010. Prediction of the chemical composition of poultry excreta by near infrared spectroscopy. J. Near Infrared Spectrosc. 18:69–77.

Bellon-Maurel, V., and A. McBratney. 2011. Near-infrared (NIR) and mid-infrared (MIR) spectroscopic techniques for assessing the amount of carbon stock in soils - Critical review and research perspectives. Soil Biol. Biochem. 43:1398–1410.

Bendit, E. G. 1967. Infrared absorption of tyrosine side chains in proteins. Biopolymers 5:525–533.

Blakeney, A. B., and P. C. Flinn. 2005. Determination of non-starch polysaccharides in cereal grains with near-infared reflectance spectroscopy. Mol. Nutr. Food Res. 49:546–550.

Blanco, M., J. Coello, H. Iturriaga, S. Maspoch, and R. G. Bano. 2000. On-line monitoring of starch enzymatic hydrolysis by near-infrared spectroscopy. Analyst 125:749–752.

Boisen, S., and J. A. Fernandez. 1997. Prediction of the total tract digestibility of energy in feedstuffs and pig diets by in vitro analyses. Anim. Feed Sci. Technol. 68:277–286.

Boval, M., D. B. Coates, P. Lecomte, V. Decruyenaere, and H. Archimede. 2004. Faecal near infrared reflectance spectroscopy (NIRS) to assess chemical composition, in vivo digestibility and intake of tropical grass by Creole cattle. Anim. Feed Sci. Technol. 114:19–29.

Bruno-Soares, A. M., I. Murray, R. M. Paterson, and J. M. F. Abreu. 1998. Use of near infrared reflectance spectroscopy (NIRS) for the prediction of the chemical composition and nutritional attributes of green crop cereals. Anim. Feed Sci. Technol. 75:15–25.

Bruun, S. W., I. Sndergaard, and S. Jacobsen. 2007. Analysis of protein structures and interactions in complex food by near-infrared spectroscopy. 1. Gluten powder. J. Agric. Food Chem. 55:7234–7243.

Buchner, G. S., R. D. Murphy, N.-V. Buchete, and J. Kubelka. 2011. Dynamics of protein folding: Probing the kinetic network of folding–unfolding transitions with experiment and theory. BBA - Proteins Proteom.

1814:1001–1020.

Budevska, B. O. 2002. Vibrational spectroscopy imaging of agricultural products. In: J. M. Chalmers and P. R. Griffiths, editors, Handbook of vibrational theory, Vol. 5. John Wiley & Sons Ltd, Chichester, UK. p. 3720–3732.

Butkute, B., and J. Ceseviciene. 2009. Development of equations for wheat grain quality assessment by a NIRS-6500 spectrometer. I. Grain quality and optical data base characterization. Zemdirbyste 96:62–77.

Byung Joo, K., P. Eui Ho, and S. Hyung Soo. 1995. Use of near infrared reflectance spectroscopy for determination of grain components in barley. Korean J. Crop Sci. 40:716–722.

Cai, S., and B. R. Singh. 2004. A distinct utility of the amide III infrared band for secondary structure estimation of aqueous protein solutions using partial least squares methods. Biochemistry 43:2541–2549.

Carbonaro, M., and A. Nucara. 2010. Secondary structure of food proteins by Fourier transform spectroscopy in the mid-infrared region. Amino Acids 38:679–690.

Castro, P., G. Flores, A. Gonzalez-Arraez, and J. Castro. 2002. Nutritive quality of herbage silages by NIRS: dried or undried samples? In: Multi-function grasslands: quality forages, animal products and landscapes. Proceedings of the 19th General meeting of the European grassland federation, La Rochelle, France. p. 190–191.

Chalmers, J. M., and P. R. Griffiths. 2002. Handbook of vibrational theory. John Wiley & Sons Ltd, Chichester, UK.

Chung, H. S., M. Khalil, and A. Tokmakoff. 2004. Nonlinear infrared spectroscopy of protein conformational change during thermal unfolding. J. Phys. Chem. B 108:15332–15342.

Coates, J. 2002. Classical methods of quantitative analysis. In: J. M. Chalmers and P. R. Griffiths, editors, Handbook of vibrational theory, Vol. 3. John Wiley & Sons Ltd, Chichester, UK. p. 2235–2257.

Coleman, S. W., and I. Murray. 1993. The use of near-infrared reflectance spectroscopy to define nutrient digestion of hay by cattle. Anim. Feed Sci. Technol. 44:237–249.

Coppa, M., A. Ferlay, C. Leroux, M. Jestin, Y. Chilliard, B. Martin, and D. Andueza. 2010. Prediction of milk fatty acid composition by near infrared reflectance spectroscopy. Int. Dairy J. 20:182–189.

Cozzolino, D., I. Murray, A. Chree, and J. R. Scaife. 2005. Multivariate determination of free fatty acids and moisture in fish oils by partial least-squares regression and near-infrared spectroscopy. LWT-Food Sci. Technol. 38:821–828.

Cremer, D. R., and G. Kaletunç. 2003. Fourier transform infrared microspectroscopic study of the chemical microstructure of corn and oat flour-based extrudates. Carbohydr. Polym. 52:53–65.

Cyr, N., R. M. Elofson, and G. W. Mathison. 1990. Determination of crystallinity of carbohydrates by 13C cross polarization/magic angle spinning NMR with applications to the nutritive value of forages. Can. J. Anim. Sci. 70:695–701.

Das, B., U. Konwar, M. Mandal, and N. Karak. 2013. Sunflower oil based biodegradable hyperbranched polyurethane as a thin film material. Ind. Crop Prod. 44:396–404.

Dauchez, M., P. Lagant, P. Derreumaux, G. Vergoten, M. Sekkal, and B. Sombret. 1994. Force field and vibrational spectra of oligosaccharides with different glycosidic linkages – Part II. Maltose monohydrate, cellobiose and gentiobiose. Spectrochim. Acta, Pt. A: Mol. Spectrosc. 50:105–118.

Deaville, E. R., and D. I. Givens. 1998. Regions of normalised near infrared reflectance difference spectra related to the rumen degradation of fresh grass, grass silage and maize silage. Anim. Feed Sci. Technol. 72:41–51.

Decandia, M., V. Giovanetti, F. Boe, G. Scanu, A. Cabiddu, G. Molle, A. Cannas, and S. Landau. 2009. Faecal NIRS to assess the chemical composition and the nutritive value of dairy sheep diets. Options Mediterraneennes. Serie A, Seminaires Mediterraneens:135–139.

Decruyenaere, V., P. Lecomte, C. Demarquilly, J. Aufrere, P. Dardenne, D. Stilmant, and A. Buldgen. 2009. Evaluation of green forage intake and digestibility in ruminants using near infrared reflectance spectroscopy (NIRS): Developing a global calibration. Anim. Feed Sci. Technol. 148:138–156.

Derkacheva, O., and D. Sukhov. 2008. Investigation of lignins by FTIR spectroscopy. Macromol. Symp. 265:61–68.

DeThomas, F. A., and P. J. Brimmer. 2002. Monochromators for near-infrared spectroscopy. In: J. M. Chalmers and P. R. Griffiths, editors, Handbook of

Vibrational Theory Vol. 1. John Wiley & Sons Ltd, Chichester, UK. p. 383–392.

Devillard, E., F. M. McIntosh, D. Paillard, N. A. Thomas, K. J. Shingfield, and R. J. Wallace. 2009. Differences between human subjects in the composition of the faecal bacterial community and faecal metabolism of linoleic acid. Microbiology (Reading) 155:513–520.

Ciolacu, D., F. Ciolacu, and V. I. Popa. 2011. Amorphous cellulose - structure and characterization. Cellul. Chem. Technol. 45:13–21.

Dixon, R., and D. Coates. 2009. Review: near infrared spectroscopy of faeces to evaluate the nutrition and physiology of herbivores. J. Near Infrared Spectrosc. 17:1–31.

Edwards, H. G. M. 2002. Spectra–structure correlations in Raman spectroscopy. In: J. M. Chalmers and P. R. Griffiths, editors, Handbook of vibrational theory, Vol. 3. John Wiley & Sons Ltd, Chichester, UK. p. 1838–1871.

Ekgasit, S., and H. Ishida. 2002. Depth profiling by ATR. In: J. M. Chalmers and P. R. Griffiths, editors, Handbook of vibrational theory, Vol. 2. John Wiley & Sons Ltd, Chichester, UK. p. 1508–1520.

Englyst, H., H. S. Wiggins, and J. H. Cummings. 1982. Determination of the non-starch polysaccharides in plant foods by gas-liquid-chromatography of constituent sugars as alditol acetates. Analyst 107:307–318.

Englyst, H. N., and J. H. Cummings. 1985. Digestion of the polysaccharides of some cereal foods in the human small-intestine. Am. J. Clin. Nutr. 42:778–787.

Fabian, H., K. Gast, V. V. Filimonov, D. F. Zamyatkin, and V. V. Rogov. 2005. Thermal unfolding of two designed monomeric λ Cro repressor variants. Vib. Spectrosc. 38:45–51.

Fabian, H., and D. Naumann. 2004. Methods to study protein folding by stopped-flow FT-IR. Methods 34:28–40.

Fabian, H., C. Schultz, D. Naumann, O. Landt, U. Hahn, and W. Saenger. 1993. Secondary structure and temperature-induced unfolding and refolding of ribonuclease T1 in aqueous solution: A Fourier transform infrared spectroscopic study. J. Mol. Biol. 232:967–981.

Fabian, H., Z. Yu, Y. Wang, and D. Naumann. 2010. Generalized 2D and time-resolved FTIR studies of protein unfolding events. J. Mol. Struct. 974:203–209.

Fanchone, A., M. Boval, P. Lecomte, and H. Archimede. 2007. Faecal indices based on near infrared spectroscopy to assess intake, in vivo digestibility and chemical composition of the herbage ingested by sheep (crude protein, fibres and lignin content). J. Near Infrared Spectrosc. 15:107–113.

Fontaine, J., J. Horr, and B. Schirmer. 2004. Amino acid contents in raw materials can be precisely analyzed in a global network of near-infrared spectrometers: collaborative trials prove the positive effects of instrument standardization and repeatability files. J. Agric. Food Chem. 52:701–708.

Fox, G. P., K. Onley-Watson, and A. Osman. 2002. Multiple linear regression calibrations for barley and malt protein based on the spectra of hordein. J. Inst. Brew. 108:155–159.

Franck, P., J. L. Sallerin, H. Schroeder, M. A. Gelot, and P. Nabet. 1996. Rapid determination of fecal fat by Fourier transform infrared analysis (FTIR) with partial least-squares regression and an attenuated total reflectance accessory. Clin. Chem. 42:2015–2020.

Fu, F. N., D. B. Deoliveira, W. R. Trumble, H. K. Sarkar, and B. R. Singh. 1994. Secondary structure estimation of proteins using the amide-III region of Fourier-transform infrared-spectroscopy - application to analyze calcium binding-induced structural-changes in calsequestrin. Appl. Spectrosc. 48:1432–1441.

Gacs, G., and D. Barltrop. 1977. Significance of Ca-soap formation for calcium absorption in the rat. Gut 18:64–68.

García, N. L., L. Famá, A. Dufresne, M. Aranguren, and S. Goyanes. 2009. A comparison between the physico-chemical properties of tuber and cereal starches. Food Res. Int. 42:976–982.

Garnsworthy, P. C., and Y. Unal. 2004. Estimation of dry-matter intake and digestibility in group-fed dairy cows using near infrared reflectance spectroscopy. Anim. Sci. 79:327–334.

Garnsworthy, P. C., J. Wiseman, and K. Fegeros. 2000. Prediction of chemical, nutritive and agronomic characteristics of wheat by near infrared spectroscopy. J. Agric. Sci. 135:409–417.

Gelbrich, J., C. Mai, and H. Militz. 2008. Chemical changes in wood degraded by bacteria. Int. Biodeterior. Biodegrad. 61:24–32.

George, C. F., R. Duane, and G. Christine. 2000. Nonstarch polysaccharides and

oligosaccharides in swine nutrition. In: A. J. Lewis and L. L. Southern, editors, Swine nutrition, second edition. CRC Press, Boca Raton, FL.

Gergely, S., and A. Salgo. 2007. Changes in protein content during wheat maturation - what is measured by near infrared spectroscopy? J. Near Infrared Spectrosc. 15:49–58.

Givens, D. I., and E. R. Deaville. 1999. The current and future role of near infrared reflectance spectroscopy in animal nutrition: a review. Aust. J. Agric. Res. 50:1131–1145.

Gonzalez-Martin, I., N. Alvarez-Garcia, and J. L. Hernandez-Andaluz. 2006. Instantaneous determination of crude proteins, fat and fibre in animal feeds using near infrared reflectance spectroscopy technology and a remote reflectance fibre-optic probe. Anim. Feed Sci. Technol. 128:165–171.

Gordon, S. H., S. C. Whatel, B. C. Wheeler, and C. James. 1993. Multivariate FTIR analysis of substrates for protein, polysaccharide, lipid and microbe content: Potential for solid-state fermentations. Biotechnol. Adv. 11:665–675.

Grdadolnik, J. 2003. Infrared difference spectroscopy: Part I. Interpretation of the difference spectrum. Vib. Spectrosc. 31:279–288.

Grdadolnik, J., and Y. Maréchal. 2003. Infrared difference spectroscopy: Part II. Spectral decomposition. Vib. Spectrosc. 31:289–294.

Griffiths, P. R. 2002a. Beer's law. In: J. M. Chalmers and P. R. Griffiths, editors, Handbook of vibrational theory, Vol. 3. John Wiley & Sons Ltd,

Chichester, UK. p. 2225–2234.

Griffiths, P. R. 2002b. Introduction to vibrational spectroscopy. In: J. M. Chalmers and P. R. Griffiths, editors, Handbook of vibrational theory, Vol. 1. John Wiley & Sons Ltd. p. 33–43.

Guy, F., S. Prache, A. Thomas, D. Bauchart, and D. Andueza. 2011. Prediction of lamb meat fatty acid composition using near-infrared reflectance spectroscopy (NIRS). Food Chem. 127:1280–1286.

Guzmán, J. L., A. Garrido, A. Gómez-Cabrera, J. E. Guerrero, and I. Murray. 1996. Use of NIRS to estimate the improvement in digestibility after ammonia treatment of cereal straws. Anim. Feed Sci. Technol. 57:149–157.

Hamilton, R. M. G., and B. B. McDonald. 1969. Effect of dietary fat source on the apparent digestibility of fat and the composition of fecal lipids of the young pig. J. Nutr. 97:33–41.

Hannah, R. W. 2002. Standard sampling techniques for infrared spectroscopy. In: J. M. Chalmers and P. R. Griffiths, editors, Handbook of vibrational theory, Vol. 3. John Wiley & Sons Ltd, Chichester, UK. p. 933–952.

Hashimoto, A., A. Yamanaka, M. Kanou, K. Nakanishi, and T. Kameoka. 2005. Simple and rapid determination of metabolite content in plant cell culture medium using an FT-IR/ATR method. Bioprocess Biosyst. Eng. 27:115–123.

Hattey, J. A., W. E. Sabbe, G. D. Baten, and A. B. Blakeney. 1994. Nitrogen and starch analysis of cotton leaves using near-infrared reflectance

spectroscopy (NIRS). Commun. Soil Sci. Plant Anal. 25:1855–1863.

Herman, R., Gao, Yong , Storer, Nicholas 2006. Acid-induced unfolding kinetics in simulated gastric digestion of proteins. Regul. Toxicol. Pharmacol. 46:93–99.

Hernandez-Uribe, J. P., G. Ramos-Lopez, H. Yee-Madeira, and L. A. Bello-Perez. 2010. Physicochemical, rheological and structural characteristics of starch in maize tortillas. Plant. Food. Hum. Nutr. 65:152–157.

Hinterstoisser, B., and L. Salmén. 2000. Application of dynamic 2D FTIR to cellulose. Vib. Spectrosc. 22:111–118.

Holtug, K., H. S. Rasmussen, and P. B. Mortensen. 1992. An in vitro study of short-chain fatty acid concentrations, production and absorption in pig (Sus scrofa) colon. Comparative Biochemistry and Physiology Part A: Physiology 103:189–197.

Hourant, P., V. Baeten, M. T. Morales, M. Meurens, and R. Aparicio. 2000. Oil and fat classification by selected bands of near-infrared spectroscopy. Appl. Spectrosc. 54:1168–1174.

Hromádková, Z., B. S. Paulsen, M. Polovka, Z. Košťálová, and A. Ebringerová. 2013. Structural features of two heteroxylan polysaccharide fractions from wheat bran with anti-complementary and antioxidant activities. Carbohydr. Polym. 93:22–30.

Htoon, A., A. K. Shrestha, B. M. Flanagan, A. Lopez-Rubio, A. R. Bird, E. P. Gilbert, and M. J. Gidley. 2009. Effects of processing high amylose maize starches under controlled conditions on structural organisation and

amylase digestibility. Carbohydr. Polym. 75:236–245.

Irudayaraj, J., and H. Yang. 2002. Depth profiling of a heterogeneous food-packaging model using step-scan Fourier transform infrared photoacoustic spectroscopy. J. Food Eng. 55:25–33.

Isao, N. 2008. Recent advancement in the field of two-dimensional correlation spectroscopy. J. Mol. Struct. 883–884:2–26.

Izydorczyk, M. S., and J. E. Dexter. 2008. Barley beta-glucans and arabinoxylans: Molecular structure, physicochemical properties, and uses in food products-a Review. Food Res. Int. 41:850–868.

Jackson, M., and H. H. Mantsch. 1995. The use and misuse of FTIR spectroscopy in the determination of protein structure. Crit. Rev. Biochem. Mol. Biol. 30:95–120.

Jakobs, B. S., M. Volmer, D. W. Swinkels, M. T. W. Hofs, S. Donkervoort, M. M. J. Joosting, B. G. Wolthers, P. de Peinder, and H. A. M. Voorbij. 2000. New method for faecal fat determination by mid-infrared spectroscopy, using a transmission cell: an improvement in standardization. Ann. Clin. Biochem. 37:343–349.

Jamme, F., P. Robert, B. Bouchet, L. Saulnier, P. Dumas, and F. Guillon. 2008. Aleurone cell walls of wheat grain: high spatial resolution investigation using synchrotron infrared microspectroscopy. Appl. Spectrosc. 62:895–900.

Jiang, H. Y., Y. J. Zhu, L. M. Wei, J. R. Dai, T. M. Song, Y. L. Yan, and S. J. Chen. 2007. Analysis of protein, starch and oil content of single intact kernels by

near infrared reflectance spectroscopy (NIRS) in maize (Zea mays L.). Plant Breeding 126:492–497.

Jinsong, B., W. Yuefei, and S. Yun. 2007. Determination of apparent amylose content, pasting properties and gel texture of rice starch by near-infrared spectroscopy. J. Sci. Food Agric. 87:2040–2048.

Jolliffe, I. T. 2002. Principal component analysis. 2nd ed. Springer, New York, NY.

Kačuráková, M., P. Capek, V. Sasinkova, N. Wellner, and A. Ebringerova. 2000. FT-IR study of plant cell wall model compounds: pectic polysaccharides and hemicelluloses. Carbohydr. Polym. 43:195–203.

Kačuráková, M., A. Ebringerova, J. Hirsch, and Z. Hromadkova. 1994. Infrared study of arabinoxylans. J. Sci. Food Agric. 66:423–427.

Kačuráková, M., N. Wellner, A. Ebringerová, Z. Hromádková, R. H. Wilson, and P. S. Belton. 1999. Characterisation of xylan-type polysaccharides and associated cell wall components by FT-IR and FT-Raman spectroscopies. Food Hydrocolloid. 13:35–41.

Kačuráková, M., and R. H. Wilson. 2001. Developments in mid-infrared FT-IR spectroscopy of selected carbohydrates. Carbohydr. Polym. 44:291–303.

Kays, S. E., and F. E. Barton, II. 2002. Rapid prediction of gross energy and utilizable energy in cereal food products using near-infrared reflectance spectroscopy. J. Agric. Food Chem. 50:1284–1289.

Kays, S. E., N. Shimizu, F. E. Barton, II, and K. Ohtsubo. 2005. Near-infrared transmission and reflectance spectroscopy for the determination of dietary

fiber in barley cultivars. Crop Sci. 45:2307–2311.

Kays, S. E., W. R. Windham, and F. E. Barton, II. 1996. Prediction of total dietary fiber in cereal products using near-infrared reflectance spectroscopy. J. Agric. Food Chem. 44:2266–2271.

Kim, K. O., and P. C. Williams. 1990. Determination of starch and energy in feed grains by near-infrared reflectance spectroscopy. J. Agric. Food Chem. 38:682–688.

Kim, Y. K., D. S. Himmelsbach, and S. E. Kays. 2007. ATR-Fourier transform mid-infrared spectroscopy for determination of trans fatty acids in ground cereal products without oil extraction. J. Agric. Food Chem. 55:4327–4333.

Koprna, R., P. Nerusil, O. Kolovrat, V. Kucera, and A. Kohoutek. 2006. Estimation of fatty acid content in intact seeds of oilseed rape (Brassica napus L.) lines using near-infrared spectroscopy. Czech J. Genet. Plant Breed. 42:132–136.

Kos, G., R. Krska, H. Lohninger, and P. R. Griffiths. 2004. A comparative study of mid-infrared diffuse reflection (DR) and attenuated total reflection (ATR) spectroscopy for the detection of fungal infection on RWA2-corn. Anal. Bioanal. Chem. 378:159–166.

Krongtaew, C., K. Messner, T. Ters, and K. Fackler. 2010. Characterization of key parameters for biotechnological lignocellulose conversion assessed by FT-NIR spectroscopy. Part 1. Qualitative analysis of pretreated straw. BioResources 5:2063–2080.

Kuhnen, S., J. B. Ogliari, P. F. Dias, E. F. Boffo, I. Correia, A. G. Ferreira, I. Delgadillo, and M. Maraschin. 2010. ATR-FTIR spectroscopy and chemometric analysis applied to discrimination of landrace maize flours produced in southern Brazil. Int. J. Food Sci. Tech. 45:1673–1681.

Landau, S., T. Glasser, and L. Dvash. 2006. Monitoring nutrition in small ruminants with the aid of near infrared reflectance spectroscopy (NIRS) technology: a review. Small Ruminant Res. 61:1–11.

Lanser, A. C., G. R. List, R. K. Holloway, and Y. L. Mounts. 1991. FTIR estimation of free fatty acid content in crude oils extracted from damaged soybeans. J. Am. Oil Chem. Soc. 68:448–449.

Larkin, P. 2011. Infrared and Raman spectroscopy: principles and spectral interpretation. Elsevier Inc., Waltham, MA.

Lewis, R., R. N. McElhaney, W. Pohle, and H. H. Mantsch. 1994. Components of the carbonyl stretching band in the infrared-spectra of hydrated 1,2-diacylglycerolipid bilayers - a reevaluation. Biophys. J. 67:2367–2375.

Liu, Y. L., F. E. Barton, II, B. G. Lyon, W. R. Windham, and C. E. Lyon. 2004. Two-dimensional correlation analysis of visible/near-infrared spectral intensity variations of chicken breasts with various chilled and frozen storages. J. Agric. Food Chem. 52:505–510.

Losada, B., P. Garcia-Rebollar, C. Alvarez, P. Cachaldora, M. A. Ibanez, J. Mendez, and J. C. de Blas. 2010. The prediction of apparent metabolisable energy content of oil seeds and oil seed by-products for poultry from its chemical components, in vitro analysis or near-infrared reflectance

spectroscopy. Anim. Feed Sci. Technol. 160:62–72.

Lu, Y., and J. D. Miller. 2002. Carboxyl stretching vibrations of spontaneously adsorbed and LB-transferred calcium carboxylates as determined by FTIR internal reflection spectroscopy. J. Colloid Interface Sci. 256:41–52.

Luypaert, J., D. L. Massart, and Y. Vander Heyden. 2007. Near-infrared spectroscopy applications in pharmaceutical analysis. Talanta 72:865–883.

Mahesar, S. A., S. T. H. Sherazi, A. A. Kandhro, M. I. Bhanger, A. R. Khaskheli, and M. Y. Talpur. 2011. Evaluation of important fatty acid ratios in poultry feed lipids by ATR FTIR spectroscopy. Vib. Spectrosc. 57:177–181.

Mark, H. 2008. Data analysis: Multilinear regression and principal component analysis. In: D. A. Burns and E. W. Ciurczak, editors, Handbook of near-infrared analysis. CRC Press, Boca Raton, FL. p. 151–187.

Mathlouthi, M., and J. L. Koenig. 1987. Vibrational spectra of carbohydrates. In: R. S. Tipson and H. Derek, editors, Adv. Carbohydr. Chem. Biochem. Vol. 44. Academic Press Inc., Orlando, FL. p. 7–89.

Mayo, D. W. 2004. Characteristic frequencies of alkanes. In: D. W. Mayo, F. A. Miller and R. W. Hannah, editors, Course notes on the interpretation of infrared and Raman spectra. John Willy & Sons, Inc., Hoboken, NJ. p. 33–72.

McCann, M. E. E., K. J. McCracken, and R. E. Agnew. 2006. The use of near infrared reflectance spectroscopy (NIRS) for prediction of the nutritive value of barley for growing pigs. Irish J. Agr. Food. Res. 45:187–195.

McCarty, G. W., and J. B. Reeves, III. 2006. Comparison of near infrared and mid

infrared diffuse reflectance spectroscopy for field-scale measurement of soil fertility parameters. Soil Sci 171:94–102.

Meineri, G., P. G. Peiretti, and G. Masoero. 2009. Appraisal of ingestion and digestibility in growing rabbits using near infrared reflectance spectroscopy (NIRS) of feeds and faeces. Ital. J. Anim. Sci. 8:75–82.

Miller, F. A. 2003. Amides, carboxylate ion, and C-O single bonds. In: D. W. Mayo, F. A. Miller and R. W. Hannah, editors, Course notes on the interpretation of infrared and Raman spectra. John Wiley & Sons, Inc., Hoboken, NJ. p. 205–215.

Miller, F. A. 2004a. Characteristic frequencies of alkenes (olefins). In: D. W. Mayo, F. A. Miller and R. W. Hannah, editors, Course notes on the interpretation of infrared and Raman spectra. John Willy & Sons, Inc., Hoboken, NJ. p. 73–84.

Miller, F. A. 2004b. Introduction. In: D. W. Mayo, F. A. Miller and R. W. Hannah, editors, Course notes on the interpretation of infrared and Raman spectra. John Willy & Sons, Inc., Hoboken, NJ. p. 1–32.

Milosevic, M. 2004. Internal reflection and ATR spectroscopy. Appl. Spectrosc. Rev. 39:365–384.

Mischnick, P., and D. Momcilovic. 2010. Chemical structure analysis of starch and cellulose derivatives. In: H. Derek, editor, Adv. Carbohydr. Chem. Biochem. Vol. 64. Academic Press, New York, NY. p. 117–210.

Mitsui, K., T. Inagaki, and S. Tsuchikawa. 2007. Monitoring of hydroxyl groups in wood during heat treatment using NIR spectroscopy.

Biomacromolecules 9:286–288.

Modzelewska, I., A. Sandak, J. Sandak, and A. Jaszczur. 2011. FT-NIR spectrophotometric analysis of paper, made of cellulose sulfate bleached deciduous pulp, with starch and resinous glue additives, subjected to mycological biodegradiation. Acta Scientiarum Polonorum - Silvarum Colendarum Ratio et Industria Lignaria 10:29–36.

Moreau, R. A., K. S. Liu, J. K. Winkler-Moser, and V. Singh. 2011. Changes in lipid composition during dry grind ethanol processing of corn. J. Am. Oil Chem. Soc. 88:435–442.

Mossoba, M. M., J. K. G. Kramer, H. Azizian, J. Kraft, P. Delmonte, A. R. F. Kia, F. J. Bueso, J. I. Rader, and J. K. Lee. 2012. Application of a novel, heated, nine-reflection ATR crystal and a portable FTIR spectrometer to the rapid determination of total trans fat. J. Am. Oil Chem. Soc. 89:419–429.

Mossoba, M. M., V. Milosevic, M. Milosevic, J. K. G. Kramer, and H. Azizian. 2007. Determination of total trans fats and oils by infrared spectroscopy for regulatory compliance. Anal. Bioanal. Chem. 389:87–92.

Mossoba, M. M., M. P. Yurawecz, and R. E. McDonald. 1996. Rapid determination of the total trans content of neat hydrogenated oils by attenuated total reflection spectroscopy. J. Am. Oil Chem. Soc. 73:1003–1009.

Moughan, P. J. 1999. In vitro techniques for the assessment of the nutritive value of feed grains for pigs: a review. Aust. J. Agric. Res. 50:871–879.

Movasaghi, Z., S. Rehman, and I. U. Rehman. 2007. Raman Spectroscopy of

Biological Tissues. Appl. Spectrosc. Rev. 42:493–541.

Moya Moreno, M. C. M., D. Mendoza Olivares, F. J. Amézquita López, V. Peris Martínez, and F. Bosch Reig. 1999. Study of the formation of carbonyl compounds in edible oils and fats by 1H-NMR and FTIR. J. Mol. Struct. 482–483:557–561.

Munck, L., B. Moller, S. Jacobsen, and I. Sondergaard. 2004. Near infrared spectra indicate specific mutant endosperm genes and reveal a new mechanism for substituting starch with (1→3,1→4)-beta-glucan in barley. J. Cereal. Sci. 40:213–222.

Nakashima, K., J. Sugiyama, and N. Satoh. 2008. A spectroscopic assessment of cellulose and the molecular mechanisms of cellulose biosynthesis in the ascidian Ciona intestinalis. Mar. Genomics 1:9–14.

Nakorn, K. N., T. Tongdang, and P. Sirivongpaisal. 2009. Crystallinity and rheological properties of pregelatinized rice starches differing in amylose content. Starch/Starke 61:101–108.

Noblet, J., and Y. Jaguelin-Peyraud. 2007. Prediction of digestibility of organic matter and energy in the growing pig from an in vitro method. Anim. Feed Sci. Technol. 134:211–222.

Noda, I. 2002. General theory of two-dimensional (2D) analysis. In: J. M. Chalmers and P. R. Griffiths, editors, Handbook of vibrational theory, Vol. 3. John Wiley & Sons Ltd, Chichester, UK. p. 2123–2134.

Nordheim, H., H. Volden, G. Fystro, and T. Lunnan. 2007. Prediction of in situ degradation characteristics of neutral detergent fibre (aNDF) in temperate

grasses and red clover using near-infrared reflectance spectroscopy (NIRS). Anim. Feed Sci. Technol. 139:92–108.

Norris, K. H., R. F. Barnes, J. E. Moore, and J. S. Shenk. 1976. Predicting forage quality by infrared reflectance spectroscopy. J. Anim. Sci. 43:889–897.

Norris, K. H., W. R. Hruschka, M. M. Bean, and D. C. Slaughter. 1989. A definition of wheat hardness using near infrared reflectance spectroscopy. Cereal Food World 34:696–705.

Oh, S. Y., D. I. Yoo, Y. Shin, H. C. Kim, H. Y. Kim, Y. S. Chung, W. H. Park, and J. H. Youk. 2005. Crystalline structure analysis of cellulose treated with sodium hydroxide and carbon dioxide by means of X-ray diffraction and FTIR spectroscopy. Carbohydr. Res. 340:2376–2391.

Olinger, J. M., and P. R. Griffiths. 1993. Effects of sample dilution and particle size/morphology on diffuse reflection spectra of carbohydrate systems in the near- and mid-infrared. Part 1. Single analytes. Appl. Spectrosc. 47:687–694.

Osawa, M., and N. Inoue. 2008. Estimation of starch digestion pattern and glycemic index of rice by near infrared reflectance spectroscopy. JPN J. Crop. Sci. 77.

Osborne, B. G., T. Fearn, and P. H. Hindle. 1993. Practical NIR spectroscopy with applications in food and beverage analysis. Longman Scientific & Technical, Harlow, Essex, England.

Pérez-Marín, D., A. Garrido-Varo, E. de Pedro, and J. E. Guerrero-Ginel. 2007. Chemometric utilities to achieve robustness in liquid NIRS calibrations:

Application to pig fat analysis. Chemometrics Intellig. Lab. Syst. 87:241–246.

Pandey, K. K., and K. S. Theagarajan. 1997. Analysis of wood surfaces and ground wood by diffuse reflectance (DRIFT) and photoacoustic (PAS) Fourier transform infrared spectroscopic techniques. Holz Roh Werkst. 55:383–390.

Philippe, S., P. Robert, C. Barron, L. Saulnier, and F. Guillon. 2006. Deposition of cell wall polysaccharides in wheat endosperm during grain development: Fourier transform-infrared microspectroscopy study. J. Agric. Food Chem. 54:2303–2308.

Philipps, P., R. Aureli, B. Cochin de Billy, and A. M. Klunter. 2005. The use of near-infrared reflectance spectroscopy to predict the protein, fat and gross energy contents of broiler ileum content and broiler excreta. In: Proc. 15th European Symp. Poultry Nutr., Balatonfured, Hungary. p. 456–458..

Picarelli, A., M. Greco, F. Di Giovambattista, A. Ramazzotti, C. Cedrone, E. Corazziari, and A. Torsoli. 1995. Quantitative determination of faecal fat, nitrogen and water by means of a spectrophotometric technique: near infrared reflectance analysis (NIRA). Assessment of its accuracy and reproducibility compared with chemical methods. Clin. Chim. Acta 234:147–156.

Pizzo, B., E. Pecoraro, and N. Macchioni. 2013. A new method to quantitatively evaluate the chemical composition of waterlogged wood by means of attenuated total reflectance Fourier transform infrared (ATR FT-IR)

measurements carried out on wet material. Appl. Spectrosc. 67:553–562.

Pla, M., P. Hernandez, B. Arino, J. A. Ramirez, and I. Diaz. 2007. Prediction of fatty acid content in rabbit meat and discrimination between conventional and organic production systems by NIRS methodology. Food Chem. 100:165–170.

Planinšek, O., D. Planinšek, A. Zega, M. Breznik, and S. Srčič. 2006. Surface analysis of powder binary mixtures with ATR FTIR spectroscopy. Int. J. Pharm. 319:13–19.

Purnomoadi, A., M. Kurihara, T. Nishida, F. Terada, and A. Abe. 1998. Prediction of feed digestibility using differences in NIRS spectra between feeds and feces at a determined region of wavelength. Anim. Sci. Technol. 69:253–258.

Qiao, Y., and T. A. T. G. van Kempen. 2004. Technical note: comparison of Raman, mid, and near infrared spectroscopy for predicting the amino acid content in animal meals. J. Anim. Sci. 82:2596–2600.

Rana, R., R. Langenfeld-Heyser, R. Finkeldey, and A. Polle. 2010. FTIR spectroscopy, chemical and histochemical characterisation of wood and lignin of five tropical timber wood species of the family of Dipterocarpaceae. Wood Sci. Technol. 44:225–242.

Rashid, I., M. H. Al Omari, S. A. Leharne, B. Z. Chowdhry, and A. Badwan. 2012. Starch gelatinization using sodium silicate: FTIR, DSC, XRPD, and NMR studies. Starch-Starke 64:713–728.

Reeves, J. B., III. 2010. Near- versus mid-infrared diffuse reflectance

spectroscopy for soil analysis emphasizing carbon and laboratory versus on-site analysis: where are we and what needs to be done? Geoderma 158:3–14.

Regmi, P. R., N. S. Ferguson, and R. T. Zijlstra. 2009. In vitro digestibility techniques to predict apparent total tract energy digestibility of wheat in grower pigs. J. Anim. Sci. 87:3620–3629.

Regmi, P. R., W. C. Sauer, and R. T. Zijlstra. 2008. Prediction of in vivo apparent total tract energy digestibility of barley in grower pigs using an in vitro digestibility technique. J. Anim. Sci. 86:2619–2626.

Regmi, P. R., T. A. T. G. van Kempen, J. J. Matte, and R. T. Zijlstra. 2011. Starch with high amylose and low in vitro digestibility increases short-chain fatty acid absorption, reduces peak insulin secretion, and modulates incretin secretion in pigs. J. Nutr. 141:398–405.

Ricard-Lespade, L., G. Longhi, and S. Abbate. 1990. The first overtone of CH stretchings in polymethylene chains: A conformationally dependent spectrum. Chem. Phys. 142:245–259.

Robert, P., M. Marquis, C. Barron, F. Guillon, and L. Saulnier. 2005. FT-IR investigation of cell wall polysaccharides from cereal grains. Arabinoxylan infrared assignment. J. Agric. Food Chem. 53:7014–7018.

Russell, J. D., I. Murray, and A. R. Fraser. 1989. Near- and mid-infrared studies of the cell wall structure of cereal straw in relation to its rumen degradability. In: A. Chesson and E. R. Ørskov, editors, Physico-chemical characterisation of plant residues for industrial and feed use. Springer

Netherlands. p. 13–24.

Schindler, R., B. Lendl, and R. Kellner. 1997. Determination of amyloglucosidase activity using flow injection analysis with Fourier transform infrared spectrometric detection. Analyst 122:531–534.

Schulz, H., and M. Baranska. 2007. Identification and quantification of valuable plant substances by IR and Raman spectroscopy. Vib. Spectrosc. 43:13–25.

Schweitzer-Stenner, R. 2006. Advances in vibrational spectroscopy as a sensitive probe of peptide and protein structure: A critical review. Vib. Spectrosc. 42:98–117.

Seefeldt, H. F., A. Blennow, B. M. Jespersen, B. Wollenweber, and S. B. Engelsen. 2009. Accumulation of mixed linkage (1→3) (1→4)-β-d-glucan during grain filling in barley: A vibrational spectroscopy study. J. Cereal. Sci. 49:24–31.

Sevenou, O., S. E. Hill, I. A. Farhat, and J. R. Mitchell. 2002. Organisation of the external region of the starch granule as determined by infrared spectroscopy. Int. J. Biol. Macromol. 31:79–85.

Shao, Y., Y. Cen, Y. He, and F. Liu. 2011. Infrared spectroscopy and chemometrics for the starch and protein prediction in irradiated rice. Food Chem. 126:1856–1861.

Shenk, J. S., J. J. Workman, and M. O. Westerhaus. 2001. Application of NIR spectroscopy to agricultural products. In: D. A. Burns and E. W. Ciurczak, editors, Handbook of near-infrared analysis. CRC Press, Boca Raton, FL.

p. 348–386.

Sherazi, S. T. H., M. Y. Talpur, S. A. Mahesar, A. A. Kandhro, and A. Sarfraz. 2009. Main fatty acid classes in vegetable oils by SB-ATR-Fourier transform infrared (FTIR) spectroscopy. Talanta 80:600–606.

Shrestha, A. K., C. S. Ng, A. Lopez-Rubio, J. Blazek, E. P. Gilbert, and M. J. Gidley. 2010. Enzyme resistance and structural organization in extruded high amylose maize starch. Carbohydr. Polym. 80:699–710.

Shurvell, H. F. 2002. Spectra–structure correlations in the mid- and far-infrared. In: J. M. Chalmers and P. R. Griffiths, editors, Handbook of vibrational theory, Vol. 3. John Wiley & Sons Ltd, Chichester, UK. p. 1783–1816.

Siesler, H. W. 2001. Basic principles of near-infrared spectroscopy. In: D. A. Burns and E. W. Ciurczak, editors, Handbook of near-infrared analysis. CRC Press, Boca Raton, FL. p. 7–19.

Sills, D. L., and J. M. Gossett. 2012. Using FTIR to predict saccharification from enzymatic hydrolysis of alkali-pretreated biomasses. Biotechnol. Bioeng. 109:353–362.

Smith, J. G. 2010. General, organic, and biological chemistry. McGraw-Hill Companies, Inc., New York, NY.

Smits, A. L. M., F. C. Ruhnau, J. F. G. Vliegenthart, and J. J. G. Van Soest. 1998. Ageing of starch based systems as observed with FT-IR and solid state NMR spectroscopy. Starch 50:478–483.

Sohn, M. Y., D. S. Himmelsbach, and F. E. Barton, II. 2004. A comparative study of Fourier transform Raman and NIR spectroscopic methods for

assessment of protein and apparent amylose in rice. Cereal Chem. 81:429–433.

Sohn, M. Y., D. S. Himmelsbach, S. E. Kays, D. D. Archibald, and F. E. Barton, II. 2005. NIR-FT/Raman spectroscopy for nutritional classification of cereal foods. Cereal Chem. 82:660–665.

Sokolowski, F., and D. Naumann. 2005. FTIR study on thermal denaturation and aggregation of recombinant hamster prion protein SHaPrP90–232. Vib. Spectrosc. 38:39–44.

Storz, E., and K. J. Steffens. 2004. Feasibility study for determination of the dextrose equivalent (DE) of starch hydrolysis products with near-infrared spectroscopy (NIRS). Starch-Starke 56:58–62.

Swift, M. L. 2003. Prediction of dry matter, crude protein degradability, and amino acid composition of corn silage and grass silage by near infrared reflectance spectroscopy (NIRS). PhD Thesis. The University of British Columbia, Canada.

Szymanska-Chargot, M., J. Cybulska, and A. Zdunek. 2011. Sensing the structural differences in cellulose from apple and bacterial cell wall materials by Raman and FT-IR spectroscopy. Sensors 11:5543–5560.

Tamaki, Y., and G. Mazza. 2011. Rapid determination of lignin content of straw using Fourier transform mid-infrared spectroscopy. J. Agric. Food Chem. 59:504–512.

Tang, Z., H. Li, and G. Lu. 2011. Rapid determination of sweetpotato resistant starch (RS) using near-infrared spectroscopy (NIRS). Jiangsu J. Agric. Sci.

27:1426–1429.

Uarrota, V. G., E. R. Amante, I. M. Demiate, F. Vieira, I. Delgadillo, and M. Maraschin. 2013. Physicochemical, thermal, and pasting properties of flours and starches of eight Brazilian maize landraces (Zea mays L.). Food Hydrocolloid. 30:614–624.

Udén, P. 2009. Estimating residual starch from in vitro fermentations by Fourier transform mid-IR transmission spectroscopy. Anim. Feed Sci. Technol. 152:133–140.

Udén, P., and L. O. Sjaunja. 2009. Estimating volatile fatty acid concentrations in rumen samples by Fourier transform mid-IR transmission spectroscopy. Anim. Feed Sci. Technol. 152:123–132.

van Barneveld, R. J., J. D. Nuttall, P. C. Flinn, and B. G. Osborne. 1999. Near infrared reflectance measurement of the digestible energy content of cereals for growing pigs. J. Near Infrared Spectrosc. 7:1–7.

van de Voort, F. R., J. Sedman, and A. A. Ismail. 1993. A rapid FTIR quality-control method for determining fat and moisture in high-fat products. Food Chem. 48:213–221.

van de Voort, F. R., J. Sedman, and S. T. H. Sherazi. 2007. Improved determination of isolated trans isomers in edible oils by Fourier transform infrared spectroscopy using spectral reconstitution. J. AOAC Int. 90:446–451.

van de Voort, F. R., J. Sedman, and T. H. Sherazi. 2008. Correcting for underlying absorption interferences in Fourier transform infrared trans analysis of

edible oils using two-dimensional correlation techniques. J. Agric. Food Chem. 56:1532–1537.

van Kempen, T., and J. C. Bodin. 1998. Near-infrared reflectance spectroscopy (NIRS) appears to be superior to nitrogen-based regression as a rapid tool in predicting the poultry digestible amino acid content of commonly used feedstuffs. Anim. Feed Sci. Technol. 76:139–147.

van Soest, J. J. G., H. Tournois, D. de Wit, and J. F. G. Vliegenthart. 1995. Short-range structure in (partially) crystalline potato starch determined with attenuated total reflectance Fourier-transform IR spectroscopy. Carbohydr. Res. 279:201–214.

Vasanthan, T., and F. Temelli. 2008. Grain fractionation technologies for cereal beta-glucan concentration. Food Res. Int. 41:876–881.

Vasko, P. D., J. Blackwell, and J. L. Koenig. 1972. Infrared and raman spectroscopy of carbohydrates. Part II: Normal coordinate analysis of α-D-glucose. Carbohydr. Res. 23:407–416.

Vongsvivut, J., P. Heraud, W. Zhang, J. A. Kralovec, D. McNaughton, and C. J. Barrow. 2012. Quantitative determination of fatty acid compositions in micro-encapsulated fish-oil supplements using Fourier transform infrared (FTIR) spectroscopy. Food Chem. 135:603–609.

Wang, L. F., P. R. Regmi, N. S. Ferguson, A. Pharazyn, and R. T. Zijlstra. 2010. Evaluation of energy digestibility among and within feedstuffs for swine using an in vitro digestibility technique. J. Anim. Sci. 88:557 (Abstr.).

Warren, F. J., P. G. Royall, S. Gaisford, P. J. Butterworth, and P. R. Ellis. 2011.

Binding interactions of alpha-amylase with starch granules: the influence of supramolecular structure and surface area. Carbohydr. Polym. 86:1038–1047.

Wei, L., Y. Yan, and J. Dai. 2004. Determination of protein and starch content in whole maize kernel by near infrared reflectance spectroscopy. Agric. Sci. China 3.

Westad, F., A. Schmidt, and M. Kermit. 2008. Incorporating chemical band-assignment in near infrared spectroscopy regression models. J. Near Infrared Spectrosc. 16:265–273.

Weyer, L. G., and S.-C. Lo. 2002. Spectra–structure correlations in the near-infrared. In: J. M. Chalmers and P. R. Griffiths, editors, Handbook of vibrational theory, Vol. 3. John Wiley & Sons Ltd, Chichester, UK. p. 1817–1837.

Williams, P. C. 1975. Application of near infrared reflectance spectroscopy to analysis of cereal grains and oilseeds. Cereal Chem. 52:561–576.

Williams, P. C., and H. M. Cordeiro. 1979. The determination of protein and moisture in HRS wheat by near-infrared reflectance spectroscopy. II. Influence of degrading factors, dockage and wheat variety. Cereal Food World 24:460.

Williams, P. C., K. R. Preston, K. H. Norris, and P. M. Starkey. 1984. Determination of amino acids in wheat and barley by near-infrared reflectance spectroscopy. J. Food Sci. 49:17–20.

Williams, P. C., and D. C. Sobering. 1993. Comparison of commercial near

infrared transmittance and reflectance instruments for analysis of whole grains and seeds. J. Near Infrared Spectrosc. 1:25–32.

Wilman, D., M. Field, S. J. Lister, and D. I. Givens. 2000. The use of near infrared spectroscopy to investigate the composition of silages and the rate and extent of cell-wall degradation. Anim. Feed Sci. Technol. 88:139–151.

Wolkers, W. F. 2009. Biomedical FTIR spectroscopy of lipids. In: A. Barth and P. I. Haris, editors, Biological and biomedical infrared spectroscopy. IOS Press, Amsterdam, Netherlands. p. 272–287.

Wong, B. T., L. Day, D. McNaughton, and M. A. Augustin. 2009. The effect of maillard conjugation of deamidated wheat proteins with low molecular weight carbohydrates on the secondary structure of the protein. Food Biophysics 4:1–12.

Workman, J., and L. Weyer. 2012. Practical guide and spectral atlas for interpretive near-infrared spectroscopy. 2nd ed. CRC Press, Boca Raton, FL.

Xie, F., F. E. Dowell, and X. Z. S. Sun. 2004. Using visible and near-infrared reflectance spectroscopy and differential scanning calorimetry to study starch, protein, and temperature effects on bread staling. Cereal Chem. 81:249–254.

Yang, D., and Y. Ying. 2011. Applications of Raman spectroscopy in agricultural products and food analysis: A review. Appl. Spectrosc. Rev. 46:539–560.

Yang, H., and J. Irudayaraj. 2000. Characterization of semisolid fats and edible oils by Fourier transform infrared photoacoustic spectroscopy. J. Am. Oil

Chem. Soc. 77:291–295.

Yang, H., J. Irudayaraj, and M. M. Paradkar. 2005. Discriminant analysis of edible oils and fats by FTIR, FT-NIR and FT-Raman spectroscopy. Food Chem. 93:25–32.

Yen, J. T. 2001. Anatomy of the digestive system and nutritional physiology. In: A. J. Lewis and L. L. Southern, editors, Swine Nutrition. CRC Press, Boca Raton, FL. p. 31–64.

Yoshida, S., and H. Yoshida. 2003. Nondestructive analyses of unsaturated fatty acid species in dietary oils by attenuated total reflectance with Fourier transform IR spectroscopy. Biopolymers 70:604–613.

Yu, P. 2005. Multicomponent peak modeling of protein secondary structures: comparison of Gaussian with Lorentzian analytical methods for plant feed and seed molecular biology and chemistry research. Appl. Spectrosc. 59:1372–1380.

Yu, P. 2008. Molecular chemistry of plant protein structure at a cellular level by synchrotron-based FTIR spectroscopy: Comparison of yellow (Brassica rapa) and Brown (Brassica napus) canola seed tissues. Infrared. Phys. Techn. 51:473–481.

Yu, P. 2010. Plant-based food and feed protein structure changes induced by gene-transformation, heating and bio-ethanol processing: a synchrotron-based molecular structure and nutrition research program. Mol. Nutr. Food Res. 54:1535–1545.

Yu, P. 2011. Study the sensitivity of molecular functional groups to bioethanol

processing in lipid biopolymer of co-products using DRIFT molecular spectroscopy. Spectrochim. Acta. A Mol. Biomol. Spectrosc. 82:1–7.

Yu, P., C. R. Christensen, D. A. Christensen, and J. J. McKinnon. 2005. Ultrastructural-chemical makeup of yellow-seeded (Brassica rapa) and brown-seeded (Brassica napus) canola within cellular dimensions, explored with synchrotron reflection FTIR microspectroscopy. Can. J. Plant. Sci. 85:533–541.

Yu, P., D. A. Christensen, C. R. Christensen, M. D. Drew, B. G. Rossnagel, and J. J. McKinnon. 2004a. Use of synchrotron FTIR microspectroscopy to identify chemical differences in barley endosperm tissue in relation to rumen degradation characteristics. Can. J. Anim. Sci. 84:523–527.

Yu, P., J. J. McKinnon, C. R. Christensen, and D. A. Christensen. 2004b. Imaging molecular chemistry of Pioneer corn. J. Agric. Food Chem. 52:7345–7352.

Yu, P., J. J. McKinnon, C. R. Christensen, D. A. Christensen, N. S. Marinkovic, and L. M. Miller. 2003. Chemical imaging of microstructures of plant tissues within cellular dimension using synchrotron infrared microspectroscopy. J. Agric. Food Chem. 51:6062–6067.

Yu, P., and W. G. Nuez-Ortin. 2010. Relationship of protein molecular structure to metabolisable proteins in different types of dried distillers grains with solubles: a novel approach. Br. J. Nutr. 104:1429–1437.

Yu, P. Q., D. Damiran, A. Azarfar, and Z. Y. Niu. 2011a. Detecting molecular features of spectra mainly associated with structural and non-structural carbohydrates in co-products from bioethanol production using DRIFT

with uni- and multivariate molecular spectral analyses. Int. J. Mol. Sci. 12:1921–1935.

Yu, X., F. van de Voort, J. Sedman, and J. Gao. 2011b. A new direct Fourier transform infrared analysis of free fatty acids in edible oils using spectral reconstitution. Anal. Bioanal. Chem. 401:315–324.

Yuen, S., S. Choi, D. L. Phillips, and C. Ma. 2009. Raman and FTIR spectroscopic study of carboxymethylated non-starch polysaccharides. Food Chem. 114:1091–1098.

Zhang, B., X. Li, J. Liu, F. Xie, and L. Chen. 2013. Supramolecular structure of A- and B-type granules of wheat starch. Food Hydrocolloid. 31:68–73.

Zhang, Y., and J. H. Han. 2006. Plasticization of pea starch films with monosaccharides and polyols. J. Food Sci. 71:E253–E261.

Zhbankov, R. G. 1992. Vibrational spectra and structure of mono- and polysaccharides. J. Mol. Struct. 275:65–84.

Zhbankov, R. G., S. P. Firsov, D. K. Buslov, N. A. Nikonenko, M. K. Marchewka, and H. Ratajczak. 2002. Structural physico-chemistry of cellulose macromolecules. Vibrational spectra and structure of cellulose. J. Mol. Struct. 614:117–125.

Zhou, G., G. Taylor, and A. Polle. 2011. FTIR-ATR-based prediction and modelling of lignin and energy contents reveals independent intra-specific variation of these traits in bioenergy poplars. Plant Methods 7:1–10.

Zijlstra, R. T., A. Owusu-Asiedu, and P. H. Simmins. 2010. Future of NSP-degrading enzymes to improve nutrient utilization of co-products and gut

health in pigs. Livest. Sci. 134:255–257.

Zijlstra, R. T., M. L. Swift, L. F. Wang, T. A. Scott, and M. J. Edney. 2011. Near infrared reflectance spectroscopy accurately predicts the digestible energy content of barley for pigs. Can. J. Anim. Sci. 91:301–304.

Zobel, H. F. 1988. Molecules to granules - A comprehensive starch review. Starch-Starke 40:44–50.

Zomeno, C., V. Juste, and P. Hernandez. 2012. Application of NIRS for predicting fatty acids in intramuscular fat of rabbit. Meat Sci. 91:155–159.

Table 3.1 Characteristic bands of mid-infrared (MIR) and near-infrared (NIR) spectra of macronutrients

Macro nutrient	MIR			NIR		
	Wavenumber, cm^{-1}	Band assignment	Reference	Wavelength, nm	Band assignment	Reference
Protein	1,650	Amide I	(Miller, 2003; Barth, 2007)	2,175-2,180	Amide I/III	(Gergely and Salgo, 2007)
	1,550	Amide II		2,055-2,065	Amide A/II	
	2,926 ± 10 2,853 ± 10	CH_2	(Mayo, 2004)	2,307, 2,347	C-H stretch and CH_2 bending	(Ricard-Lespade et al., 1990)
Fat or fatty acids	1,742-1,749	Ester C=O	(Yang and Irudayaraj, 2000)			
	1,710-1,712	C=O in free fatty acids	(Yu et al., 2011b)			
	3,010	-C=C-H	(Yoshida and Yoshida, 2003)			

Macro nutrient	MIR			NIR		
	Wavenumber, cm^{-1}	Band assignment	Reference	Wavelength, nm	Band assignment	Reference
Starch	1,076-1,079	C-O, C-C, and C-OH of Glucose	(Vasko et al., 1972)	2,280	C-H stretching and CH_2 deformation	(Kim and Williams, 1990; Workman and Weyer, 2012)
	1,047	Crystalline starch	(Nakorn et al., 2009)			
	1,022	Amorphous starch	(García et al., 2009)			
	995	Crystallinity	(van Soest et al., 1995)			
	929, 860	C-H bending, anomer	(Zhbankov, 1992)			
Fiber	898	β-glycosidic linkage	(Kačuráková et al., 2000)	2,336	C-H,	(Munck et al., 2004; Modzelewska et al., 2011)
	1,033	Cellulose	(Philippe et al., 2006)	2,270	CH_2	
	1,039	α-linked arabinan	(Kačuráková et al., 2000)	1,672,1,446	Lignin	(Krongtaew et al., 2010)

Macro nutrient	MIR			NIR		
	Wavenumber, cm^{-1}	Band assignment	Reference	Wavelength, nm	Band assignment	Reference
	1,505-1,510	Lignin	(Derkacheva and Sukhov, 2008)			

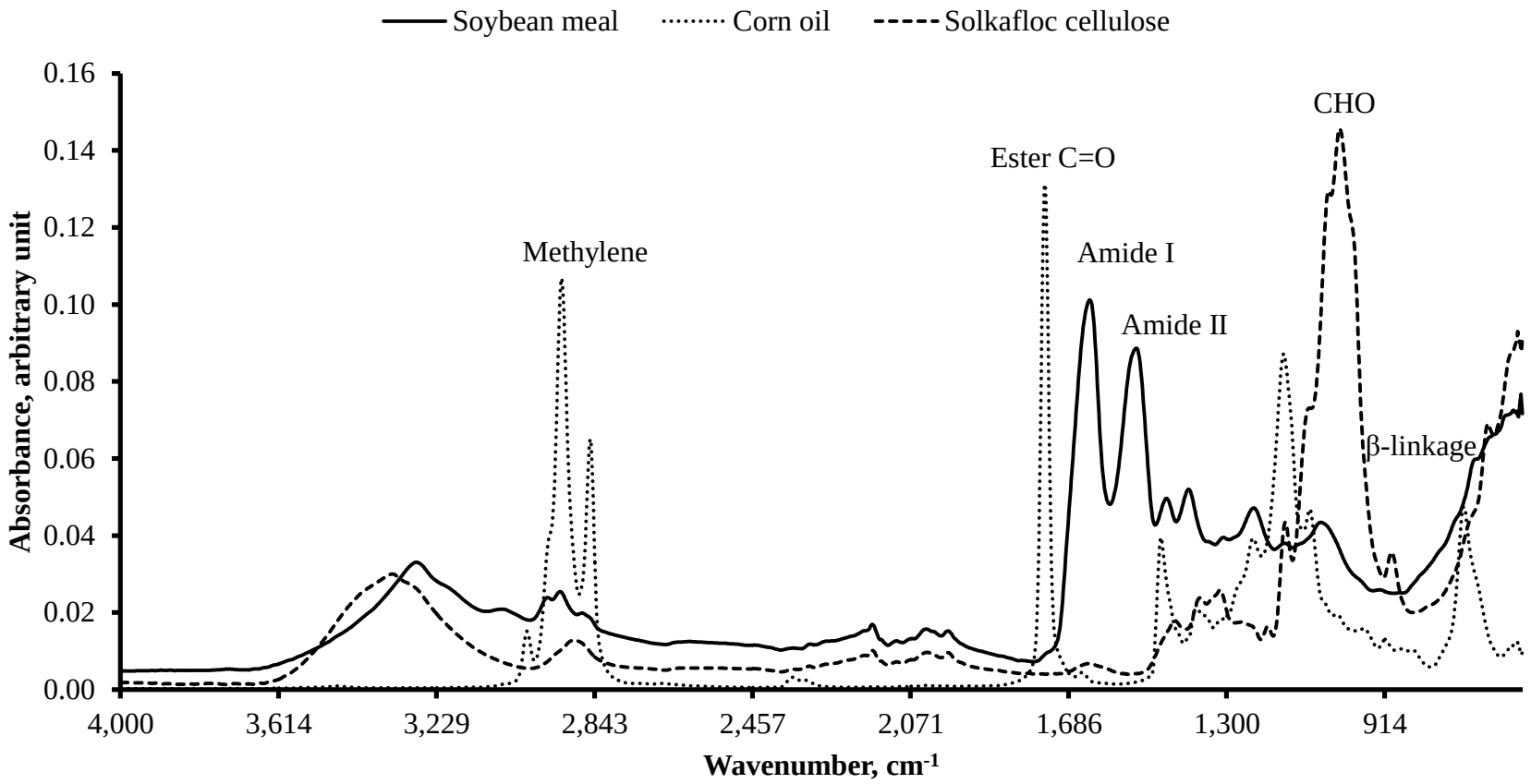

Figure 3.1 Example of mid-infrared (MIR) spectra of soybean meal, corn oil, and Solkfloc cellulose acquired using an attenuated total reflection (ATR) Fourier transform infrared (FT-IR) spectrometer

Chapter 4 Prediction of the apparent total tract digestibility of energy of co-products in pigs with in vitro digestion and chemical analyses

4.1 Abstract

In vitro digestion (IVD) and chemical analyses have been used to predict the apparent total tract digestibility (ATTD) of energy for cereal grains. However, IVD and chemical analyses have not been rigorously tested for co-products rich in fiber, protein, and/or fat. To examine efficacy of an IVD model and chemical analyses on predicting ATTD of energy for co-products, 30 samples of co-products of cereal grains (n = 17) and oilseeds (n = 13) were tested in growing pigs to determine the ATTD of energy, and were tested with an IVD model and chemical analyses. The IVD model explained 69% of the variation in ATTD of energy (RMSE = 3.4, root mean standard error) among the co-products. Within the co-products, the IVD model described the variation of ATTD of energy for wheat millrun (R^2 = 0.79; n = 9), but not for canola meal (R^2 = 0.19; n = 8), corn distillers dried grain with solubles (DDGS; R^2 = 0.29; n = 8), or soybean meal (R^2 = 0.24; n = 5). Moreover, the IVD assay underestimated the ATTD of energy of co-products, especially for corn DDGS and wheat millrun. Using NDF as a single predictor, chemical analyses explained 66% of the variation of ATTD of energy of co-products (RMSE = 3.5). Using ADF, hemicellulose, ether extract, and ash as multiple predictors, prediction accuracy increased (R^2 = 0.88, $P < 0.01$, RMSE = 2.2) for the ATTD of energy of co-products. Chemical analyses of nutrients also explained the variation (R^2 = 0.56-0.84) of ATTD of energy within co-products.

Overall, chemical analyses had greater accuracy than current IVD to predict ATTD of energy among and within the co-products. The IVD model, which worked well for cereal grains, requires improvement to predict energy digestibility for co-products with high fat and high fiber.

4.2 Introduction

Feed cost accounts for approximately two thirds of the cost of pig production (Williams et al., 2011), with dietary energy cost as its largest proportion. However, digestible energy (**DE**) values varied up to 25% within cereal grains and their co-products (van Barneveld, 1999; Zijlstra and Beltranena, 2009). The pork industry attempts to formulate energy levels in swine diets to within a tolerance of 1.5% (Fairbairn et al., 1999). Such a goal is difficult to achieve with widely fluctuating DE values of primary ingredients. Without a proper strategy to manage ingredient DE variability, precision of diet formulation is reduced, resulting in less predictable pig growth performance, increased feed cost and nutrient excretion, or reduced carcass quality (Fairbairn et al., 1999). Thus, knowing actual DE values of feedstuffs is important to ensure that feed energy supply matches energy requirements of pigs (Noblet and Perez, 1993).

Evaluation of energy digestibility is a prerequisite to determine DE values of feed. In vitro digestion (**IVD**) models are promising to evaluate feedstuffs quality (Boisen and Fernandez, 1997) and can predict (R^2 = 0.82-0.97) apparent total tract digestibility (**ATTD**) of energy of cereal grains (Regmi et al., 2008, 2009). However, IVD may lack accuracy for predicting DE value of corn co-

products in pigs (Anderson, 2009), and thus require rigorous testing on co-products. Chemical analyses can predict (R^2 = 0.75-0.94) DE values of wheat grain and among 114 diets in pigs (Noblet and Perez, 1993; Zijlstra et al., 1999), but their accuracy to predict the DE value or energy digestibility of co-products was not tested rigorously.

We hypothesized that both IVD and chemical analyses could predict the ATTD of energy of co-products from cereal grains and oilseeds in pigs. Thus, the objective of present study was to examine the performance of an IVD model to predict the ATTD of energy of co-products from corn, wheat, soybean, and canola in pigs, and compare these to predictions based on chemical analyses.

4.3 Materials and methods

4.3.1 Ingredients, diets, and pig trials

The animal protocols were approved by the University of Alberta Animal Care Committee to ensure adherence to the Canadian Council on Animal Care guidelines (CCAC, 1993). The pig experiments were conducted at the Swine Research and Technology Centre at the University of Alberta (Edmonton, Alberta, Canada).

Thirty co-product samples, including 8 solvent extracted canola meal, 8 corn distillers dried grain with solubles (**DDGS**), 5 soybean meal, and 9 wheat millrun, were mixed with basal diets (Table 4.1) and tested in 4 pig trials to determine the ATTD of energy. Each diet was fed to 4 growing pigs (initial BW: 30~52kg) in 2 periods (each period included 5 days for test diet acclimation and 5

days for fecal collection) following a cross-over experimental design. Diets contained Cr_2O_3 as indigestible marker.

4.3.2 In vitro digestion

All samples of co-products were tested in triplicate using a 3-step IVD model, which was used previously for wheat grain (Regmi et al., 2009) and adapted from its original model (Boisen and Fernandez, 1997). Briefly, 0.5 g sample (ground through 1 mm screen) was incubated with freshly prepared porcine pepsin from gastric mucosa (P-7000, Sigma-Aldrich; 800-200 units/mg protein) for 2 h to mimic the digestion in stomach. The slurry was then incubated with freshly prepared porcine pancreatin (P-7545; Sigma-Aldrich; 8 x USP specifications) for 4 h to mimic the digestion in small intestine. The digesta was then incubated with a multi-enzyme complex Viscozyme L (Sigma-Aldrich; St. Louis, MO; cell wall degrading enzyme complex from *Aspergillus sp*) for 18 h to mimic the digestion in large intestine. At the end of digestion, the undigested residues of IVD were collected after filtration using distilled water in a porcelain filtration funnel lined with pre-weighed filter paper (pore size, 20~25 µm; Whatman no. 54; Whatman Inc., Florham Park, NJ), and then dried overnight at 80 ℃.

4.3.3 Chemical analyses and calculations

All ingredients, diets, and freeze-dried feces were ground in a centrifugal mill through a 1-mm screen; and analyzed for dry matter (**DM**; method 930.15; AOAC, 2006). All ingredients were analyzed for ash (method 942.05), acid detergent fiber (**ADF**; method 973.18), crude fiber (**CF,** method 978.10), crude

protein (**CP**; N × 6.25; method 990.03), ether extract (**EE**, method 920.39) as described by AOAC (2006), and neutral detergent fiber (**NDF**; van Soest et al., 1991). Hemicellulose fraction was calculated as NDF minus ADF (Noblet and Perez, 1993). All samples were analyzed for gross energy (**GE**) using an adiabatic bomb calorimeter (model 5003, Ika-Werke GMBH & Co. KG, Staufen, Germany). Chromic oxide content of diets and feces was determined by spectrophotometry at 440 nm after ashing at 450 ˚C overnight (Fenton and Fenton, 1979). The ATTD of GE of test diets and basal diets was determined using the indicator method (Eq. 1); and the ATTD of GE of test ingredients was determined using the difference method (Eq. 2) according to ATTD of GE of test and basal diets (Adeola, 2001).

$$ATTD\ of\ GE\ of\ diet, \% =$$

$$100 - 100 \times \frac{Concentration\ of\ Cr_2O_3\ in\ diet}{Concentration\ of\ Cr_2O_3\ in\ feces} \times \frac{Concentration\ of\ energy\ in\ feces}{Concentration\ of\ energy\ in\ diet} \quad \text{(Eq. 1)}$$

$$ATTD\ of\ GE\ of\ ingredient, \% = 100 \times \frac{T \times T_p - B \times B_p}{A_p} \quad \text{(Eq. 2)}$$

where T is the ATTD of GE of test diet (basal diet plus the test co-product ingredient); B is the ATTD of GE of basal diet; B_p is the proportion, %, of GE in the test diet contributed by the basal diet; A_p is the proportion, %, of GE in test diet contributed by test co-product ingredient; $T_p = B_p + A_p$.

4.3.4 Statistical analysis

The descriptive statistics, ANOVA and regression analysis were performed using the MEANS, MIXED and REG procedures respectively in SAS 9.3 (SAS Inst. Inc., Cary, NC, USA). Co-product was the experimental unit. The in vitro energy digestibility (**ivED**) was compared with the ATTD of energy of co-products. The model used for ANOVA was: $Y_{ij} = \mu + T_i + e_{ij}$, where Y_{ij} was an

observation of the dependent variable ij (energy digestibility); μ was the population mean for the variable; T_i was the method to determine energy digestibility (IVD or in vivo digestion) as a fixed effect, and e_{ij} was the random error associated with the observation ij. Significance was declared at $P < 0.05$. The ATTD of energy and ivED were reported as least squares means. Partial R^2 of individual chemical predictor was obtained from multiple linear regression analyses with 'Selection = Stepwise' option for the predictions of the ATTD of energy and difference of energy digestibility (as ATTD of energy minus ivED) between IVD and in vivo digestion.

According to predictors entered into the regression model using stepwise selection, an equation to predict the difference of energy digestibility of co-products between IVD and in vivo digestion was generated (Eq. 3).

$$Difference\ of\ digestibility, \% = 10.10 + 0.93 \times EE + 0.47 \times Hemicellulose - 0.40 \times ADF - 0.23 \times CP \quad \text{(Eq. 3)}$$

Similarly, an equation to predict ATTD of energy of co-products using multiple chemical predictors was generated (Eq. 4).

$$ATTD\ of\ energy, \% = 96.06 - 0.41 \times Ash - 0.93 \times ADF - 0.39 \times Hemicellulose - 0.59 \times EE \quad \text{(Eq. 4)}$$

4.4 Results

4.4.1 Chemical characteristics of co-products

The 4 co-products were rich in fiber, protein, and/or fat; and the nutrient content in the 30 samples varied widely (Table 4.2). Within co-products, soybean

co-products were relatively low in fiber (3.9% CF), but high in protein (48.9% CP); wheat co-products were relatively low in fat (4.1% EE), but high in fiber (8.3% CF); while corn DDGS was high in fat, fiber, and protein (12% EE; 6.0% CF; 31.0% CP; respectively).

4.4.2 Measurements of apparent total tract digestibility of energy and predictions with in vitro digestion

The ATTD of energy of 30 co-product samples varied by 23.3 %-units; whereas ivED varied by 42.4 %-units (Table 4.3). Within the co-products, the range of ATTD of energy was small, due to limited number of samples, except for wheat millrun.

Among the co-products, the ivED of co-products related (R^2 = 0.69, P < 0.01; Figure 4.1) to the ATTD of energy. However, the root mean standard error (**RMSE**) of prediction was large (RMSE = 3.4; Table 4.3). Furthermore, the slope of 0.40 of the regression equation (Figure 4.1) was less than the ideal slope of 1.0 with a large intercept of 47.5.

Within co-products, the IVD model severely underestimated the ATTD of energy for corn DDGS and wheat millrun by more than 14 %-units, but did not for canola meal and soybean meal (Table 4.3). The IVD model described the variation of ATTD of energy for wheat millrun (R^2 = 0.79, P < 0.01; Figure 4.2A), but did not for canola meal (R^2 = 0.19, P = 0.28; Figure 4.2B), corn DDGS (R^2 = 0.29, P = 0.17; Figure 4.2C), or soybean meal (R^2 = 0.24, P = 0.41; Figure 4.2D). The difference of energy digestibility (as in vivo ATTD of energy minus ivED) between IVD and in vivo digestion among the co-products was predicted (R^2 =

0.90, $P < 0.01$; Figure 4.3) by the content of hemicellulose (partial $R^2 = 0.67$), EE (partial $R^2 = 0.20$), ADF (partial $R^2 = 0.02$), and CP (partial $R^2 = 0.02$) of co-products using Eq. 3.

4.4.3 Predicting apparent total tract digestibility of energy using chemical analyses

With chemical analyses, the ATTD of energy of co-products was predicted ($R^2 = 0.66$, $P < 0.01$, RMSE = 3.5; Figure 4.4) using NDF as a single predictor. The prediction accuracy for the ATTD of energy of co-products was further increased ($R^2 = 0.88$, $P < 0.01$, RMSE = 2.2; Figure 4.5) with multiple predictors of ADF (partial $R^2 = 0.41$), hemicellulose (partial $R^2 = 0.32$), EE (partial $R^2 = 0.13$), and ash (partial $R^2 = 0.03$) as per Eq. 4. The combination of IVD and chemical analyses did not increase the prediction accuracy of ATTD of energy among the co-products ($R^2 = 0.88$; Table 4.3) with predictors of ivED (partial $R^2 = 0.69$, $P < 0.01$), ADF (partial $R^2 = 0.18$, $P < 0.01$), and ash (partial $R^2 = 0.01$, $P = 0.15$).

Within the co-products, EE content in canola meal, CF and ash content in corn DDGS, CP content in soybean meal, and CF content in wheat millrun predicted the ATTD of energy of canola meal ($R^2 = 0.56$, $P = 0.03$; Table 4.3), corn DDGS ($R^2 = 0.81$, $P = 0.02$), soybean meal ($R^2 = 0.84$, $P = 0.03$), and wheat millrun ($R^2 = 0.80$, $P < 0.01$), respectively. The combination of IVD and chemical analyses slightly increased the prediction accuracy of ATTD of energy only for wheat millrun ($R^2 = 0.86$, $P < 0.01$).

4.5 Discussion

4.5.1 Challenges of co-products

The 30 samples of co-products covered a wide range of chemical composition, such as for protein, fiber, and fat, that was in agreement with other investigations (Serena and Knudsen, 2007; Ortin and Yu, 2009; Zijlstra and Beltranena, 2009). Correspondingly, the ATTD of energy of co-products varied widely (Landero et al., 2011; Yanez et al., 2011; Shrestha, 2012). Consequently, the samples were a representative set of co-products to challenge the prediction accuracy of IVD and predictions based on chemical analyses.

4.5.2 In vitro digestion for co-products

Among the co-products, the IVD model explained 69% of the variation of the ATTD of energy; however, that was largely attributed to the increased range of the ATTD of energy. In comparison, the IVD model explained 82-97% of variation in ATTD of energy for cereal grains (Regmi et al., 2008, 2009). The regression line was away from ideal (slope =1) and much smaller than the regression slope of 1.07 using a IVD model tested on 34 feed mixtures (Boisen and Fernandez, 1997), indicating inconsistent IVD of co-products. The IVD model was thus not sufficiently robust to evaluate energy digestibility among the co-products (Anderson, 2009).

Within the co-products, the number of samples of each co-product for pig trials was small (n = 5-9) and the range of ATTD of energy was also narrow for each co-product except for wheat millrun. The IVD model underestimated the ATTD of energy for corn DDGS and wheat millrun. Corn DDGS is rich in fat,

fiber, and protein (Belyea et al., 2004); whereas wheat millrun is especially rich in fiber (Shrestha, 2012). Hemicellulose and EE content in the co-products explained most of the variation of the difference of energy digestibility between IVD and in vivo digestion. High partial R^2 of hemicellulose and EE in the regression model indicated that IVD of fiber and fat might be an issue for the current IVD model to evaluate energy digestibility of co-products. The ATTD of energy was not underestimated for the other 2 co-products, solvent extracted canola meal and soybean meal. Both canola meal and soybean meal were rich in protein and relatively low in fat, indicating that IVD of protein might be not an issue for the current IVD model. Indeed, prediction accuracy for CP and amino acid (**AA**) digestibility was high with an IVD model (Boisen and Fernandez, 1995). Some suggest that an IVD model may replace surgically-modified pigs to analyze apparent ileal digestibility (**AID**) of AA in protein sources (Boisen, 2007). However, the IVD model poorly described the variation of ATTD of energy of canola meal, corn DDGS, and soybean meal. The range of ATTD of energy was a factor for the low R^2, but not the only factor. Simulation by IVD reflecting in vivo digestion is important. The IVD model described the variation of ATTD of energy for wheat millrun. However, the ATTD of energy of wheat millrun was severely underestimated by the IVD model. The current IVD is incapable to detect small fluctuations of ATTD of energy within co-products, although this capability is desired for a potent IVD model (Moughan, 1999).

4.5.3 Limitations of the current in vitro digestion model

Fat content of co-products was associated with discrepancies of energy digestibility between IVD and in vivo digestion. Digestion of fat requires pancreatic lipase, colipase, phospholipase, calcium, and bile salts (Carey et al., 1983; Embleton and Pouton, 1997). The IVD model does not have a fully functional fat digestion step, thus, enzymatic digestion of fat is not expected to mimic in vivo digestion. The IVD model used in the present study has been used in our lab for cereal grains and did not have an additional filtration step with acetone at the end of IVD (Regmi et al., 2008, 2009). Thus, undigested fat was expected still in the undigested residues without filtration using acetone (Boisen and Fernandez, 1997). Cereal grains are low in fat, thus, the filtration using acetone might be not critical for the evaluation of energy digestibility. Indeed, the IVD model accurately predicted the ATTD of energy of wheat and barley grains (Regmi et al., 2008, 2009). For co-products rich in fat, enzymatic digestion of fat or removal of fat with filtration using acetone would be critical. However, even with filtration using acetone, the IVD model did not describe the variation of DE for corn co-products (Anderson, 2009), indicating that fat is not the only factor affecting prediction accuracy of IVD models. Fat removal is easy to fulfill with filtration using acetone, but would not reflect fat digestion and microflora modification of fat in the hindgut (Duran-Montgé et al., 2007). Major amounts of fat could be excreted in feces in the form of soap as a loss of dietary energy (Bendsen et al., 2008).

Fiber content might be also associated with the discrepancies of energy digestibility between IVD and in vivo digestion. Fat may restrict enzyme access to digest fiber, because the addition of 0.3 g fat to 1 g of cereal and legume samples during gelatinization decreased in vitro digestibility of carbohydrates (Madhuri et al., 1996). However, even with filtration using acetone at end of IVD (Boisen and Fernandez, 1997), digestion of fiber was not affected.

Compared to other investigations not showing underestimation of ATTD of energy (Boisen and Fernandez, 1997), pore size of filtration unit might be a factor affecting the absolute value of ivED. The pore size of filter paper used in the present IVD model was 20~25 μm, whereas it was 40~90 μm for glass fibre crucible (Boisen and Fernandez, 1997). The larger pore may allow loss of undigested feed particles and therefore overestimate nutrient digestibility (Qiao and Thacker, 2001).

4.5.4 Predictions of energy digestibility with chemical analyses

As a single predictor, NDF can predict the ATTD of energy for co-products, indicating fiber digestion is a major factor affecting ATTD of energy of co-products. Indeed, fiber analyses such as ADF and NDF best predicted the DE values of wheat, barley, and 40 compound pig feeds (Fairbairn et al., 1999; Spanghero and Volpelli, 1999; Zijlstra et al., 1999). Although multiple chemical predictors predicted the ATTD of energy more accurately than a single predictor, the use of multiple chemical analyses is a disadvantage for application.

Within co-products, chemical analyses also predicted the ATTD of energy for corn DDGS, soybean meal, and wheat millrun. For corn DDGS, CF and ash

content best predicted the ATTD of energy. But, methods to determine CF are empirical and any modification (e.g., particle size of sample and pore size of filter) yields a different CF fraction (Thiex, 2009), and hence may affect the accuracy to predict the ATTD of energy of corn DDGS. Furthermore, predictors and corresponding predicting equations differed for each co-product, and among the co-products, indicating the best equation to predict the ATTD of energy for co-products was largely dependent on the sample set used for regression analyses.

4.5.5 Limitations of predictions based on chemical analyses

Although predictions based on chemical analyses were more accurate than the IVD model for co-products, the predictions were based on the amount of analyzed chemical component. Chemical analyses did not account for chemical structure, such as for fiber and starch, and the interaction of digestion among nutrients. For instance, the type and extent of links between polymers and lignin rather than the amount of lignin are important in determining degradability (Glits et al., 2000). Because fiber is the main predictor for the ATTD of energy of co-products, analytical error for fiber is a concern (Wolters et al., 1992). Unlike total dietary fiber or non-starch polysaccharides (NSP), NDF may not account for pectins, galactans, and β-glucans (van Soest et al., 1991). Thus, chemical analyses in the present study covered limited information of the carbohydrates profile.

Another challenge for predictions based on chemical analyses was the selection of samples to cover a wide range of chemical profiles to avoid extrapolation of prediction equations. Although both IVD and chemical analyses accurately predicted DE value of 40 compound feeds in pigs (Spanghero and

Volpelli, 1999), the current IVD model requires improvement to achieve better prediction accuracy than the predictions based on chemical analyses for co-products.

In conclusion, the IVD model described the ATTD of energy among the co-products with a large error, and could not detect small fluctuations of energy digestibility within the co-products. The IVD model underestimated the ATTD of energy for corn DDGS rich in fat and wheat millrun rich in fiber, but not for solvent extracted canola meal and soybean meal rich in protein. Predictions based on chemical analyses were more accurate than the current IVD model to predict the ATTD of energy among and within co-products from corn, wheat, soybean, and canola in pigs. Nevertheless, ivED predicted the ATTD of energy among the co-products better than any single chemical predictor. However, IVD technique requires improvement to fit the evaluation of energy digestibility for co-products.

4.6 References

Adeola, O. 2001. Digestion and balance techniques in pigs. In: A. J. Lewis and L. L. Southern, editors, Swine nutrition. CRC Press LLC, Boca Raton, FL. p. 903–916.

Anderson, P. 2009. Energy determination of corn co-products in finishing pigs and the use of an in vitro organic matter digestibility assay to predict in vivo energy. MSc Diss. Iowa State University, Ames, IA.

AOAC. 2006. Official methods of analysis. 18th ed. Assoc. Off. Anal. Chem., Arlington, VA.

Belyea, R. L., K. D. Rausch, and M. E. Tumbleson. 2004. Composition of corn and distillers dried grains with solubles from dry grind ethanol processing. Bioresour. Technol. 94:293–298.

Bendsen, N. T., A. L. Hother, S. K. Jensen, J. K. Lorenzen, and A. Astrup. 2008. Effect of dairy calcium on fecal fat excretion: a randomized crossover trial. Int. J. Obesity 32:1816–1824.

Boisen, S. 2007. In vitro analyses for predicting standardised ileal digestibility of protein and amino acids in actual batches of feedstuffs and diets for pigs. Livest. Sci. 109:182–185.

Boisen, S., and J. A. Fernandez. 1995. Prediction of the apparent ileal digestibility of protein and amino-acids in feedstuffs and feed mixtures for pigs by in-vitro analyses. Anim. Feed Sci. Technol. 51:29–43.

Boisen, S., and J. A. Fernandez. 1997. Prediction of the total tract digestibility of energy in feedstuffs and pig diets by in vitro analyses. Anim. Feed Sci. Technol. 68:277–286.

Carey, M. C., D. M. Small, and C. M. Bliss. 1983. Lipid digestion and absorption. Annu. Rev. Physiol. 45:651–677.

CCAC. 1993. Guide to the care and use of experimental animals. Vol. 1. 2nd ed. Canadian Council on Animal Care (CCAC), Ottawa, ON, Canada.

Duran-Montgé, P., R. Lizardo, D. Torrallardona, and E. Esteve-Garcia. 2007. Fat and fatty acid digestibility of different fat sources in growing pigs. Livest. Sci. 109:66–69.

Embleton, J. K., and C. W. Pouton. 1997. Structure and function of gastro-intestinal lipases. Adv. Drug Del. Rev. 25:15–32.

Fairbairn, S. L., J. F. Patience, H. L. Classen, and R. T. Zijlstra. 1999. The energy content of barley fed to growing pigs: characterizing the nature of its variability and developing prediction equations for its estimation. J. Anim. Sci. 77:1502–1512.

Fenton, T. W., and M. Fenton. 1979. An improved procedure for the determination of chromic oxide in feed and feces. Can. J. Anim. Sci. 59:631–634.

Glits, L. V., B. B. Jensen, and K. E. B. Knudsen. 2000. In vitro fermentation of rye carbohydrates including arabinoxylans of different structure. J. Sci. Food Agric. 80:1211–1218.

Landero, J. L., E. Beltranena, M. Cervantes, A. Morales, and R. T. Zijlstra. 2011. The effect of feeding solvent-extracted canola meal on growth performance and diet nutrient digestibility in weaned pigs. Anim. Feed Sci. Technol. 170:136–140.

Madhuri, K., S. Pratima, and B. Y. Rao. 1996. Effect of processing on in vitro carbohydrate digestibility of cereals and legumes. J. Food Sci. Technol. 33:493–497.

Moughan, P. J. 1999. In vitro techniques for the assessment of the nutritive value of feed grains for pigs: a review. Aust. J. Agric. Res. 50:871–879.

Noblet, J., and J. M. Perez. 1993. Prediction of digestibility of nutrients and energy values of pig diets from chemical-analysis. J. Anim. Sci. 71:3389–3398.

Ortin, W. G. N., and P. Yu. 2009. Nutrient variation and availability of wheat DDGS, corn DDGS and blend DDGS from bioethanol plants. J. Sci. Food Agric. 89:1754–1761.

Qiao, S., and P. A. Thacker. 2001. A comparison of washed and unwashed bags to determine the apparent fecal digestibility of dry matter, energy and crude protein in feeds for swine using the mobile nylon bag technique. Can. J. Anim. Sci. 81:371–378.

Regmi, P. R., N. S. Ferguson, and R. T. Zijlstra. 2009. In vitro digestibility techniques to predict apparent total tract energy digestibility of wheat in grower pigs. J. Anim. Sci. 87:3620–3629.

Regmi, P. R., W. C. Sauer, and R. T. Zijlstra. 2008. Prediction of in vivo apparent total tract energy digestibility of barley in grower pigs using an in vitro digestibility technique. J. Anim. Sci. 86:2619–2626.

Serena, A., and K. E. B. Knudsen. 2007. Chemical and physicochemical characterisation of co-products from the vegetable food and agro industries. Anim. Feed Sci. Technol. 139:109–124.

Shrestha, D. R. 2012. Effects of supplemented NSP-degrading enzymes on nutrient digestibility of diets containing co-products fed to grower pigs. MSc Diss. University of Alberta, Edmonton.

Spanghero, M., and L. A. Volpelli. 1999. A comparison of the predictions of digestible energy content of compound feeds for pigs by chemical or in vitro analysis. Anim. Feed Sci. Technol. 81:151–159.

Thiex, N. 2009. Evaluation of analytical methods for the determination of moisture, crude protein, crude fat, and crude fiber in distillers dried grains with solubles. J. AOAC Int. 92:61–73.

van Barneveld, R. J. 1999. Chemical and physical characteristics of grains related to variability in energy and amino acid availability in pigs: a review. Aust. J. Agric. Res. 50:667–687.

van Soest, P. J., J. B. Robertson, and B. A. Lewis. 1991. Methods for dietary fiber, neutral detergent fiber, and non-starch polysaccharides in relation to animal nutrition. J. Dairy Sci. 74:3583–3597.

Williams, N. H., S. Klenk, and B. Christianson. 2011. Production costs in the Americas. In: Proc. 2011 Banff Pork Seminar, Banff, Alberta. p. 277–282.

Wolters, M. G. E., C. Verbeek, J. J. M. van Westerop, R. J. J. Hermus, and A. G. J. Voragen. 1992. Comparison of different methods for determination of dietary fiber. J. AOAC Int. 75:626–634.

Yanez, J. L., E. Beltranena, M. Cervantes, and R. T. Zijlstra. 2011. Effect of phytase and xylanase supplementation or particle size on nutrient digestibility of diets containing distillers dried grains with solubles cofermented from wheat and corn in ileal-cannulated grower pigs. J. Anim. Sci. 89:113–123.

Zijlstra, R. T., and E. Beltranena. 2009. Variability of quality in biofuel co-products. In: P. C. Garnsworthy and J. Wiseman, editors, Recent advances in animal nutrition – 2008. Nottingham Academic Press, Nottingham, UK. p. 313–326.

Zijlstra, R. T., C. F. M. de Lange, and J. F. Patience. 1999. Nutritional value of wheat for growing pigs: chemical composition and digestible energy content. Can. J. Anim. Sci. 79:187–194.

Table 4.1 Ingredient composition of the test and basal diets (as fed basis) for in vivo determination of apparent total tract digestibility (ATTD) of energy of co-products in pigs[1]

	Test diets				Basal diets		
Ingredient, %	CM	Corn DDGS	SBM	WM	CM	Corn DDGS	Others[2]
Canola meal	40.0	–	–	–	–	–	–
Corn DDGS	–	60.0	–	–	–	–	–
Soybean meal	–	–	40.0	–	–	–	–
Wheat millrun	–	–	–	40.0	–	–	–
Wheat	55.2	–	–	–	95.2	–	–
Corn starch[3]	–	33.9	–	–	–	85.32	–
Corn	–	–	56.0	56.0	–	–	96.0
Canola oil	–	0.78	–	–	–	2.0	–
Sugar	–	1.95	–	–	–	5.0	–
Solka-Floc[4]	–	–	–	–	–	3.0	–
Limestone	1.2	1.5	1.2	1.2	1.2	1.0	1.2
Mono-dicalcium phosphate	–	–	–	–	–	1.2	–
$CaHPO_4$	0.8	–	0.8	0.8	0.8	–	0.8
Salt	0.4	0.5	0.5	0.5	0.4	0.5	0.5
Mineral premix[5]	0.5	0.5	0.5	0.5	0.5	0.5	0.5
Vitamin premix[6]	0.5	0.5	0.5	0.5	0.5	0.5	0.5
KCO_3 (56% K)	–	–	–	–	–	0.5	–
MgO (58% Mg)	–	–	–	–	–	0.1	–
Celite[7]	1.0	–	–	–	1.0	–	–
Chromic oxide	0.4	0.38	0.5	0.5	0.4	0.38	0.5

[1]CM = canola meal; DDGS = distillers dried grains with solubles; SBM = soybean meal; WM = wheat millrun.

[2]SBM and WM.

[3]Melojel (National Starch and Chemical Co., Bridgewater, NJ).

[4]International Fiber Corp., North Tonawanda, NY.

[5]Provided per kilogram of diet: iron, 80 mg; zinc, 100 mg; manganese, 25 mg; copper, 50 mg; iodine, 0.5 mg; and selenium, 0.1 mg

[6]Provided per kilogram of diet: vitamin A, 8250 IU; vitamin D, 825 IU; vitamin E 40 IU; vitamin K, 4.0 mg; thiamine,1.0 mg; riboflavin, 5.0 mg; pantothenic acid, 15.0 mg; niacin, 35.0 mg; folacin, 2.0 mg; biotin, 0.2 mg; and vitamin B_{12}, 0.03 mg.

[7]World Minerals Inc., Santa Barbara, CA.

Table 4.2 Analyzed nutrient content of canola meal, corn DDGS, soybean meal, and wheat millrun for both in vivo and in vitro trials (%, dry matter basis)[1]

	Canola meal (n = 8)			Corn DDGS (n = 8)			Soybean meal (n = 5)			Wheat millrun (n = 9)			All (n = 30)		
Item, %	Min	Max	Mean	Min	Max	Mean	Min	Max	Mean	Min	Max	Mean	Min	Max	Mean
Ash	6.7	8.6	7.6	4.2	16.4	6.5	5.8	16.7	8.6	5.2	7.5	6.2	4.2	16.7	7.0
EE	2.4	4.3	3.0	9.6	14.1	12.0	1.0	7.5	3.8	2.9	5.5	4.1	1.0	14.1	5.9
CP	36.2	41.3	39.0	26.5	33.6	31.0	44.3	53.3	48.9	15.9	27.8	20.2	15.9	53.3	32.9
CF	8.3	10.1	9.3	5.1	6.9	6.0	2.7	5.1	3.9	5.2	12.0	8.3	2.7	12.0	7.2
ADF	15.2	18.1	16.5	9.2	16.3	12.6	4.5	6.9	5.7	8.0	15.5	12.3	4.5	18.1	12.4
NDF	18.7	24.9	21.4	23.4	29.6	26.5	6.6	11.3	9.2	22.9	49.1	33.4	6.6	49.1	24.3

[1]CF, crude fiber; DDGS, dried distillers grains with solubles; EE, ether extract.

Table 4.3 The apparent total tract digestibility (ATTD) of energy and in vitro energy digestibility (ivED) of co-products, and prediction performance for ATTD of energy with ivED and chemical analyses[1]

Item	Canola meal (n = 8)	Corn DDGS (n = 8)	Soybean meal (n = 5)	Wheat millrun (n = 9)	All co-products (n = 30)
ATTD of energy, %					
Mean	73.6	68.7	83.7	71.7	73.4
Range	70.9-76.0	67.1-70.0	81.9-85.9	62.6-81.9	62.6-85.9
ivED, %					
Mean	74.6	53.8*	81.3	57.1*	64.9*
Range	71.5-79.3	50.2-61.7	75.3-87.1	45.7-69.1	45.7-87.1
Prediction of ATTD of energy					
Using ivED					
R^2	0.19	0.29	0.24	0.79	0.69
RMSE, %	1.44	0.89	1.60	2.76	3.37
Using chemical analyses					
R^2	0.56	0.81	0.84	0.80	0.88
RMSE, %	1.07	0.50	0.74	2.66	2.17
Predictors	EE	Ash CF	CP	CF	Ash ADF Hemicellulose EE
Using ivED and chemical analyses					
R^2	0.59	0.83	0.84	0.86	0.88
RMSE, %	1.13	0.53	0.89	2.40	2.19
Predictors	ivED EE	ivED Ash CF	ivED CP	ivED CF	ivED Ash ADF

[1]CF, crude fiber; DDGS, dried distillers grains with solubles; EE, ether extract; RMSE, root mean standard error.
*Within a column, means of ivED with superscript (*) differ with means of ATTD of energy

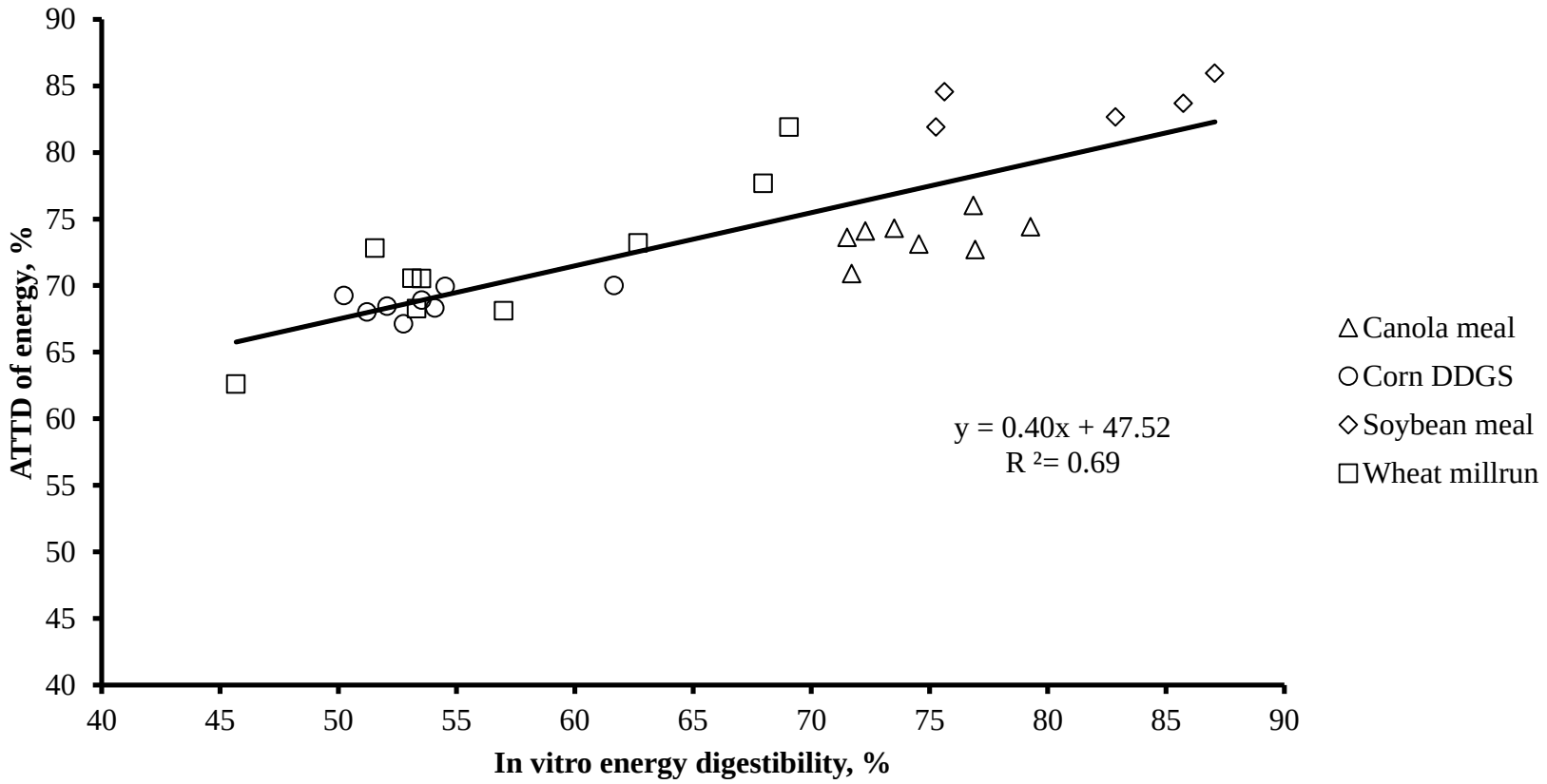

Figure 4.1 Relationship between in vivo apparent total tract digestibility (ATTD) and in vitro energy digestibility among co-products (n = 30). DDGS = dried distillers grains with solubles.

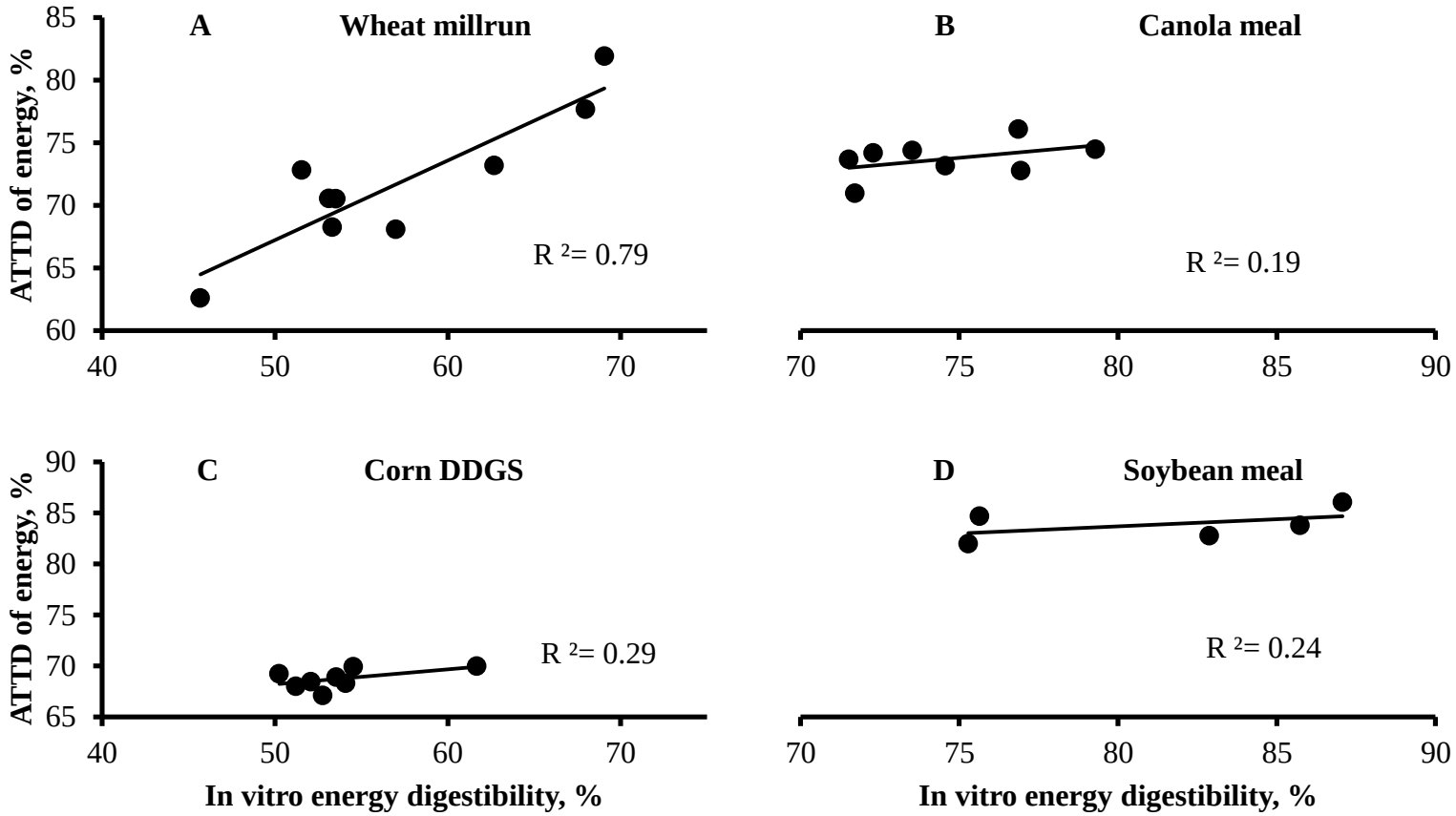

Figure 4.2 Relationship between in vivo apparent total tract digestibility (ATTD) of energy and in vitro energy digestibility within co-products: wheat millrun (A), canola meal (B), corn dried distillers grains with solubles (DDGS; C), and soybean meal (D).

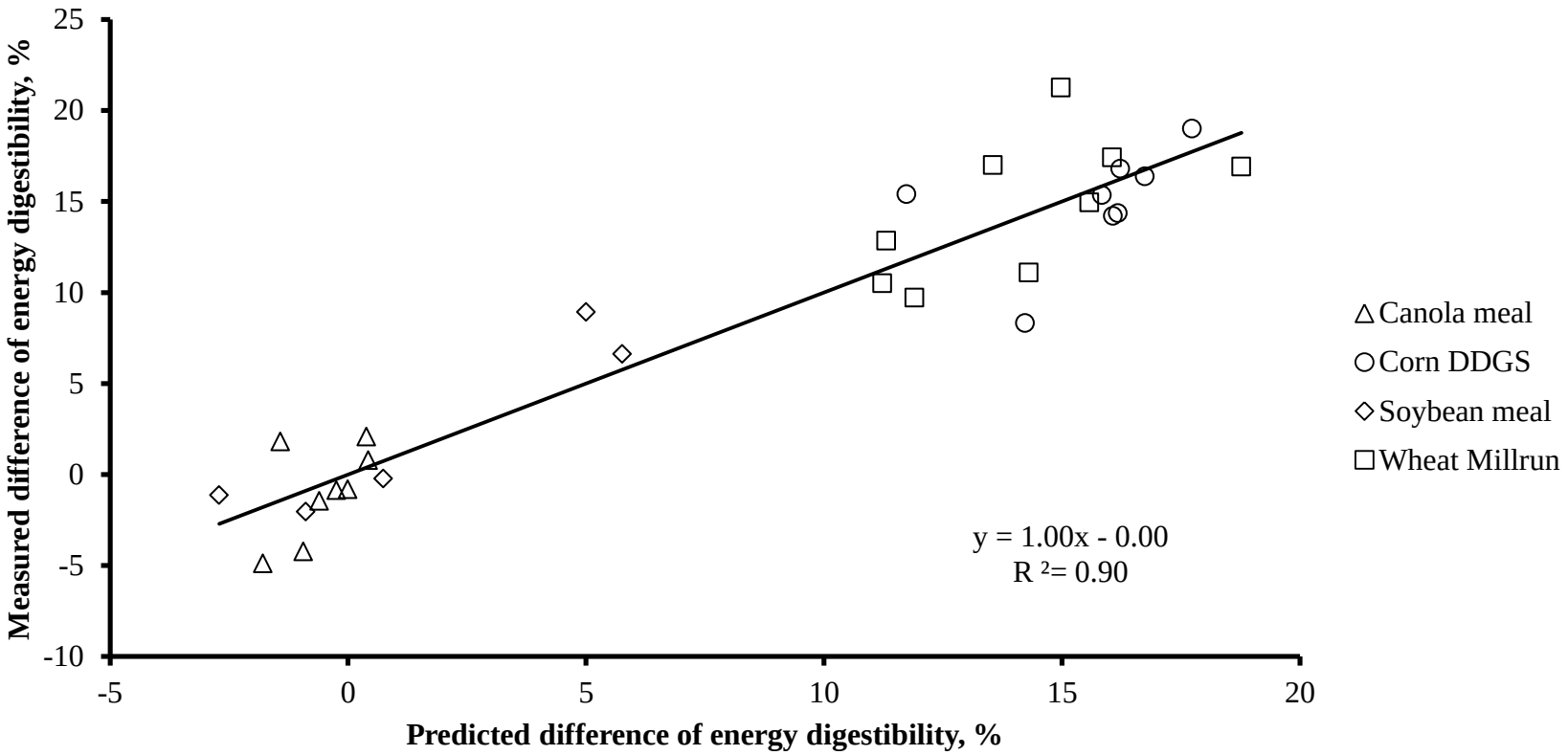

Figure 4.3 Relationship between predicted difference of energy digestibility (as ATTD of energy minus in vitro energy digestibility) by ether extract (EE), acid detergent fiber (ADF), and hemicellulose (as NDF minus ADF) content and measured difference of energy digestibility of co-products (n = 30). DDGS = dried distillers grains with solubles.

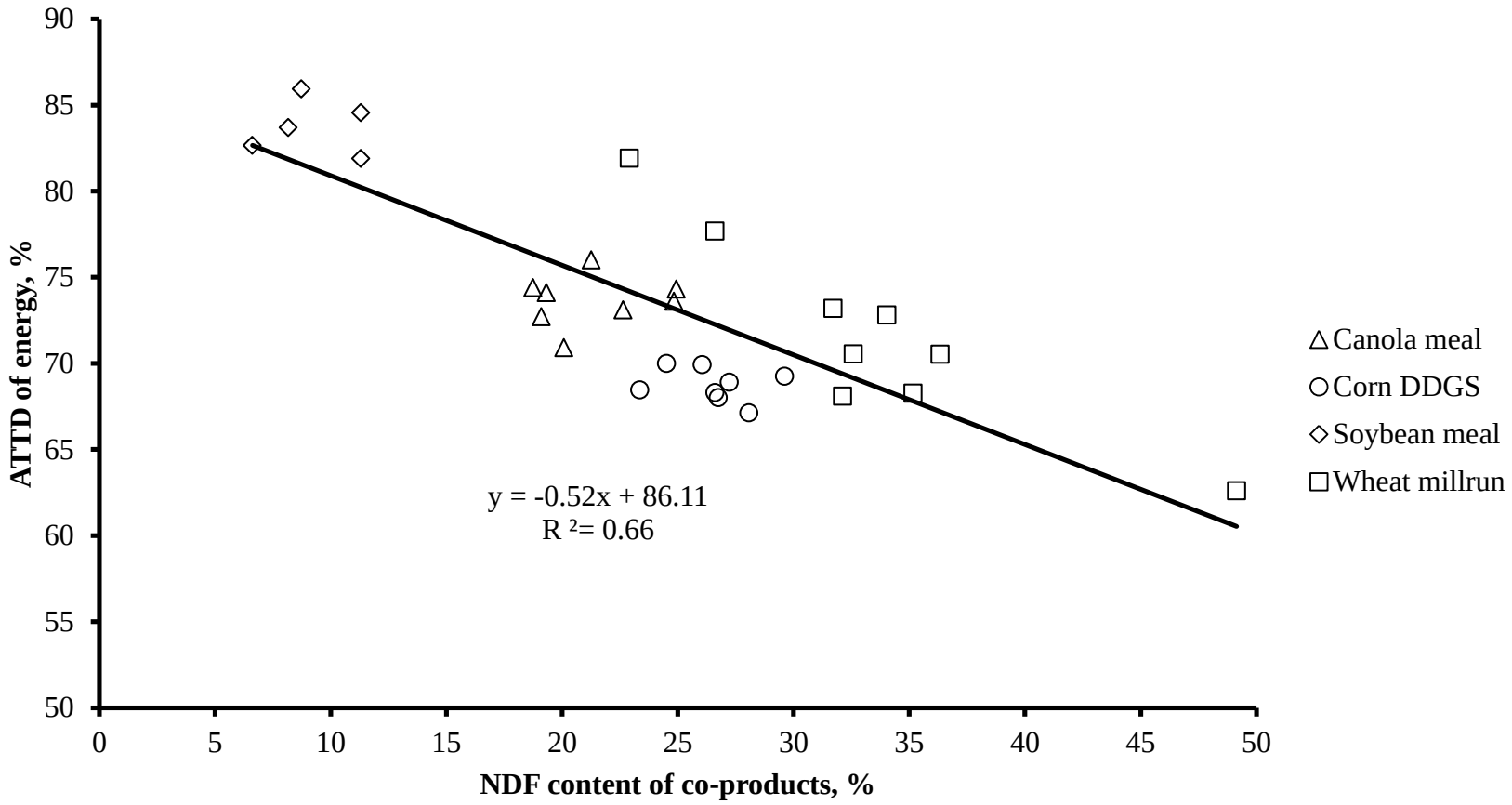

Figure 4.4 Relationship between neutral detergent fiber (NDF) content and measured apparent total tract digestibility (ATTD) of energy of co-products (n = 30). DDGS = dried distillers grains with solubles.

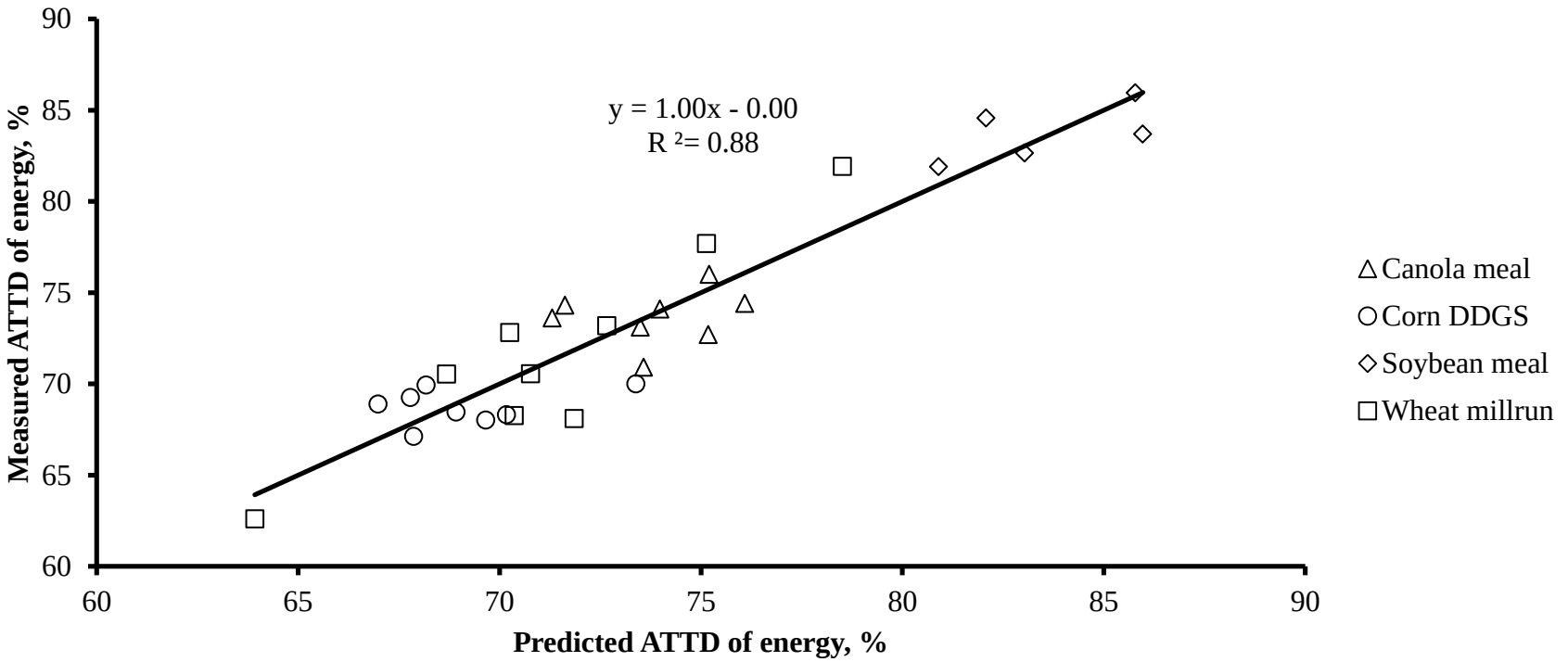

Figure 4.5 Relationship between predicted apparent total tract digestibility (ATTD) of energy using ash, acid detergent fiber (ADF), hemicellulose (as NDF minus ADF), and ether extract (EE) from chemical analyses and measured ATTD of energy of co-products (n = 30). The ATTD of energy was predicted using: 96.06 - 0.41 ×Ash - 0.93 × ADF - 0.39 × Hemicellulose - 0.59 × EE (Eq. 4). DDGS = dried distillers grains with solubles.

Chapter 5 A novel approach for a functional group to predict protein in undigested residue and protein digestibility by mid-infrared spectroscopy[1]

5.1 Abstract

To evaluate nutrient digestibility of feedstuffs, we propose the novel approach of functional group digestibility (FGD). The FGD was based on the absorbance of specific Fourier transform infrared (FT-IR) peaks and the ratio of an inorganic indigestible marker in diet and digesta, without calibration. For application, samples of diet and digesta of wheat with predetermined crude protein (CP) digestibility were scanned on an FT-IR spectrometer equipped with a single-reflection attenuated total reflection (ATR) attachment. The FGD in the amide I region (1,689-1,631 cm^{-1}) of digesta spectra was strongly related (R^2 = 0.99) with CP digestibility. The diet CP digestibility ranged from 60.4 to 87.8% was predicted with a standard error of prediction of 1.09%. In conclusion, instead of predictions based on calibrations, FGD can be calculated directly from spectra provided that the ratio of marker in diet and undigested residue is known.

5.2 Introduction

Nutrient digestibility is one of key concerns of nutritionists and defines the quantity of a nutrient that is digested and presumably absorbed. Nutrient

[1] A version of this chapter has been published. Wang, L. F., M. L. Swift, and R. T. Zijlstra. 2013. A novel approach for a functional group to predict protein in undigested residue and protein digestibility by mid-infrared spectroscopy. Appl. Spectrosc. 67:1343–1347.
L. F. Wang, M. L. Swift, and R. T. Zijlstra designed research; L. F. Wang conducted research and analyzed data; L. F. Wang, M. L. Swift, and R. T. Zijlstra wrote the paper.

concentration of undigested residue (digesta, feces) alone does not predict nutrient digestibility, because diet mass is reduced drastically following digestion. When all undigested residue mass cannot be collected, nutrient digestibility is determined with the indicator method by analyzing the concentration of a nutrient and an inorganic indigestible marker, such as chromic oxide (Cr_2O_3), in diet and undigested residue (Adeola, 2001). Due to digestion and absorption of nutrients, marker concentration will be higher in undigested residue than diet (reflecting mass change) and, combined with the ratio of nutrient in diet and undigested residue, nutrient digestibility can be measured.

Spectroscopy may predict nutrient concentration of undigested residues and thereby assist determination of nutrient digestibility (Givens and Deaville, 1999; Zijlstra et al., 2011). However, predictions are based on equations from regressing wet chemistry data on absorption data of a large number of samples. Occasionally, undigested residue mass is not sufficient for chemical analyses of nutrients, for instance, for in vitro [lab-based] assays that mimic nutrient digestion in animals. Due to the small quantity (< 200 mg) of residue remaining after in vitro digestion, chemical analyses are impossible. Fourier transform infrared (**FT-IR**) spectroscopy may provide a solution, because FT-IR spectra contain a wealth of information about chemical structure. Strong peaks above 1,500 cm^{-1} of mid-infrared spectra can be assigned confidently to specific functional groups (Miller, 2004b). According to Beer's law, absorbance of spectra is proportional to concentration of analytes (Griffiths, 2002a). Thus, absorbance of a peak indicates the molar concentration of a functional group. We proposed the term functional

group digestibility (**FGD**) to predict digestibility of specific nutrients.

We hypothesized that 1) absorbance in the amide I region (induced by vibrations of protein molecules) reflects crude protein (**CP**) in undigested residue, and 2) CP digestibility of wheat grain can be predicted directly by calculating FGD in the amide I region using the spectra of diet and undigested residue multiplied by the ratio of the indigestible marker concentration in diet and digesta. The objective was to develop a novel approach to estimate CP digestibility of wheat grain in pigs using FT-IR and inorganic indigestible marker data.

5.3 Materials and methods

5.3.1 Pig trial

The animal protocol was approved by the University of Alberta Animal Care Committee and Use Committee for Livestock. Experimental methods were described recently (Kandel, 2011). Briefly, one diet (14.5% CP) containing 96.3% ground wheat grain and 0.4% Cr_2O_3 as indigestible marker was fed to eight cross-bred barrows (initial body weight, 80 ± 2.5 kg). Pigs were surgically fitted with a T-cannula at the distal ileum to collect ileal digesta.

5.3.2 Analyses and calculations

Ground wheat diet and ground freeze-dried ileal digesta were analyzed for dry matter (**DM**; AOAC method 930.15), CP (AOAC method 990.03) (AOAC, 2006), and Cr_2O_3 using spectrophotometry (model 80-2097-62, KBUltraspec III, Pharmacia, Cambridge, UK) at 440 nm after ashing at 450°C overnight (Fenton and Fenton, 1979). Particle size of diet and digesta was measured with a laser

diffraction particle size analyzer (Beckman Coulter LS 13320, Mississauga, ON, Canada). The CP digestibility was determined using the indicator method (Adeola, 2001).

5.3.3 Spectra acquisition, processing, and conversion

Samples of ground wheat diet (mean particle size, 0.11 mm) and ground freeze-dried ileal digesta (mean particle size, 0.25 mm) were scanned in triplicate on a FT-IR spectrometer (MB 3000, ABB, Montréal, QC, Canada) equipped with a deuterated triglycine sulfate detector. An attachment of single-bounce attenuated total reflection (**ATR**) with a diamond internal reflection element (**IRE**) (MIRacle ATR, PIKE Technologies, Madison, WI) was installed in the FT-IR spectrometer for spectra acquisition. Spectra were obtained using Horizon MB FT-IR software (ABB) in the range of 4,000-578 cm^{-1} with a resolution setting of 4 cm^{-1} and 32 co-added scans. The diamond IRE of ATR was cleaned carefully with lint-free tissue between each sample to avoid cross contamination. Constant pressure was applied to ensure consistent contact of the sample with the diamond plate. Spectra of three repacked subsamples of each individual sample were averaged into one spectrum. Spectra were preprocessed with Savitzky-Golay smoothing with seven points convolution at both sides and multiplicative scatter correction in The Unscrambler X (CAMO Software AS, Oslo, Norway).

5.3.4 Statistical analyses

Normality, correlation and linear regression analyses were performed using the UNIVARIATE, CORR and REG procedures, respectively, in SAS 9.2 (SAS Inst. Inc., Cary, NC).

5.4 Calculation of digestibility of functional groups

According to Beer-Lambert-Bouguer's law (Griffiths, 2002a), the absorbance of spectra is proportional to the concentration of the analyte and is a function of pathlength, absorptivity, and concentration:

$$A = K \times C \times L \qquad \textbf{(1)}$$

where A is the measured absorbance, K is the absorptivity, C is the concentration of analyte, and L is the optical pathlength (Coates, 2002).

For FT-IR with ATR, pathlength is not constant throughout the mid-infrared region, it is a function of the angle of incidence and wavelength (Coates, 2002). In our approach, the angle of incidence was fixed. If we take one wavenumber (representing a peak induced by a functional group), the pathlength is theoretically the same for wheat and undigested residue. Assuming absorptivity is also the same, we have $K_{diet} = K_{digesta}$ and $L_{diet} = L_{digesta}$. We then deduced a formula (Eq. 2), which means that at a specific wavenumber, the ratio of absorbance equals the ratio of concentration of the analyte. This also eliminates the effect of pathlength change for each wavenumber.

$$\frac{A_{diet}}{A_{digesta}} = \frac{C_{diet}}{C_{digesta}} \qquad \textbf{(2)}$$

For nutrient digestibility using the indicator method (Adeola, 2001), the formula to calculate ileal digestibility of a nutrient was:

$$Digestiblity\ (\%) = 100 - 100 \times \frac{C_{marker\ in\ diet}}{C_{marker\ in\ digesta}} \times \frac{C_{nutrient\ in\ digesta}}{C_{nutrient\ in\ diet}} \qquad \textbf{(3)}$$

Mass of nutrient in undigested residue was determined with nutrient concentration in digesta sample and ratio of marker concentration in diet and

digesta samples (Stein et al., 2007):

$$Undigested\ nutrient\ mass\ (\%\ of\ diet) =$$

$$\frac{C_{marker\ in\ diet}}{C_{marker\ in\ digesta}} \times C_{nutrient\ in\ digesta} \quad \textbf{(4)}$$

Using Eq. 2 and 3, we calculated the FGD:

$$FGD\ (\%) = 100 - 100 \times \frac{C_{marker\ in\ diet}}{C_{marker\ in\ digesta}} \times \frac{A_{digesta}}{A_{diet}} \qquad \textbf{(5)}$$

The FDG was calculated using the Visual Basic for Applications (**VBA**) Macro programming in Microsoft Excel.

5.5 Results

The undigested mass of DM and CP and CP concentrations differed among digesta samples collected from eight pigs fed the same wheat-based diet, resulting in a range of CP digestibility (Figure 5.1). Wheat diet and freeze-dried ileal digesta were similar in DM content (89% vs. 87%; data not shown). The integrated area of absorbance in the amide I region (1,689-1,631 cm^{-1}) without use of a baseline was related (R^2 = 0.80, P < 0.01) to the CP concentration in digesta samples (Figure 5.2). Absorbance in the amide I region was related weakly (R^2 = 0.13, P = 0.38; Figure 5.3) to CP digestibility. The FGD in the amide I region was related strongly (R^2 = 0.99, P < 0.01; Figure 5.4) to CP digestibility with a standard error of prediction of 1.09%.

5.6 Discussion

We proposed calculating FGD from ATR FT-IR spectra to evaluate nutrient digestibility, without calibration. In the present study, we used the ratio of

absorbance in the amide I region of FT-IR spectra multiplied with the ratio of marker in diet and digesta to calculate FGD to predict CP digestibility. Predictions of the absolute concentration of CP in diet and undigested residue using FT-IR were thus not required.

The FGD approach is required when the quantity of sample of undigested residue is not sufficient for nutrient concentration analysis. For instance, in vitro digestion models only leave 50-200 mg of undigested residue. To determine in vitro energy digestibility, this residue was used entirely for bomb calorimetry (Regmi et al., 2008; Regmi et al., 2009), so that mechanisms underlying changes in digestibility cannot be studied. The mass change after in vitro digestion could be measured accurately by weighing the undigested residue. In pig trials, indigestible markers are used to measure the mass change. Thus, concentrations of Cr_2O_3 in diets and digesta were analyzed using wet chemistry and not FT-IR (Fenton and Fenton, 1979). The ratio of marker concentration in diet versus digesta represented the change in mass of DM following digestion. The FGD approach must be validated with enough undigested residue to conduct chemical analyses; thus, we selected pig samples with determined ileal CP digestibility.

The amide I region of spectra is an envelope containing vibrations of protein structures such as α-helices, β-sheets, turns, and random coils. These vibrations are induced primarily by carbonyl (C=O) stretching plus minor contributions from C-N stretching of peptide links in the secondary amide of protein and polypeptides (Barth, 2007a). This region might be affected by HOH bending vibrations at ca. 1,640–1,631 cm^{-1} from water and cis C=C double bond

stretching at ca. 1,653 cm^{-1} in unsaturated fat or fatty acids (Al-Alawi et al., 2005; Chalmers, 2002; Christy and Egeberg, 2006). However, our samples were low in water and fat. The amide I region may not account for other nonprotein N sources in digesta such as free amino acids and urea, because these do not have peptide links and, hence, do not have α-helix and β-sheet vibrations. Side chains of amino acids may absorb in the amide I region and may account for 15–20% of absorbance (Fabian and Mantele, 2002). Urea also has peaks adjacent to the amide I region (Shaw and Mantsch, 2002). However, ileal digesta contains minimal free amino acids and urea; thus, the error to determine CP concentration is small (Miner-Williams et al., 2009). Combined, the absorbance of the amide I region might be ideal to reflect CP concentration, according to Beer's law (Griffiths, 2002a).

The CP concentration or mass change alone is not equivalent to CP digestibility. The mass change is basically DM digestibility at the distal ileum. Combining CP concentration changes between diet and digesta with DM digestibility determines CP digestibility. As demonstrated, absorbance in the amide I region of digesta spectra was related weakly to CP digestibility, indicating that absorbance of spectra independently does not represent CP digestibility. Instead, digestibility is determined using nutrient concentration changes and change in mass between diet and digesta as reflected by marker ratio. Absorbance changes in the amide I region combined with mass change as FGD of amide I predicted CP digestibility of wheat diet accurately.

Further research remains to be conducted to implement FGD. The mass

change after in vitro digestion can be measured accurately. In pig samples, in contrast, the poor signal to noise ratio in the cutoff region of the diamond crystal of ATR hampers accurate prediction of Cr_2O_3 concentration. Research on selection of instrumentation or use of distinctive markers may enable accurate prediction of marker concentration with FT-IR and thereby rapid determination of FGD in pigs using FT-IR. Finally, absorbance of amide I was used in our novel approach. In FT-IR spectra, peaks or regions above 1,500 cm^{-1} might be reliably assigned to functional groups that indicate other nutrients such as fat (Miller, 2004b). Thus, the FGD approach may be used for other functional groups.

In conclusion, absorbance in the amide I region of FT-IR spectra is indicative of CP concentration and the novel approach to calculate FGD can predict CP digestibility of wheat diet accurately. The proposed approach avoids the need for calibrations; thus, reference data are not required thereby avoiding the need of proximate analyses for nutrient concentration.

5.7 References

Adeola, O. 2001. Digestion and balance techniques in pigs. In: A. J. Lewis and L. L. Southern, editors, Swine nutrition. CRC Press LLC, Boca Raton, FL. p. 903-916.

Al-Alawi, A., F. R. van de Voort, and J. Sedman. 2005. A new Fourier transform infrared method for the determination of moisture in edible oils. Appl. Spectrosc. 59:1295-1299.

AOAC. 2006. Official methods of analysis. 18th ed. Assoc. Off. Anal. Chem.,

Arlington, VA.

Barth, A. 2007. Infrared spectroscopy of proteins. Biochim. Biophys. Acta, Bioenerg. 1767:1073-1101.

Chalmers, J. M. 2002. Mid-infrared spectroscopy: anomalies, artifacts and common errors. In: J. M. Chalmers and P. R. Griffiths, editors, Handbook of vibrational theory No. 3. John Wiley and Sons Ltd, Chichester, UK. p. 2327-2347.

Christy, A. A., and P. K. Egeberg. 2006. Quantitative determination of saturated and unsaturated fatty acids in edible oils by infrared spectroscopy and chemometrics. Chemometrics Intellig. Lab. Syst. 82:130-136.

Coates, J. 2002. Classical methods of quantitative analysis. In: J. M. Chalmers and P. R. Griffiths, editors, Handbook of vibrational theory No. 3. John Wiley and Sons Ltd, Chichester, UK. p. 2235-2257.

Fabian, H., and W. Mantele. 2002. Infrared spectroscopy of proteins. In: J. M. Chalmers and P. R. Griffiths, editors, Handbook of Vibrational Theory No. 5. John Wiley and Sons Ltd, Chichester, UK. p. 3399-3425.

Fenton, T. W., and M. Fenton. 1979. An improved procedure for the determination of chromic oxide in feed and feces. Can. J. Anim. Sci. 59:631-634.

Givens, D. I., and E. R. Deaville. 1999. The current and future role of near infrared reflectance spectroscopy in animal nutrition: a review. Aust. J. Agric. Res. 50:1131-1145.

Griffiths, P. R. 2002. Beer's law. In: J. M. Chalmers and P. R. Griffiths, editors, Handbook of vibrational theory No. 3. John Wiley and Sons Ltd,

Chichester, UK. p. 2225-2234.

Kandel, K. P. 2011. Nutritional characterization of wheat distillers dried grains with solubles in grower-finisher pigs. M.Sc. Thesis. University of Alberta, Edmonton.

Miller, F. A. 2004. Introduction. In: D. W. Mayo, F. A. Miller and R. W. Hannah, editors, Course notes on the interpretation of infrared and Raman spectra. John Willy and Sons, Inc. p. 1-32.

Miner-Williams, W., P. J. Moughan, and M. F. Fuller. 2009. Endogenous components of digesta protein from the terminal ileum of pigs fed a casein-based diet. J. Agric. Food Chem. 57:2072-2078.

Regmi, P. R., N. S. Ferguson, and R. T. Zijlstra. 2009. In vitro digestibility techniques to predict apparent total tract energy digestibility of wheat in grower pigs. J. Anim. Sci. 87:3620-3629.

Regmi, P. R., W. C. Sauer, and R. T. Zijlstra. 2008. Prediction of in vivo apparent total tract energy digestibility of barley in grower pigs using an in vitro digestibility technique. J. Anim. Sci. 86:2619-2626.

Shaw, R. A., and H. H. Mantsch. 2002. Vibrational spectroscopy applications in clinical chemistry. In: J. M. Chalmers and P. R. Griffiths, editors, Handbook of Vibrational Theory No. 5. John Wiley and Sons Ltd, Chichester, UK. p. 3295-3308.

Stein, H. H., B. Seve, M. F. Fuller, P. J. Moughan, and C. F. M. de Lange. 2007. Invited review: amino acid bioavailability and digestibility in pig feed ingredients: terminology and application. J. Anim. Sci. 85:172-180.

Zijlstra, R. T., M. L. Swift, L. F. Wang, T. A. Scott, and M. J. Edney. 2011. Near infrared reflectance spectroscopy accurately predicts the digestible energy content of barley for pigs. Can. J. Anim. Sci. 91:301-304.

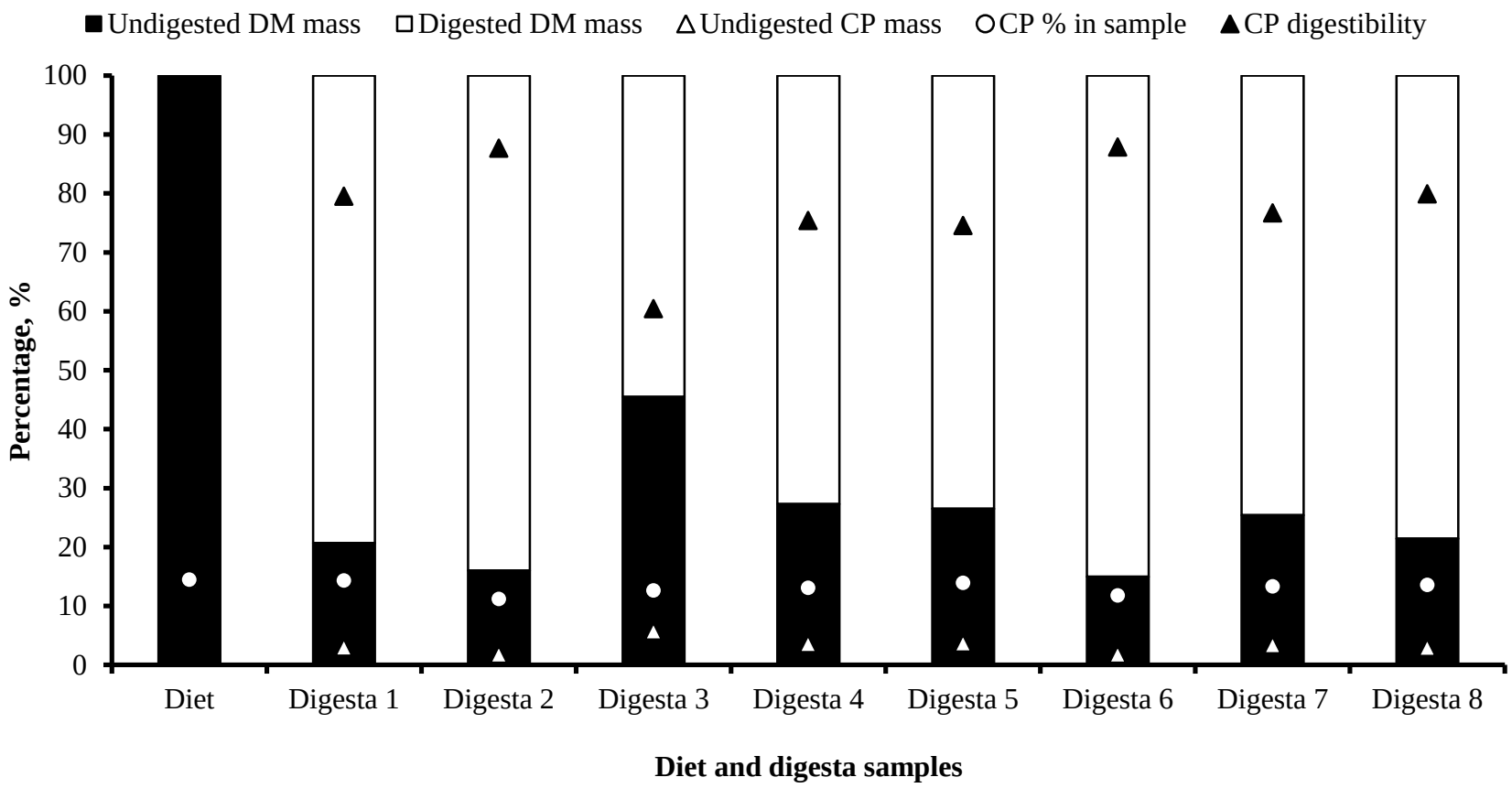

Figure 5.1 Dry matter (DM) and crude protein (CP) mass before (diet) and after digestion (digesta) and CP digestibility. Undigested CP mass (as % of diet) was calculated by multiplying CP % in digesta with the ratio of indigestible marker in diet and digesta.

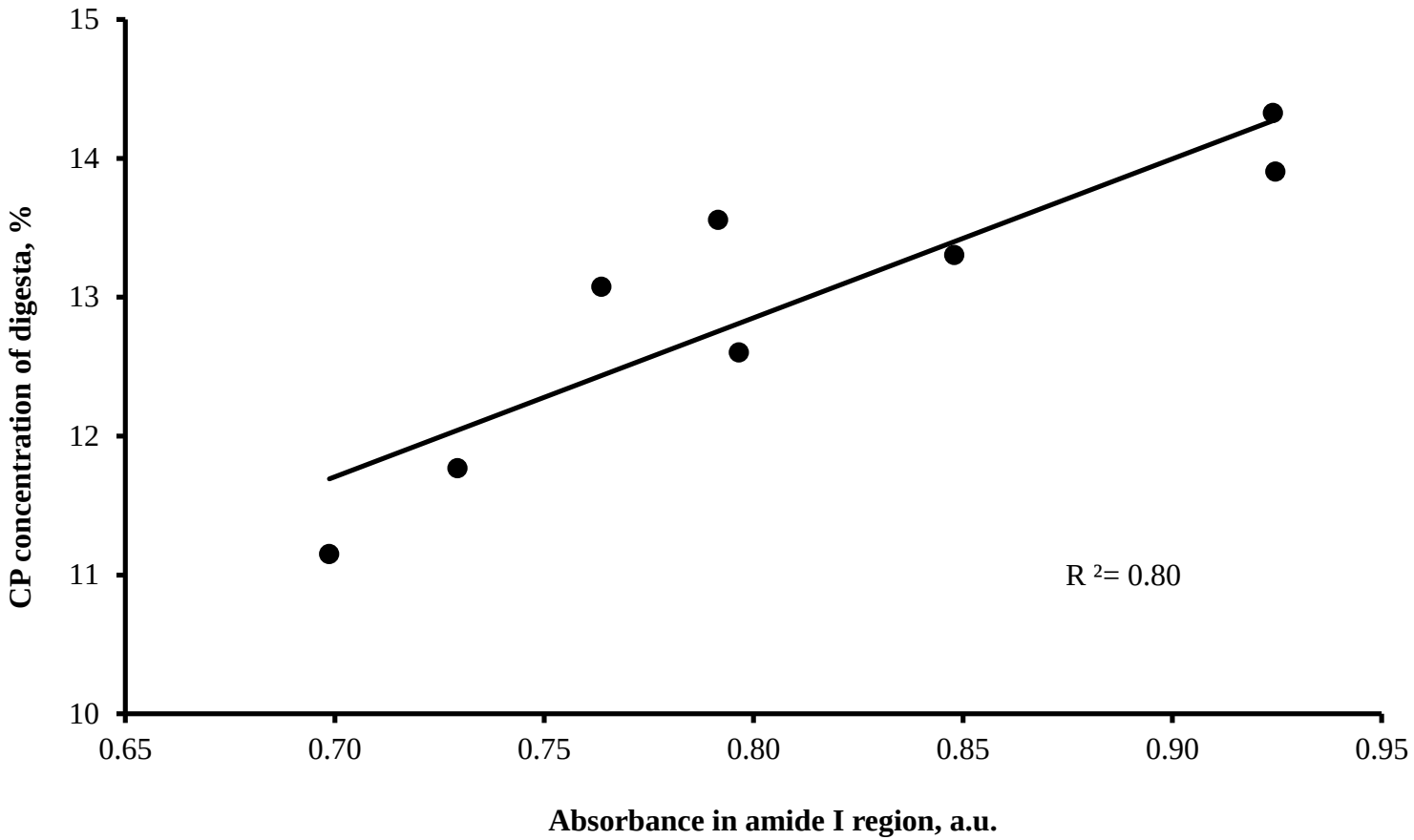

Figure 5.2 Relation between crude protein (CP) concentration of undigested residue (digesta) of wheat diet and absorbance in the amide I region (1,689-1,631 cm^{-1}). a.u. = arbitrary unit.

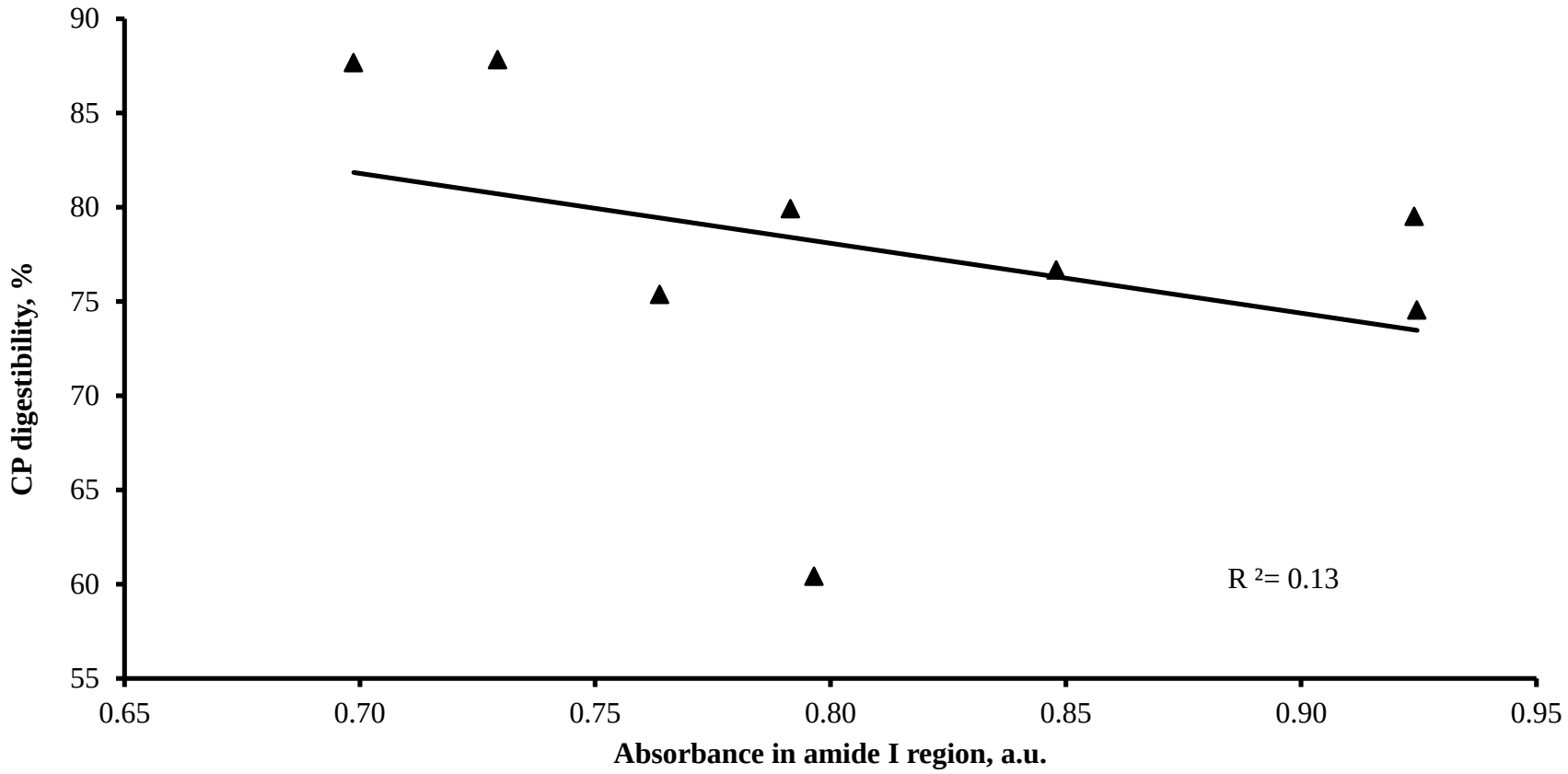

Figure 5.3 Relation between crude protein (CP) digestibility of wheat diet and absorbance of the amide I region (1,689-1,631 cm^{-1}) of digesta spectra. a.u. = arbitrary unit.

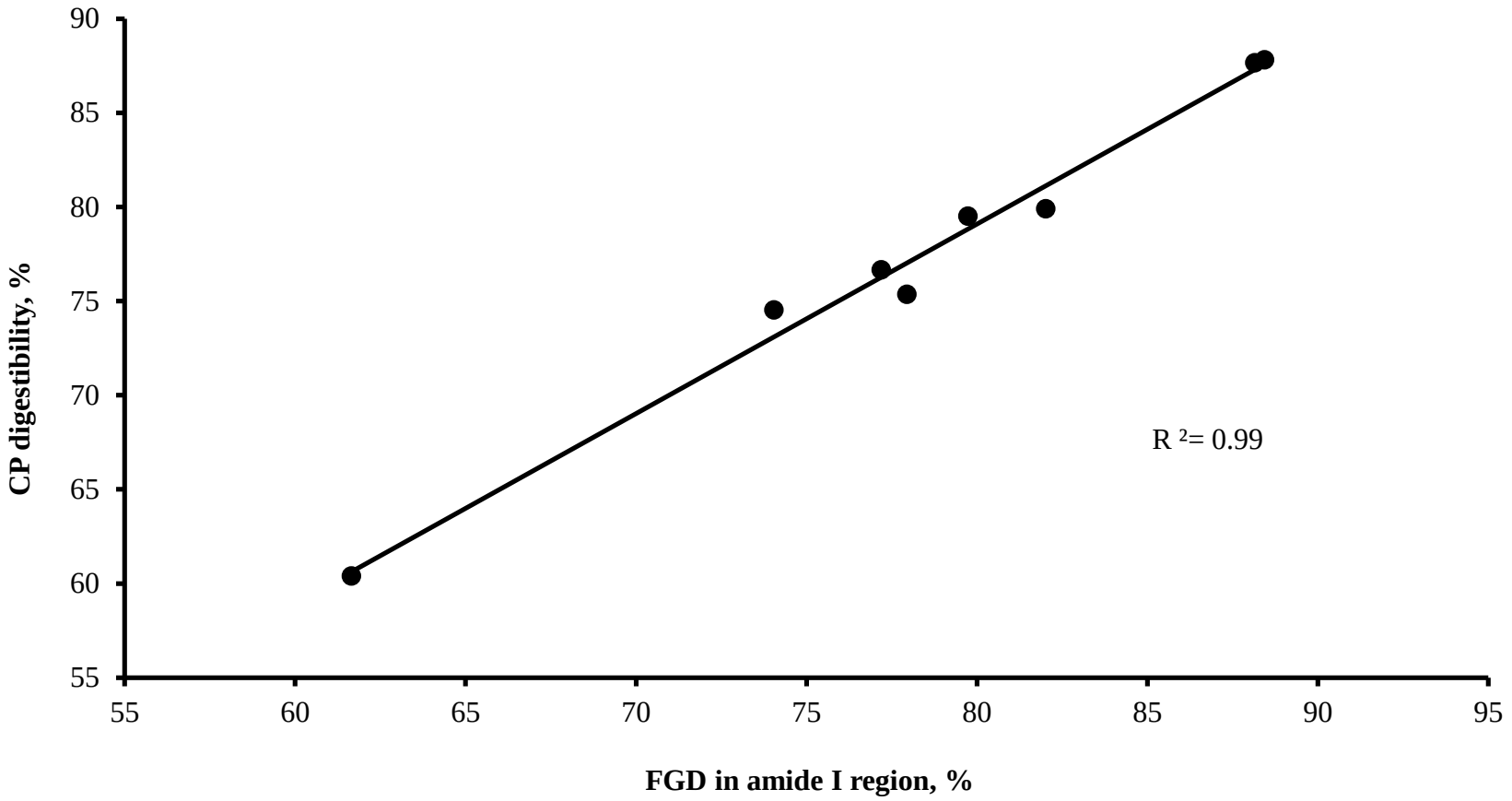

Figure 5.4 Relation between functional group digestibility (FGD) of the amide I region (1,689-1,631 cm^{-1}) and crude protein (CP) digestibility of wheat diet.

Chapter 6 A non-calibration spectroscopic method to estimate ether extract and fatty acid digestibility of feed and its validation with flaxseed and field pea in pigs[2]

6.1 Abstract

Digestibility of ether extract (EE) or fatty acids (FA) is traditionally measured by chemical analyses for EE or gas-liquid chromatography (GLC) method for FA combined with marker concentration in diet and digesta or feces. We hypothesized that digestibility of EE or FA might also be predicted by marker concentrations and spectral analyses of diet and digesta or feces. Based on Beer's law, a non-calibration spectroscopic method, which used functional group digestibility (FGD) determined with marker concentration and peak intensity of spectra of diets and undigested residues [digesta or feces], was developed to predict the apparent ileal digestibility (AID) of total FA and apparent total tract digestibility (ATTD) of EE. To validate the proposed method, 4 diets containing 30% flaxseed and field pea co-extruded with 4 extruder treatments and a wheat and soybean basal diet with predetermined AID of total FA and ATTD of EE were used. Samples of ingredients, diets, and freeze-dried digesta and feces were scanned on a Fourier transform infrared (FT-IR) instrument with a single-reflection attenuated total reflection (ATR) attachment. The intensity of either the

[2] A version of this chapter has been submitted to Journal of Animal Science for publication: Wang, L. F., M. L. Swift, and R. T. Zijlstra. 2013. A non-calibration spectroscopic method to estimate ether extract and fatty acid digestibility of feed and its validation with flaxseed and field pea in pigs.
L. F. Wang, M. L. Swift, and R. T. Zijlstra designed research; L. F. Wang conducted research and analyzed data; L. F. Wang, M. L. Swift, and R. T. Zijlstra wrote the manuscript.

methylene (CH_2) anti-symmetric stretching peak at ca. 2,923 cm^{-1} ($R^2 = 0.90$, $P < 0.01$) or symmetric stretching peak at ca. 2,852 cm^{-1} ($R^2 = 0.86$, $P < 0.01$) of ingredients, diet, and digesta spectra was related strongly to the concentration of total FA. The AID of total FA of diets measured using GLC was estimated by spectroscopic method using FGD at ca. 2,923 cm^{-1} and ca. 2,852 cm^{-1} ($R^2 = 0.75$, $P < 0.01$) with a bias of 0.54 ± 3.78% and -1.35 ± 3.74%, respectively. The accumulated peak intensity in the region between 1,766-1,695 cm^{-1} of spectra was related to EE concentration in ingredients and diets ($R^2 = 0.61$, $P = 0.01$), and feces ($R^2 = 0.88$, $P < 0.01$). The relation was improved by using 2nd derivative spectra of the sum of peak intensity at 1,743 and 1,710 cm^{-1} for ingredients and diets ($R^2 = 0.90$, $P = 0.01$), at 1,735 and 1,710 cm^{-1} for feces ($R^2 = 0.92$, $P < 0.01$). The ATTD of EE of test diets determined with proximate analysis was estimated by the FGD of non-derivative spectra with or without baseline ($R^2 = 0.90$, $P < 0.01$) with a bias of 3.15 ± 3.14% and 3.50 ± 3.24%, respectively. In conclusion, instead of using chemical analyses and GLC method for measuring chemical content, or predictions based on calibrations, the AID of total FA and ATTD of EE can be estimated directly from ATR FT-IR spectra, provided the ratio of marker in diets and undigested residue is known.

6.2 Introduction

Digestibility of ether extract (**EE**) or total fatty acids (**FA**) are major criteria for gauging fat quality of feedstuffs. However, determination of EE or FA is time-consuming and requires sample preparation (Sukhija and Palmquist,

1988). Spectroscopy may predict EE or FA concentration in feed or feces, but predictions are based on multivariate calibrations from regressing wet chemistry data on absorption data of samples (Franck et al., 1996; Jakobs et al., 2000; Mahesar et al., 2011). In certain situations, the amount of sample is not sufficient for chemical analyses, such as for the 50 to 200 mg undigested residues from in vitro digestion models (Regmi et al., 2009); thus, calibration development is limited.

Intensity of a single peak or area under the curve in spectra reflects concentration of an analyte (Coates, 2002). However, the overlap of neighboring peaks and a baseline shift may also contribute to peak intensity and distort the relation to concentration of an analyte. Baseline correction or derivative transformation may increase prediction accuracy (Mossoba et al., 2007; Li et al., 2011). Functional group digestibility (**FGD**) is calculated directly [without calibration] from infrared spectra peaks and indigestible marker concentration in diet and undigested residue and can accurately estimate protein digestibility of wheat in pigs (Wang et al., 2013). Whether FGD can estimate FA or EE digestibility is unknown.

We hypothesized that 1) the intensity of mid-infrared spectra peaks induced by fat molecules reflects concentration of total FA or EE; 2) derivative transformation and baseline correction can increase prediction accuracy of concentration and digestibility of total FA and EE; and 3) FGD can estimate the apparent ileal digestibility (**AID**) of total FA and apparent total tract digestibility (**ATTD**) of EE. The objective was to test these hypotheses in diets containing co-

extruded flaxseed and field pea ingredients, and resulting swine digesta, and feces.

6.3 Materials and methods

6.3.1 Animal study

The animal protocol was approved by the University of Alberta Animal Care and Use Committee for Livestock, followed guidelines established by the Canadian Council of Animal Care (CCAC, 1993), and was described previously (Htoo et al., 2008). Briefly, a 50:50 (wt/wt) mix of flaxseed and field pea was co-extruded with 3 extrusion treatments. Four test diets containing 30% raw or co-extruded flaxseed and field pea and 1 basal diet comprised of wheat and soybean meal were fed to 5 barrows in a 5 × 5 Latin square. Diets contained Cr_2O_3 as indigestible marker. Pigs were fitted with a T-cannula at the distal ileum to collect ileal digesta.

6.3.2 Chemical analyses

Ingredients, diets, and freeze-dried digesta and feces were analyzed for DM (method 930.15; AOAC, 2006) and EE (method 920.39). The Cr_2O_3 in diets, digesta, and feces samples was determined by spectrophotometry (model 80-2097-62, KBUltraspec III, Pharmacia, Cambridge, UK) at 440 nm after ashing at 450°C overnight (Fenton and Fenton, 1979). Total FA in ingredients, diets, and freeze-dried digesta were analyzed using gas-liquid chromatography (**GLC**; Sukhija and Palmquist, 1988), as the sum of palmitic (C16:0), stearic (C18:0), arachidic (C20:0), oleic (C18:1ω9), vaccenic (C18:1ω7), linoleic (C18:2), and

linolenic (C18:3) acids. The AID of total FA and ATTD of EE were determined using the indicator method (Adeola, 2001).

6.3.3 Spectra acquisition and analyses

A total of 59 samples were used: 4 ingredients, 5 diets, 25 digesta, and 25 feces. These samples were ground in a centrifugal mill (Retsch GmbH, Haan, Germany) passing through a 0.5-mm screen and were scanned in triplicate on a Fourier transform infrared (**FT-IR**) spectrometer (MB3000; ABB, Montreal, QC, Canada) equipped with a deuterated triglycine sulfate detector. An attachment of single-reflection attenuated total reflection (**ATR**) with a diamond internal reflection element (**IRE**; MIRacle ATR; PIKE Technologies, Madison, WI) was installed in the FT-IR spectrometer for spectra acquisition.

The spectra were obtained using Horizon MB FT-IR software (ABB) in the range of 4,000 to 578 cm^{-1} with a resolution of 4 cm^{-1} and 32 co-added scans. The diamond IRE of ATR was carefully cleaned with lint-free tissue between each sample to avoid cross contamination. Constant pressure was applied to ensure consistent contact with the diamond plate. A reference scan was collected prior to triplicate scans of each sample. Spectra of 3 repacked sub-samples of each individual sample were averaged to 1 spectrum. All spectra were preprocessed with the Savitzy-Golay smoothing with 7 points at both sides to alleviate spectra noise, and with multiplicative scatter correction (**MSC**) to address possible path length variation (Isaksson and Naes, 1988). For comparison, spectra were also transformed using the Savitzy-Golay 2nd derivative procedure with the 3th polynomial order in The Unscrambler X (CAMO Software AS., Oslo, Norway).

We defined peak intensity without baseline correction as the absolute peak height, and peak intensity with baseline correction as the absolute difference between baseline and peak height (Li et al., 2011). Baselines were 3,045-2,777, 2,945-2,902, 3,045-2,777, and 2,869-2,835 cm^{-1} for the peak at 2,923 cm^{-1} without derivative or with 2nd derivative and the peak at 2,852 cm^{-1} without derivative or with 2nd derivative, respectively. The accumulated peak intensity in carbonyl (C=O) region (1,766-1,695 cm^{-1}) was defined as the sum of peak intensity at each wavenumber in the region of non-derivative spectra. Derivative spectra do not preserve spectra shape; thus, the sum of intensity of the ester C=O peak at ca. 1,743 cm^{-1} and the carboxylic acid C=O peak at ca. 1,710 cm^{-1} was used as intensity of 2nd derivative spectra in the C=O region (1,766-1,695 cm^{-1}). Baselines were 1,822 cm^{-1} for the non-derivative spectra region at 1,766-1,695 cm^{-1}, 1,753-1,722 cm^{-1} for 2nd derivative spectra at 1,735 cm^{-1}, and 1,722-1,702 cm^{-1} for 2nd derivative spectra at 1,710 cm^{-1}.

6.3.4 Calculation of digestibility of functional groups

According to Beer-Lambert-Bouguer's law (Griffiths, 2002), the absorbance of spectra is proportional to the analyte's concentration, and is a function of absorptivity, concentration, and path length (Eq. 1, Coates, 2002).

$$A = K \times C \times L \qquad \textbf{(Eq. 1)}$$

where A is the measured absorbance, K is the absorptivity, C is the concentration of analyte, and L is the optical path length.

However, for ATR FT-IR, the path length is not constant throughout the mid-infrared range, and is a function of the angle of incidence and wavenumber

(Coates, 2002). In our approach, the angle of incidence was fixed. For 1 wavenumber that represents a peak induced by 1 functional group, path length is theoretically the same for diet and undigested residue. Assuming that the absorptivity is also the same, we have theoretical assumptions of $K_{diet} = K_{digesta}$ and $L_{diet} = L_{digesta}$. We then deduced formula (Eq. 2), which means in specific wavenumber, the ratio of absorbance equals to the ratio of concentration of the analyte, and eliminates the effect of path length change for each wavenumber.

$$\frac{A_{diet}}{A_{digesta}} = \frac{C_{diet}}{C_{digesta}} \qquad \textbf{(Eq. 2)}$$

Using the indicator method (Adeola, 2001), the AID of FA was calculated as:

$$AID\ of\ FA\ (\%) = 100 - 100 \times \frac{Cr_2O_{3_{diet}}}{Cr_2O_{3_{digesta}}} \times \frac{Concentration\ of\ FA\ in\ digesta}{Concentration\ of\ FA\ in\ diet}$$

(Eq. 3)

According to Eq. 2 and 3, we calculated the FGD:

$$FGD\ (\%) = 100 - 100 \times \frac{Cr_2O_{3_{diet}}}{Cr_2O_{3_{digesta}}} \times \frac{A_{digesta}}{A_{diet}} \qquad \textbf{(Eq. 4)}$$

The Eq. 3 and 4 were also applied on feces. The FGD was calculated with peak intensity of non-derivative or derivative spectra using the Microsoft Visual Basic for Applications (**VBA**) Macro programming in Microsoft Excel.

6.3.5 Statistical analyses

The difference between AID of FA or ATTD of EE and FGD, the effect of baseline treatment, and the effect of derivative transformation treatment were analyzed by paired t-test using the TTEST procedure in SAS 9.2 (SAS Inst. Inc., Cary, NC), respectively. Linear regression analysis was performed using the REG

procedure. The Pearson correlation coefficients between peak intensity at each wavenumber with 2 cm^{-1} interval in 4,000-578 cm^{-1} and concentrations of FA or EE were calculated using Microsoft VBA Macro programming in Microsoft Excel. The performance of the non-calibration spectroscopic method was reported as the coefficients of determination, and bias (mean and SD of residual as FGD minus AID or ATTD) between FGD and AID or ATTD. Significance was declared at $P < 0.05$.

6.4 Results

6.4.1 Concentration and digestibility of total fatty acids and ether extract

Concentration of total FA and EE in the ingredients ranged from 12.3 to 15.0% and 17.3 to 19.6% respectively; and in the 4 test diets ranged from 6.5 to 7.9% and 7.2 to 8.7% respectively, and was 2.7% in the basal diet. Concentration of total FA in digesta ranged from 3.8 to 8.6% for the 4 test diets and from 0.8 to 1.7% for the basal diet. Concentration of EE in feces ranged from 4.4 to 12.6% for the 4 test diets and from 2.4 to 3.6% for the basal diet.

The AID of total FA was weakly related ($R^2 = 0.26$, $P = 0.01$; data not shown) to AID of DM, but strongly related ($R^2 = 0.79$, $P < 0.01$) to concentration of total FA in digesta. The ATTD of EE was moderately related to either ATTD of DM of diets ($R^2 = 0.41$, $P < 0.01$; data not shown) or EE concentration in feces ($R^2 = 0.52$, $P < 0.01$).

6.4.2 Relationship between spectra and concentration of total fatty acids or ether extract

The concentration of total FA in ingredients, diets, and digesta, or EE in ingredients, diets, or feces were all strongly correlated with peak intensity of non-derivative spectra at 2,923, 2,852, 1,744-1,710, ca. 1,460, and ca. 721 cm^{-1} (Figure 6.1). With or without using baseline correction and using derivative spectra or not, the peak intensity at 2,923 cm^{-1} was strongly related ($R^2 = 0.90$, $P < 0.01$; Figure 6.2) to the concentration of total FA in ingredients, diets, and digesta. The peak intensity at 2,852 cm^{-1} was strongly related ($R^2 = 0.86$, $P < 0.01$; Table 6.1) to these concentrations.

With non-derivative spectra, accumulated peak intensity in the C=O region (1,766-1,695 cm^{-1}) with baseline correction was strongly related ($R^2 = 0.88$, $P < 0.01$; Table 6.2) to the EE concentration in feces, and moderately related ($R^2 = 0.61$, $P < 0.05$) to the EE concentration in ingredients and diets. Diet spectra clearly showed 1 C=O peak at ca. 1,743 cm^{-1} that represents ester C=O in triglycerides and another C=O peak at ca. 1,710 cm^{-1} that represents C=O in free FA (**FFA**, Figure 6.3). Furthermore, the ester C=O peak shifted to 1,735 cm^{-1} in feces.

Using 2nd derivative spectra in the C=O region, the sum of peak intensity at 1,743 and 1,710 cm^{-1} was highly related ($R^2 = 0.88$-0.90, $P < 0.05$; Table 6.2) to EE concentration of ingredients and diets. Moreover, the sum of peak intensity at 1,735 and 1,710 cm^{-1} was highly related ($R^2 = 0.83$-0.92, $P < 0.01$; Table 6.2) to EE concentration of feces. The slope of regression between sum of peak

intensity and EE concentration was higher for feces than ingredients and diets (Figure 6.4). The sum of peak intensity was better related to EE concentration of ingredients and diets than individual peak intensity at either 1,743 or 1,710 cm^{-1} (R^2 = 0.88-0.90 vs. 0.67, $P < 0.01$ or R^2 = 0.05, $P = 0.58$, respectively; data not shown).

6.4.3 Prediction of apparent ileal digestibility of total fatty acids

The FGD calculated with peak intensity of non-derivative spectra at 2,923 cm^{-1} with baseline correction was related (R^2 = 0.75, $P < 0.01$; Figure 6.5) to AID of total FA, with a mean residual of 0.54 and SD of 3.78 (Table 6.1). Using peak intensity of non-derivative spectra at 2,852 cm^{-1} with baseline correction yielded lower ($P < 0.05$; Table 6.1) FGD than at 2,923 cm^{-1} but related similarly to AID of total FA. Using derivative spectra did not increase the relation between FGD and AID of total FA, but reduced the residual at 2,923 cm^{-1} (Table 6.1). Although relations between FGD and AID of total FA were similar for 2,923 cm^{-1} and 2,852 cm^{-1} regardless of baseline correction, mean residual and SD were lower using baseline correction. Using peak intensity at 2,923 or 2,852 cm^{-1} of non-derivative spectra without baseline correction yielded 3 %-units lower ($P < 0.05$; Table 6.1) FGD than with baseline correction.

6.4.4 Fecal fat and prediction of apparent total tract digestibility of ether extract

Properties of fat in feces differed from fat in ingredients, diets, or digesta. The methylene symmetric stretching peak shifted from 2,854 to 2,848 cm^{-1}, the anti-symmetric stretching peak shifted from 2,923 to 2,918 cm^{-1}, and the ester

C=O peak shifted from 1,743 to 1,735 cm^{-1} (Figure 6.3). Moreover, a strong doublet appeared at 1,575 and 1,539 cm^{-1} whereas the olefinic hydrocarbon (-C=C-H) peak at 3,008 cm^{-1} almost disappeared in feces spectra. Peak intensity at 1,575 cm^{-1} was strongly related to peak intensity at 2,918 ($R^2 = 0.96$, $P < 0.01$; Figure 6.6) and 721 cm^{-1} ($R^2 = 0.95$, $P < 0.01$) of 2nd derivative fecal spectra.

The FGD determined with accumulated peak intensity at 1,766-1,695 cm^{-1} of non-derivative spectra with baseline correction was strongly related ($R^2 = 0.90$, $P < 0.01$; Figure 6.7) to ATTD of EE of test diets, but FGD was 3.5 %-units higher than ATTD of EE. However, including the basal diet reduced the relation between ATTD of EE and FGD ($R^2 = 0.61$, $P < 0.01$; data not shown). The use of 2nd derivative spectra did not increase the relation between FGD and ATTD of EE of test diets (Table 6.2). In addition, the residual between FGD and the ATTD of EE was increased.

6.5 Discussion

6.5.1 Determinants for digestibility of total fatty acids or ether extract

Concentration of indigestible marker and fat in diets and undigested residue are two crucial measurements needed to determine fat digestibility using the indicator method (Adeola, 2001). Independently, ratio of marker concentration reflecting DM digestibility or feces EE concentration were only moderately correlated with fat digestibility in the present study, indicating that these are not good single estimators of AID of FA or ATTD of EE.

6.5.2 Relation between spectra and concentration of total fatty acids and ether extract

To determine the overall relationship between absorbance at each wavenumber in entire spectral region and concentration of EE or total FA, we did not check for or remove potential outliers. The intensity of peaks associated with fat or FA molecules was strongly correlated with concentration of EE or total FA, reflecting Beer's law and vibrational theory (Griffiths, 2002; Shurvell, 2002). These peaks included symmetric or anti-symmetric methylene ($-CH_2$) peaks at ca. 2,923 and 2,852 cm^{-1}, ester C=O in triglycerides and C=O stretching in FFA at 1,744-1,710 cm^{-1}, the anti-symmetric deformation modes of C-H peaks at ca. 1,460 cm^{-1}, and the all-in-phase rocking mode of methylene group with chain length greater than 4 ($[-CH_2-]_n$) at ca. 721 cm^{-1} (Mayo, 2004). These peaks were used to investigate fat structure (Abeysekara et al., 2012) and predict fat or FA concentrations (Yoshida and Yoshida, 2003; Christy and Egeberg, 2006). The symmetric and anti-symmetric methylene stretching peaks best indicated total FA concentration: they were strong, had less overlap with other strong peaks, and the strength of the 2 peaks increased with increasing hydrocarbon chain length in fat (Mayo, 2004).

The peak of ester C=O at 1,748 cm^{-1} predicted fat content (van de Voort et al., 1993), while the peak of C=O in carboxylic acids at 1,710 cm^{-1} predicted FFA concentration (Yu et al., 2011). In present study, we used the spectral region covering both peaks to predict EE concentration, instead of the single ester C=O peak centered at 1,743 cm^{-1} in ingredients and diets, or 1,735 cm^{-1} in feces. We

did so because FFA was clearly present in ingredients, diets, and digesta or feces, as indicated by the peak at 1,710 cm^{-1} (Yu et al., 2011). For chemical analyses of EE, the solvent also extracted FFA. Thus, inclusion of the peak induced by FFA was necessary to represent EE concentration. Using 2nd derivative spectra, the sum of 2 peaks of C=O (ester and carboxylic acid) was used, rather than accumulated peak intensity in the C=O region, because derivative transformation does not preserve the integrated areas of individual components (Fabian and Mantele, 2002). Mathematic manipulation of peaks, e.g., ratio, addition, or subtraction, is commonly used in spectroscopic analyses (Moya Moreno et al., 1999; Yu et al., 2011). For FFA present in samples, the sole use of ester C=O at 1,743 cm^{-1} did not completely represent EE concentration, as indicated by the stronger relation between EE concentration and peak intensity for using the sum of 2 peaks as compared to using either peak individually.

6.5.3 Non-calibration approach

In the present study, total FA and EE concentrations were not determined spectroscopically following calibration to calculate AID of total FA or ATTD of EE. Rather, the ratio of peak intensity associated with fat determined their AID or ATTD. Thus, calibration development with reference data was circumvented. This is a useful approach in certain situations. For example, for in vitro digestibility assays, DM digestibility is determined by weighing the diet sample to be digested and its undigested residue; the resulting ratio is equivalent to the ratio of indigestible marker to DM in diets fed and resulting feces. With our proposed method, in vitro digestibility of total FA or EE can then be estimated.

6.5.4 Prediction of apparent ileal digestibility of total fatty acids

The low residual and strong relation between FGD of methylene peaks at both 2,923 and 2,852 cm^{-1} and the AID of total FA indicated that this FGD estimated the AID of total FA. However, the FGD at 2,923 cm^{-1} predicted the AID of FA with lower residual than the FGD at 2,852 cm^{-1}, a difference that might be attributed to stronger intensity of anti-symmetric stretching than of symmetric stretching of methylene. We used total FA that covered major FA in oilseeds (Koprna et al., 2006). However, short- or medium-chain FA, or FA with more than 20 C were not included in our estimate of total FA, because the relative amount of these FA was expected to be small in the samples (Azizian and Kramer, 2005; Martínez-Ramírez et al., 2010). The peak of methylene stretching was induced by all FA presented in the samples.

6.5.5 Fecal fat and prediction of apparent total tract digestibility of ether extract

Fat present in feces differs from fat in ingredients, diets, or digesta, because the hind gut microflora may modify fat extensively (Devillard et al., 2009). A major part of fecal lipids are FA in the soap form (Hamilton and McDonald, 1969). Fecal spectra reflected the fat property changes, e.g., the peak shift for ester C=O indicated possible mono- or di-glycerides in feces vs. triglycerides in diets (Lewis et al., 1994). The ester C=O peak of lipids in a fiber matrix was observed at 1,736 cm^{-1} in spectra of corn pericarp (Yu et al., 2004). The strong methylene stretching peak corresponded with the strong asymmetric carboxylate peak at 1,575 cm^{-1} in fecal spectra, indicating deprotonation of the

head carboxylic group (Potapova et al., 2010). Together with the strong peak at 1,539 cm^{-1}, this doublet is characteristic for dicarboxylate salt, such as Ca distearate (Lu and Miller, 2002). The shift of symmetric and asymmetric methylene stretching peaks from 2,923 to 2,918 cm^{-1} and 2,852 to 2,848 cm^{-1}, indicated conformational packing geometry alterations (Mendelsohn and Moore, 1998) or surface property changes (Lu and Miller, 2002; Shi et al., 2006; Lin et al., 2011). Saturation of fat or FA by losing double bonds may cause conformational change (Smith, 2010). The absent olefinic hydrocarbon (-C=C-H) peak at 3,008 cm^{-1}, weak ester C=O peak at 1,735 cm^{-1}, and strong carboxylate peak at 1,575 cm^{-1} indicated that in feces, saturated FA in the form of soap, and not unsaturated fat, mainly induced the methylene stretching peaks, which differed from those for ingredients, diets, and digesta. Besides, FA salts, e.g., Ca palmitic acid salt, do not have peaks in the ester C=O region (Larkin, 2011). Thus, intensity of the ester C=O peak is not affected by FA in the form of soap in feces, in contrast to the strong ester C=O peak induced by mono-, di-, or triglyceride as EE measurements.

The strong relation between FGD of the C=O region and ATTD of EE indicates that FGD of C=O in ester and FFA region estimate ATTD of EE well. However, fecal samples from the basal diet were excluded from regression analysis. The EE concentration in feces from the basal diet was lower than that from test diets; correspondingly, the ester C=O peak was weak in fecal spectra from the basal diet. Using ATR FT-IR might then be an approach with limitations due to shallow penetration depth (Ekgasit and Ishida, 2002), while quality of

reference data was another concern. Comparing to total FA, EE concentration does not precisely define fat, as waxes and pigments in samples were extracted, whereas soaps were not (Sukhija and Palmquist, 1988).

6.5.6 Baseline selection and derivative transformation

In the present study, non-derivative and 2nd derivative spectra with or without baseline correction were compared. Although peak intensity determination without baseline correction was not advised for non-derivative spectra (Griffiths, 2002), relations to concentration of total FA did not change much either with or without use of baseline for the methylene stretching peaks at 2,923 or 2,852 cm^{-1}. Thus, baseline selection or derivative transformation was not critical for using peak intensity to reflect concentration of total FA.

Using non-derivative spectra to calculate FGD, baseline correction reduced residuals to estimate AID of total FA as compared to without baseline correction, which might be attributed to removal of contributions from overlapping peaks and baselines. However, the baseline selected for correction is subjective (Griffiths, 2002). Using derivative spectra may eliminate baseline selection (Coates, 2002), while Beer's law remains valid (Rieppo et al., 2012). Using 2nd derivative spectra without baseline correction had similar relation between FGD and AID of total FA compared with using non-derivative spectra with baseline correction, and lowered the residual between FGD at 2,923 cm^{-1} and AID of total FA, indicating that 2nd derivative spectra of ileal digesta can determine FGD. However, the baseline correction for 2nd derivative spectra did not further improve estimation of AID of FA in the present study. The

effectiveness of other novel baseline correction methods for derivative spectra to estimate AID of FA requires further investigation (Li et al., 2011).

Using a 2nd derivative transformation, the relation between peak intensity and EE concentration in ingredients and diets was stronger than using non-derivative spectra, because the FFA peak was pronounced in the spectra. The peak of C=O in FFA at 1,710 cm^{-1} could overlap with the β-sheet peak of protein centered at 1,684 cm^{-1} (Barth, 2007). Derivative transformation may resolve overlapping peaks (Saarinen and Kauppinen, 2002). Using 2nd derivative spectra improved an official method to predict trans FA content (Mossoba et al., 1996; Mossoba et al., 2007). However, FGD determined with 2nd derivative fecal spectra overestimated ATTD of EE, which might be due to different sensitivity of peak intensity changes for diets and feces after derivative transformation (Mark and Workman, 2007).

6.5.7 Advantage and weakness of the proposed method

With the proposed method, extraction or esterification of fat was not required. Steps not required will facilitate the use of this method for rapid estimation of digestibility of EE or total FA, especially to investigate in vitro digestion with micro amount of undigested residue. The single reflection ATR was signal-limited compared to transmission spectroscopy (van de Voort et al., 2007). Thus, use of instrumentation such as multiple-reflection ATR FT-IR for the extended detection limit might improve the prediction accuracy, especially for low fat samples (Mossoba et al., 2012).

In conclusion, intensity of methylene stretching peaks indicated

concentration of total FA. Likewise, accumulated peak intensity in the C=O region induced by ester and FFA indicated EE concentration. Direct calculation of FGD using intensity of methylene stretching peaks can estimate AID of total FA. Baseline correction or derivative transformation of non-derivative spectra may improve the prediction accuracy for AID of total FA. Direct calculation of FGD using C=O of ester and FFA can estimate ATTD of EE, but neither baseline correction nor derivative transformation improved prediction accuracy. Instead of GLC-based methods or predictions based on calibrations, the AID of total FA and ATTD of EE can be estimated directly from ATR FT-IR spectra, provided the ratio of marker in diets and undigested residue is known. The proposed method was tested with a few samples; thus, further validation with more samples is required.

6.6 References

Abeysekara, S., Samadi, and P. Yu. 2012. Response and sensitivity of lipid related molecular structure to wet and dry heating in Canola tissue. Spectrochim. Acta. A Mol. Biomol. Spectrosc. 90:63–71.

Adeola, O. 2001. Digestion and balance techniques in pigs. In: A. J. Lewis and L. L. Southern, editors, Swine nutrition. CRC Press LLC, Boca Raton, FL. p. 903–916.

AOAC. 2006. Official methods of analysis. 18th ed. Assoc. Off. Anal. Chem., Arlington, VA.

Azizian, H., and J. Kramer. 2005. A rapid method for the quantification of fatty acids in fats and oils with emphasis on trans fatty acids using Fourier

transform near infrared spectroscopy (FT-NIR). Lipids 40:855–867.

Barth, A. 2007. Infrared spectroscopy of proteins. Biochim. Biophys. Acta - Bioenergetics 1767:1073–1101.

Canadian Council on Animal Care (CCAC). 1993. Guide to the care and use of experimental animals. Vol. 1. 2nd ed. CCAC, Ottawa, ON, Canada.

Christy, A. A., and P. K. Egeberg. 2006. Quantitative determination of saturated and unsaturated fatty acids in edible oils by infrared spectroscopy and chemometrics. Chemometrics Intellig. Lab. Syst. 82:130–136.

Coates, J. 2002. Classical methods of quantitative analysis. In: J. M. Chalmers and P. R. Griffiths, editors, Handbook of vibrational theory, Vol. 3. John Wiley & Sons Ltd, Chichester, UK. p. 2235–2257.

Devillard, E., F. M. McIntosh, D. Paillard, N. A. Thomas, K. J. Shingfield, and R. J. Wallace. 2009. Differences between human subjects in the composition of the faecal bacterial community and faecal metabolism of linoleic acid. Microbiology (Reading) 155:513–520.

Ekgasit, S., and H. Ishida. 2002. Depth profiling by ATR. In: J. M. Chalmers and P. R. Griffiths, editors, Handbook of vibrational theory, Vol. 2. John Wiley & Sons Ltd, Chichester, UK. p. 1508–1520.

Fabian, H., and W. Mantele. 2002. Infrared spectroscopy of proteins. In: J. M. Chalmers and P. R. Griffiths, editors, Handbook of vibrational theory Vol. 5. John Wiley & Sons Ltd, Chichester, UK. p. 3399–3425.

Fenton, T. W., and M. Fenton. 1979. An improved procedure for the determination of chromic oxide in feed and feces. Can. J. Anim. Sci. 59:631–634.

Franck, P., J. L. Sallerin, H. Schroeder, M. A. Gelot, and P. Nabet. 1996. Rapid determination of fecal fat by Fourier transform infrared analysis (FTIR) with partial least-squares regression and an attenuated total reflectance accessory. Clin. Chem. 42:2015–2020.

Griffiths, P. R. 2002. Beer's law. In: J. M. Chalmers and P. R. Griffiths, editors, Handbook of vibrational theory Vol. 3. John Wiley & Sons Ltd, Chichester, UK. p. 2225–2234.

Hamilton, R. M. G., and B. B. McDonald. 1969. Effect of dietary fat source on the apparent digestibility of fat and the composition of fecal lipids of the young pig. J. Nutr. 97:33–41.

Htoo, J. K., X. Meng, J. F. Patience, M. E. R. Dugan, and R. T. Zijlstra. 2008. Effects of coextrusion of flaxseed and field pea on the digestibility of energy, ether extract, fatty acids, protein, and amino acids in grower-finisher pigs. J. Anim. Sci. 86:2942–2951.

Isaksson, T., and T. Naes. 1988. The effect of multiplicative scatter correction (MSC) and linearity improvement in NIR spectroscopy. Appl. Spectrosc. 42:1273–1284.

Jakobs, B. S., M. Volmer, D. W. Swinkels, M. T. W. Hofs, S. Donkervoort, M. M. J. Joosting, B. G. Wolthers, P. de Peinder, and H. A. M. Voorbij. 2000. New method for faecal fat determination by mid-infrared spectroscopy, using a transmission cell: an improvement in standardization. Ann. Clin. Biochem. 37:343–349.

Koprna, R., P. Nerusil, O. Kolovrat, V. Kucera, and A. Kohoutek. 2006.

Estimation of fatty acid content in intact seeds of oilseed rape (Brassica napus L.) lines using near-infrared spectroscopy. Czech J. Genet. Plant Breed. 42:132–136.

Larkin, P. 2011. Infrared and Raman spectroscopy: principles and spectral interpretation. Elsevier Inc., Waltham, MA.

Lewis, R., R. N. McElhaney, W. Pohle, and H. H. Mantsch. 1994. Components of the carbonyl stretching band in the infrared-spectra of hydrated 1,2-diacylglycerolipid bilayers. A reevaluation. Biophys. J. 67:2367–2375.

Li, N., X. Li, Z. Zou, L. Lin, and Y. Li. 2011. A novel baseline-correction method for standard addition based derivative spectra and its application to quantitative analysis of benzo(a)pyrene in vegetable oil samples. Analyst 136:2802–2810.

Lin, Y., H. Chen, C. Chan, and J. Wu. 2011. Nucleating effect of calcium stearate coated CaCO3 nanoparticles on polypropylene. J. Colloid Interface Sci. 354:570–576.

Lu, Y., and J. D. Miller. 2002. Carboxyl stretching vibrations of spontaneously adsorbed and LB-transferred calcium carboxylates as determined by FTIR internal reflection spectroscopy. J. Colloid Interface Sci. 256:41–52.

Mahesar, S. A., S. T. H. Sherazi, A. A. Kandhro, M. I. Bhanger, A. R. Khaskheli, and M. Y. Talpur. 2011. Evaluation of important fatty acid ratios in poultry feed lipids by ATR FTIR spectroscopy. Vib. Spectrosc 57:177–181.

Mark, H., and J. Workman. 2007. Chemometrics in spectroscopy. Academic Press, Burlington, MA.

Martínez-Ramírez, H. R., J. K. G. Kramer, and C. F. M. de Lange. 2010. Fatty acid profiles, including CLA isomers and long chain PUFA, in ileal digesta of growing gilts fed flaxseed or tallow containing diets. Livest. Sci. 134:65–67.

Mayo, D. W. 2004. Characteristic frequencies of alkanes. In: D. W. Mayo, F. A. Miller, and R. W. Hannah, editors, Course notes on the interpretation of infrared and Raman spectra. John Wiley & Sons, Inc. p. 33–72.

Mendelsohn, R., and D. J. Moore. 1998. Vibrational spectroscopic studies of lipid domains in biomembranes and model systems. Chem. Phys. Lipids 96:141–157.

Mossoba, M. M., J. K. G. Kramer, H. Azizian, J. Kraft, P. Delmonte, A. R. F. Kia, F. J. Bueso, J. I. Rader, and J. K. Lee. 2012. Application of a novel, heated, nine-reflection ATR crystal and a portable FTIR spectrometer to the rapid determination of total trans fat. J. Am. Oil Chem. Soc. 89: 419–429.

Mossoba, M. M., V. Milosevic, M. Milosevic, J. K. G. Kramer, and H. Azizian. 2007. Determination of total trans fats and oils by infrared spectroscopy for regulatory compliance. Anal. Bioanal. Chem. 389:87–92.

Mossoba, M. M., M. P. Yurawecz, and R. E. McDonald. 1996. Rapid determination of the total trans content of neat hydrogenated oils by attenuated total reflection spectroscopy. J. Am. Oil Chem. Soc. 73:1003–1009.

Moya Moreno, M. C. M., D. Mendoza Olivares, F. J. Amézquita López, J. V. Gimeno Adelantado, and F. Bosch Reig. 1999. Determination of

unsaturation grade and trans isomers generated during thermal oxidation of edible oils and fats by FTIR. J. Mol. Struct. 482–483:551–556.

Potapova, E., M. Grahn, A. Holmgren, and J. Hedlund. 2010. The effect of calcium ions and sodium silicate on the adsorption of a model anionic flotation collector on magnetite studied by ATR-FTIR spectroscopy. J. Colloid Interface Sci. 345:96–102.

Regmi, P. R., N. S. Ferguson, and R. T. Zijlstra. 2009. In vitro digestibility techniques to predict apparent total tract energy digestibility of wheat in grower pigs. J. Anim. Sci. 87:3620–3629.

Rieppo, L., S. Saarakkala, T. Närhi, H. J. Helminen, J. S. Jurvelin, and J. Rieppo. 2012. Application of second derivative spectroscopy for increasing molecular specificity of Fourier transform infrared spectroscopic imaging of articular cartilage. Osteoarthr. Cartil. 20:451–459.

Saarinen, P. E., and J. K. Kauppinen. 2002. Resolution enhancement approaches. In: J. M. Chalmers and P. R. Griffiths, editors, Handbook of vibrational theory, Vol. 3. John Wiley & Sons Ltd, Chichester, UK. p. 2185–2214.

Shi, L., L. Wang, and Y. Wang. 2006. The investigation of argon plasma surface modification to polyethylene: Quantitative ATR-FTIR spectroscopic analysis. Eur. Polym. J. 42:1625–1633.

Shurvell, H. F. 2002. Spectra–structure correlations in the mid- and far-infrared. In: J. M. Chalmers and P. R. Griffiths, editors, Handbook of vibrational theory, Vol. 3. John Wiley & Sons Ltd, Chichester, UK. p. 1783–1816.

Smith, J. G. 2010. General, organic, and biological chemistry. McGraw-Hill

Companies, Inc., New York, NY.

Sukhija, P. S., and D. L. Palmquist. 1988. Rapid method for determination of total fatty acid content and composition of feedstuffs and feces. J. Agric. Food Chem. 36:1202–1206.

van de Voort, F. R., J. Sedman, and A. A. Ismail. 1993. A rapid FTIR quality-control method for determining fat and moisture in high-fat products. Food Chem. 48:213–221.

van de Voort, F. R., J. Sedman, and S. T. H. Sherazi. 2007. Improved determination of isolated trans isomers in edible oils by Fourier transform infrared spectroscopy using spectral reconstitution. J. AOAC Int. 90:446–451.

Wang, L. F., M. L. Swift, and R. T. Zijlstra. 2013. A novel approach for a functional group to predict protein in undigested residue and protein digestibility by mid-infrared spectroscopy. Appl. Spectrosc. 67:1343–1347.

Yoshida, S., and H. Yoshida. 2003. Nondestructive analyses of unsaturated fatty acid species in dietary oils by attenuated total reflectance with Fourier transform IR spectroscopy. Biopolymers 70:604–613.

Yu, P., J. J. McKinnon, C. R. Christensen, and D. A. Christensen. 2004. Imaging molecular chemistry of Pioneer corn. J. Agric. Food Chem. 52:7345–7352.

Yu, X., F. van de Voort, J. Sedman, and J. Gao. 2011. A new direct Fourier transform infrared analysis of free fatty acids in edible oils using spectral reconstitution. Anal. Bioanal. Chem. 401:315–324.

Table 6.1 The apparent ileal digestibility (AID) of total fatty acids (FA) measured using gas-liquid chromatography (GLC) and functional group digestibility (FGD) calculated using FT-IR at ca. 2,923 and ca. 2,852 cm^{-1}, without derivative or with 2nd derivative, and with or without baseline correction (BC) of FT-IR spectra; and relationship between peak intensity and concentration of total FA of ingredients, diets, and digesta of pigs[1,2]

	FT-IR								GLC
	2,923, cm^{-1}				2,852, cm^{-1}				AID of
	Without derivative		2nd derivative		Without derivative		2nd derivative		total
Item	Without BC	With BC[3]	Without BC	With BC	Without BC	With BC	Without BC	With BC	FA, %
Relation to FA[4]	0.90	0.90	0.90	0.90	0.86	0.86	0.86	0.86	-
FGD, %	80.0^{cd}	83.0^{a}	82.7^{a}	82.0^{b}	77.7^{e}	81.1^{bc}	80.5^{c}	80.6^{cd}	82.4^{ab}
SD	3.4	5.5	6.1	6.3	3.1	6.0	7.1	7.1	7.0
Relation to AID[5]	0.77	0.75	0.74	0.74	0.74	0.75	0.77	0.77	-
Residual[6]									
Mean	-2.46	0.54	0.24	-0.45	-4.76	-1.35	-1.92	-1.83	-
SD	4.39	3.78	3.80	3.77	4.59	3.74	3.81	3.78	-

[a-e]Within a row, means without a common superscript differ ($P < 0.05$).

[1]FT-IR = Fourier transform infrared.

[2]Total FA were defined as the sum of palmitic (C16:0), stearic (C18:0), arachidic (C20:0), oleic (C18:1ω9), vaccenic (C18:1ω7), linoleic (C18:2), and linolenic (C18:3).

[3]Baselines were 3,045-2,777, 2,945-2,902, 3,045-2,777, and 2,869-2,835 cm^{-1} for the peak at 2,923 cm^{-1} without derivative or with 2nd derivative and the peak at 2,852 cm^{-1} without derivative or with 2nd derivative, respectively.

[4]Coefficients of determination between concentration of total FA of ingredients, diets, and digesta and peak intensity of FT-IR spectra (n = 33, $P < 0.01$).

[5]Coefficients of determination between AID of total FA and FGD (n = 24, $P < 0.01$).

[6]Residual was defined as FGD minus AID of FA.

Table 6.2 The apparent total tract digestibility (ATTD) of ether extract (EE) measured using chemical analysis and functional group digestibility (FGD) calculated using FT-IR at ca. 1,766-1,695 cm^{-1} without or with 2nd derivative, and without or with baseline corrections (BC) of FT-IR spectra; and relationship between peak intensity and EE concentration of ingredients, diets, or feces[1]

	FT-IR; area (1,766-1,695 cm^{-1})				
	Without derivative[2]		2nd derivative[3]		Chemical analysis
Item	Without BC	With BC[4]	Without BC	With BC	ATTD of EE, %
Relation to EE					
Ingredients and diets[5]	0.55	0.61	0.90	0.88	-
Feces[6]	0.88	0.88	0.92	0.83	-
FGD, %	88.8[d]	89.1[c]	97.0[a]	94.6[b]	85.6[e]
SD	3.3	3.3	3.0	3.4	5.1
Relation to ATTD[7]	0.90	0.90	0.88	0.88	-
Residual[8]					
Mean	3.15	3.50	11.41	8.98	-
SD	3.14	3.24	3.53	4.88	-

[a-e]Within a row, means without a common superscript differ ($P < 0.01$).

[1]FT-IR = Fourier transform infrared.

[2]Accumulated peak intensity, defined as the sum of peak intensity at each wavenumber in the carbonyl (C=O) region (1,766-

1,695 cm^{-1}), was used to calculate FGD and for analyses.

[3]Sum of peak intensity at 1,743 and 1,710 cm^{-1} for ingredients and diets, and at 1,735 and 1,710 cm^{-1} for feces was used to calculate FGD and for analyses.

[4]Baselines were 1,822 for non-derivative spectra at 1,766-1,695 cm^{-1}, 1,753-1,722 for 2nd derivative spectra at 1,735 cm^{-1}, and 1,722-1,702 cm^{-1} for 2nd derivative spectra at 1,710 cm^{-1}.

[5]Coefficients of determination between EE concentration in ingredients and diets and peak intensity of FT-IR spectra ($n = 9$, $P < 0.05$).

[6]Coefficients of determination between EE concentration in feces and peak intensity of FT-IR spectra ($n = 24$, $P < 0.01$).

[7]Coefficients of determination between ATTD of EE of test diets and FGD ($n = 19$, $P < 0.01$).

[8]Residual was defined as FGD minus ATTD of EE.

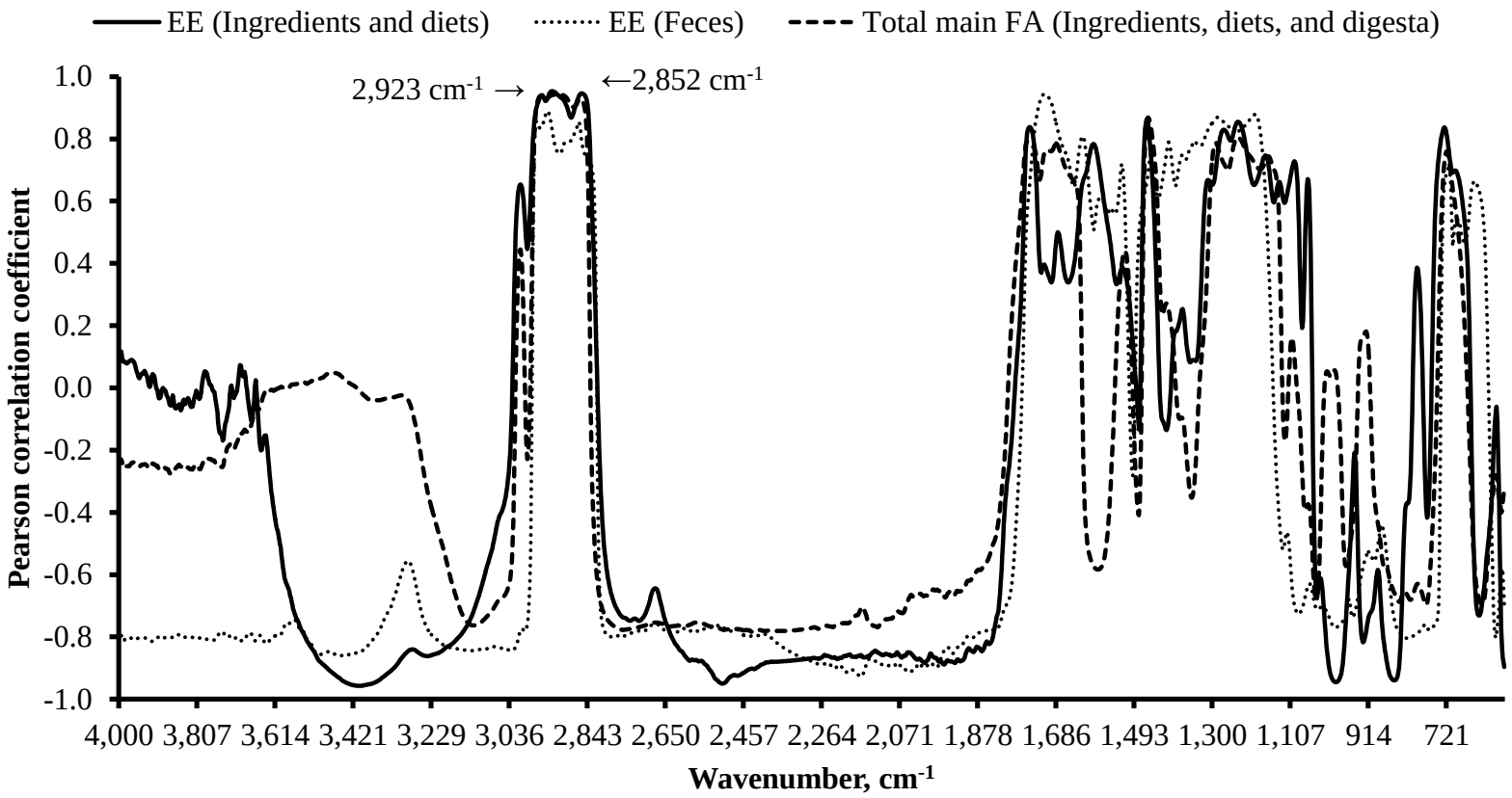

Figure 6.1 Correlation between concentrations of ether extract (EE) and total fatty acids (FA) in ingredient, diets, and feces and peak intensity from 4,000 to 578 cm^{-1} with a 2 cm^{-1} interval of Fourier transform infrared spectra of ingredients, diets, and feces (n = 34).

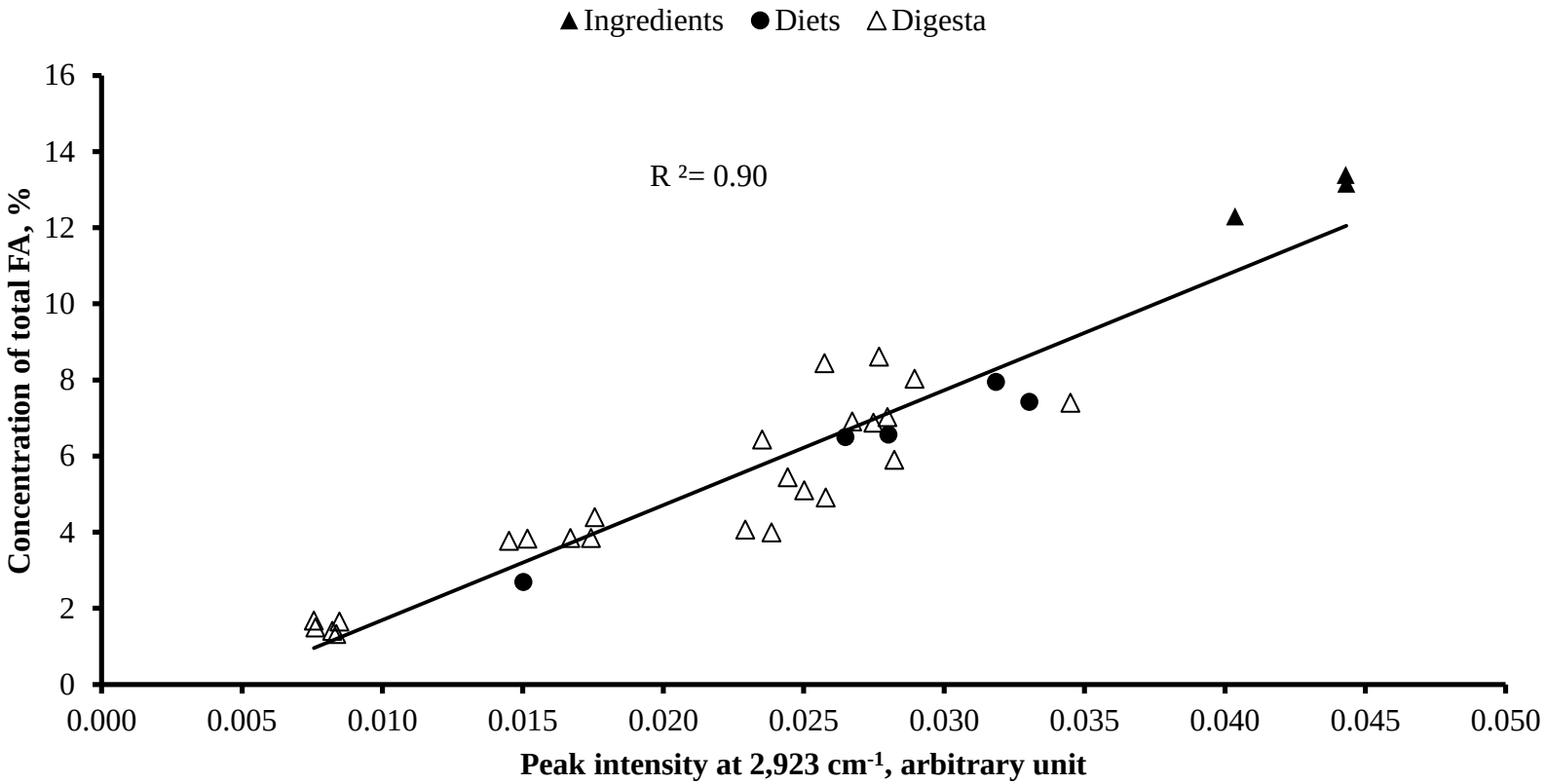

Figure 6.2 Relation between peak intensity at ca. 2,923 cm^{-1} of spectra with baseline at ca. 3,045-2,777 cm^{-1} and concentrations of total fatty acids (FA) in ingredients, diets, and digesta (n = 34).

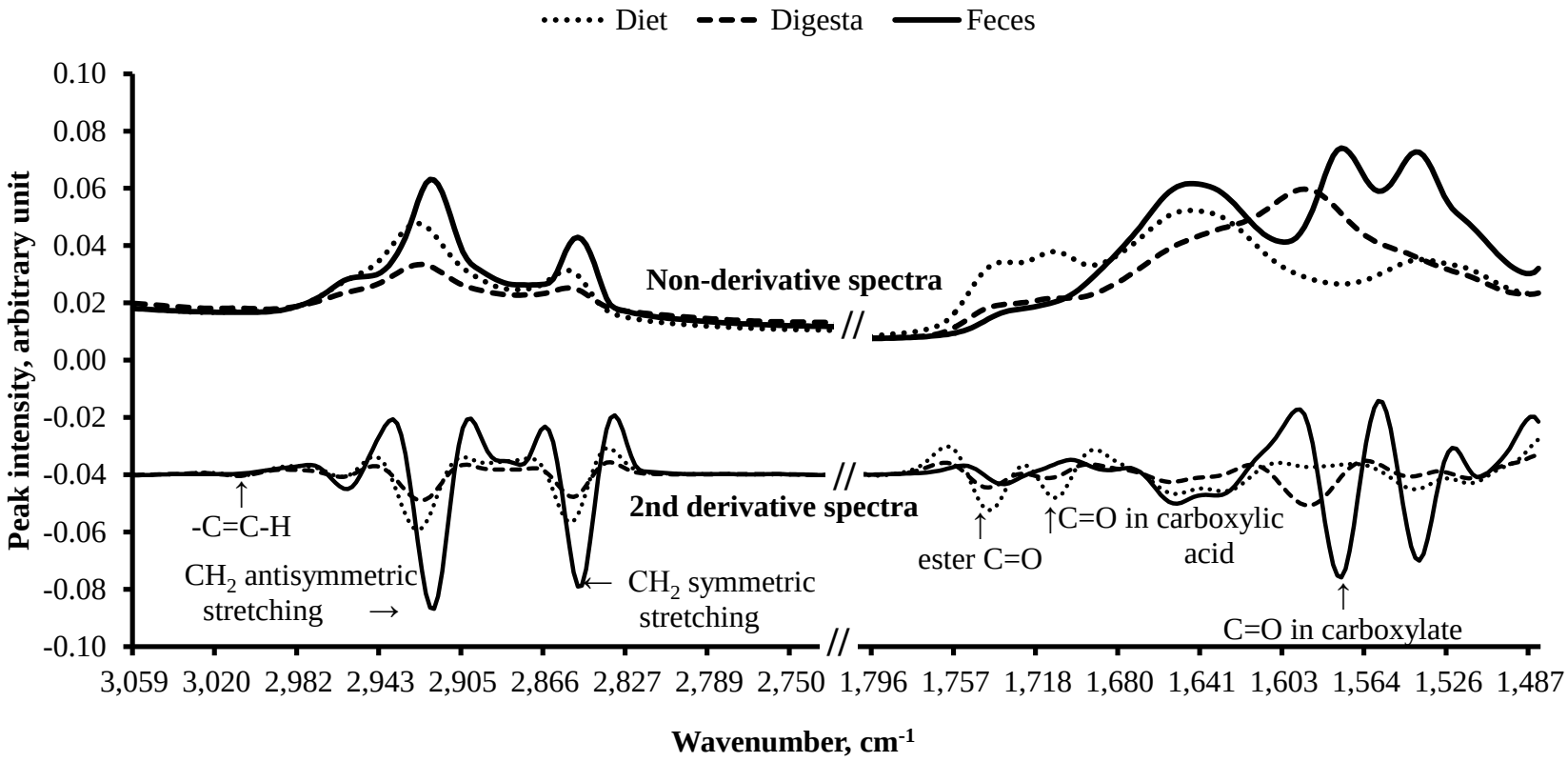

Figure 6.3 Example non-derivative and 2nd derivative Fourier transform infrared spectra of diet, digesta, and feces of flaxseed and field pea at 3,058-1,483 cm^{-1}. The 2nd derivative spectra were multiplied by 50 and added offset by -0.04.

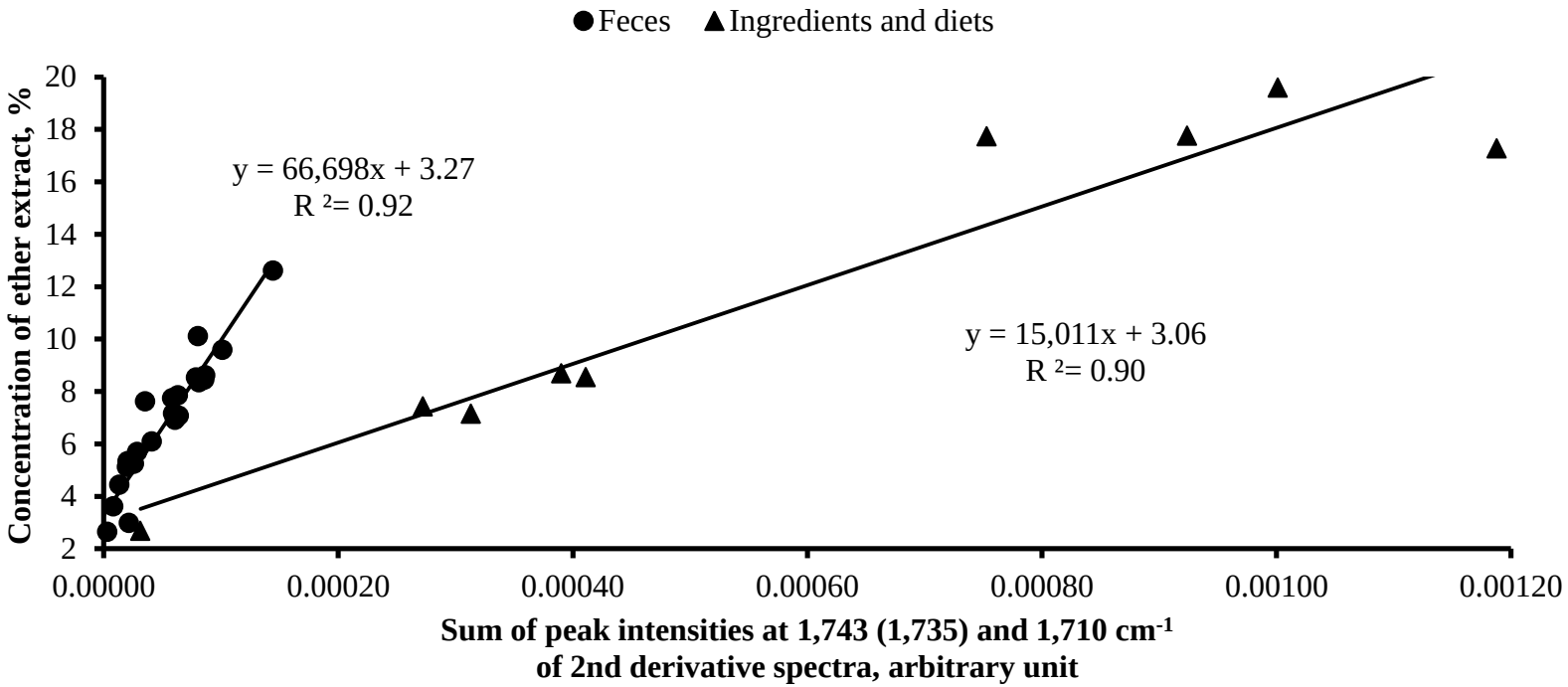

Figure 6.4 Relation between the sum of C=O peak intensities of 2nd derivative Fourier transform infrared spectra at ca. 1,743 and ca. 1,710 cm^{-1} for ingredients and diets or at ca. 1,735 and ca. 1,710 cm^{-1} for feces that reflect triglyceride and FFA, respectively, and the concentrations of ether extract (EE).

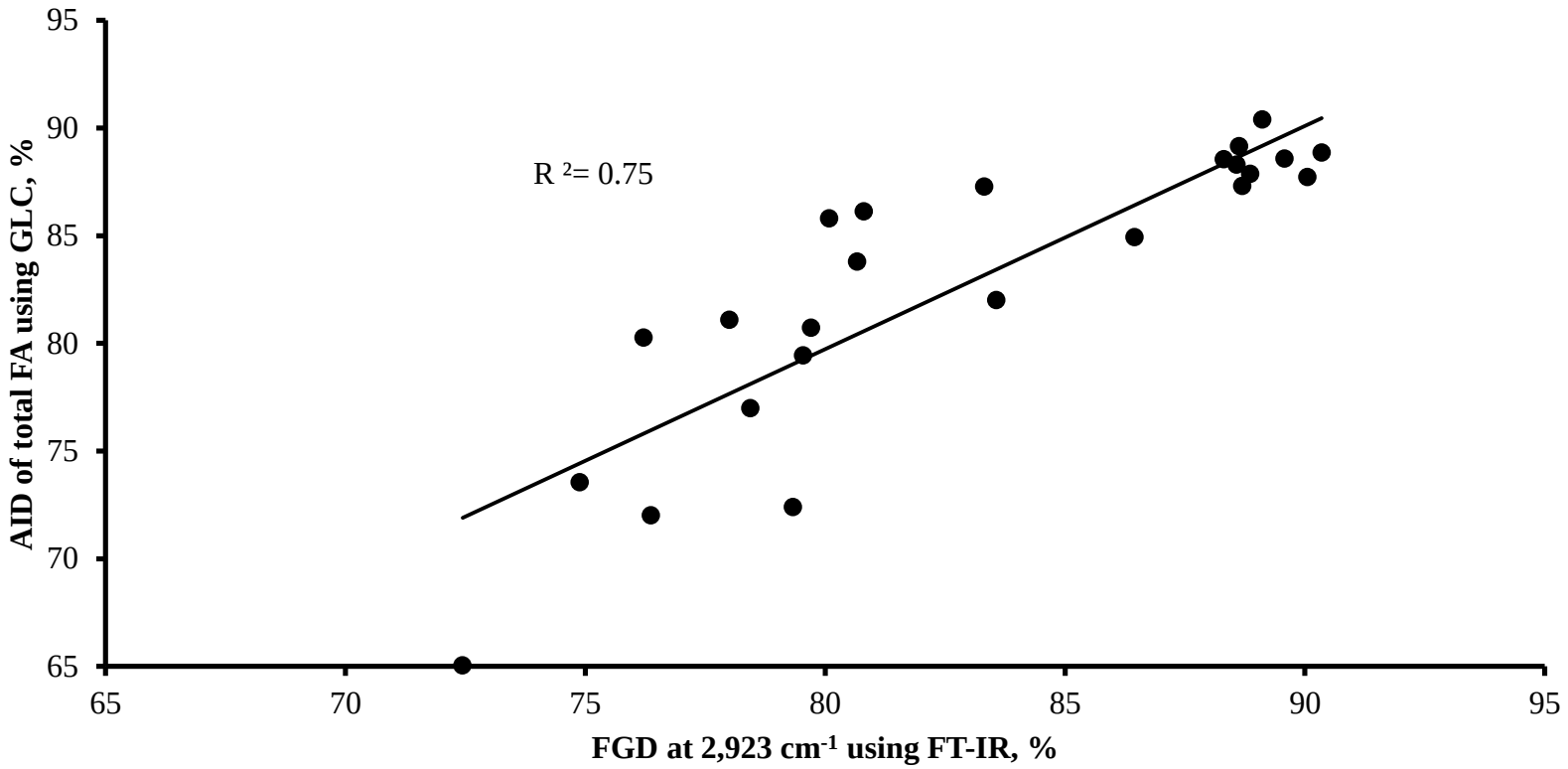

Figure 6.5 Relation between functional group digestibility (FGD) determined with Fourier transform infrared spectra and apparent ileal digestibility (AID) of total fatty acids (FA) with gas-liquid chromatography (GLC).

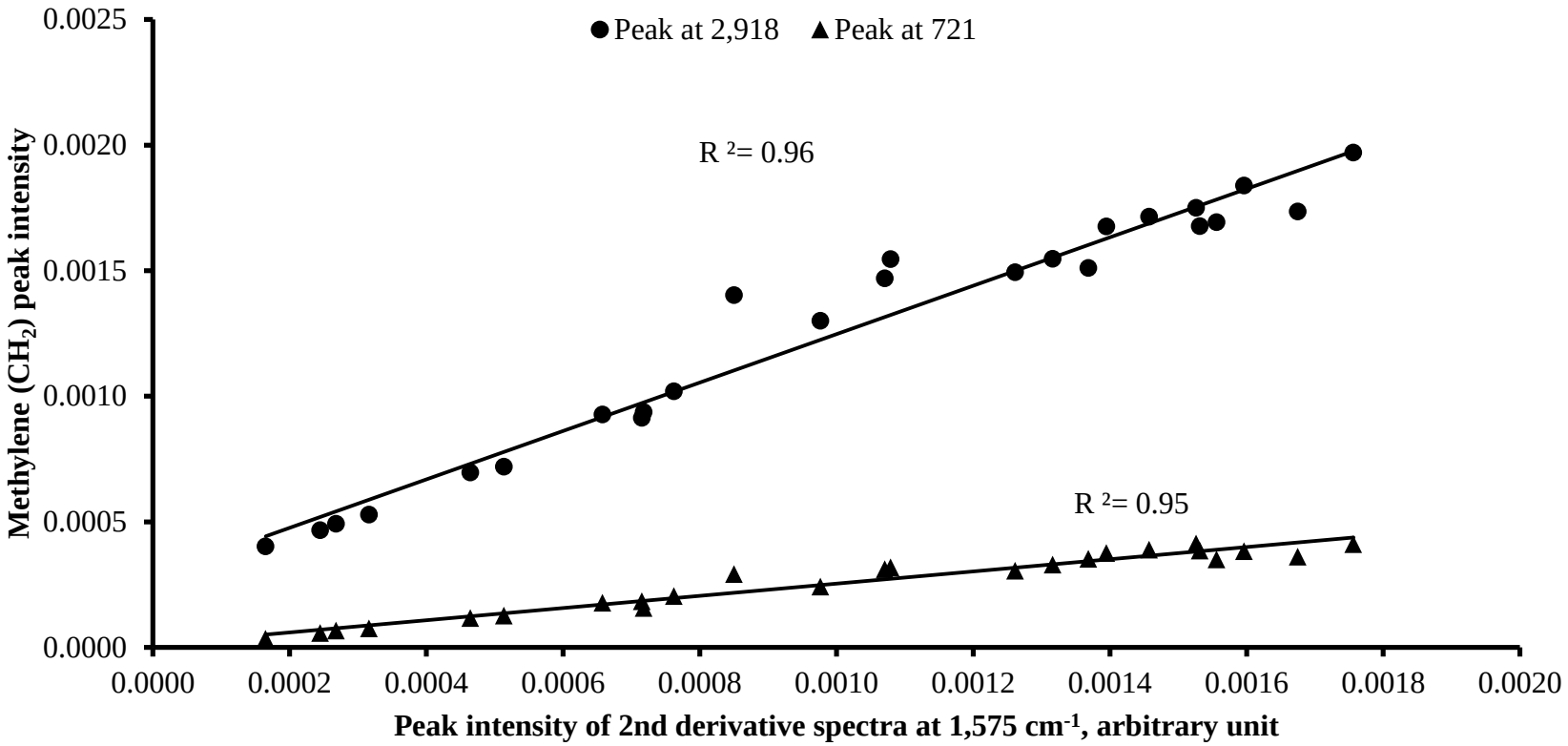

Figure 6.6 Relation between peak intensity of carboxylate peak at ca. 1,575 cm^{-1} with methylene peak at ca. 2,918 and ca. 721 cm^{-1} of 2nd derivative spectra of feces.

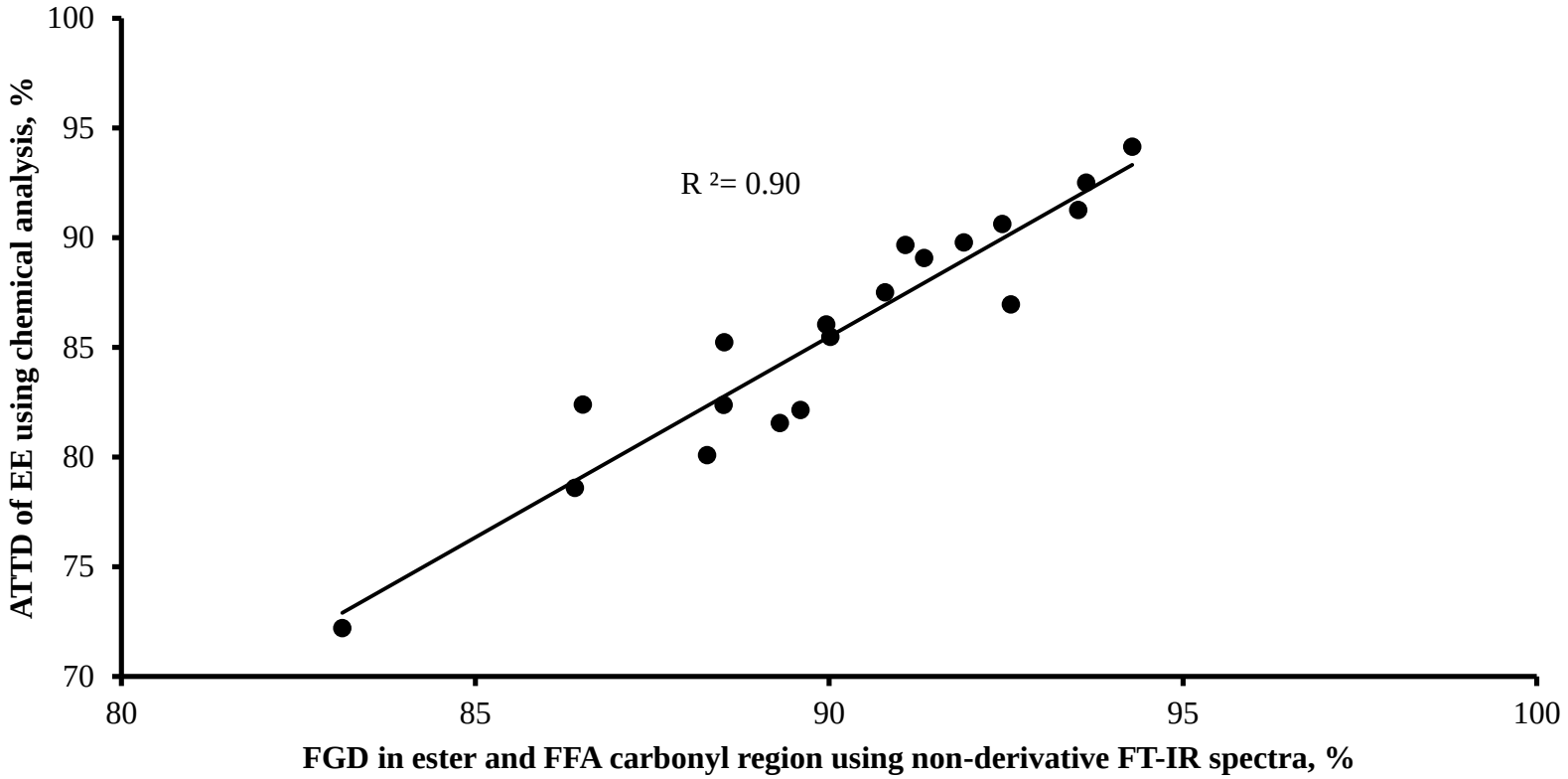

Figure 6.7 Relation between functional group digestibility (FGD) in carbonyl region (ca. 1,766 to 1,695 cm^{-1}) with Fourier transform infrared (FT-IR) and the apparent total tract digestibility (ATTD) of ether extract (EE).

Chapter 7 General discussion

7.1 In vitro evaluation of energy digestibility

The competitive use of cereal grains, legumes, and oilseeds as food source by humans and as feedstock by the expanding biofuel industry has reduced their use in swine diets. Consequently, co-products from cereal grain, legumes, and oilseed processing are increasingly used as alternative feedstuffs (Zijlstra and Beltranena, 2013). However, the nutritional quality of these co-products varies widely (Zijlstra and Beltranena, 2008). For routine evaluation of a large number of samples of feedstuffs, the use of animal model to characterize nutritional quality is expensive and not practical; thus, rapid and accurate feed quality evaluation methods are required. The in vitro digestion (**IVD**) model has been used to evaluate feed quality and has advantages against other methods, such as predictions based on physical measurements or chemical analyses (Chapter 2). The IVD models accurately predicted the apparent total tract digestibility (**ATTD**) of energy for cereal grains (Regmi et al., 2008, 2009). However, the existing IVD models were inaccurate to evaluate energy digestibility for co-products (Chapter 2). Unlike their parent cereal grains or oilseeds, co-products are rich in fiber, protein, or fat. Thus, efficacy of IVD models for co-products needs to be tested rigorously.

A 3-step IVD model was problematic for the evaluation of ATTD of energy for co-products of cereal grains and oilseeds (Chapter 4). Although the IVD model explained 69% of the variation in ATTD of energy among 30 co-product samples, the prediction error was large. The IVD model severely

underestimated ATTD of energy for co-products rich in fiber or fat, such as corn distillers dried grain with solubles (**DDGS**) and wheat millrun. Also, the IVD model did not detect small differences in energy digestibility within co-products. Chemical analyses with multiple predictors had greater accuracy than the IVD model to predict ATTD of energy for both among and within co-products. However, the IVD model explained more variation of ATTD of energy among co-products than any single chemical predictor. Chemical predictors and corresponding predicting equations differed for each co-product, and among co-products. The best equation to predict ATTD of energy or DE value of feedstuffs depends largely on the sample set for regression analysis (Noblet and Perez, 1993; Fairbairn et al., 1999; Zijlstra et al., 1999). Thus, IVD models are promising to evaluate energy digestibility for co-products, but requires further improvement.

To improve IVD models, we require knowledge about digestion of individual energy-yielding macronutrients that do not adequately simulate in vivo digestion. However, the amount of undigested in vitro residue (**ivR**) is usually less than 200 mg. The small quantity of ivR limits the use of laboratory analyses to determine the concentration of macronutrients and hence their digestibility.

To identify discrepancies between IVD and in vivo digestion of nutrients, appropriate methods are required. Infrared (**IR**) spectroscopy is a potential solution (Chapter 3). However, conventional IR spectroscopy to predict concentration or digestibility of nutrients is based on multivariate calibrations from regressing wet chemistry data on absorption data of samples (van Kempen and Bodin, 1998; Zijlstra et al., 2011). For IVD models, the amount of sample is

not sufficient for chemical analyses; thus, prediction calibrations cannot be developed. Non-calibration spectroscopic methods can overcome this bottleneck (Wang et al., 2013; Chapters 5 and 6), and may assist to identify discrepancies between IVD and in vivo digestion of energy-yielding macronutrients (Wang et al., 2012).

7.2 Summary of novel findings

We proposed a novel spectroscopic method using functional group digestibility (**FGD**) to estimate protein digestibility (Chapter 5). The FGD was calculated without calibration using the absorbance of specific Fourier transform infrared (**FT-IR**) peaks and the ratio of an inorganic indigestible marker in diet and digesta that was determined with laboratory analyses. With this approach, 99% of the variation in apparent ileal digestibility (**AID**) of CP of a wheat diet was explained by the FGD in the amide I region (1,689-1,631 cm^{-1}). The measured diet CP digestibility ranged from 60.4 to 87.8% was accurately estimated. The sole use of the absorbance of spectra was incomplete to evaluate digestibility of CP and might be misleading (Chapter 5). Absorbance is proportional to concentration of an analyte, which is the essence of the Beer's law (Griffiths, 2002). The concentration of CP in digesta was also largely affected by digestion of other nutrients, collectively measured as DM digestibility of a diet.

According to the concept of FGD, non-calibration methods to estimate digestibility of ether extract (**EE**) and total fatty acids (**FA**) were proposed and validated (Chapter 6). The AID of total FA was estimated with the FGD at 2,923

cm^{-1} or 2,852 cm^{-1}. Similarly, the sum of peak intensities of ester carbonyl (C=O) at 1743 cm^{-1} for ingredients and diets or 1,735 cm^{-1} for feces and C=O in carboxylic acids at 1,710 cm^{-1} reflected the concentration of EE in ingredients, diets, and feces. The FGD in the C=O area (1,766-1,695 cm^{-1}) was used to estimate the ATTD of EE. We also observed the shift of methylene stretch peaks and appearance of carboxylate peaks, indicating fat property of diets was changed through digestive tract of pigs.

7.3 Challenges and limitations

Although the tested co-product samples covered a wide range of chemical profiles and ATTD of energy, the sample size was small and the range of ATTD of energy was narrow for each individual co-product, except for wheat millrun. A small sample set with a narrow range is a limit to examine efficacy of IVD model to evaluate the ATTD of energy for within co-products. Similarly, the range of chemical profile of co-product samples is essential for predictions based on chemical analyses to avoid extrapolation of prediction equations. However, to prepare such ideal sample sets is a challenge.

Another limit of the present thesis is the use of an IVD model without a filtration step using acetone (Boisen and Fernandez, 1997). This missing step might be not critical for cereal grains (Regmi et al., 2008, 2009), but might be important for co-products rich in fat. However, by simply including filtration with acetone at the end of digestion, IVD model may still not accurately predict DE

values of co-products rich in fat (Anderson, 2009). Thus, the IVD models either with or without filtration using acetone need improvement.

The investigations of spectroscopic methods used the ATR technique. Working with ATR on biological samples is a great challenge, especially for ivR less than 0.2 g, to reach homogenized conditions. Furthermore, the penetration depth of ATR is typically 0.3 to 3 μm (Fitzpatrick and Reffner, 2002), which is smaller than the particle size of starch granules (Sevenou et al., 2002). Other types of IR spectroscopy may overcome this limit, such as diffuse reflectance infrared Fourier transformed spectroscopy (**DRIFTS**) with a penetration depth of 20 to 160 μm (Zavarin et al., 1991) or near infrared spectroscopy (**NIRS**) with a penetration depth greater than 0.1 mm (DeThomas and Brimmer, 2002).

We validated the non-calibration methods with limited number of in vivo samples. Thus, the proposed methods should be validated with an expanded sample set.

7.4 Future research

Fat has a high energy density; thus, adequate simulation of fat digestion is important for co-products rich in fat. For pigs, certain amount of fat could be excreted in feces in the form of soap and is an energy loss (Bendsen et al., 2008). The quantitative evaluation of fat in soap, ester, and free fatty acid form with IR spectroscopy would be beneficial for the characterization of discrepancies between 3-step IVD model and in vivo total tract digestion of fat.

As starch and fiber are major energy-yielding macronutrients, the evaluation of starch and fiber digestibility with IR spectroscopy should be future

topics. However, similar or overlapped starch and fiber peaks in IR spectra may pose challenges to evaluate starch and fiber digestibility separately (Kačuráková and Wilson, 2001).

For the proposed non-calibration methods, the concentration of indigestible marker (Cr_2O_3) was pre-determined with a lab-based method (Fenton and Fenton, 1979) other than IR spectroscopy. The poor signal to noise ratio in the cut-off region of diamond internal reflection element (**IRE**) of ATR hampered the estimation of concentration of the marker using spectroscopy. Further research on selection of instrumentation or markers that are distinctive spectroscopically will benefit rapid spectroscopic determination of FGD for in vivo samples.

Finally, the ultimate goal is to develop an IVD model to evaluate energy digestibility for co-products. To achieve this ultimate goal, both identification of weakness of IVD of all energy-yielding macronutrients and understanding of digestion processes in pigs are essential.

7.5 Conclusions and implications

In conclusion, current IVD models do not fit to evaluate energy digestibility of co-products rich in fat and fiber. The non-calibration spectroscopic methods were capable to estimate the digestibility of CP, EE, and total FA. The FGD concept might be used to develop non-calibration spectroscopic methods to determine digestibility for other energy-yielding macronutrients such as starch and fiber. Thus, the discrepancies between IVD and in vivo digestion of energy-yielding macronutrients can be revealed with the aid of IR spectroscopy. The

findings support the future improvement of IVD models to evaluate energy digestibility for co-products. Such improved IVD models may be used as an effective and economical method to supply reference data for NIRS calibration and facilitate the establishment of a rapid feed quality evaluation network. Rapid feed quality evaluation benefits the feed and livestock industries.

7.6 References

Anderson, P. 2009. Energy determination of corn co-products in finishing pigs and the use of an in vitro organic matter digestibility assay to predict in vivo energy. MSc Diss. Iowa State University, Ames, IA.

Bendsen, N. T., A. L. Hother, S. K. Jensen, J. K. Lorenzen, and A. Astrup. 2008. Effect of dairy calcium on fecal fat excretion: a randomized crossover trial. Int. J. Obesity 32:1816–1824.

Boisen, S., and J. A. Fernandez. 1997. Prediction of the total tract digestibility of energy in feedstuffs and pig diets by in vitro analyses. Anim. Feed Sci. Technol. 68:277–286.

DeThomas, F. A., and P. J. Brimmer. 2002. Monochromators for near-infrared spectroscopy. In: J. M. Chalmers and P. R. Griffiths, editors, Handbook of Vibrational Theory Vol. 1. John Wiley and Sons Ltd, Chichester, UK. p. 383–392.

Fairbairn, S. L., J. F. Patience, H. L. Classen, and R. T. Zijlstra. 1999. The energy content of barley fed to growing pigs: characterizing the nature of its

variability and developing prediction equations for its estimation. J. Anim. Sci. 77:1502–1512.

Fenton, T. W., and M. Fenton. 1979. An improved procedure for the determination of chromic oxide in feed and feces. Can. J. Anim. Sci. 59:631–634.

Fitzpatrick, J., and J. A. Reffner. 2002. Macro and micro internal reflection accessories. In: J. M. Chalmers and P. R. Griffiths, editors, Handbook of vibrational theory Vol. 2. John Wiley and Sons Ltd, Chichester, UK. p. 1103–1116.

Griffiths, P. R. 2002. Beer's law. In: J. M. Chalmers and P. R. Griffiths, editors, Handbook of vibrational theory Vol. 3. John Wiley and Sons Ltd, Chichester, UK. p. 2225–2234.

Kačuráková, M., and R. H. Wilson. 2001. Developments in mid-infrared FT-IR spectroscopy of selected carbohydrates. Carbohydr. Polym. 44:291–303.

Noblet, J., and J. M. Perez. 1993. Prediction of digestibility of nutrients and energy values of pig diets from chemical-analysis. J. Anim. Sci. 71:3389–3398.

Regmi, P. R., N. S. Ferguson, and R. T. Zijlstra. 2009. In vitro digestibility techniques to predict apparent total tract energy digestibility of wheat in grower pigs. J. Anim. Sci. 87:3620–3629.

Regmi, P. R., W. C. Sauer, and R. T. Zijlstra. 2008. Prediction of in vivo apparent total tract energy digestibility of barley in grower pigs using an in vitro digestibility technique. J. Anim. Sci. 86:2619–2626.

Sevenou, O., S. E. Hill, I. A. Farhat, and J. R. Mitchell. 2002. Organisation of the external region of the starch granule as determined by infrared spectroscopy. Int. J. Biol. Macromol. 31:79–85.

van Kempen, T., and J. C. Bodin. 1998. Near-infrared reflectance spectroscopy (NIRS) appears to be superior to nitrogen-based regression as a rapid tool in predicting the poultry digestible amino acid content of commonly used feedstuffs. Anim. Feed Sci. Technol. 76:139–147.

Wang, L. F., M. L. Swift, and R. T. Zijlstra. 2012. Evaluation of energy digestibility of canola coproducts by in vitro analyses and characterization of fat digestion using spectroscopy. J. Anim. Sci. 90:251–253.

Wang, L. F., M. L. Swift, and R. T. Zijlstra. 2013. A novel approach for a functional group to predict protein in undigested residue and protein digestibility by mid-infrared spectroscopy. Appl. Spectrosc. 67:1343–1347.

Zavarin, E., L. G. Cool, and S. J. Jones. 1991. Analysis of Solid Wood Surfaces by Internal Reflection Fourier Transform Infrared Spectroscopy (FTIR-IRS). J. Wood Chem. Technol. 11:41–56.

Zijlstra, R. T., C. F. M. de Lange, and J. F. Patience. 1999. Nutritional value of wheat for growing pigs: chemical composition and digestible energy content. Can. J. Anim. Sci. 79:187–194.

Zijlstra, R. T., and E. Beltranena. 2008. Variability of quality in biofuel co-products. In: Recent advances in animal nutrition 2008. 42nd University of Nottingham Feed Conference, Sutton Bonington Campus, Nottingham, UK, 2-4 September 2008. p 313–326.

Zijlstra, R. T., and E. Beltranena. 2013. Swine convert co-products from food and biofuel industries into animal protein for food. Animal Frontiers 3:48–53.

Zijlstra, R. T., M. L. Swift, L. F. Wang, T. A. Scott, and M. J. Edney. 2011. Near infrared reflectance spectroscopy accurately predicts the digestible energy content of barley for pigs. Can. J. Anim. Sci. 91:301–304.